

Implications of Anthocyanin Instability and Metabolism: Impact on Discovery of Intake Biomarkers and *In Vitro* Mechanisms of Action

Michael James Smith, BSc. (Hons)

Registration number: 0345709

A Thesis presented to the University of East Anglia in accordance with the requirements for the Degree of Doctor of Philosophy

Norwich Medical School

November 2016

This copy of the thesis has been supplied on condition that anyone who consults it is understood to recognise that its copyright rests with the author and that use of any information derived there from must be in accordance with current UK Copyright Law. In addition, any quotation or extract must include full attribution.

Abstract

Anthocyanins are polyphenol pigments responsible for the blue/red colouring of many fruits and vegetables whose consumption is associated with reduced risk of cardiovascular disease. Due to instability at neutral pH and reported low bioavailability of anthocyanins, the focus has shifted to their phenolic metabolites to explain the observed bioactivity. The hypothesis of the present study was that greater sensitivity and higher throughput could be achieved by developing existing analytical methodology, metabolite biomarkers of anthocyanin intake could be identified, and physiologically relevant anthocyanin metabolite profiles could reduce expression of proinflammatory cytokines *in vitro*. Stability of cyanidin-3-glucoside and 17 metabolites in serum was assessed. Unlike the parent anthocyanin, metabolite recovery was unaffected by either pH or freeze/thaw cycling suggesting that acidification and aliquoting of samples may be unnecessary for quantifying anthocyanin metabolites only. HPLC-ESI-MS/MS methodology was developed to increase sensitivity and sample throughput. Initial and developed methods were validated against FDA guidelines and found to have acceptable linearity, specificity and sensitivity with limits of detection of 9.5 ± 13.0 nM and 96.7 ± 541.7 nM respectively. Accuracy and precision were acceptable at 50 μ M but outside guidelines at 1.56 μ M and 0.098 μ M for both methods. Biomarkers of anthocyanin intake were explored using samples from a ^{13}C -labelled cyanidin-3-glucoside trial to compare ^{13}C -labelled metabolites against ^{12}C metabolites from the background diet. Gallic acid was consistently found above background levels in urine and represented the best biomarker candidate. Finally, effect of anthocyanin metabolite profiles on proinflammatory cytokines in CD40L and TNF- α -stimulated HUVEC was investigated. Incubation with metabolite profiles reduced expression of sVCAM-1 by 47-58% and IL-6 by 16-37% following TNF- α stimulation. In conclusion, the present thesis develops methodology for the quantification of anthocyanin metabolites in biological matrices and provides insight into their use as biomarkers of anthocyanin intake and role in maintaining cardiovascular health.

Table of Contents

ABSTRACT	2
TABLE OF CONTENTS	3
LIST OF TABLES	5
LIST OF FIGURES	7
ACKNOWLEDGEMENTS.....	11
 CHAPTER 1. ANTHOCYANINS: A REVIEW OF CURRENT LITERATURE.....	13
1.1. Introduction.....	13
1.2. Chemistry	16
1.3. Role in Nature.....	18
1.4. Dietary Consumption	19
1.5. Bioavailability	20
1.6. Metabolism	22
1.7. Cardiovascular Health	25
1.8. Summary and Aims.....	31
 CHAPTER 2. INVESTIGATING THE EFFECT OF ACIDIFICATION AND FREEZE/THAW CYCLES ON ANTHOCYANIN METABOLITE STABILITY IN CLINICAL SAMPLES.	33
2.1. Introduction.....	33
2.2. Methods	34
2.3. Results	39
2.4. Discussion.....	49
2.5. Conclusion	52
 CHAPTER 3. DEVELOPMENT OF HPLC-ESI-MS/MS METHODS FOR QUANTIFYING ANTHOCYANIN METABOLITES IN HUMAN SERUM AND URINE.	53
3.1. Introduction.....	53
3.2. Methods	54
3.3. Results	62
3.4. Discussion.....	71
3.5. Conclusion	75
 CHAPTER 4. VALIDATION OF HPLC-ESI-MS/MS METHODS FOR QUANTIFYING ANTHOCYANIN METABOLITES IN HUMAN SERUM AND URINE.	77
4.1. Introduction.....	77
4.2. Methods	78
4.3. Results	89
4.4. Discussion.....	98
4.5. Conclusion	103

CHAPTER 5. ESTABLISHING ROBUST METABOLIC BIOMARKERS OF ANTHOCYANIN CONSUMPTION.....	104
5.1. Introduction.....	104
5.2. Methods	106
5.3. Results	114
5.4. Discussion	125
5.5. Conclusion	128
CHAPTER 6. THE EFFECTS OF DIFFERENT METABOLITE PROFILES ON SVCAM-1 AND IL-6 EXPRESSION IN TNF-A AND CD40L-STIMULATED HUVEC.....	129
6.1. Introduction.....	129
6.2. Methods	131
6.3. Results	135
6.4. Discussion	145
6.5. Conclusion	153
CHAPTER 7. GENERAL DISCUSSION AND FUTURE PERSPECTIVES	154
7.1. General Discussion	154
7.2. Future Perspectives	161
GLOSSARY	167
BIBLIOGRAPHY	171

List of Tables

Table 1.1 Polyphenol subgroups, common structures, and main dietary sources.	14
Table 1.2 Flavonoid subgroups, common structures and main dietary sources.....	15
Table 1.3 Anthocyanin content of common dietary sources.	19
Table 1.4 Pharmacokinetic data from human anthocyanin bioavailability studies.	21
Table 2.1 sMRM schedule used to analyse the extracted serum samples on the AB SCIEX 3200 QTRAP® instrument.	39
Table 2.2 Statistical significance of the effect of acidification on anthocyanin metabolite stability in serum when stored at -80°C for 240 hours.	40
Table 2.3 Statistical significance of the effect of five freeze/thaw cycles on anthocyanin metabolite stability in serum.....	45
Table 2.4 Variation in scopoletin internal standard peak areas using the HPLC-ESI-MS/MS method.	51
Table 3.1 MRM parameters used to analyse samples on the AB SCIEX 3200 QTRAP® instrument.	61
Table 3.2 Comparison of initial 32 minute HPLC-ESI-MS/MS method and optimised 15 minute HPLC-ESI-MS/MS method parameters.	75
Table 4.1 Metabolite composition of urine mixed standard.....	82
Table 4.2 sMRM schedule used to analyse serum samples on the AB SCIEX 3200 QTRAP® instrument.	84
Table 4.3 sMRM schedule used to analyse urine samples on the AB SCIEX 3200 QTRAP® instrument.	86
Table 4.4 Validation criteria and acceptable limits.	88
Table 4.5 Validation of specificity, limit of detection, and linearity of a 32 minute HPLC-ESI-MS/MS method for quantifying cyanidin-3-glucoside, its phenolic metabolites, and two internal standards in serum.....	90
Table 4.6 Validation of accuracy and precision of a 32 minute HPLC-ESI-MS/MS method for quantifying cyanidin-3-glucoside, its phenolic metabolites, and two internal standards in serum.....	91
Table 4.7 Validation of specificity, limit of detection, linearity, and accuracy of a 15 minute HPLC-ESI-MS/MS method for quantifying cyanidin-3-glucoside, its phenolic metabolites, and two internal standards in urine.	93

Table 4.8 Validation of precision and extraction efficiency of a 15 minute HPLC-ESI-MS/MS method for quantifying cyanidin-3-glucoside, its phenolic metabolites, and two internal standards in urine.....	96
Table 5.1 sMRM schedule used to analyse the extracted serum samples on the AB SCIEX 3200 QTRAP® instrument.....	110
Table 5.2 sMRM schedule used to analyse the extracted urine samples on the AB SCIEX 3200 QTRAP® instrument.....	112
Table 5.3 Anthocyanin metabolite concentrations from ¹³ C ₅ -cyanidin-3-glucoside intervention compared to ¹² C background levels in serum samples.	114
Table 5.4 Anthocyanin metabolite concentrations from ¹³ C ₅ -cyanidin-3-glucoside intervention compared to ¹² C background levels in urine samples.	118
Table 5.5 QC sample response obtained in the present study compared to expected response based on previous QC samples.....	127
Table 6.1 Composition of treatments P-1, P-6, and P-24.	133
Table 6.2 Composition of treatments.....	146
Table 6.3 Structural composition of treatments.	148
Table 6.4 Structural information on metabolites included in treatments.	149

List of Figures

Figure 1.1 Common structures of anthocyanidins.	17
Figure 1.2 pH-dependent structures of anthocyanins.	18
Figure 1.3 Potential mechanisms for anthocyanin metabolism and absorption.	23
Figure 1.4 Progression of atherosclerosis.	27
Figure 1.5 Selectins and adhesion molecules involved in the initial stages of atherosclerosis.	28
Figure 1.6 Activation of MAPK and NF- κ B signalling pathways via TNF- α and CD40L stimulation.....	30
Figure 2.1 Compounds included in the mixed standard; cyanidin-3-glucoside and 17 of its phenolic metabolites as reported following consumption of ^{13}C -labelled cyanidin-3- glucoside.....	36
Figure 2.2 Experimental design of anthocyanin metabolite stability study showing acidified vs non-acidified serum samples and freeze/thaw vs control serum samples.....	37
Figure 2.3 Metabolite concentration as a percentage of initial concentration in acidified and non-acidified serum samples across 240 hours of storage at -80°C	42
Figure 2.4 Metabolite concentration as a percentage of initial concentration in control and freeze/thaw serum samples across five freeze/thaw cycles.....	46
Figure 2.5 Scopoletin internal standard peak area as a percentage of initial peak area during the present study.	51
Figure 3.1 Compounds included in the mixed standard; cyanidin-3-glucoside and 17 of its phenolic metabolites as reported following consumption of ^{13}C -labelled cyanidin-3-glucoside	56
Figure 3.2 Experimental design of extraction method development protocol showing the differences between the various extraction methods tested. Current method is solid-phase extraction (4x concentrated) as previously reported.....	59
Figure 3.3 Signal-to-noise ratio observed using ammonium-buffered mobile phases compared to the current 0.1% formic acid mobile phase.....	62
Figure 3.4 Peak width observed using ammonium-buffered mobile phases compared to the current 0.1% formic acid mobile phase.....	63
Figure 3.5 Limit of detection observed using alternative extraction methods compared to the current solid-phase extraction (4x concentrated) method.	64

Figure 3.6 Chromatography of initial 32 minute method using column diameter of 4.6 mm (A) and following optimisation of column diameter to 2.1 mm (B) during development of an HPLC-ESI-MS/MS method with reduced run time for the quantification of cyanidin-3-glucoside and its phenolic metabolites.	65
Figure 3.7 Chromatography using column temperature of 37°C (A) and following optimisation of column temperature to 40°C (B) during development of an HPLC-ESI-MS/MS method with reduced run time for the quantification of cyanidin-3-glucoside and its phenolic metabolites.	66
Figure 3.8 Chromatography using mobile phase flow rate of 1.5 mL min ⁻¹ / 1.0 mL min ⁻¹ with 4.6 mm diameter column (A) and following optimisation of mobile phase flow rate to 0.6 mL min ⁻¹ with 2.1 mm diameter column (B) during development of an HPLC-ESI-MS/MS method with reduced run time for the quantification of cyanidin-3-glucoside and its phenolic metabolites.	67
Figure 3.9 Chromatography using gradient profile of 32 minutes (1% B at 0 min, 7.5% B at 7 min, 7.6% B at 14 min, 10% B at 17 min, 12% B at 18.5 min, 12.5% B at 20 min, 30% B at 24 min, 90% B at 25 to 28 min, 1% B at 29 to 32 min) (A) and following optimisation of gradient profile to 15 minutes (1% B at 0 min, 7.5% B at 7 min, 7.6% B at 9 min, 90% B at 9.5 to 11.5 min, 1% B at 12 to 15 min) (B) during development of an HPLC-ESI-MS/MS method with reduced run time for the quantification of cyanidin-3-glucoside and its phenolic metabolites.	68
Figure 3.10 Chromatography using mobile phase formic acid concentration of 1% (A) and optimised mobile phase formic acid concentration of 0.1% (B) during development of an HPLC-ESI-MS/MS method with reduced run time for the quantification of cyanidin-3-glucoside and its phenolic metabolites.	69
Figure 3.11 Chromatography using column length of 100 mm (A) and following optimisation of column length to 50 mm (B) during development of an HPLC-ESI-MS/MS method with reduced run time for the quantification of cyanidin-3-glucoside and its phenolic metabolites.	70
Figure 3.12 Chromatography using injection volume of 1 µL (A) and final optimised 15 minute method with injection volume of 5 µL (B) following development of an HPLC-ESI-MS/MS method with reduced run time for the quantification of cyanidin-3-glucoside and its phenolic metabolites.	71
Figure 3.13 Comparison of (A) initial 32 minute HPLC-ESI-MS/MS method and (B) optimised 15 minute HPLC-ESI-MS/MS method chromatography	76

Figure 4.1 Compounds included in the mixed standard; cyanidin-3-glucoside and 17 of its phenolic metabolites as reported following consumption of ^{13}C -labelled cyanidin-3-glucoside.....	81
Figure 4.2 sMRM chromatograms showing the separation of cyanidin-3-glucoside and its phenolic metabolites in serum using optimised negative (A) and positive (B) 32 minute HPLC-ESI-MS/MS methods.....	85
Figure 4.3 sMRM chromatograms showing the separation of cyanidin-3-glucoside and its phenolic metabolites in urine using optimised negative (A) and positive (B) 15 minute HPLC-ESI-MS/MS methods.....	87
Figure 5.1 Background adjusted concentrations of cyanidin-3-glucoside and its serum metabolites detected in eight participants following a $^{13}\text{C}_5$ -cyanidin-3-glucoside intervention.	115
Figure 5.2 ^{13}C -labelled serum metabolite concentration compared to ^{12}C background concentration throughout 48 hours following $^{13}\text{C}_5$ -cyanidin-3-glucoside intervention.....	116
Figure 5.3 Background adjusted concentrations of urinary B-ring-derived metabolites detected in eight participants following a $^{13}\text{C}_5$ -cyanidin-3-glucoside intervention.	121
Figure 5.4 Background adjusted concentrations of urinary A-ring-derived metabolites detected in eight participants following a $^{13}\text{C}_5$ -cyanidin-3-glucoside intervention.	122
Figure 5.5 ^{13}C -labelled B-ring-derived urinary metabolite concentration compared to ^{12}C background concentration throughout 48 hours following $^{13}\text{C}_5$ -cyanidin-3-glucoside intervention.....	123
Figure 5.6 ^{13}C -labelled A-ring-derived urinary metabolite concentration compared to ^{12}C background concentration throughout 48 hours following $^{13}\text{C}_5$ -cyanidin-3-glucoside intervention.....	124
Figure 6.1 Pharmacokinetic data from a ^{13}C -labelled cyanidin-3-glucoside feeding trial showing total ^{13}C metabolite concentration in serum across 48 hours in eight participants.	131
Figure 6.2 Cytotoxicity of treatment compounds in HUVEC as measured by WST-1 assay following 24 hour incubation.	136
Figure 6.3 sVCAM-1 production in TNF- α -stimulated HUVEC.....	137
Figure 6.4 sVCAM-1 production in TNF- α -stimulated HUVEC.....	137
Figure 6.5 sVCAM-1 production following treatment with anthocyanin metabolites in TNF- α -stimulated HUVEC.	138

Figure 6.6 sVCAM-1 production following treatment with anthocyanin metabolites in TNF- α -stimulated HUVEC.	139
Figure 6.7 IL-6 production in TNF- α -stimulated HUVEC.	139
Figure 6.8 IL-6 production in TNF- α -stimulated HUVEC.	140
Figure 6.9 IL-6 production following treatment with anthocyanin metabolites in TNF- α -stimulated HUVEC.	140
Figure 6.10 IL-6 production following treatment with anthocyanin metabolites in TNF- α -stimulated HUVEC.	141
Figure 6.11 sVCAM-1 production in CD40L-stimulated HUVEC.	141
Figure 6.12 sVCAM-1 production following treatment with anthocyanin metabolites in CD40L-stimulated HUVEC.	142
Figure 6.13 sVCAM-1 production following treatment with anthocyanin metabolites in CD40L-stimulated HUVEC.	143
Figure 6.14 IL-6 production in CD40L-stimulated HUVEC.	143
Figure 6.15 IL-6 production following treatment with anthocyanin metabolites in CD40L-stimulated HUVEC.	144
Figure 6.16 IL-6 production following treatment with anthocyanin metabolites in CD40L-stimulated HUVEC.	144
Figure 6.17 Activation of MAPK and NF- κ B signalling pathways via TNF- α and CD40L stimulation.	151
Figure 7.1 Experimental scheme for the assessment of stability, quantification methods, biomarker utility, and bioactivity of anthocyanin metabolites.	155

Acknowledgements

In many respects, writing a thesis must be similar to the process of raising a child: sleepless nights, loneliness, self-doubt, endless worry, but, ultimately, hugely rewarding. It is said that it takes a village to raise a child and the same can be said for writing a thesis. As such, there are many people to which I would like to express my gratitude.

Firstly, I would like to thank my primary supervisor, Colin Kay. Thank you for all your help, advice, and encouragement. Thank you for your immense patience and for believing in me when I did not. You taught me the value of asking, “So what?” and improved my writing beyond all recognition. You made me a better scientist.

I would also like to thank Maria O’Connell, my secondary supervisor, for your guidance and support. Thank you to all past Kay Lab members for your input, especially Rachel de Ferrars for helping me to understand the world of mass spectrometry. Thank you to Emily Warner and Jessica di Gesso for your help with cell culture and for inspiring me to work harder just to keep up with you both. More importantly, thank you for your friendship.

Thank you to the Faculty of Medicine and Health Sciences at the University of East Anglia for the funding and facilities that made this work possible. Thank you to the Department of Nutrition for your support, especially Vera van der Velpen for your help with statistics.

Increased coffee consumption and unusual hobbies must be two of the biggest clichés associated with postgraduate study. After ticking off the first of these within weeks of starting, it wasn’t until my third year that I fulfilled the second by joining the UEA Blue Sox Baseball and Softball Club and discovering a sporting passion that will last beyond my time at UEA with the formation of Norwich Iceni Baseball Club. Thank you to everyone involved with both clubs for providing a welcome distraction when times were tough.

Thank you to all my friends for your encouragement and for not forgetting about me when I disappeared into the lab. I look forward to finding out what everyone has been up to for the last few years. On behalf of myself and my wife, I would like to particularly thank our friends in Norwich: Michael Twigg, Colin Lockwood, and Joanna & Jesse Roberts. Your friendship has been indispensable in getting us both through an often difficult time. We look forward to many more happy times over good food, cheap wine, and Settlers of Catan.

Thank you to my family, especially my parents, Bob Smith and Rosaline Smith, for your support and for providing me with the work ethic, curiosity, and determination that got me to this point. Thank you to Monty and Mabel for always hanging out with me at the end of a long day.

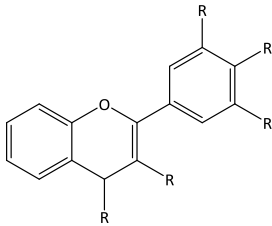
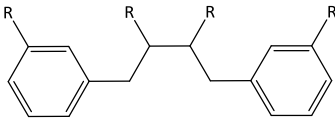
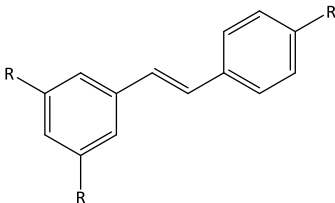
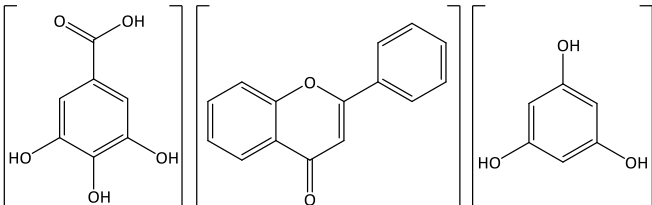
Finally, and most importantly, I would like to thank my incredible wife, Jenny Lane-Smith. Jen, I know that I haven't been the easiest person to live with for the last few years but you have been the constant source of love, encouragement, and belief that has given me the confidence to continue. Thank you for the many sacrifices that you accepted to allow me to follow my ambition. Thank you for taking responsibility for the vast swathes of our life that I have sadly neglected. Thank you for picking me up and putting me back together every time I needed it. The fact that I got this far is more your achievement than mine. I look forward to moving on to the next stage of our lives together and reading these words in the future, laughing about how important all this seemed at the time.

Chapter 1. Anthocyanins: A Review of Current Literature

1.1. Introduction

Polyphenols are a group of phytochemicals that can be divided into four main subgroups: flavonoids, lignans, stilbenes, and tannins (**Table 1.1**). These groups retain a basic multiple aromatic ring structure differentiated by various functional groups and are found in many dietary sources including fruits, vegetables, tea, and chocolate (Manach *et al.* 2004, Crozier *et al.* 2009). Interest in polyphenols as bioactive dietary components grew in the early 1990s as epidemiological studies reported a link between increased polyphenol intake and reduced mortality (Hertog *et al.* 1993, Hertog *et al.* 1994) with initial theories to explain these observations focusing on the antioxidant properties of polyphenols (Rice-Evans 1995, Hollman *et al.* 1996). Whilst the consensus has moved away from free-radical scavenging as a mechanism for their bioactivity (Scalbert *et al.* 2005), polyphenol-rich diets have continued to be linked to a range of beneficial health effects relating to cognition (Lamport *et al.* 2012, Rabassa *et al.* 2015), obesity (Wu *et al.* 2003, Hughes *et al.* 2008), cancer prevention (Hui *et al.* 2013, Zamora-Ros *et al.* 2013), and cardiovascular disease (Tresserra-Rimbau *et al.* 2014, Rangel-Huerta *et al.* 2015).

Table 1.1 Polyphenol subgroups, common structures, and main dietary sources.

Subgroup	Structure	Main dietary sources
Flavonoids		Fruit and vegetables
Lignans		Flax seed, sesame seed, cereals
Stilbenes		Almonds, grapes
Tannins ^a		Cocoa, black and green tea, berries, walnuts, wine

R, functional group (-H, -OH, -OCH₃). ^aTannins exist as polymers consisting of gallic acid, flavone or phloroglucinaldehyde monomers. Adapted from (Scalbert and Williamson 2000, Neveu *et al.* 2010).

With over 6,000 compounds identified to date across a wide range of fruits and vegetables (Harborne and Williams 2000), flavonoids are the most commonly consumed polyphenol group and have been widely studied in relation to their bioavailability and bioactivity (Kay *et al.* 2012, Thilakarathna and Rupasinghe 2013, Rodriguez-Mateos *et al.* 2014). Flavonoid compounds share the same phenolic structure and can be further divided into six main subgroups based on the functional groups attached to the heterocyclic C-ring: anthocyanidins, flavan-3-ols, flavanones, flavones, flavonols, and isoflavonoids (**Table 1.2**).

Table 1.2 Flavonoid subgroups, common structures and main dietary sources.

Subgroup	Structure	Main dietary sources
Anthocyanidins		Berries, blackcurrants, black grapes, red cabbage
Flavan-3-ols		Cocoa, black and green tea, apples
Flavanones		Oranges, grapefruit, lemons
Flavones		Globe artichoke, celery, oregano, sage, thyme
Flavonols		Black and green tea, onions, cumin
Isoflavonoids		Soybean

R, functional group (-H, -OH, -OCH₃). Adapted from (Crozier *et al.* 2009, Neveu *et al.* 2010).

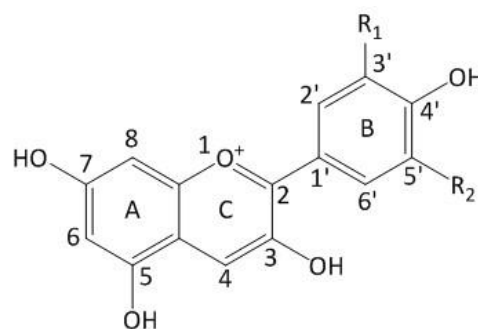
Anthocyanins (from Greek, *Anthos* meaning flower and *kyanos* meaning blue) are the more stable, glycosylated form of anthocyanidins found in plants (Castañeda-Ovando *et al.* 2009). One of three main plant pigment groups alongside betalains and carotenoids, anthocyanins are water-soluble pigments responsible for the red/blue colour of the flowers, leaves and fruit of many plants including dietary sources such as berries, grapes and red cabbage (Crozier *et al.* 2009, Del Rio *et al.* 2010a). Anthocyanin consumption has been linked to a range of health benefits including reduced rates of obesity (Prior *et al.* 2008, Wu *et al.* 2013), improved cognition (Kent *et al.* 2015, Whyte *et al.* 2015), reduced risk of cancer (Peiffer *et al.* 2014, Charepalli *et al.* 2015), and cardiovascular disease (Cassidy *et al.* 2013, Wang *et al.* 2014a). However, due to the reported low bioavailability of anthocyanins (Scalbert and Williamson 2000, Kay *et al.* 2005, Manach *et al.* 2005), recent studies have suggested that the phenolic metabolites of anthocyanins may be responsible for the observed bioactivity (di Gesso *et al.* 2015, Warner *et al.* 2016). The present study focuses on the stability of anthocyanin metabolites in biological samples, their utility as biomarkers of anthocyanin intake and their effect on early-stage biomarkers of cardiovascular disease.

1.2. Chemistry

The basic anthocyanin structure is based on the 2-phenylbenzopyrylium (flavylium) cation with substitutions in the glycosylation, acylation, hydroxylation, and methoxylation differentiating between the 600+ anthocyanin compounds identified to date (Wallace 2011). The aglycones, known as anthocyanidins, contain conjugated double bonds that show absorption maxima within the visible spectrum between 465 – 550 nm (resulting in the red/blue colour visible to the human eye) and within the UV spectrum between 270 – 280 nm (Hong and Wrolstad 1990). 23 anthocyanidins have been identified to date with six predominant anthocyanidins (cyanidin, delphinidin, pelargonidin, peonidin, petunidin, and malvidin), differing in the number and position of hydroxyl and methoxy groups on the cation B-ring, accounting for over 90% of identified anthocyanins (**Figure 1.1**) (Castañeda-Ovando *et al.* 2009, Wallace 2011).

Figure 1.1 Common structures of anthocyanidins.

Anthocyanidin	R ₁	R ₂	Distribution
Cyanidin	-OH	-H	50%
Delphinidin	-OH	-OH	12%
Pelargonidin	-H	-H	12%
Peonidin	-OCH ₃	-H	12%
Malvidin	-OCH ₃	-OCH ₃	7%
Petunidin	-OCH ₃	-OH	7%



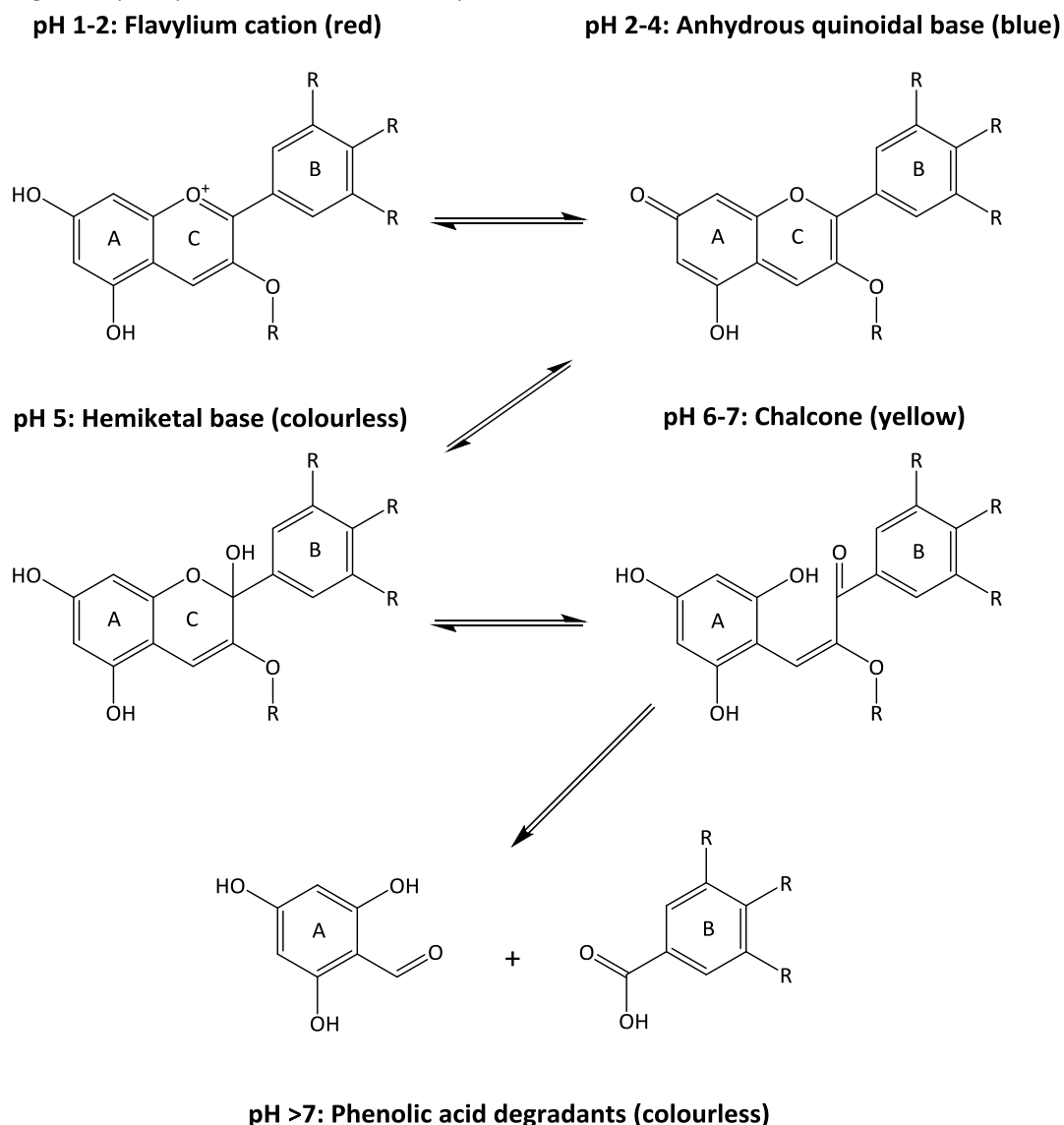
R₁, R₂, functional groups (-H, -OH, -OCH₃). Adapted from (Kong *et al.* 2003).

Glycosylation of anthocyanidins to form anthocyanins is essential in plants to improve stability and solubility of the pigments in water (Stintzing and Carle 2004). Glycosylation typically occurs at the 3-hydroxyl or 5-hydroxyl positions but can also occur at the 3', 4', 5' or 7-hydroxyl positions (Fossen *et al.* 2003, Crozier *et al.* 2009). Anthocyanins exist most commonly as monoglycosides containing glucose, galactose, rhamnose, arabinose, or xylose moieties but di- and triglycosides containing rutinose, sambubiose and sophorose have also been identified (Wu *et al.* 2004, Del Rio *et al.* 2010a). Cyanidin-3-glucoside is the most commonly consumed anthocyanin in the western diet (Wu *et al.* 2006).

Anthocyanins can also be acylated via ester bonding of aromatic phenolic acids and aliphatic dicarboxylic acids to the glycoside molecule. Common phenolic acids acylated to anthocyanins include hydroxycinnamic acids such as coumaric acid, and hydroxybenzoic acids such as gallic acid (Harborne 1958, Sadilova *et al.* 2006).

Whilst more stable than the anthocyanidin aglycones, anthocyanins are still relatively unstable compounds that are sensitive to a range of environmental conditions including temperature, presence of enzymes, proteins and metallic ions, solvents, light and pH (Rein 2005, Castañeda-Ovando *et al.* 2009). Anthocyanins are particularly sensitive to changes in pH; most stable in acidic conditions and susceptible to degradation into their A- and B-ring derivatives at neutral pH (**Figure 1.2**).

Figure 1.2 pH-dependent structures of anthocyanins.



R, functional group (-H, -OH, -OCH₃, glycoside). Adapted from (McGhie and Walton 2007, Castañeda-Ovando *et al.* 2009).

1.3. Role in Nature

Anthocyanins are produced by a wide range of plants and stored in the vacuoles where they act as pigments amongst other roles (Gould 2004). Anthocyanin synthesis occurs within the cytosol, beginning with coumaroyl-CoA and malonyl-CoA precursors, and involves enzymes from various families including glucosyltransferases, cytochromes p450, and 2-oxoglutarate-dependent dioxygenases (Tanaka *et al.* 2008). The most visible role of anthocyanins in plants is to provide colour to leaves, petals, and fruit to attract animals for pollination and seed dispersal (Gould 2004, Stintzing and Carle 2004). A number of additional functions for anthocyanins within plants have been suggested including absorption of high-intensity light to protect chloroplasts from photoinhibition (Pietrini *et al.* 2002), protection of plant tissues

from photooxidative damage during nutrient retrieval following autumn senescence (Feild *et al.* 2001), and osmotic adjustment of cells to protect tissues during drought and freezing temperatures (Chalker-Scott 1999).

1.4. Dietary Consumption

Anthocyanins are present in many commonly consumed fruits and vegetables that display red, blue or purple colouring with the main dietary sources of anthocyanins being grapes and berries (Wu *et al.* 2006). Even within particular fruit or vegetable species, anthocyanin content can vary considerably depending on a range of factors including cultivar, growing conditions, maturity, processing, and storage conditions (Anttonen and Karjalainen 2005, Amarowicz *et al.* 2009, Wang *et al.* 2009) but typical anthocyanin concentrations can range between 4 mg/100 g fresh weight (FW) in red lettuce and 1317 mg/100 g FW in black elderberry (**Table 1.3**).

Table 1.3 Anthocyanin content of common dietary sources.

Dietary source	Mean content (mg/100 g FW)						Total
	Cy	Dp	Pg	Pn	Mv	Pt	
Black elderberry	1315	-	2	-	-	-	1317
Blackcurrant	187	392	2	1	-	10	592
Red cabbage	210	-	-	-	-	-	210
Blackberry	173	-	-	-	-	-	173
Highbush blueberry	10	46	-	2	48	29	135
Aubergine	-	86	-	-	-	-	86
Strawberry	5	-	68	-	-	-	73
Black grape	1	3	-	6	59	3	72
Red raspberry	65	-	6	-	1	-	72
American cranberry	14	-	-	36	-	-	50
Red onion	3	7	-	-	-	-	10
Red lettuce	4	-	-	-	-	-	4

Mean content represents combined total for all glycosylated forms of anthocyanidins. Cy, cyanidin; Dp, delphinidin; Pg, pelargonidin; Pn, peonidin; Mv, malvidin; Pt, petunidin. Adapted from (Neveu *et al.* 2010, Bhagwat *et al.* 2011).

Estimated intakes of anthocyanins within global diets range between 3 to 65 mg/day [3 mg/day, USA (Chun *et al.* 2007); 28 mg/day, China (Li *et al.* 2013); 57 mg/day, France (Pérez-Jiménez *et al.* 2011); 19 – 65 mg/day, Europe (Zamora-Ros *et al.* 2011)] with intakes of over 500 mg of anthocyanins achievable within a single serving of anthocyanin-rich foods (Table 1.3). The accuracy of anthocyanin intake estimates is dependent on the quality of data obtained from dietary assessment methods, such as food frequency questionnaires (FFQs),

and the suitability of data contained within anthocyanin content databases, such as Phenol-Explorer (Neveu *et al.* 2010) or USDA Database for the Flavonoid Content of Selected Foods (Bhagwat *et al.* 2011). Alternatively, dietary intake can be monitored via the detection of characteristic metabolites within the body known as biomarkers of intake (Hedrick *et al.* 2012) but while a small number of biomarkers for consumption of anthocyanin-rich foods have been suggested (van Dorsten *et al.* 2010, Urpi-Sarda *et al.* 2015), these have yet to be accepted as robust metabolic biomarkers of anthocyanin intake.

1.5. Bioavailability

Studies investigating the bioavailability of flavonoids have reported anthocyanins to be amongst the least bioavailable of the flavonoid sub-classes with plasma concentrations of anthocyanins in the nanomolar range compared to micromolar concentrations achieved by more bioavailable flavonoid groups such as flavanones or isoflavonoids (Manach *et al.* 2005). Plasma/serum concentrations of anthocyanins have been reported to peak around 2 to 200 nM at 0.5 to 4 hours following consumption, with typically less than 1% of the intake recovered in the urine (**Table 1.4**). The low concentrations of anthocyanins observed following consumption, combined with the sensitivity of the anthocyanin structure to changes in pH and temperature, prompted suggestions that anthocyanins may be subject to rapid degradation to their phenolic acid derivatives within the body. The degradation products could then be further metabolised, resulting in considerable underestimation of anthocyanin bioavailability until the contribution of these phenolic metabolites was quantified (Kay 2006, Kay *et al.* 2009). This theory is supported by recent studies that have reported the detection of phenolic acid metabolites within plasma/serum and urine following consumption of anthocyanins (Rodriguez-Mateos *et al.* 2013, de Ferrars *et al.* 2014b, Pimpão *et al.* 2015). Importantly, a recent human feeding trial was able to demonstrate a direct link between the parent anthocyanins and the phenolic metabolites via the use of stable isotope-labelled cyanidin-3-glucoside (Czank *et al.* 2013). This study used five ¹³C labels within the aglycone structure, three on the A-ring and two on the B-ring, to trace the lineage of the phenolic metabolites identified in biological samples through the A-ring and B-ring degradants, phloroglucinaldehyde and protocatechuic acid respectively, back to the parent ¹³C₅-C3G compound. However, despite a comprehensive sampling regime involving serum, urine, faeces, and breath samples being collected, only 43.9% of the ingested ¹³C label was recovered leaving the fate of over half of the labelled compound unknown, possibly remaining in the lower intestine.

Table 1.4 Pharmacokinetic data from human anthocyanin bioavailability studies.

Dietary source	Anthocyanin intake (mg)	Study duration (h)	Plasma/serum C_{max} (nM)	Plasma/serum T_{max} (h)	Plasma/serum $T_{1/2}$ (h)	Urinary recovery (%)	Reference
Red cabbage	648	24	86.39	2.0	2.73	0.09	(Wiczowski <i>et al.</i> 2016)
Fermented red cabbage	554	24	64.02	2.0	3.02	0.07	(Wiczowski <i>et al.</i> 2016)
Grape and blueberry juice	277	24	13.19	1.2	-	-	(Kuntz <i>et al.</i> 2015b)
Grape and blueberry smoothie	325	24	9.86	1.3	-	-	(Kuntz <i>et al.</i> 2015b)
Blueberry juice	216	24	-	-	-	0.0752	(Kalt <i>et al.</i> 2014)
Cranberry juice	95	3	4.64	3	-	0.79	(Milbury <i>et al.</i> 2010)
Bilberry and lingonberry purée	650	48	138	1.5	-	-	(Nurmi <i>et al.</i> 2009)
Blood orange juice	71	24	1.9	0.5	-	1.2	(Vitaglione <i>et al.</i> 2007)
Cranberry juice	651	24	-	-	-	5.00	(Ohnishi <i>et al.</i> 2006)
Chokeberry extract	721	24	96.1	2.8	1.5	0.15	(Kay <i>et al.</i> 2005)
Blackberry	431	24	-	-	-	0.16	(Felgines <i>et al.</i> 2005)
Hibiscus extract	147	7	7.6	1.5	2.6	0.018	(Frank <i>et al.</i> 2005)
Elderberry juice	3570	5	-	-	-	0.053	(Bitsch <i>et al.</i> 2004b)
Blackcurrant juice	145	7	-	-	1.7	0.04	(Bitsch <i>et al.</i> 2004a)
Elderberry extract	147	7	-	-	1.7	0.37	(Bitsch <i>et al.</i> 2004a)
Chokeberry extract	1300	24	592	-	-	-	(Kay <i>et al.</i> 2004)
Red wine	280	7	222.7	0.5	1.83	0.23	(Frank <i>et al.</i> 2003)
Red grape juice	283	7	95.5	1.5	1.52	0.18	(Frank <i>et al.</i> 2003)
Blackcurrant juice	345	7	-	-	-	0.029	(McGhie <i>et al.</i> 2003)
Boysenberry extract	189	7	-	-	-	0.064	(McGhie <i>et al.</i> 2003)
Blueberry extract	439	7	-	-	-	0.020	(McGhie <i>et al.</i> 2003)
Strawberry	77	24	-	-	-	1.9	(Felgines <i>et al.</i> 2003)
Blackcurrant juice	1239	4	-	0.7	-	0.07	(Nielsen <i>et al.</i> 2003)
Blackcurrant juice	716	4	-	0.7	-	0.05	(Nielsen <i>et al.</i> 2003)
Elderberry juice	1900	6	-	-	-	0.03	(Mülleider <i>et al.</i> 2002)
Blueberry extract	1200	4	29.2	4.0	-	0.003	(Mazza <i>et al.</i> 2002)
Blueberry	690	6	-	-	-	0.004	(Wu <i>et al.</i> 2002)
Red wine	68	6	1.47	0.3	-	0.03	(Bub <i>et al.</i> 2001)
Dealcoholised red wine	56	6	1.7	1.5	-	0.03	(Bub <i>et al.</i> 2001)
Red grape juice	117	6	2.8	3.0	-	0.03	(Bub <i>et al.</i> 2001)

C_{max} , maximal concentration; T_{max} , time of maximal concentration; $T_{1/2}$, half-life of elimination. Adapted from (Fernandes *et al.* 2015).

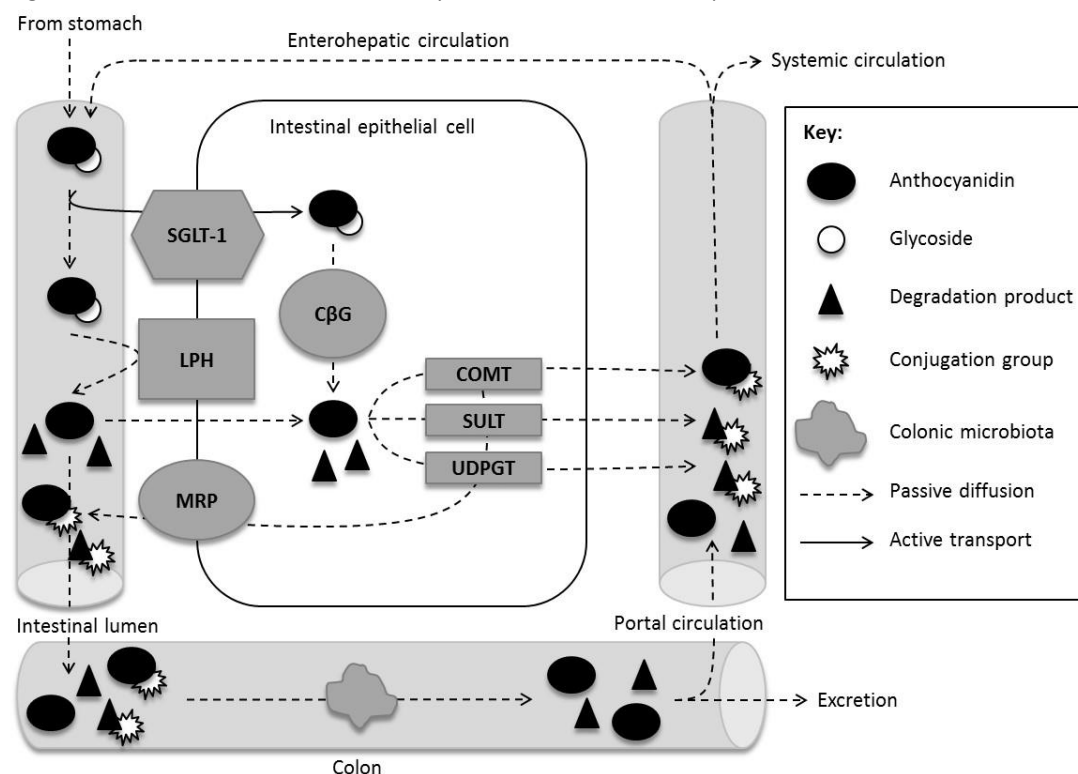
1.6. Metabolism

The low bioavailability of anthocyanins was previously believed to be a result of poor absorption within the body. However, whilst the absorption of anthocyanins is not yet fully understood, recent studies have demonstrated that the low concentrations observed within the circulation following consumption is likely due to the extensive degradation, metabolism and catabolism of anthocyanins within the gastrointestinal tract and subsequent phase I and II metabolism within the liver and kidneys (Kay 2006, Fang 2014, Fernandes *et al.* 2015).

The rapid appearance of anthocyanins within the blood following consumption (Milbury *et al.* 2002, Mullen *et al.* 2008) has led to suggestions that the first site for anthocyanin absorption in the gastrointestinal tract is the stomach. However, despite a limited number of studies reporting evidence claiming to support gastric absorption, this is not believed to be a major route due to the size and polarity of anthocyanins. One possible mechanism that has been suggested is via an anion membrane carrier protein expressed by epithelial cells in the stomach called bilitranslocase. Previous work has observed interaction between anthocyanins and bilitranslocase (Passamonti *et al.* 2002) but transport of anthocyanins via bilitranslocase has yet to be demonstrated and is thought to be unlikely due to the predominance of anthocyanins in the cation form in the acidic environment present within the stomach. Recent studies have reported transport of anthocyanins by MKN-28 differentiated adenocarcinoma stomach epithelial cells (Fernandes *et al.* 2012), possibly via the GLUT1 and GLUT3 glucose transporters (Oliveira *et al.* 2015) but this has yet to be observed in other cell models or *in vivo*. A small number of studies have reported gastric absorption of anthocyanins in rats (Talavéra *et al.* 2003, Passamonti *et al.* 2005, Vanzo *et al.* 2008) but due to differences in absorption, distribution, metabolism, and excretion (ADME) mechanisms between rats and humans, and the lack of supporting studies demonstrating *in vivo* gastric absorption in humans, further work is required to establish the extent of the stomach's role in the absorption of anthocyanins.

One of the main areas of anthocyanin absorption is thought to be in the lumen of the small intestine and this absorption can be broken down into two routes (**Figure 1.3**). The first potential route involves direct absorption of the glycosylated anthocyanin via sodium-dependent glucose transporter-1 (SGLT-1) which is present in the membrane of intestinal epithelium cells. Studies investigating absorption of the structurally similar quercetin-4'-glucoside, have demonstrated that the intact glucoside can be detected in intestinal epithelium cells following incubation and that this absorption is reduced in the presence of phloridzin, an SGLT-1 inhibitor (Walgren *et al.* 2000, Day *et al.* 2003).

Figure 1.3 Potential mechanisms for anthocyanin metabolism and absorption.



CβG, cytosolic β-glucosidase; COMT, catechol-O-methyltransferase; LPH, Lactase phloridzin hydrolase; MRP, multidrug resistance protein; SGLT-1, Sodium-dependent glucose transporter-1; SULT, sulfotransferase; UDPGT, uridine 5'-diphospho-glucuronosyltransferase. Adapted from (Kay 2006).

A recent study has reported decreased absorption of cyanidin-3-glucoside by human intestinal epithelial (Caco-2) cells following inhibition of SGLT-1 and glucose transporter 2 (GLUT2) suggesting that there may be a range of glucose transporters involved in the intestinal absorption of anthocyanins (Zou *et al.* 2014). Once inside the cell, the flavonoid glycoside is able to diffuse across the basolateral membrane and enter the portal circulation. Glycosides inside the cells are hydrolysed by cytosolic β-glucosidase (CβG) to produce the flavonoid aglycone (**Figure 1.3**) (Day *et al.* 1998, Lambert *et al.* 1999). These metabolised compounds are then able to enter the hepatic portal circulation.

The second possible route of absorption in the small intestine involves deglycosylation of the hydrophilic anthocyanin molecule by lactase phloridzin hydrolase (LPH) to produce the anthocyanidin aglycone molecule (**Figure 1.3**). Following deglycosylation, the more lipophilic, less polar aglycone is able to passively diffuse across the epithelial cell membrane and into the cytosol. It is thought that anthocyanins may be a substrate for LPH as other structurally similar flavonoid glycosides have been shown to be hydrolysed by LPH (Day *et al.* 2000, Sesink *et al.* 2003) and it has been demonstrated that the uptake of quercetin glycosides is reduced in the presence of LPH inhibitors (Day *et al.* 2003). However, possibly

due to the difficulties caused by the instability of anthocyanins at neutral pH, there has been limited investigation of the enzymatic deglycosylation of anthocyanins and hydrolysis of anthocyanins by LPH or any other β -glucosidase has yet to be demonstrated either *in vitro* or *in vivo*. Some studies have suggested that anthocyanins may not be hydrolysed by LPH (Németh *et al.* 2003) and could instead act as substrates for α -glucosidases (Williamson 2013). Further research is required to confirm the mechanisms involved in intestinal deglycosylation of anthocyanins.

Inside the epithelial cytosol the aglycone is subject to phase II metabolism reactions with enzymes such as catechol-*O*-methyltransferase (COMT), sulfotransferase (SULT) and uridine 5'-diphospho-glucuronosyltransferase (UDPGT) (**Figure 1.3**). These enzymes catalyse conjugation reactions leading to methyl, sulfate and glucuronide conjugates of the flavonoid aglycone respectively. These conjugate molecules are then able to cross the cell membrane into the portal circulation either by passive diffusion or via active transport by multidrug resistance proteins (MRP). MRP can also efflux flavonoid glycosides and metabolites back across the epithelium into the small intestine (**Figure 1.3**). From the portal circulation the flavonoid molecules are transported to the liver where they may undergo phase I metabolism (hydroxylation and demethylation) but this is believed to be minimal as it would not achieve the goal of increasing polarity for excretion via the kidneys. The liver is also a site for further methyl, sulfate and glucuronide conjugation reactions before the conjugated metabolites are released into the systemic circulation and unconjugated metabolites are recirculated back into the small intestine via enterohepatic circulation. Conjugation to glutathione, a tripeptide present in millimolar concentrations in the cytosol, is also possible during this process. Glutathione is made up of glutamic acid, cysteine and glycine and it has been reported to form conjugates with quercetin *in vivo* (Hong and Mitchell 2006) and there is some work showing formation of anthocyanin-glutathione conjugates *in vitro* (Fernandes *et al.* 2009) but this has yet to be proven to occur *in vivo*.

Anthocyanin aglycones present in the small intestine that are not absorbed will degrade over time as a result of the neutral pH, aided by the gut microbiota. This degradation of the aglycone will produce aldehyde and phenolic acid derivatives that are able to diffuse across the apical membrane into the epithelium (**Figure 1.3**). Within the cytosol, the degradation products are subject to the same conjugation reactions and MRP recycling as the aglycones. The degradation products and their conjugated forms can then enter the portal circulation for transport to the liver.

Anthocyanin glycosides and metabolites that are unabsorbed after passing through the small intestine will then enter the large intestine. In the large intestine these compounds can be metabolised by the colonic microbiota (**Figure 1.3**). There is evidence to suggest that metabolism by colonic bacteria may play an important role in the overall bioavailability of anthocyanins (Keppler and Humpf 2005, Forester and Waterhouse 2008, Selma *et al.* 2009, Sánchez-Patán *et al.* 2012, Czank *et al.* 2013). Differences in the microbiota population of the colon may influence the types and levels of anthocyanin metabolites seen in the circulation (Selma *et al.* 2009, Boto-Ordóñez *et al.* 2014). Anthocyanins can be deglycosylated in the colon and the aglycone absorbed across the intestinal epithelium. Alternatively, aglycones can undergo ring fission by the colonic microflora and the degradation products can be dehydroxylated and demethylated prior to absorption (Selma *et al.* 2009). Any metabolites not absorbed during transit through the large intestine will be excreted, along with any remaining parent anthocyanins, via the faeces (**Figure 1.3**) (Czank *et al.* 2013).

1.7. Cardiovascular Health

Cardiovascular disease (CVD) is a group of disorders of the heart and blood vessels including coronary heart disease, peripheral artery disease, and stroke. CVD is the number one cause of death globally with an estimated 17.5 million deaths caused by CVD in 2012 representing nearly a third of total deaths worldwide (World Health Organisation 2014).

Recent epidemiological studies have reported a link between increased anthocyanin intake and improved cardiovascular health. Specifically, studies have reported a 9% reduction in risk of CVD mortality from diets containing anthocyanins compared to an anthocyanin-free diet (Mink *et al.* 2007), an increase in anthocyanin intake from 6 mg/day to 19 mg/day was associated with an 8% reduction in risk of hypertension (Cassidy *et al.* 2011), an increase in anthocyanin intake from 8 mg/day to 24 mg/day was associated with a 3 mm Hg reduction in central systolic blood pressure (Jennings *et al.* 2012), and an increase in anthocyanin intake from 1.8 mg/day to 32 mg/day was associated with a decrease in a range of inflammatory biomarkers (Cassidy *et al.* 2015). A recent systematic review of 14 cohort studies reported an 11% reduced risk of CVD mortality when comparing the highest and lowest categories of anthocyanin intake (Wang *et al.* 2014a).

Randomised controlled trials (RCTs) investigating the effect of anthocyanin consumption have also observed positive effects on markers of cardiovascular health. Recent studies have shown that 4 hours after intake of a cranberry juice drink (containing 835 mg polyphenols,

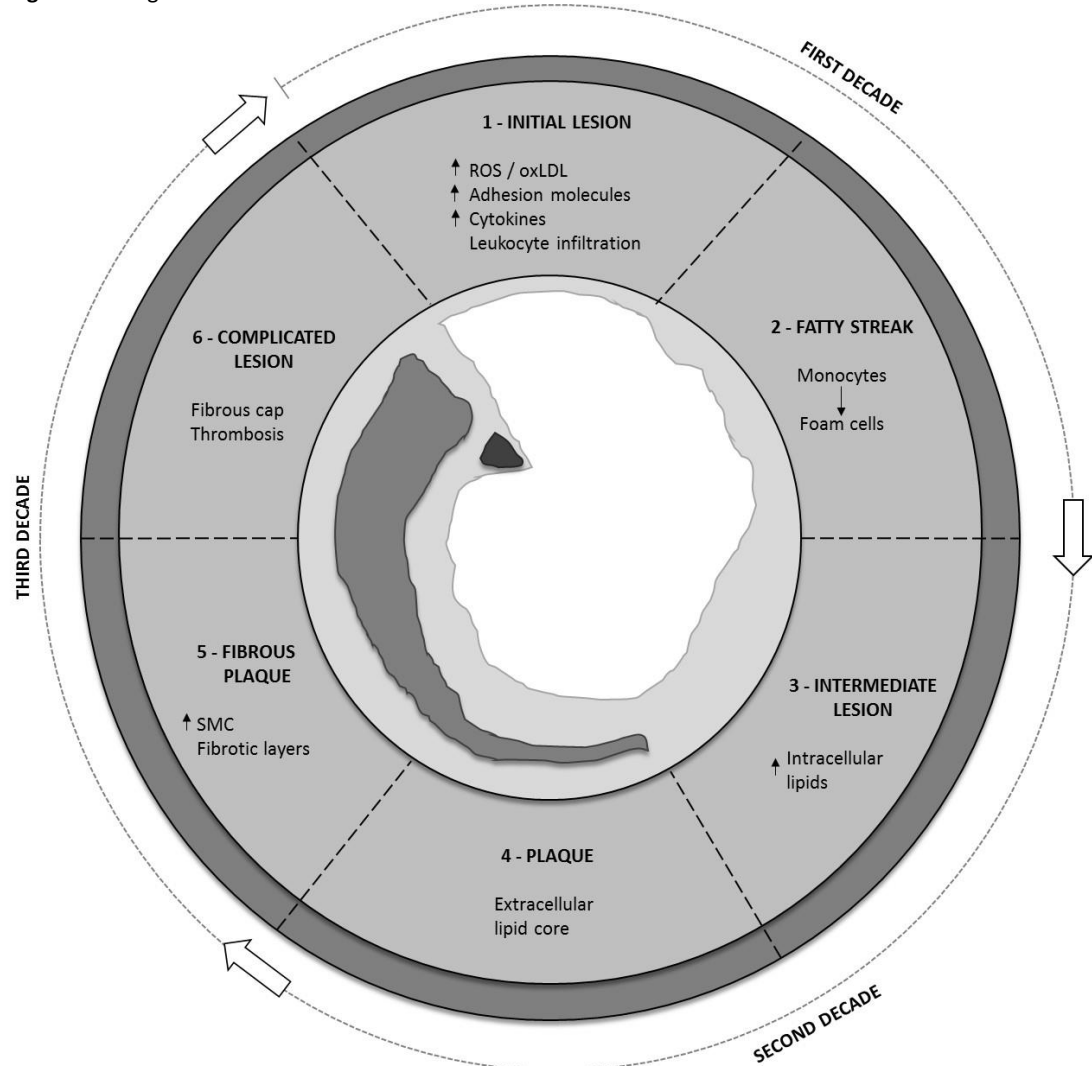
of which 94 mg were anthocyanins) flow-mediated dilation (FMD) increased from 7.7% to 8.7% (Dohadwala *et al.* 2011), carotid-femoral PWV was reduced from 8.3 m/s to 7.8 m/s after 4 weeks consumption of the same cranberry juice drink (Dohadwala *et al.* 2011) and intake of a blueberry drink (containing between 319 – 1791 mg polyphenols, of which between 129 – 724 mg were anthocyanins) improved FMD within 6 hours of consumption (Rodriguez-Mateos *et al.* 2013). A recent meta-analysis of 22 RCTs observed significant improvement of a range of cardiovascular risk factors including low-density lipoprotein (LDL)-cholesterol levels and systolic blood pressure following consumption of anthocyanin-rich foods (Huang *et al.* 2016).

Inflammation is the process by which the body defends itself against tissue damage from harmful agents via the migration of leukocytes to the site of injury, infection, or other insult. (Libby *et al.* 2002). Inflammation can be classified as either acute or chronic. Acute inflammation is the term used to describe the immediate immune response and is generally seen as beneficial in the healing process (Libby *et al.* 2002). Chronic inflammation is the long-term, persistent state of immune response associated with the development of many disorders including atherosclerosis (Epstein and Ross 1999).

Atherosclerosis is the process by which vascular walls develop lesions and plaques resulting in thickening, hardening and occlusion of blood vessels (**Figure 1.4**).

Progression of atherosclerosis can take many decades and is initially characterised as a chronic state of endothelial dysfunction. In the healthy endothelium, blood pressure is regulated via the production of various vasodilators and vasoconstrictors by enzymes within endothelial cells, such as the production of nitric oxide (NO) from L-arginine by endothelial nitric oxide synthase (eNOS) (Zhao *et al.* 2015). This process is disrupted following activation of the endothelium by stimuli such as smoking or high levels of LDL cholesterol, as production of NO is reduced and levels of reactive oxygen species (ROS) such as superoxide (O_2^-) increase leading to the formation of hydrogen peroxide (H_2O_2) by superoxide dismutase (SOD) (Cai 2005). The build-up of H_2O_2 within the endothelium results in expression of inducible nitric oxide synthase (iNOS) to boost production of NO to quench the ROS, and upregulation of cytokines such as NF- κ B to trigger an inflammatory response to defend against injury whilst the causative agent is removed (Aktan 2004).

Figure 1.4 Progression of atherosclerosis.

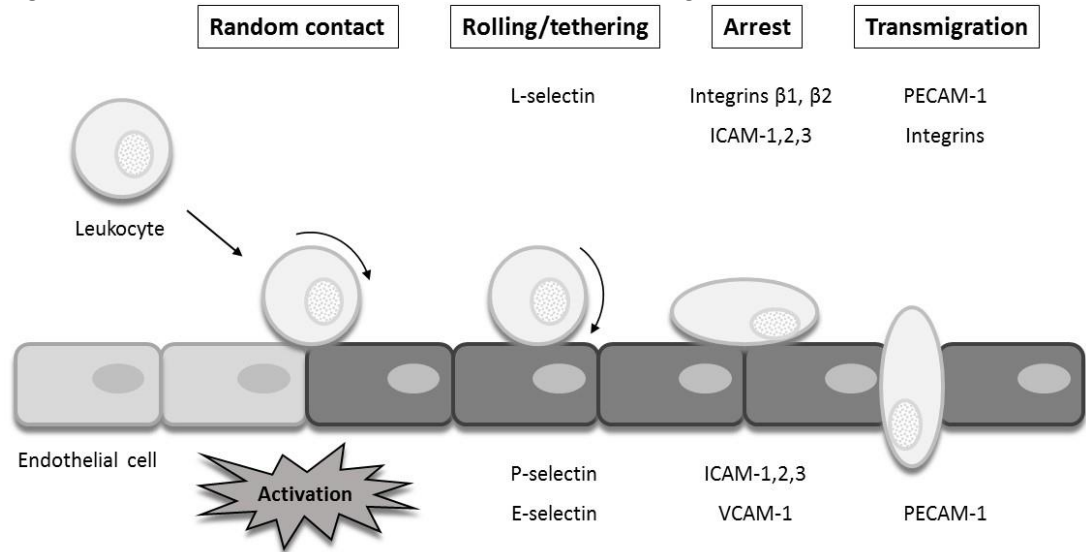


ROS, reactive oxygen species; oxLDL, oxidised low-density lipoprotein; SMC, smooth muscle cells. Adapted from (Epstein and Ross 1999, Vassiliadis *et al.* 2012).

If the causative agent persists, chronic inflammation ensues and levels of peroxynitrite (ONOO^-) increase due to the reaction between NO and O_2^- resulting in increased levels of oxidised low-density lipoprotein (oxLDL), monocyte infiltration, and lipid accumulation within the endothelium (Graham *et al.* 1993, Epstein and Ross 1999). The end result of this process is the formation of fatty streaks and fibrotic plaques within the endothelium that can occlude blood vessels and rupture causing potentially fatal ischemia and infarction (Libby *et al.* 2002, Hansson 2005).

Following proatherogenic stimuli, expression of adhesion molecules such as selectins and cell adhesion molecules is upregulated within activated arterial endothelial cells leading to the recruitment and infiltration of leukocytes (**Figure 1.5**).

Figure 1.5 Selectins and adhesion molecules involved in the initial stages of atherosclerosis.



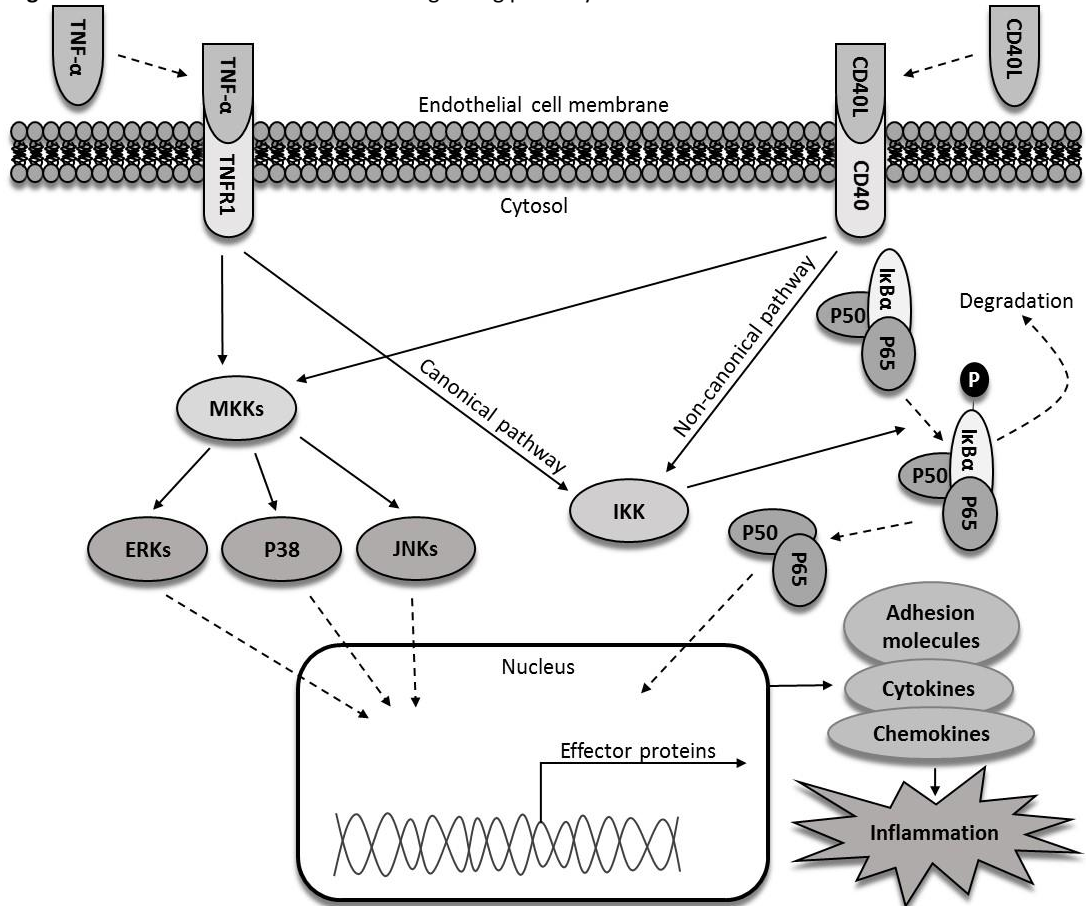
ICAM, intercellular adhesion molecule; VCAM, vascular cell adhesion molecule; PECAM, platelet endothelial cell adhesion molecule. Adapted from (Blankenberg *et al.* 2003).

The initial stages of atherosclerotic progression are facilitated by the interaction between leukocyte-expressed L-selectin and endothelium-expressed E- and P-selectins which promotes the rolling and tethering of leukocytes at the endothelial surface (Blankenberg *et al.* 2003). Intercellular adhesion molecules (ICAM) -1, -2, and -3, platelet endothelial cell adhesion molecule-1 (PECAM-1), and vascular cell adhesion molecule-1 (VCAM-1) are expressed at endothelial cell junctions and interact with leukocyte-expressed integrins $\beta 1$ and $\beta 2$ to promote the adhesion of leukocytes to the endothelium before migration into the intercellular matrix (Blankenberg *et al.* 2003). VCAM-1 is induced by various cytokines including tumour necrosis factor- α (TNF- α) and cluster of differentiation 40 ligand (CD40L) (Karmann *et al.* 1995, Maaser *et al.* 2001), and also has a role in signalling the endothelial shape change that allows leukocytes to pass through the endothelium via interaction with integrin $\alpha 4 \beta 1$ and activation of NADPH oxidase (NOX) (Matheny *et al.* 2000). A number of studies have investigated the effect of anthocyanins on the expression of VCAM-1 as a possible mechanism for downregulating the inflammatory response and inhibiting atherosclerotic progression. Inhibition of VCAM-1 expression in endothelial cells following incubation with anthocyanins has been reported by *in vitro* studies (Xia *et al.* 2009, Chao *et al.* 2013, Huang *et al.* 2014, Kuntz *et al.* 2015a) while consumption of anthocyanins has been shown to reduce levels of circulating VCAM-1 in human (Zhu *et al.* 2013) and animal trials (Miyazaki *et al.* 2008).

In addition to cell adhesion molecules, many other cytokines and chemokines are upregulated within leukocytes and vascular endothelial cells as part of the inflammatory response to proatherogenic stimuli. These proinflammatory signalling molecules mediate every stage of the atherosclerotic process with an extensive range of cytokines reported to be involved including monocyte chemoattractant protein-1 (MCP-1) and interleukin-8 (IL-8) stimulating the transmigration of leukocytes across the vascular endothelium (Libby *et al.* 2002, Tedgui and Mallat 2006), activation of T-cells induced by TNF- α and IL-2 (Epstein and Ross 1999), macrophage colony-stimulating factor (M-CSF) and IL-1 promoting the differentiation of monocytes into macrophages and lipid-filled foam cells (Epstein and Ross 1999), and proliferation of smooth muscle cells induced by fibroblast growth factor 2 (FGF2) and IL-6 (Epstein and Ross 1999, Tedgui and Mallat 2006).

During chronic inflammation, a number of signalling pathways are stimulated that act as positive feedback loops, perpetuating the inflammatory response. CD40L is a proinflammatory cytokine, part of the TNF family of proteins, and is produced by leukocytes, platelets and vascular cells in response to induction by various proinflammatory cytokines such as IL-1, IL-3, IL-4, interferon- γ (IFN- γ), and TNF- α (Tedgui and Mallat 2006, Pamukcu *et al.* 2011). CD40L binds to the CD40 receptor to stimulate the mitogen-activated protein kinase (MAPK) and nuclear factor- κ B (NF- κ B) signalling pathways which can also be activated via the binding of TNF- α to its receptor, TNF receptor 1 (TNFR1) leading to the upregulation of many proinflammatory cytokines and adhesion molecules (**Figure 1.6**).

Figure 1.6 Activation of MAPK and NF- κ B signalling pathways via TNF- α and CD40L stimulation.



CD40(L), cluster of differentiation 40 (ligand); ERK, extracellular signal-regulated kinase; I κ B α , NF- κ B inhibitory protein; IKK, inhibitory- κ B kinase; JNK, c-Jun N-terminal kinase; MKK, mitogen-activated protein kinase kinase; P, phosphate; p38, mitogen-activated protein kinase; p50, nuclear factor- κ B p50 subunit; p65, NF- κ B p65 subunit; TNF- α , tumour necrosis factor- α ; TNFR1, TNF receptor 1. Adapted from (Pamukcu *et al.* 2011, Hayden and Ghosh 2014, Sabio and Davis 2014).

Inactive NF- κ B exists in the cytosol of leukocytes and vascular cells and consists of two subunits, P50 and P65, bound to NF- κ B inhibitory protein (I κ B α) (Hayden and Ghosh 2014). TNF- α and CD40L act upon NF- κ B via two distinct pathways; the canonical signalling pathway is activated by TNF- α while CD40L activates the non-canonical signalling pathway (Brasier 2010). Both pathways result in the upregulation of inhibitory- κ B kinase (IKK) which signals the activation of NF- κ B via phosphorylation and subsequent degradation of I κ B α (Pamukcu *et al.* 2011). This allows NF- κ B to translocate into the nucleus where it triggers the expression of various proinflammatory cytokines including IL-6 and TNF- α (Brasier 2010). A number of studies have reported the ability of anthocyanins to inhibit NF- κ B activation and translocation *in vitro* (Paixão *et al.* 2012, Lee *et al.* 2014) and *in vivo* (Blanco-Colio *et al.* 2000, Karlsen *et al.* 2007) suggesting a possible mechanism for the observed bioactivity of anthocyanins.

MAPKs are a family of cytokines consisting of extracellular signal-regulated kinases (ERKs), p38, and c-Jun N-terminal kinases (JNKs) (Sabio and Davis 2014). The MAPK signalling pathway is activated by many of the same proinflammatory cytokines as the NF- κ B pathway, including TNF- α and CD40L (Pamukcu *et al.* 2011, Hayden and Ghosh 2014), which act via downstream signalling to induce mitogen-activated protein kinase kinases (MKKs) activation of MAPKs and subsequent expression of proinflammatory cytokines, including TNF- α (Sabio and Davis 2014). Recent *in vitro* studies demonstrating inhibition of MAPK signalling by anthocyanins suggest that this pathway may also play a role in the bioactive effect exerted by anthocyanins (Xia *et al.* 2009, Xie *et al.* 2011, Jeong *et al.* 2013).

1.8. Summary and Aims

Anthocyanins are phytochemicals commonly consumed within the normal diet and their consumption has been associated with a reduced risk of cardiovascular disease (Wallace *et al.* 2016). However, the poor bioavailability of anthocyanins observed in feeding trials (Manach *et al.* 2005) combined with the results of recent studies demonstrating the extensive metabolism of anthocyanins *in vivo* (Czank *et al.* 2013, de Ferrars *et al.* 2014b) has shifted the focus onto the phenolic metabolites of anthocyanins to explain the reported bioactivity.

The present study intended to provide information on the analysis and clinical utility of anthocyanin metabolites by seeking to achieve the following aims:

1. Determine best practice for storage of clinical samples to maximise anthocyanin metabolite recovery (Chapter 2).

Whilst the factors affecting the stability of anthocyanins in biological matrices are understood (Sadiłova *et al.* 2006, Woodward *et al.* 2009), little is known about the stability of phenolic metabolites. The present thesis investigated the effect of pH and freeze/thaw cycling during storage on the recovery of anthocyanin metabolites in biological samples.

2. Increase the sensitivity and throughput of current methodology for quantifying anthocyanin metabolites in biological samples (Chapter 3).

An HPLC-ESI-MS/MS method capable of detecting over 35 phenolic metabolites of anthocyanins in clinical samples has recently been reported (de Ferrars *et al.* 2014c). However, results from a recent tracer study utilising this method to track the metabolism of an isotopically-labelled anthocyanin molecule *in vivo* have suggest that many more

metabolites remain undetected (Czank *et al.* 2013). In order to gain a comprehensive understanding of anthocyanin metabolism, more sensitive analytical methods are needed. The present thesis explored the effect of using ammonium-buffered mobile phase on method sensitivity. In addition, alternative sample preparation techniques were investigated and HPLC parameters were optimised with the aim of increasing the throughput of the methodology.

3. Validate methodology for quantifying anthocyanin metabolites in biological samples (Chapter 4).

To have confidence in the reliability of the results obtained when quantifying anthocyanin metabolites in biological samples, the developed methods were validated according to accepted guidelines. The present study conducted validations of both the previously reported method (de Ferrars *et al.* 2014c) and the newly-developed method described in Chapter 3.

4. Determine the viability of phenolic metabolites as biomarkers of anthocyanin intake (Chapter 5).

Studies investigating the bioactivity of anthocyanins typically use traditional methods such as food frequency questionnaires to measure anthocyanin intake (Cassidy *et al.* 2015) leading to possible inaccuracies (Thompson *et al.* 2010). An alternative method for monitoring dietary intake is to analyse the concentration of characteristic metabolites in biological samples (Hedrick *et al.* 2012). The present study used samples from a recent ¹³C-labelled anthocyanin feeding trial (Czank *et al.* 2013) to investigate the phenolic metabolites as potential biomarkers of anthocyanin intake.

5. Determine the effect of anthocyanin metabolic profiles on inflammatory biomarkers in a vascular cell model (Chapter 6).

Whilst the *in vitro* bioactivity of anthocyanins has been extensively studied (Speciale *et al.* 2014), few studies have explored the bioactivity of the phenolic metabolites. Studies that have investigated the bioactivity of anthocyanin metabolites have used metabolite compounds either in isolation (Amin *et al.* 2015, Edwards *et al.* 2015) or in equimolar combinations (di Gesso *et al.* 2015, Warner *et al.* 2016), neither of which accurately represent the *in vivo* situation (Czank *et al.* 2013). The present study incubated TNF- α and CD40L-stimulated human umbilical vein endothelial cells (HUVEC) with previously reported anthocyanin metabolite profiles (de Ferrars *et al.* 2014a) to investigate the effect on expression of sVCAM-1 and IL-6 proinflammatory cytokines.

Chapter 2. Investigating the Effect of Acidification and Freeze/thaw Cycles on Anthocyanin Metabolite Stability in Clinical Samples.

2.1. Introduction

Epidemiological studies have shown that diets high in anthocyanins are associated with beneficial health effects, including reducing the risk of cardiovascular disease (CVD) (Hollman *et al.* 1996, de Pascual-Teresa *et al.* 2010, Cassidy *et al.* 2011, Jennings *et al.* 2012, Cassidy *et al.* 2013). This epidemiological evidence has prompted many researchers to investigate the bioavailability and bioactivity of anthocyanins in clinical interventions (Mazza *et al.* 2002, Milbury *et al.* 2002, Felgines *et al.* 2003, Hooper *et al.* 2008, Dohadwala *et al.* 2011). Typically these studies involve asking volunteers to ingest a high dose of anthocyanins either through consuming food or beverages containing high concentrations of these pigments or via an anthocyanin extract. Biological samples such as blood and urine are then collected and stored in freezers until analyses of anthocyanin levels take place. The standard procedure is to first acidify the samples to pH 1-3 using either formic acid or hydrochloric acid (Mülleder *et al.* 2002, Mullen *et al.* 2008) prior to storage due to anthocyanins structural instability at neutral pH (Jurd 1963, Castañeda-Ovando *et al.* 2009). In recent years the focus of many investigations into anthocyanin bioactivity has shifted towards exploring their degradation products and phase II metabolites because of the observed low bioavailability of the parent anthocyanins (Kay *et al.* 2009). It is not clear what effect acidification of clinical samples has on the metabolite profiles observed.

It is also unclear how stable phenolic metabolites of anthocyanins are through multiple freeze/thaw cycles. This information is important for clinical studies involving phenolic metabolites as often samples are thawed for analysis and refrozen. Presently the effect of multiple freeze thaw cycles on metabolite stability/recovery is unknown. Previous work on the parent anthocyanins suggests that they are stable in acidified solution through at least six freeze/thaw cycles (Woodward *et al.* 2009). However, little work has been done to investigate the stability of phenolic metabolites of anthocyanins.

The present study aimed to provide information on the effect of acidification and freeze/thaw cycling on the stability of phenolic metabolites of anthocyanins in clinical samples. The hypothesis was that the phenolic metabolites would demonstrate greater

stability in clinical samples when stored at neutral pH and following multiple freeze/thaw cycles than the parent anthocyanins. To investigate this hypothesis, serum samples were spiked with a mixed standard containing cyanidin-3-glucoside and 17 of its phenolic metabolites. The spiked serum samples were then split into two groups; one group was acidified to pH 2.4 using formic acid while the other group was left unacidified. The two spiked serum sample groups were then split into two further groups; one group was put through five freeze/thaw cycles while the other group was stored at -80°C and only thawed once prior to analysis. All samples were stored at -80°C and analysed at five time-points to monitor the effect of acidification and freeze/thaw on metabolite stability over time. It is intended that the findings of the present study will inform future clinical studies of the appropriate sample preparation procedures required to maximise anthocyanin metabolite recovery from biological samples.

2.2. Methods

2.2.1. Materials and reagents

Acetonitrile and methanol were purchased from Fisher Scientific (Loughborough, UK). Strata-X™ 33 µm polymeric sorbent 500 mg/6 mL solid-phase extraction cartridges, Kinetex® pentafluorophenyl (PFP) high-performance liquid chromatography (HPLC) column (2.6 µm, 100 x 4.6 mm, 100 Å) and SecurityGuard® cartridges (PFP, 4.6 x 2.0 mm) were purchased from Phenomenex (Macclesfield, UK). Cyanidin-3-glucoside (kuromanin chloride) was purchased from Extrasynthese (Genay, France). The phase II conjugates of phenolic acids (protocatechuic acid-3-glucuronide, protocatechuic acid-4-glucuronide, protocatechuic acid-3-sulfate, protocatechuic acid-4-sulfate, isovanillic acid-3-glucuronide, vanillic acid-4-glucuronide, isovanillic acid-3-sulfate, vanillic acid-4-sulfate, benzoic acid-4-glucuronide) were synthesised by the School of Chemistry and Centre for Biomolecular Sciences, University of St. Andrews (UK) using published methods (Zhang *et al.* 2012). Methyl 3,4-dihydroxybenzoate (3,4-dihydroxy-benzoic acid methyl ester) was purchased from Alfa Aesar (Heysham, UK). All other materials, reagents, and standards were purchased from Sigma-Aldrich (Dorset, UK), including: Acrodisc PTFE syringe filters (13 mm, 0.45 µm), human serum from human male AB plasma (Product No.: H4522), formic acid (FA), dimethyl sulfoxide (DMSO), 4-hydroxybenzaldehyde, ferulic acid (4-hydroxy-3-methoxycinnamic acid), hippuric acid (benzoylaminoacetic acid), isovanillic acid (3-hydroxy-4-methoxybenzoic acid), protocatechuic acid (PCA, 3,4-dihydroxybenzoic acid), phloroglucinaldehyde (PGA, 2,4,6-trihydroxybenzaldehyde), phloridzin (phloridzin dihydrate), scopoletin (7-hydroxy-5-

methoxycoumarin), and vanillic acid (4-hydroxy-3-methoxybenzoic acid). Water was 18MΩ/cm Milli-Q quality and all solvents were LC-MS grade.

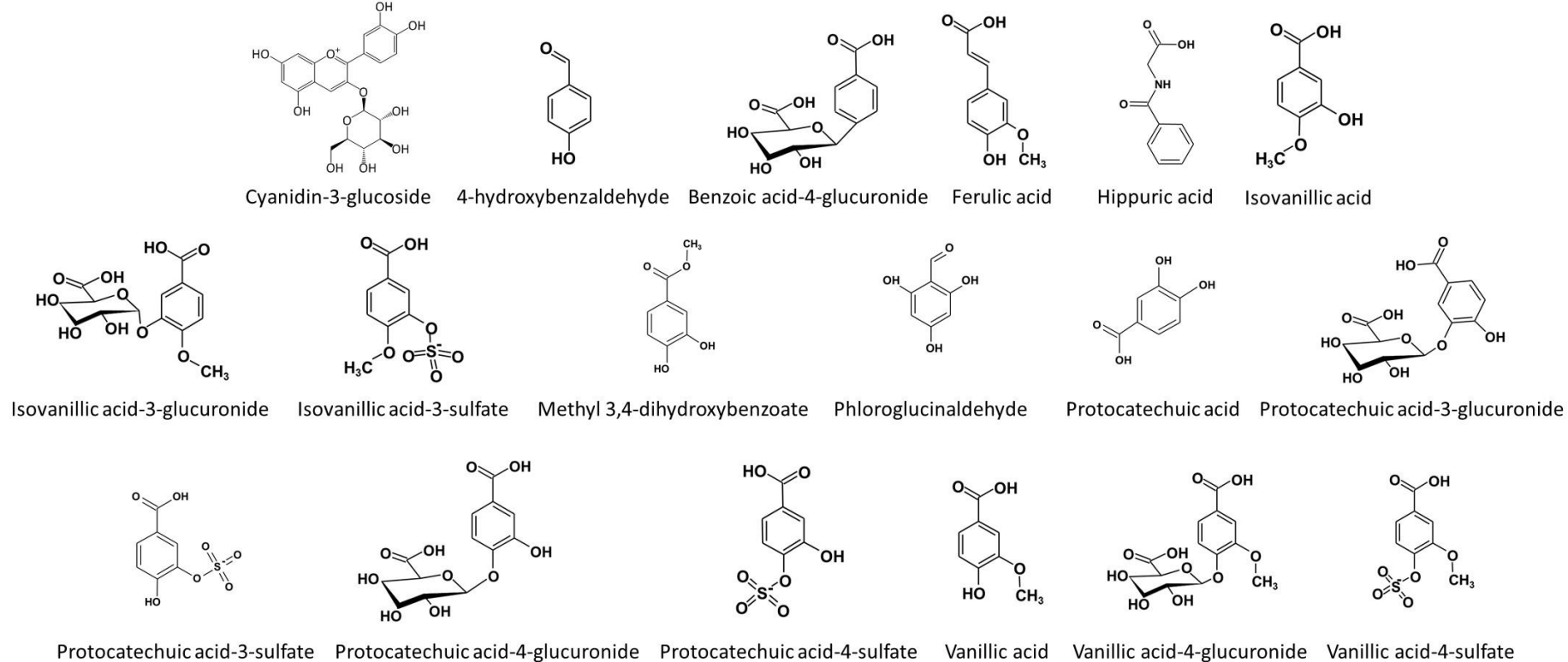
2.2.2. Solid-phase extraction (SPE)

40 mL of commercially-sourced human serum was extracted via SPE following previously reported methodology (Czank *et al.* 2013, de Ferrars *et al.* 2014c). Briefly, SPE cartridges were preconditioned with 6 mL of acidified methanol (acidified to pH 2.4 using formic acid) followed by 6 mL of acidified water (acidified to pH 2.4 using formic acid). Cartridges were loaded with 1 mL acidified water followed by 1 mL of serum. Samples were eluted at a flow rate of approximately 1 drop/second. Cartridges were washed with 12 mL of acidified water before being dried under vacuum for 30 mins. 5 mL of acidified methanol was added to the cartridges and left to soak for 10 mins before the samples were eluted with a total of 7mL acidified methanol. The eluent was evaporated to approximately 50 µL on a rotary evaporator (Thermo SPD Speedvac). Following evaporation, half the samples were reconstituted with 200 µL water and half reconstituted with 200 µL of acidified water. The samples were then sonicated for 10 mins with the ultrasonic water bath kept cool using ice, followed by vortex mixing for 10 seconds and filtration through a 0.45 µm syringe filter. Filtrates were combined to provide approximately 5 mL of non-acidified extracted matrix and 5 mL of acidified extracted matrix to be used as blank serum during sample preparation.

2.2.3. Sample Preparation

A mixed standard was composed of cyanidin-3-glucoside and 17 of its serum metabolites, as reported following consumption of ¹³C-labelled cyanidin-3-glucoside (Czank *et al.* 2013, de Ferrars *et al.* 2014a). The 18 compounds included in the mixed standard were cyanidin-3-glucoside, 4-hydroxybenzaldehyde, benzoic acid-4-glucuronide, ferulic acid, hippuric acid, isovanillic acid, isovanillic acid-3-glucuronide, isovanillic acid-3-sulfate, methyl 3,4-dihydroxybenzoate, protocatechuic acid, protocatechuic acid-3-glucuronide, protocatechuic acid-3-sulfate, protocatechuic acid-4-glucuronide, protocatechuic acid-4-sulfate, phloroglucinaldehyde, vanillic acid, vanillic acid-4-glucuronide, and vanillic acid-4-sulfate (Figure 2.1).

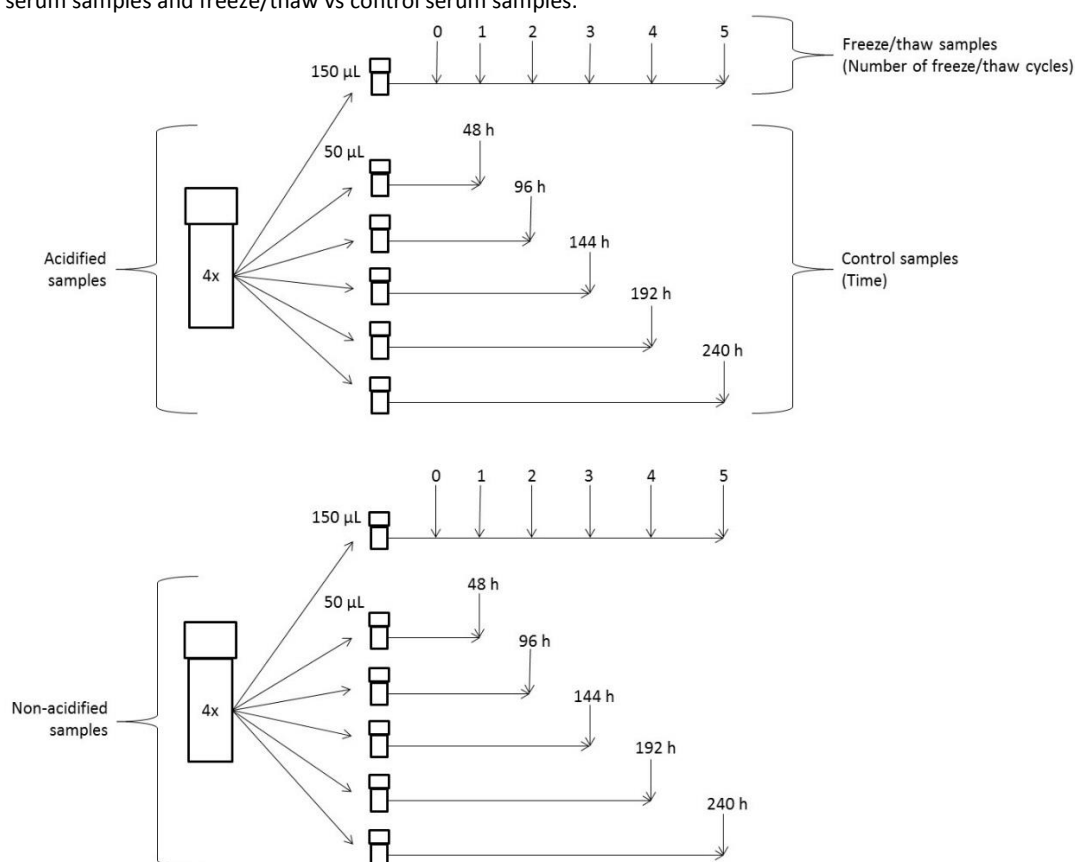
Figure 2.1 Compounds included in the mixed standard; cyanidin-3-glucoside and 17 of its phenolic metabolites as reported following consumption of ^{13}C -labelled cyanidin-3-glucoside.



Adapted from (Czank *et al.* 2013, de Ferrars *et al.* 2014a).

The non-acidified and acidified blank serum samples were each split into four 1 mL aliquots before the mixed standard was added along with either water for the non-acidified samples or formic acid for the acidified samples, and two internal standards, scopoletin and phloridzin, to give 1 μ M non-acidified and acidified samples (**Figure 2.2**). The non-acidified and acidified samples were then split into six smaller aliquots; one aliquot was used as the freeze/thaw sample (frozen, thawed and analysed every 48 hours over 240 hours for a total of five occasions) while the other five aliquots were used as control samples (one aliquot thawed and analysed every 48 hours over 240 hours).

Figure 2.2 Experimental design of anthocyanin metabolite stability study showing acidified vs non-acidified serum samples and freeze/thaw vs control serum samples.



Samples were prepared in solid-phase extracted commercial serum at 1 μ M using a mixed standard containing cyanidin-3-glucoside and 17 of its metabolite. Samples were stored at -80°C between analyses.

One freeze/thaw cycle consisted of 48 hours storage at -80°C followed by 20 min defrost at ambient room temperature prior to analysis. Metabolite concentrations were monitored at each time-point by HPLC-ESI-MS/MS analysis with samples stored at -80°C between analyses. By this method, differences in the stability of the metabolites within the non-acidified and acidified samples as well as the freeze/thaw and control samples could be identified.

2.2.4. Chromatography

HPLC-ESI-MS/MS analysis was carried out using an Agilent (Stockport, UK) 1200 series HPLC equipped with a Diode Array Detector (DAD) coupled to an AB SCIEX (Warrington, UK) 3200 series QTRAP® MS/MS system with Turbo V™ electrospray ionisation source using previously established methods (Czank *et al.* 2013, de Ferrars *et al.* 2014c). Briefly, a Kinetex® pentafluorophenyl (PFP) (2.6 µm, 100 x 4.6 mm) RP-HPLC column was used with a PFP SecurityGuard® cartridge (4.6 x 2.0 mm). The column temperature was set at 37°C, injector temperature of 4°C and injection volume of 5 µL. Mobile Phase A was 0.1% (v/v) formic acid in water and Mobile Phase B was 0.1% (v/v) formic acid in acetonitrile at a flow rate of 1.5 mL min⁻¹ at 0 min, 1 mL min⁻¹ at 7 to 14 min and 1.5 mL min⁻¹ at 14 to 32 min. The gradient consisted of 1% B at 0 min, 7.5% B at 7 min, 7.6% B at 14 min, 10% B at 17 min, 12% B at 18.5 min, 12.5% B at 20 min, 30% B at 24 min, 90% B at 25 to 28 min, 1% B at 29 to 32 min.

MS/MS source parameters included ionspray voltage, -4000 V / +5500 V; temperature, 700°C; curtain gas, 40 psi; nebulizer gas and auxiliary gas, 60 psi. Scheduled multiple reaction monitoring (sMRM) scans were performed using parameters optimised for the detection of analytical standards (**Table 2.1**).

Samples were analysed in negative and positive ionisation modes. Retention time and the detection of three or more of the relevant ion transitions were used to confirm the identity of the metabolites. For quantification, the peak area of the most intense ion transition was used. Metabolite concentrations were calculated by comparison of the analyte peak area and the scopoletin internal standard peak area at each time-point.

2.2.5. Statistical analysis

Two-way analysis of variance (ANOVA) with Bonferroni post-hoc test was performed on four replicates using SPSS for Windows statistical software package (version 22, IBM, New York, USA). Significance was determined at the 5% confidence level. Statistical analysis was conducted on raw data with mean values graphed as percentage metabolite concentration relative to the initial 1 µM concentration with error bars representing standard deviation.

Table 2.1 sMRM schedule used to analyse the extracted serum samples on the AB SCIEX 3200 QTRAP® instrument.

Compound	Transitions (m/z) precursor/product ions	Scan time range (min)	Scan mode
Benzoic acid-4-glucuronide	313/175,113,93*	2.0 – 4.0	-
Protocatechuic acid-4-glucuronide	329.01/153*,113,109	2.4 – 4.4	-
Protocatechuic acid	153.01/108*,91,81	3.2 – 5.2	-
Protocatechuic acid-3-glucuronide	329.01/153*,113,109	3.4 – 5.4	-
Vanillic acid-4-glucuronide	343.01/167,152,113*	4.6 – 6.6	-
Isovanillic acid-3-glucuronide	343.01/167,152,113*	4.6 – 6.6	-
Hippuric acid	177.9/133.9*,77.1,131.8	5.0 – 7.0	-
Protocatechuic acid-3/4-sulfate ^a	233.01/153,109*,189	6.3 – 8.3	-
4-hydroxybenzaldehyde	121.2/107.8,92*,65.1	7.0 – 9.0	-
Isovanillic acid	169.01/151.1,125,93*	7.3 – 11.3	+
Vanillic acid	167.03/152*,123,108	8.8 – 10.8	-
(Iso)vanillic acid-3/4-sulfate ^a	247/167*,152,108	8.9 – 10.9	-
Methyl 3,4-dihydroxybenzoate	167/107.8*,107.1,91.2	11.5 – 13.5	-
Cyanidin-3-glucoside	449/287*,213,137	11.9 – 15.9	+
Phloroglucinaldehyde	153/151*,125,107	13.7 – 15.7	-
Ferulic acid	193/178,149,134*	17.8 – 19.8	-
Scopoletin	193/133.2*,122,94.1	17.1 – 21.1	+
Scopoletin	191/104*,147.9,120	18.1 – 20.1	-
Phloridzin	437/275,169,107*	22.1 – 26.1	+
Phloridzin	435/273*,167,123,81	23.1 – 25.1	-

*Transition used for quantitation. ^aIsomers of this metabolite were unresolvable using this HPLC-ESI-MS/MS method so were quantified as a single analyte.

2.3. Results

2.3.1. Acid effect

Metabolite concentrations within the control (not subjected to freeze/thaw cycling) serum samples were analysed, for both the non-acidified and acidified groups, every 48 hours for a total of 240 hours. The results of the two groups were then compared using statistical methods (Table 2.2).

Table 2.2 Statistical significance of the effect of acidification on anthocyanin metabolite stability in serum when stored at -80°C for 240 hours.

Analyte	Time effect	Acid effect	Time*Acid effect	Time					
	(p-value)	(p-value)	(p-value)	0 hours ^a	48 hours ^a	96 hours ^a	144 hours ^a	192 hours ^a	240 hours ^a
4-hydroxybenzaldehyde	0.018	NS	NS	a	a	b	b	b	b
Benzoic acid-4-glucuronide	0.043	NS	NS	a	a	a	a	a	a
Cyanidin-3-glucoside	NS	<0.001	NS	NS	NS	NS	NS	NS	NS
Ferulic acid	NS	NS	NS	NS	NS	NS	NS	NS	NS
Hippuric acid	NS	NS	0.030	NS	NS	NS	NS	NS	NS
Isovanillic acid	0.010	NS	NS	a,b	b	c,d	a,d	a,b,c,d	c,d
Isovanillic acid-3-glucuronide	NS	NS	NS	NS	NS	NS	NS	NS	NS
(Iso)vanillic acid-3/4-sulfate	NS	NS	NS	NS	NS	NS	NS	NS	NS
Methyl 3,4-dihydroxybenzoate	0.006	NS	NS	a	a	b	b,c	c	c
Protocatechuic acid	0.044	NS	NS	a	a,b	b,c	c	c	c
Protocatechuic acid-3-glucuronide	NS	NS	NS	NS	NS	NS	NS	NS	NS
Protocatechuic acid-3/4-sulfate	NS	NS	NS	NS	NS	NS	NS	NS	NS
Protocatechuic acid-4-glucuronide	NS	NS	NS	NS	NS	NS	NS	NS	NS
Phloroglucinaldehyde	0.045	NS	NS	a,b	b	a	a,b	a	a
Vanillic acid	NS	NS	NS	NS	NS	NS	NS	NS	NS
Vanillic acid-4-glucuronide	NS	NS	NS	NS	NS	NS	NS	NS	NS

p≤0.05, n=4, two-way repeated measures ANOVA with Bonferroni post-hoc test. NS, not statistically significant. ^aDifferent letters represent statistical differences between groups. Time effect indicates that there was a significant change in metabolite concentration compared to the initial 1 µM concentration during the 240 hour study period. Acid effect indicates that the difference in sample pH resulted in significantly different metabolite concentrations in the acidified samples compared to the non-acidified samples. Time*Acid effect indicates that the sample pH had a differential effect on metabolite concentration depending on the time-point.

A significant time effect was observed for six analytes: 4-hydroxybenzaldehyde, benzoic acid-4-glucuronide, isovanillic acid, methyl 3,4-dihydroxybenzoate, protocatechuic acid, and phloroglucinaldehyde. This indicates that these metabolites showed a significant change in concentration compared to the initial 1 μ M concentration during the 240 hour study period. Five of the six metabolites (4-hydroxybenzaldehyde, benzoic acid-4-glucuronide, methyl 3,4-dihydroxybenzoate, protocatechuic acid, and phloroglucinaldehyde) demonstrated an increase in concentration compared to the initial 1 μ M concentration after the 240 hour study period. Of the six analytes showing a significant time effect, post-hoc Bonferroni test indicated that four of these metabolites (4-hydroxybenzaldehyde, isovanillic acid, methyl 3,4-dihydroxybenzoate, protocatechuic acid) were significantly different from the initial concentration of 1 μ M following 96 hours storage ($p \leq 0.05$) (**Figure 2.3**). Benzoic acid-4-glucuronide also showed an increase in concentration following 96 hours storage, however, post-hoc analysis suggested there were no statistically significant differences between individual timepoints, likely due to the variation in concentration observed with this metabolite. A significant acid effect was observed for cyanidin-3-glucoside indicating that the difference in sample pH resulted in significantly different cyanidin-3-glucoside concentrations in the acidified samples compared to the non-acidified samples. Cyanidin-3-glucoside was found at a higher percentage concentration compared to the initial concentration in the acidified samples ($97.2 \pm 14.9\%$) relative to the non-acidified samples ($36.5 \pm 7.6\%$) after 240 hours. A significant interaction effect between time and sample pH was observed for hippuric acid indicating that the sample pH had a differential effect on the stability of this metabolite depending on the time-point.

Figure 2.3 Metabolite concentration as a percentage of initial concentration in acidified and non-acidified serum samples across 240 hours of storage at -80°C.

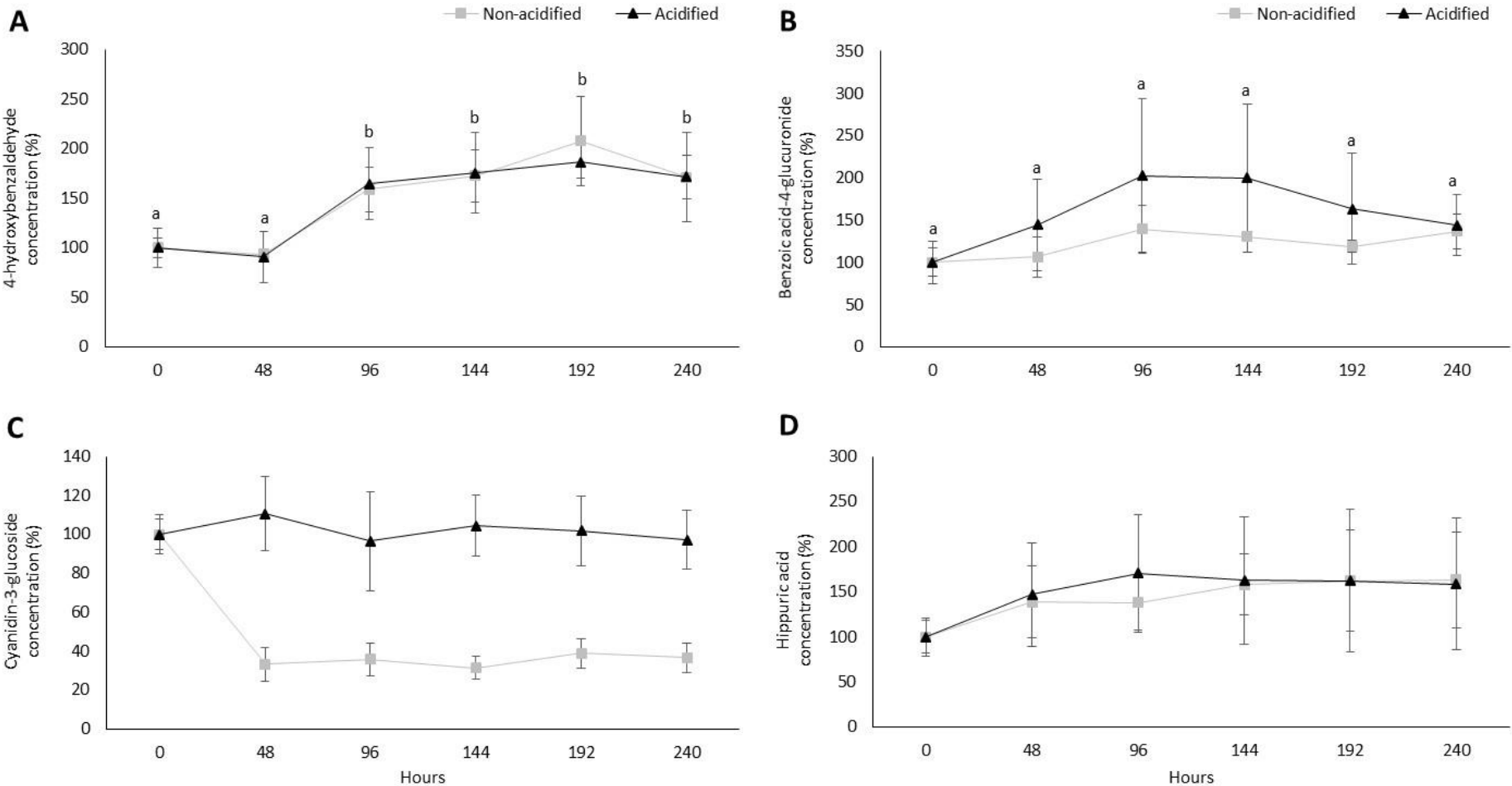
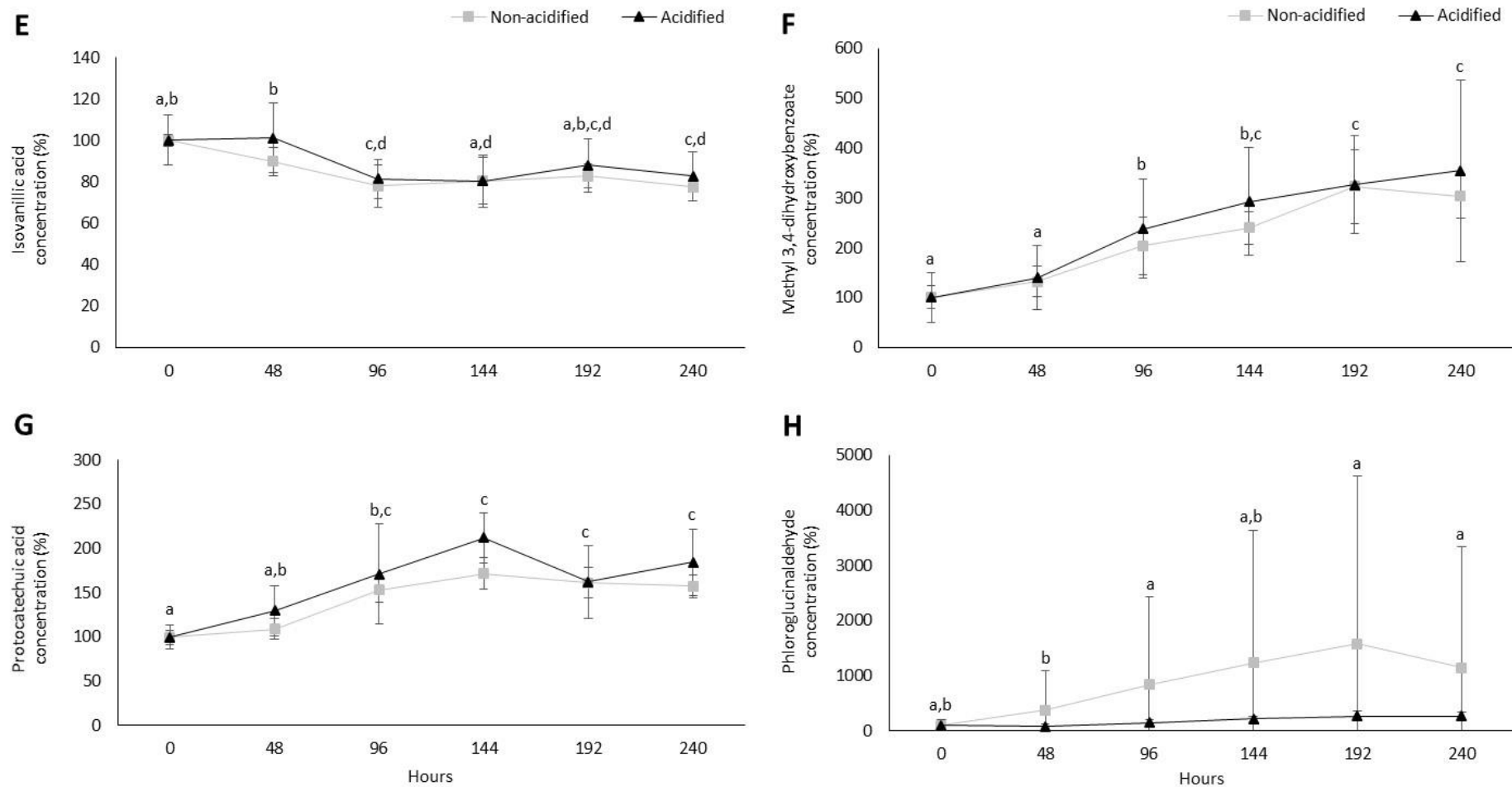


Figure 2.3 (Continued)



(A) 4-hydroxybenzaldehyde. (B) benzoic acid-4-glucuronide. (C) cyanidin-3-glucoside. (D) hippuric acid. (E) isovanillic acid. (F) methyl 3,4-dihydroxybenzoate. (G) protocatechuic acid. (H) phloroglucinaldehyde. Raw data corrected relative to the scopoletin internal standard. Results expressed as mean \pm SD, n=4.

2.3.2. Freeze/thaw effect

Metabolite concentrations within the acidified serum samples were analysed, for both the control (not subjected to freeze/thaw cycling) and freeze/thaw groups, every 48 hours for a total of five freeze/thaw cycles over 240 hours. The results of the two groups were then compared using statistical methods (**Table 2.3**). A significant time effect was observed for ten analytes: 4-hydroxybenzaldehyde, cyanidin-3-glucoside, ferulic acid, isovanillic acid, methyl 3,4-dihydroxybenzoate, protocatechuic acid, protocatechuic acid-3/4-sulfate, phloroglucinaldehyde, vanillic acid, and vanillic acid-4-sulfate. This indicates that these metabolites showed a significant change in concentration compared to the initial 1 μ M concentration during the five freeze/thaw cycles or 240 hour study period. Eight of the ten metabolites (4-hydroxybenzaldehyde, ferulic acid, methyl 3,4-dihydroxybenzoate, protocatechuic acid, protocatechuic acid-3/4-sulfate, phloroglucinaldehyde, vanillic acid, and vanillic acid-4-glucuronide) demonstrated an increase in concentration compared to the initial 1 μ M concentration after the five freeze/thaw cycles or 240 hour study period.

Of the ten analytes showing a significant time effect, post-hoc Bonferroni test indicated that six of these metabolites (4-hydroxybenzaldehyde, isovanillic acid, methyl 3,4-dihydroxybenzoate, protocatechuic acid, protocatechuic acid-3/4-sulfate, vanillic acid-4-glucuronide) were significantly different from the initial concentration of 1 μ M following two freeze/thaw cycles or 96 hours ($p \leq 0.05$) (**Figure 2.4**). A significant freeze/thaw effect was observed for cyanidin-3-glucoside indicating that the difference in the number of freeze/thaw cycles to which the sample groups were subjected resulted in significantly different cyanidin-3-glucoside concentrations in the control samples compared to the freeze/thaw samples. Cyanidin-3-glucoside was found at a higher percentage concentration compared to the initial concentration in the control samples ($97.2 \pm 14.9\%$) relative to the freeze/thaw samples ($15.3 \pm 5.5\%$) after five freeze/thaw cycles. A significant interaction effect between time and the number of freeze/thaw cycles was observed for cyanidin-3-glucoside and vanillic acid-4-glucuronide indicating that the number of freeze/thaw cycles had a differential effect on the stability of these metabolites depending on the time-point.

Table 2.3 Statistical significance of the effect of five freeze/thaw cycles on anthocyanin metabolite stability in serum.

Analyte	Time effect	FT effect	Time*FT effect	Freeze/thaw cycles					
	(p-value)	(p-value)	(p-value)	0 ^a	1 ^a	2 ^a	3 ^a	4 ^a	5 ^a
4-hydroxybenzaldehyde	0.018	NS	NS	a	a	b	b	b	b
Benzoic acid-4-glucuronide	NS	NS	NS	NS	NS	NS	NS	NS	NS
Cyanidin-3-glucoside	0.008	<0.001	0.005	a	a,b	a,b	a	b	c
Ferulic acid	0.011	NS	NS	a,b,c	b	a,b	a,c	c	a,c
Hippuric acid	NS	NS	NS	NS	NS	NS	NS	NS	NS
Isovanillic acid	0.022	NS	NS	a	a,b	b	b	a,b	a,b
Isovanillic acid-3-glucuronide	NS	NS	NS	NS	NS	NS	NS	NS	NS
(Iso)vanillic acid-3/4-sulfate	NS	NS	NS	NS	NS	NS	NS	NS	NS
Methyl 3,4-dihydroxybenzoate	0.027	NS	NS	a	b	c	c,d	d	d
Protocatechuic acid	0.015	NS	NS	a	b	b	b	a,b	b
Protocatechuic acid-3-glucuronide	NS	NS	NS	NS	NS	NS	NS	NS	NS
Protocatechuic acid-3/4-sulfate	0.042	NS	NS	a	b	b,c	c	c	c
Protocatechuic acid-4-glucuronide	NS	NS	NS	NS	NS	NS	NS	NS	NS
Phloroglucinaldehyde	0.016	NS	NS	a,b	a	b,c	c,d	e	d,e
Vanillic acid	0.013	NS	NS	a,b	b	a,b,c	c,d	d	a,c,d
Vanillic acid-4-glucuronide	<0.001	NS	0.003	a	b	c	b,c	b,c	b,c

p≤0.05, n=4, two-way repeated measures ANOVA with Bonferroni post-hoc test. FT, freeze/thaw; NS, not statistically significant. ^aDifferent letters represent statistical differences between groups. Time effect indicates that there was a significant change in metabolite concentration compared to the initial 1 µM concentration during the five freeze/thaw cycles or 240 hour study period. FT effect indicates that the difference in the number of freeze/thaw cycles to which the sample groups were subjected resulted in significantly different metabolite concentrations in the control samples (not subjected to freeze/thaw cycling) compared to the freeze/thaw samples. Time*FT effect indicates that the number of freeze/thaw cycles had a differential effect on metabolite concentration depending on the time-point.

Figure 2.4 Metabolite concentration as a percentage of initial concentration in control and freeze/thaw serum samples across five freeze/thaw cycles.

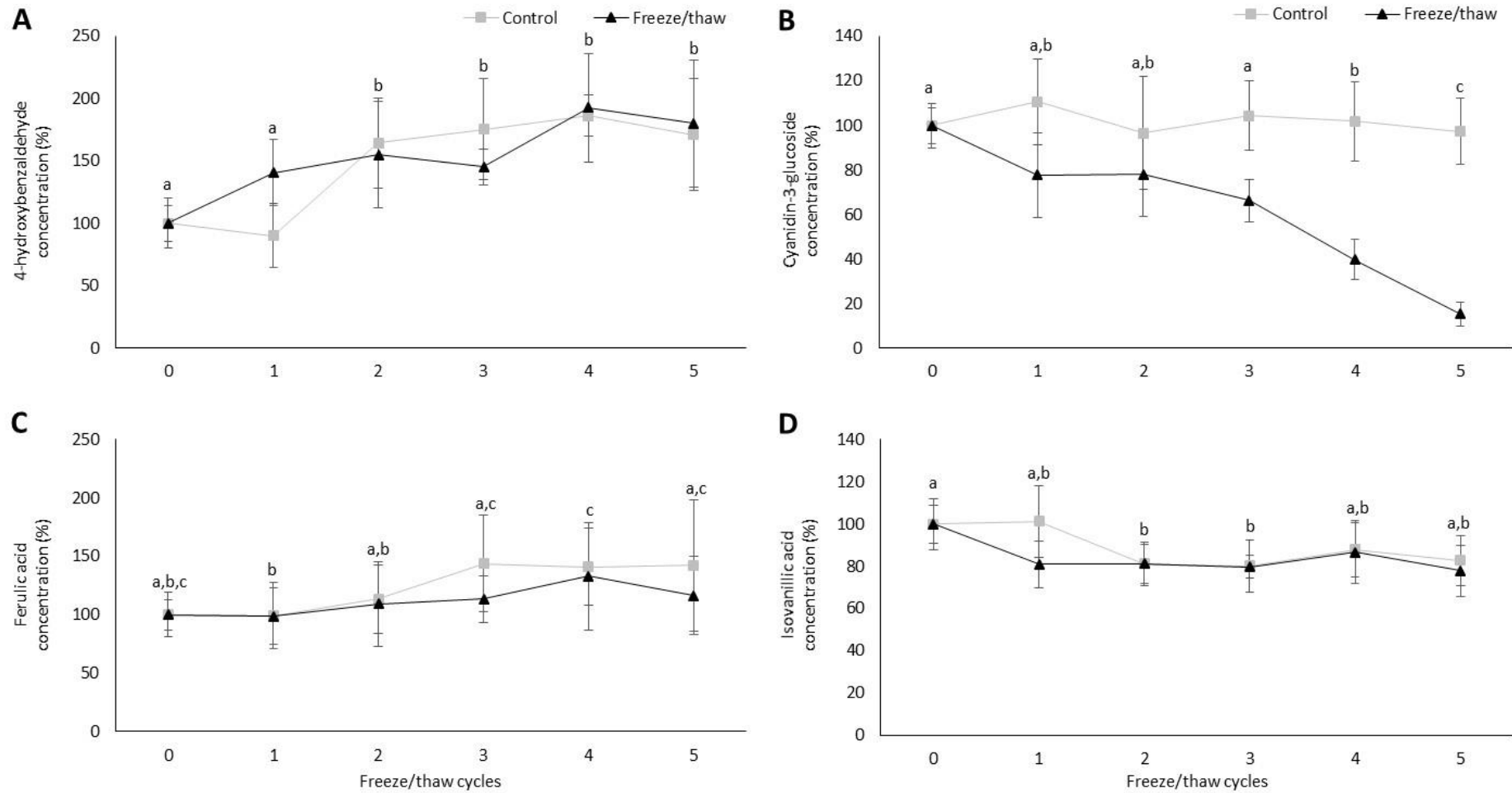


Figure 2.4 (Continued)

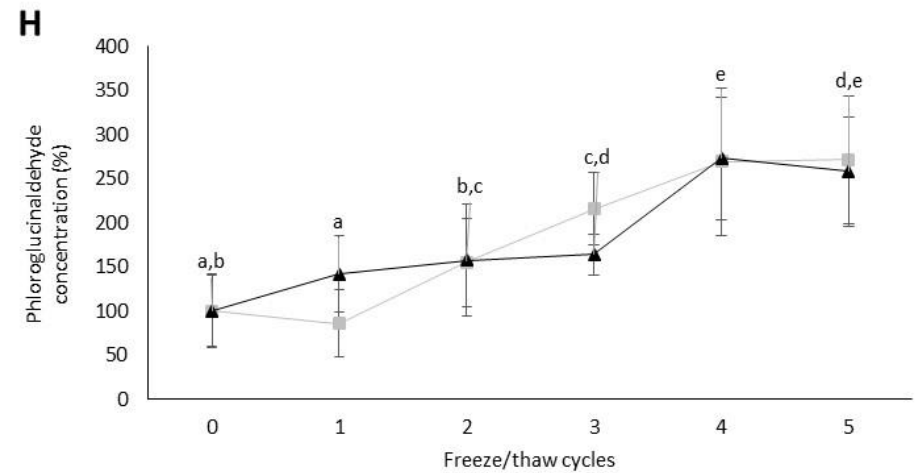
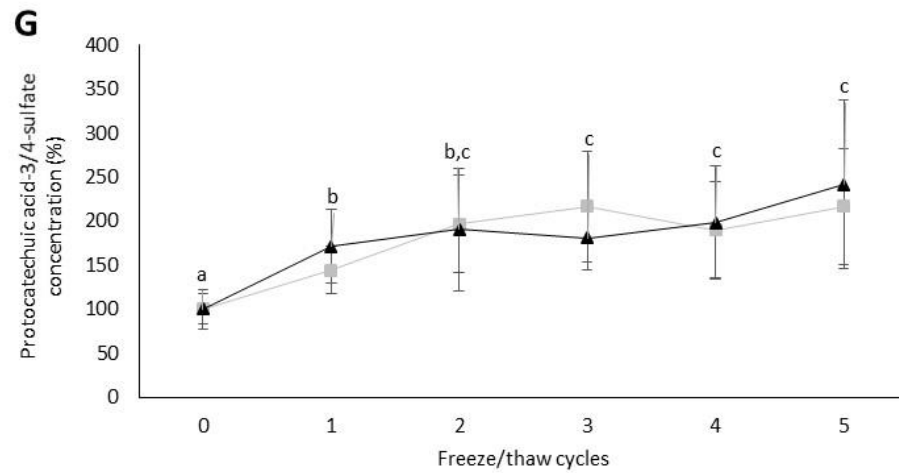
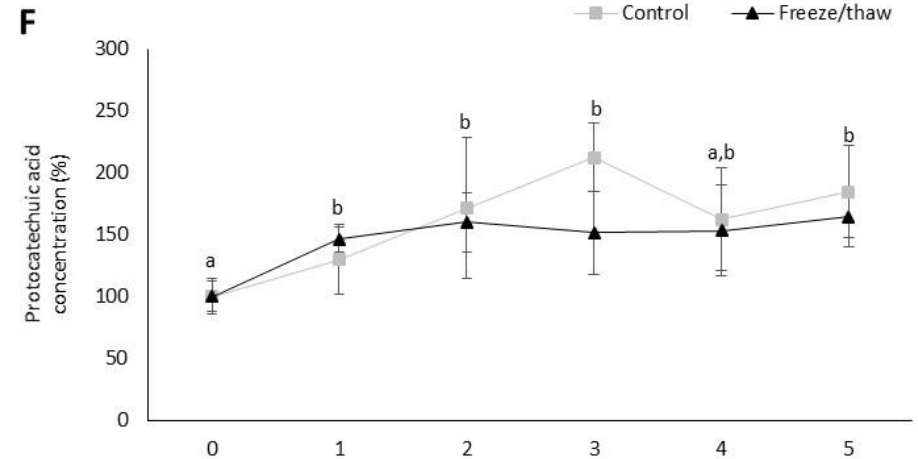
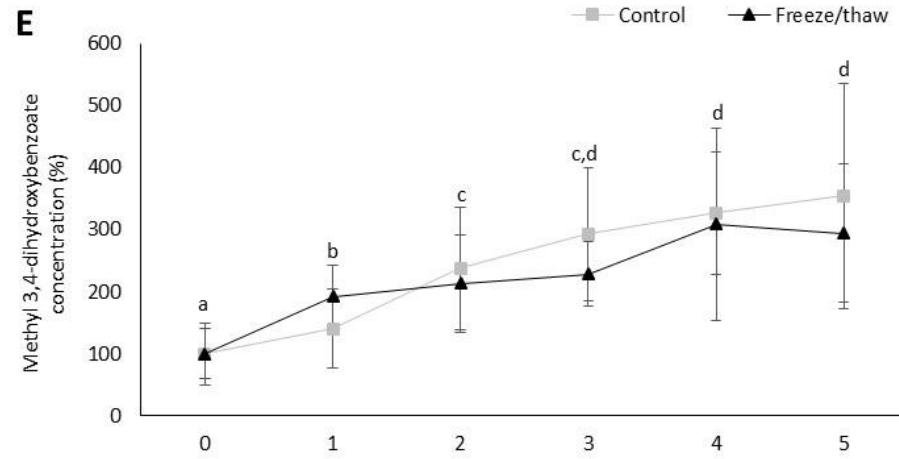
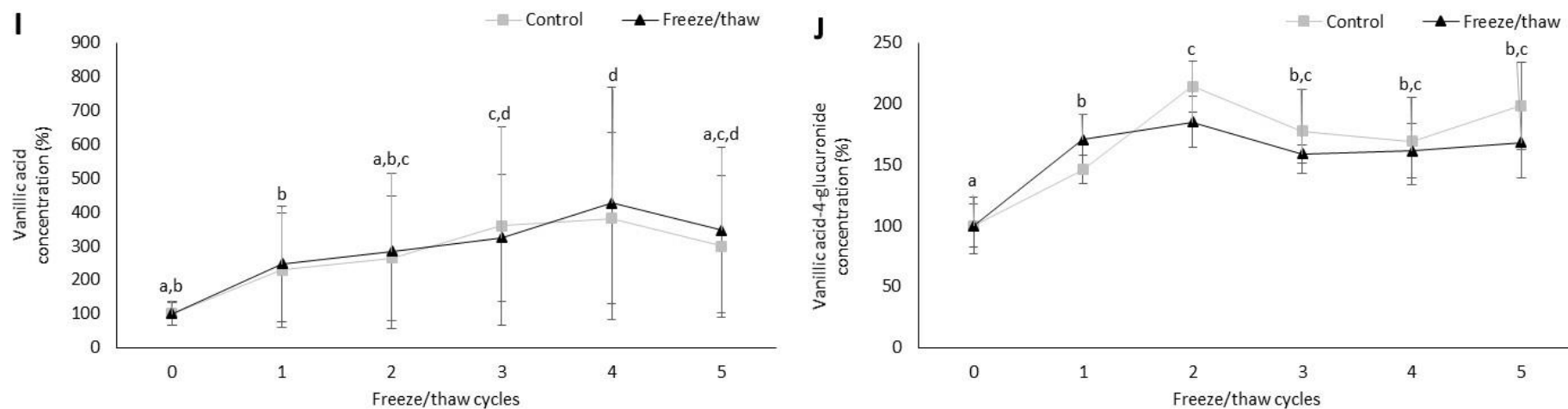


Figure 2.4 (Continued)



(A) 4-hydroxybenzaldehyde. (B) cyanidin-3-glucoside. (C) ferulic acid. (D) isovanillic acid. (E) methyl 3,4-dihydroxybenzoate. (F) protocatechuic acid. (G) protocatechuic acid-3/4-sulfate. (H) phloroglucinaldehyde. (I) vanillic acid. (J) vanillic acid-4-glucuronide. Raw data corrected relative to the scopoletin internal standard. Results expressed as mean \pm SD, n=4.

2.4. Discussion

The present study aimed to inform future clinical studies by providing information on how the stability of anthocyanins and their phenolic serum metabolites is affected by different storage conditions. The effect of acidifying serum samples to pH 2.4 using formic acid prior to storage was investigated by monitoring metabolite concentrations in non-acidified and acidified serum samples stored at -80°C for 240 hours. This analysis found that, of the 16 analytes tested, only the parent anthocyanin, cyanidin-3-glucoside, was affected by sample storage pH. After 48 hours, cyanidin-3-glucoside concentration in the non-acidified samples had decreased to $33.3 \pm 8.7\%$ of the initial concentration while there was no change in the acidified samples. The structural instability of anthocyanins in mildly acidic, neutral and basic environments is well-established (Rein 2005, Fleschhut *et al.* 2006, Woodward *et al.* 2009), however, the effect of pH on the stability on phenolic metabolites of anthocyanins is less clear. The results of the present study suggest that the stability of phenolic metabolites in serum samples is unaffected by pH. As a result, future clinical studies looking to detect metabolites of anthocyanins and not the parent anthocyanins themselves, may wish to consider foregoing the time-consuming process of sample acidification prior to storage due to the minimal effect on metabolite recovery.

The effect of submitting serum samples to numerous freeze/thaw cycles was also investigated by monitoring metabolite concentrations in samples stored continuously at -80°C (i.e. control samples not subjected to freeze/thaw cycling) and samples exposed to between one and five freeze/thaw cycles. This analysis also found that it was only cyanidin-3-glucoside that was affected by freeze/thaw cycling. Following one freeze/thaw cycle, cyanidin-3-glucoside concentration had decreased to $77.6 \pm 19.0\%$ of the starting concentration and continued decreasing until it had reached $15.3 \pm 5.5\%$ following five freeze/thaw cycles. At the equivalent time-points, cyanidin-3-glucoside concentration in the control was unaltered. This observation contradicts previous work carried out within our lab that showed that anthocyanins are stable through at least six freeze/thaw cycles (Woodward *et al.* 2009). However, whilst the present study used a solid-phase extracted serum matrix, the previous study investigated the stability of anthocyanins in an acidified buffer solution (10 mM Na/K phosphate buffer in 2% HCl). Woodward *et al.* reported increased stability of anthocyanin compounds over 24 hours at 37°C in the buffer solution compared to water. This suggests that the presence of the buffer salts is important in maintaining the stability of the anthocyanin compounds. The removal of buffer salts along with proteins and other impurities from the serum matrix during the SPE process may explain the instability of

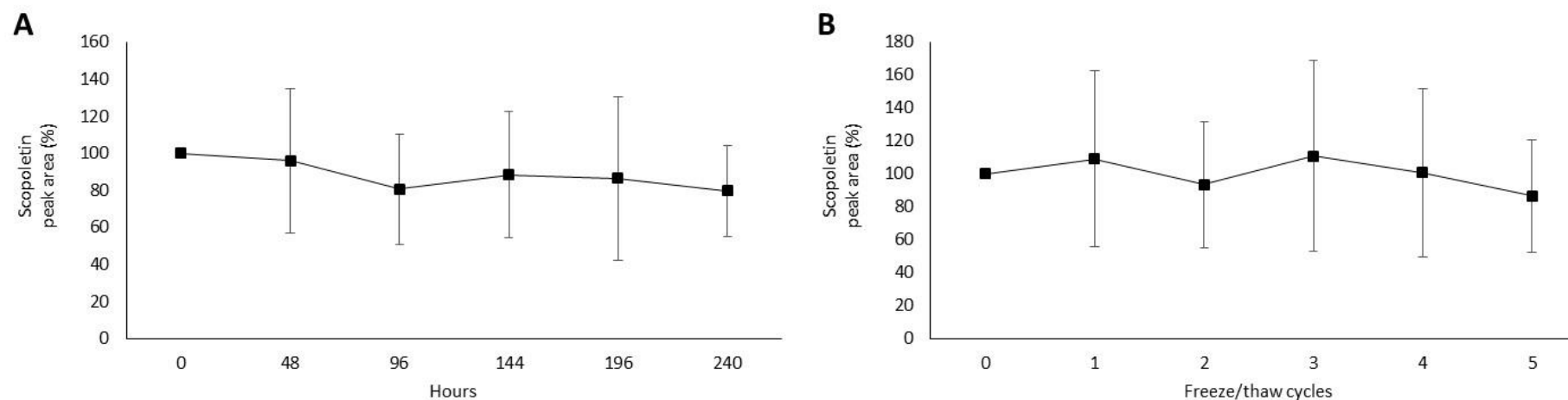
cyanidin-3-glucoside caused by freeze/thaw cycling observed in the present study. Little work has been done to establish the effect of freeze/thaw cycling on the stability of phenolic metabolites of anthocyanins. The results of the present study suggest that future clinical studies looking to detect metabolites of anthocyanins, and not the parent anthocyanins themselves, should not be concerned with subjecting clinical samples to up to five freeze/thaw cycles due to the minimal effect on metabolite recovery.

Across both analyses, 11 of the 16 metabolites tested showed a significant change in concentration compared to the initial concentration during the five freeze/thaw cycles or 240 hour study period with an average change in concentration of $43.3 \pm 34.7\%$ after 48 hours or 1 freeze/thaw cycle. Of the 11 metabolites that showed a significant change in concentration, nine exhibited an increase in metabolite concentration compared to the initial concentration during the study period. With regards to phloroglucinaldehyde and protocatechuic acid, this increase in concentration may be explained by the degradation of the parent anthocyanin, cyanidin-3-glucoside, into its A-ring and B-ring derivatives; (phloroglucinaldehyde and protocatechuic acid, respectively) a process has been reported to take place rapidly *in vitro* (Woodward *et al.* 2009). However, spontaneous formation of the remaining phenolic metabolites has not been demonstrated *in vivo* and does not provide an adequate explanation for the increase in methylated, sulfated and glucuronidated phase II metabolites which are mainly formed within the liver in the presence of methyltransferase, sulfotransferase and UDP-glucuronosyltransferase proteins (Kay 2006). A more likely explanation for the observed increases in metabolite concentration is that they are the result of the variability of the analytical method leading to poor reproducibility of the sample analysis. Whilst the scopoletin internal standard peak areas were within the normal expected range (**Table 2.4**), the scopoletin response at the final time-point had decreased to $78.1 \pm 10.1\%$ of the response at the first time-point (**Figure 2.5**) which suggests that changes in internal standard response are responsible for the changes in metabolite concentration across time-points. Future studies would benefit from using alternative methods of accounting for sample variation such as isotope-labelled internal standards. Another possible explanation for the increases in concentration observed during this study is the reduction in matrix effects during the study. Condensation of ion suppressing factors such as proteins and phospholipids that remained within the extracted matrix would lead to an increase in analyte response over the length of the study. This issue could be addressed in the future by comparing samples against both a fresh standard curve prepared on the day of analysis and a standard curve subject to the same storage protocol as the samples.

Table 2.4 Variation in scopoletin internal standard peak areas using the HPLC-ESI-MS/MS method.

Ionisation mode	Present study	Overall	
	Mean peak area (counts per second)	Mean peak area (counts per second)	Peak area range (counts per second)
Negative	$1.86 \times 10^6 \pm 1.98 \times 10^5$	$1.43 \times 10^6 \pm 4.51 \times 10^5$	$4.05 \times 10^5 - 2.38 \times 10^6$
Positive	$3.00 \times 10^6 \pm 2.36 \times 10^5$	$3.34 \times 10^6 \pm 9.43 \times 10^5$	$4.18 \times 10^5 - 5.02 \times 10^6$

Scopoletin peak areas observed in both negative and positive ionisation modes, during the sample runs associated with the metabolite stability study (Present study) and during the sample runs associated with the entire project (Overall) to assess the relative response of the internal standard. Results expressed as mean \pm SD, or min – max range.

Figure 2.5 Scopoletin internal standard peak area as a percentage of initial peak area during the present study.

(A) Acid effect samples. (B) freeze/thaw effect samples. Results expressed as mean \pm SD, n=4.

The present study suggests that while the parent anthocyanins are sensitive to pH and freeze/thaw cycling, the stability of phenolic metabolites in serum samples is unaffected by either the serum pH or the number of freeze/thaw cycles to which samples are subjected as phenolic metabolites were found to maintain their initial concentrations during the study period.

Future studies should investigate the stability of phenolic metabolites in urine samples to establish whether acidification or freeze/thaw cycles affects stability in this matrix. The present study spiked a mixed standard of anthocyanin metabolites into a pre-extracted serum matrix. Future studies may wish to investigate the stability of anthocyanin metabolites in a matrix that more closely matches the clinical situation where serum samples are collected, acidified and frozen prior to extraction and further storage. As reported previously (Woodward *et al.* 2009), the mix of buffer salts and proteins present in serum may affect the stability of anthocyanins and their metabolites in storage and further investigation of this effect may yield important information about the optimal storage procedures for clinical samples containing anthocyanins and their phenolic metabolites.

2.5. Conclusion

The present study provides valuable information for future clinical studies investigating anthocyanins and their phenolic metabolites. The results of the present study suggest that the stability of phenolic metabolites in serum samples is unaffected by either sample pH or number of freeze/thaw cycles to which samples are subjected whereas the stability of the parent anthocyanins are affected by both factors. Future clinical studies that are interested in the phenolic metabolites of anthocyanins and not the parent anthocyanins themselves, may wish to reduce the burden of sample processing by foregoing sample acidification and sample aliquoting to minimise the number of freeze/thaw cycles as the effect on metabolite recovery is likely to be minimal.

Chapter 3. Development of HPLC-ESI-MS/MS Methods for Quantifying Anthocyanin Metabolites in Human Serum and Urine.

3.1. Introduction

Diets including a high intake of anthocyanins have been linked to a reduced risk of cardiovascular disease (Jennings *et al.* 2012, Cassidy *et al.* 2013) but due to the low bioavailability of the parent anthocyanins (Felgines *et al.* 2003, Kay *et al.* 2005) it has been suggested that the observed bioactivity may be caused by the phenolic metabolites of anthocyanins (Czank *et al.* 2013, Rodriguez-Mateos *et al.* 2013). An HPLC-ESI-MS/MS (HPLC coupled to an electrospray ionisation source and tandem mass spectrometer) method was developed previously by our group for the detection and quantification of anthocyanin metabolites in biological samples (Czank *et al.* 2013, de Ferrars *et al.* 2014c). However, the nanomolar concentrations at which many of these metabolites are reported (Czank *et al.* 2013, de Ferrars *et al.* 2014a) are close to the limits of detection (LOD) for the current HPLC-ESI-MS/MS method, making reliable detection and accurate quantification difficult. In addition, the current HPLC-ESI-MS/MS method utilises solid-phase extraction (SPE) of serum and urine samples and had a run time of 32 minutes per sample resulting in time-consuming sample extraction and long run times when analysing large numbers of samples.

Mobile phase additives such as ammonium formate and ammonium acetate have been shown to have mixed results depending on the analytes tested (Mallet *et al.* 2004) but previous studies have demonstrated that when analysing flavonoids, sensitivity can be optimised through the use of ammonium buffers in the mobile phase (Rauha *et al.* 2001, de Rijke *et al.* 2003). To improve the reliability of quantification for the metabolites found at low concentrations and enable detection of any novel metabolites present at levels below the LOD of the current method, it was hypothesised that improvements in ionisation efficiency may be achieved via the addition of ammonium buffer salts to the aqueous mobile phase.

SPE can be a time-consuming method of sample extraction but is important for mass spectrometric analysis of serum or plasma samples due to the high level of salts, proteins, and phospholipids present in these matrices that, if not removed, can lead to ion suppression and reduced sensitivity (Bylda *et al.* 2014). Urine, however, has much lower levels of ion-

suppressing matrix components (Adachi *et al.* 2006, Chang *et al.* 2007) and therefore it was hypothesised that urine sample extraction time may be reduced via the use of alternative techniques such as dilution (often referred to as 'dilute-and-shoot'; D&S) and protein precipitation (PPT) without negatively affecting the sensitivity of the current method.

Our current HPLC-ESI-MS/MS method is capable of chromatographically separating and quantifying over 40 phenolic metabolites of cyanidin-3-glucoside at nanomolar concentrations over a 32 minute run time (Czank *et al.* 2013, de Ferrars *et al.* 2014c). It was hypothesised that further development of this method via optimisation of HPLC parameters and the use of alternative column dimensions may enable similar or better chromatographic separation, peak shape and method sensitivity to be achieved within a shorter run time, therefore reducing sample analysis times.

The aims of the present study were to improve method sensitivity via the use of ammonium-buffered mobile phase, investigate alternative extraction techniques suitable for processing urine samples prior to analysis, and to reduce sample run time from 32 minutes.

3.2. Methods

3.2.1. Materials and reagents

Acetonitrile and methanol were purchased from Fisher Scientific (Loughborough, UK). Strata-X™ 33 µm polymeric sorbent 500 mg/6 mL solid-phase extraction cartridges, Kinetex® pentafluorophenyl (PFP) high-performance liquid chromatography (HPLC) columns (2.6 µm, 100 x 4.6 mm, 100 Å; 2.6 µm, 100 x 2.1 mm, 100 Å; 2.6 µm, 50 x 2.1 mm, 100 Å) and SecurityGuard® cartridges (PFP, 4.6 x 2.0 mm and 2.1 x 2.0 mm) were purchased from Phenomenex (Macclesfield, UK). Cyanidin-3-glucoside (kuromanin chloride) was purchased from Extrasynthese (Genay, France). The phase II conjugates of phenolic acids (protocatechuic acid-3-glucuronide, protocatechuic acid-4-glucuronide, protocatechuic acid-3-sulfate, protocatechuic acid-4-sulfate, isovanillic acid-3-glucuronide, vanillic acid-4-glucuronide, isovanillic acid-3-sulfate, vanillic acid-4-sulfate, benzoic acid-4-glucuronide) were synthesised by the School of Chemistry and Centre for Biomolecular Sciences, University of St. Andrews (UK) using published methods (Zhang *et al.* 2012). Methyl 3, 4-dihydroxybenzoate (3, 4-dihydroxy-benzoic acid methyl ester) was purchased from Alfa Aesar (Heysham, UK). All other materials, reagents, and standards were purchased from Sigma-Aldrich (Dorset, UK), including: Acrodisc PTFE syringe filters (13 mm, 0.45 µm), formic acid (FA), dimethyl sulfoxide (DMSO), 4-hydroxybenzaldehyde, ferulic acid (4-hydroxy-3-methoxycinnamic acid), hippuric acid (benzoylaminoacetic acid), isovanillic acid (3-hydroxy-

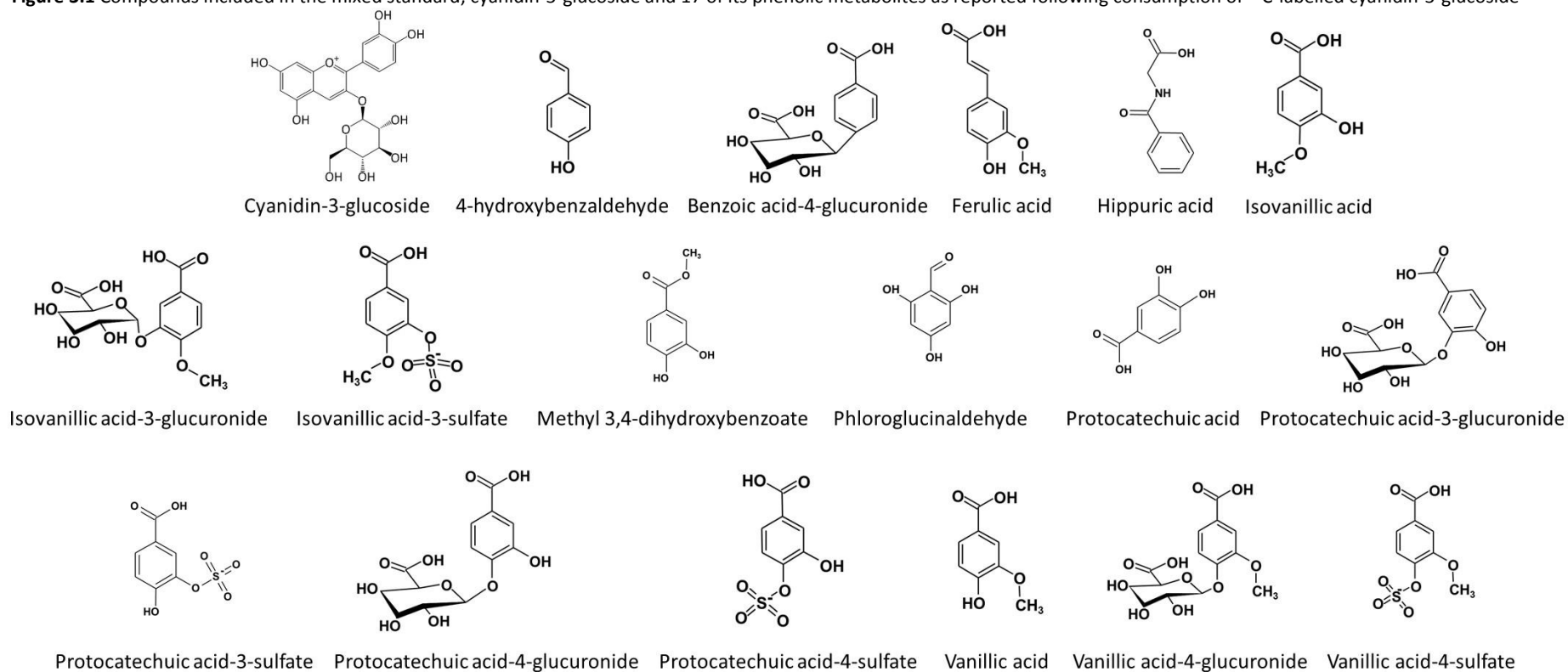
4-methoxybenzoic acid), protocatechuic acid (PCA, 3,4-dihydroxybenzoic acid), phloroglucinaldehyde (PGA, 2,4,6-trihydroxybenzaldehyde), phloridzin (phloridzin dihydrate), scopoletin (7-hydroxy-5-methoxycoumarin), and vanillic acid (4-hydroxy-3-methoxybenzoic acid). Water was 18M Ω /cm Milli-Q quality and all solvents were LC-MS grade.

3.2.2. Mobile phase development: sample preparation

A mixed standard was composed of cyanidin-3-glucoside and 17 of its phenolic metabolites, as reported following consumption of ^{13}C -labelled cyanidin-3-glucoside (Czank *et al.* 2013, de Ferrars *et al.* 2014a). The 18 compounds included in the mixed standard were cyanidin-3-glucoside, 4-hydroxybenzaldehyde, benzoic acid-4-glucuronide, ferulic acid, hippuric acid, isovanillic acid, isovanillic acid-3-glucuronide, isovanillic acid-3-sulfate, methyl 3,4-dihydroxybenzoate, phloroglucinaldehyde, protocatechuic acid, protocatechuic acid-3-glucuronide, protocatechuic acid-3-sulfate, protocatechuic acid-4-glucuronide, protocatechuic acid-4-sulfate, vanillic acid, vanillic acid-4-glucuronide, and vanillic acid-4-sulfate (**Figure 3.1**). The mixed standard was added to mobile phase diluent (0.1/5/94.9 v/v/v formic acid/methanol/water), along with scopoletin and phloridzin internal standards, to give 50 μM samples.

Ammonium formate was dissolved in water to give three solutions at 10 mM which were then separately adjusted to pH 3, pH 4 and pH 5 using formic acid. Ammonium acetate was also dissolved in water to give three solutions at 10 mM which were then separately adjusted to pH 4, pH 5 and pH 6 using acetic acid. These solutions were used in place of Mobile Phase A (0.1% [v/v] formic acid in water [pH 2.4]) to investigate the effect of ammonium buffers on method sensitivity.

Figure 3.1 Compounds included in the mixed standard; cyanidin-3-glucoside and 17 of its phenolic metabolites as reported following consumption of ^{13}C -labelled cyanidin-3-glucoside



Adapted from (Czank *et al.* 2013, de Ferrars *et al.* 2014a).

3.2.3. Extraction method development: clinical intervention study design

Banked urine samples from a previously conducted anthocyanin intervention (Czank *et al.* 2013) were used for the present analysis. Briefly, samples were originally collected from healthy males (n=8; age, 27.8 ± 8.1 y; BMI, 23.2 ± 1.5 kg/m²) prior to (t=0 h) and after consuming a 500 mg bolus of isotopically labelled cyanidin-3-glucoside containing three ¹³C-atoms on the A-ring and two ¹³C-atoms on the B-ring (6,8,10,3',5'-¹³C₅-C3G, hereafter referred to as ¹³C₅-C3G). Participants were asked to arrive on the study day in a fasted state (minimum 8 h). Individual urine samples were collected during the 6 hour study day and total urine voids were collected during the 6-24h and 24-48 hour periods. An anthocyanin-free meal was provided between 2-4 hours post-bolus. Participants were asked to maintain a low anthocyanin diet for the next 48 hours. Participants were also asked to avoid any foods containing high levels of anthocyanins and ¹³C (Morrison *et al.* 2000) over the 7 day run-in period and during the intervention. Upon collection, the urine samples were combined with 100 mg of ascorbate per 500 mL of urine and were also acidified manually to pH 2.4 using formic acid. All samples were stored at -80°C until analysis.

3.2.4. Extraction method development: sample preparation

A mixed standard was composed of cyanidin-3-glucoside and six of its serum metabolites, as reported following consumption of ¹³C-labelled cyanidin-3-glucoside (Czank *et al.* 2013, de Ferrars *et al.* 2014a). The seven compounds included in the mixed standard were cyanidin-3-glucoside, benzoic acid-4-glucuronide, ferulic acid, hippuric acid, phloroglucinaldehyde, protocatechuic acid, and vanillic acid-4-sulfate. The mixed standard was added to pool acidified baseline urine from the ¹³C₅-C3G intervention, along with phloridzin internal standard, to give 1 µM samples.

3.2.5. Extraction method development: solid-phase extraction (SPE)

1 µM samples were extracted via SPE following previously reported methodology (Czank *et al.* 2013, de Ferrars *et al.* 2014c). Briefly, SPE cartridges were preconditioned with 6 mL of acidified methanol (acidified to pH 2.4 using formic acid) followed by 6 mL of acidified water (acidified to pH 2.4 using formic acid). Cartridges were loaded with 1 mL acidified water followed by 1 mL of sample. Samples were eluted at a flow rate of approximately 1 drop/second. Cartridges were washed with 12 mL of acidified water before being dried under vacuum for 30 mins. 5 mL of acidified methanol was added to the cartridges and left to soak for 10 mins before the samples were eluted with a total of 7 mL acidified methanol. For the 7x diluted samples (**Figure 3.2**), scopoletin volume control standard was added and the samples stored at -80°C until analysis. For the undiluted, 2x concentrated, and 4x

concentrated samples, the eluent was evaporated to approximately 50 μL on a rotary evaporator (Thermo SPD Speedvac). Following evaporation, the samples were reconstituted with either 200 μL , 450 μL , 950 μL of acidified water and scopoletin volume control standard added (Figure 3.2). The samples were then sonicated for 10 mins with the ultrasonic water bath kept cool using ice, followed by vortex mixing for 10 seconds and filtration through a 0.45 μm syringe filter. Samples were stored at -80°C until analysis.

3.2.6. Extraction method development: dilute-and-shoot (D&S)

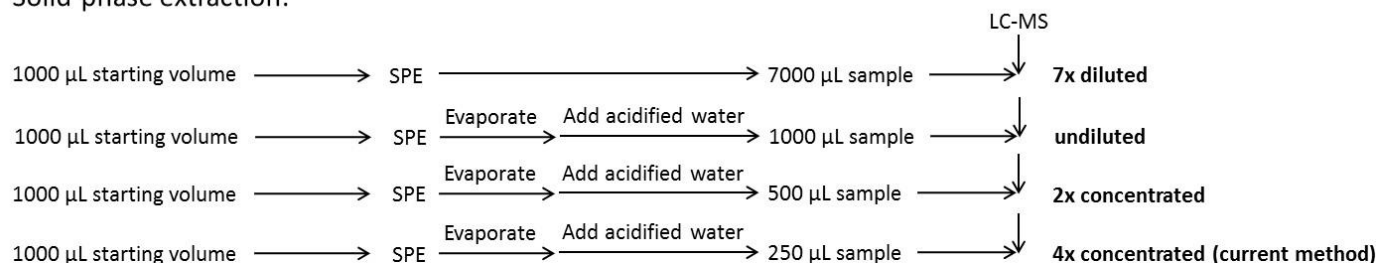
1 μM samples were extracted via D&S extraction based on previously reported methodology (Gustavsson *et al.* 2007, Fitzgerald *et al.* 2012, Warth *et al.* 2012). 200 μL samples were spiked with either 0 μL , 800 μL or 1800 μL of mobile phase diluent (0.1/5/94.9 v/v/v formic acid/methanol/water) (Figure 3.2) followed by vortex mixing for 10 seconds and filtration through a 0.45 μm syringe filter. Samples were stored at -80°C until analysis.

3.2.7. Extraction method development: protein precipitation (PPT)

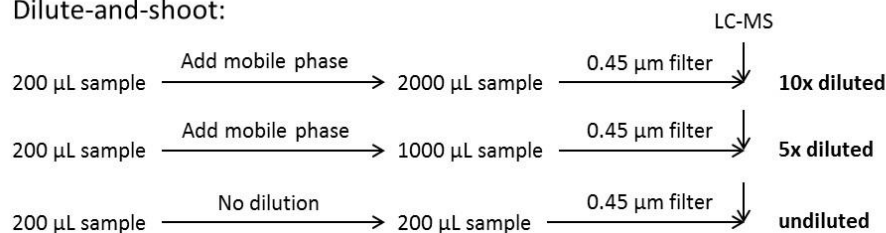
1 μM samples were extracted via PPT based on previously reported methodology (Chang *et al.* 2007, Fernández-Peralbo and Luque de Castro 2012, Raju *et al.* 2012). 200 μL samples were spiked with 800 μL of acetonitrile containing 0.1% v/v formic acid, mixed by vortex for 10 seconds, stored at -20°C for 30 mins and centrifuged at $4000 \times g$, 8°C for 10 mins. After centrifugation, the supernatant was removed, placed into a test tube and evaporated to dryness on a Thermo Speedvac concentrator. Samples were reconstituted with either 50 μL , 100 μL , 200 μL or 1000 μL of mobile phase diluent (0.1/5/94.9 v/v/v formic acid/methanol/water) (Figure 3.2). Samples were sonicated for 10 mins with the ultrasonic water bath kept cool using ice, followed by vortex mixing for 10 seconds and filtration through a 0.45 μm syringe filter. Samples were stored at -80°C until analysis.

Figure 3.2 Experimental design of extraction method development protocol showing the differences between the various extraction methods tested. Current method is solid-phase extraction (4x concentrated) as previously reported.

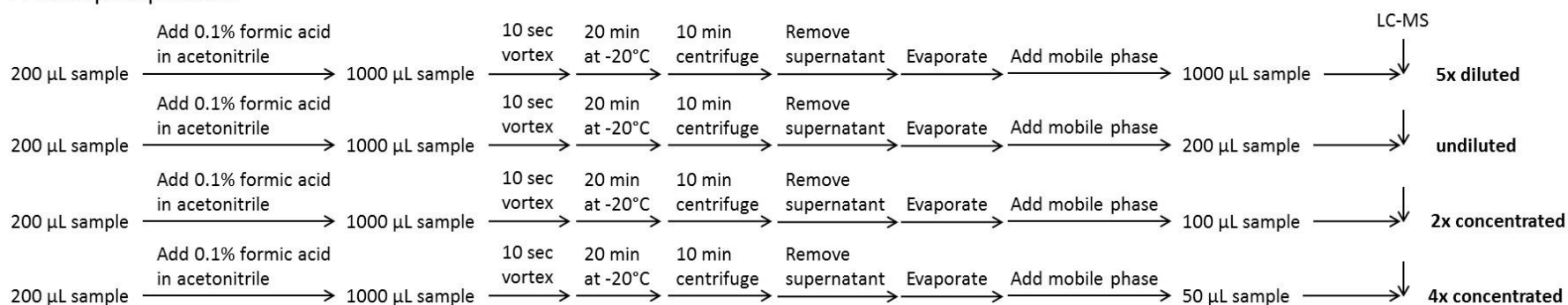
Solid-phase extraction:



Dilute-and-shoot:



Protein precipitation:



Adapted from (Czank *et al.* 2013, de Ferrars *et al.* 2014c).

3.2.8. Chromatography

HPLC-ESI-MS/MS analysis was carried out using an Agilent (Stockport, UK) 1200 series HPLC equipped with a Diode Array Detector (DAD) coupled to an AB SCIEX (Warrington, UK) 3200 series QTRAP® MS/MS system with Turbo V™ electrospray ionisation source using previously established methods (Czank *et al.* 2013, de Ferrars *et al.* 2014c). Briefly, a Kinetex® pentafluorophenyl (PFP) (2.6 µm, 100 x 4.6 mm) RP-HPLC column was used with a PFP SecurityGuard® cartridge (4.6 x 2.0 mm). The column temperature was set at 37°C, injector temperature of 4°C and injection volume of 5 µL. Mobile Phase A was 0.1% (v/v) formic acid in water and Mobile Phase B was 0.1% (v/v) formic acid in acetonitrile at a flow rate of 1.5 mL min⁻¹ at 0 min, 1 mL min⁻¹ at 7 to 14 min and 1.5 mL min⁻¹ at 14 to 32 min. The gradient consisted of 1% B at 0 min, 7.5% B at 7 min, 7.6% B at 14 min, 10% B at 17 min, 12% B at 18.5 min, 12.5% B at 20 min, 30% B at 24 min, 90% B at 25 to 28 min, 1% B at 29 to 32 min. MS/MS source parameters included ionspray voltage, -4000 V / +5500 V; temperature, 700°C; curtain gas, 40 psi; nebulizer gas and auxiliary gas, 60 psi. Multiple reaction monitoring (MRM) scans were performed using parameters optimised for the detection of analytical standards (**Table 3.1**). Samples were analysed in negative ionisation mode and in positive ionisation mode, with internal standards included in both methods. Retention time and the detection of three or more of the relevant ion transitions were used to confirm the identity of the metabolites. For quantification, the peak area of the most intense ion transition was used. A seven-point calibration (0 – 5 µM) curve was prepared for quantification of extraction method development samples by spiking a standard mixture of the compounds into a matched-matrix (blank urine) and coefficients of determination (R²) were established as linear (0.992 ± 0.010).

Table 3.1 MRM parameters used to analyse samples on the AB SCIEX 3200 QTRAP® instrument.

Compound	Transitions (m/z) precursor/product ion	Scan mode
Benzoic acid-4-glucuronide	313/175,113,93*	-
Protocatechuic acid-4-glucuronide	329.01/153*,113,109	-
Protocatechuic acid	153.01/108*,91,81	-
Protocatechuic acid-3-glucuronide	329.01/153*,113,109	-
Vanillic acid-4-glucuronide	343.01/167,152,113*	-
Isovanillic acid-3-glucuronide	343.01/167,152,113*	-
Hippuric acid	177.9/133.9*,77.1,131.8	-
Protocatechuic acid-3/4-sulfate ^a	233.01/153,109*,189	-
4-hydroxybenzaldehyde	121.2/107.8,92*,65.1	-
Isovanillic acid	169.01/151.1,125,93*	+
Vanillic acid	167.03/152*,123,108	-
(Iso)vanillic acid-3/4-sulfate ^a	247/167*,152,108	-
Methyl 3,4-dihydroxybenzoate	167/107.8*,107.1,91.2	-
Cyanidin-3-glucoside	449/287*,213,137	+
Phloroglucinaldehyde	153/151*,125,107	-
Ferulic acid	193/178,149,134*	-
Scopoletin	193/133.2*,122,94.1	+
Scopoletin	191/104*,147.9,120	-
Phloridzin	437/275, 169, 107*	+
Phloridzin	435/273*,167,123	-

*Transition used for quantitation. ^aIsomers of this metabolite were unresolvable using this HPLC-ESI-MS/MS method so were quantified as a single analyte.

3.2.9. Statistical analysis

For mobile phase and extraction method development data, one-way analysis of variance (ANOVA) with LSD post-hoc test was performed on 20 (mobile phase) or nine (extraction method) replicates using SPSS for Windows statistical software package (version 22, IBM, New York, USA). Significance was determined at the 5% confidence level. Statistical analysis was conducted on raw data with mean values graphed as percentage of current method for signal-to-noise ratio and peak width (mobile phase), and LOD (extraction method) with error bars representing standard deviation.

3.2.10. HPLC-ESI-MS/MS method development

With the aim of developing a new method with a shorter run time while maintaining the current method sensitivity, peak shape, and resolution, the HPLC chromatographic conditions were further optimised with respect to column diameter (2.1 mm; 4.6 mm), column temperature (37°C; 40°C; 50°C; 60°C; 70°C), mobile phase flow rate (0.45 mL min⁻¹ / 0.3 mL min⁻¹; 0.6 mL min⁻¹; 0.6 mL min⁻¹ / 0.4 mL min⁻¹; 0.8 mL min⁻¹; 1.5 mL min⁻¹ / 1 mL min⁻¹), gradient profile (15 min [1% B at 0 min, 7.5% B at 7 min, 7.6% B at 9 min, 90% B at 9.5 to 11.5 min, 1% B at 12 to 15 min]; 20 min [1% B at 0 min, 7.5% B at 7 min, 7.6% B at 14 min, 90% B at 14 to 17 min, 1% B at 17 to 20 min]; 32 min [1% B at 0 min, 7.5% B at 7 min, 7.6% B at 14 min, 10% B at 17 min, 12% B at 18.5 min, 12.5% B at 20 min, 30% B at 24 min, 90% B at

25 to 28 min, 1% B at 29 to 32 min]], mobile phase formic acid concentration (0.1%; 1%), column length (50 mm; 100 mm), and injection volume (1 μ L; 5 μ L).

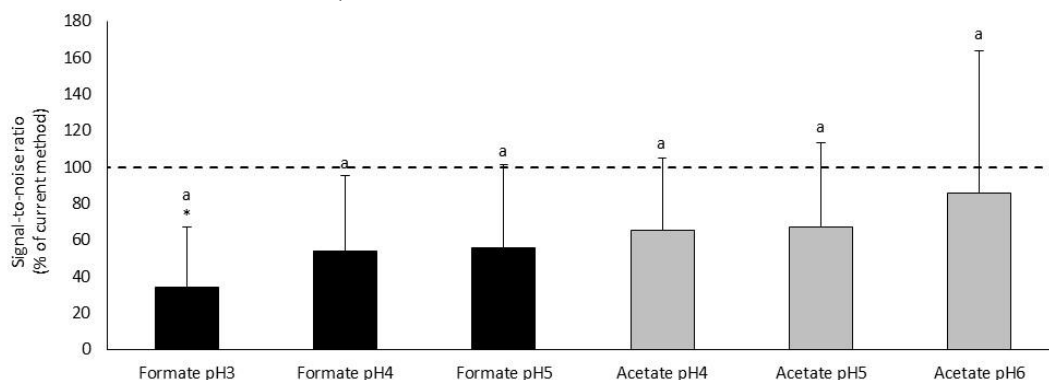
A mixed standard was composed of cyanidin-3-glucoside and 17 of its serum metabolites, as reported following consumption of ^{13}C -labelled cyanidin-3-glucoside (Czank *et al.* 2013, de Ferrars *et al.* 2014a) (Figure 3.1). The mixed standard was added to mobile phase diluent (0.1/5/94.9 v/v/v formic acid/methanol/water), along with scopoletin and phloridzin internal standards, to give 50 μM samples for use in method optimisation.

3.3. Results

3.3.1. Mobile phase development

None of the six alternative mobile phases (10 mM ammonium formate, pH 3, pH 4, pH 5; 10 mM ammonium acetate, pH 4, pH 5, pH 6) tested showed a significant increase in signal-to-noise ratio compared to the current method using 0.1% formic acid mobile phase (pH 2.4) (Figure 3.3). 10 mM Ammonium formate adjusted to pH 3 showed a significant decrease ($65.7 \pm 32.8\%$) in signal-to-noise ratio compared to the current method.

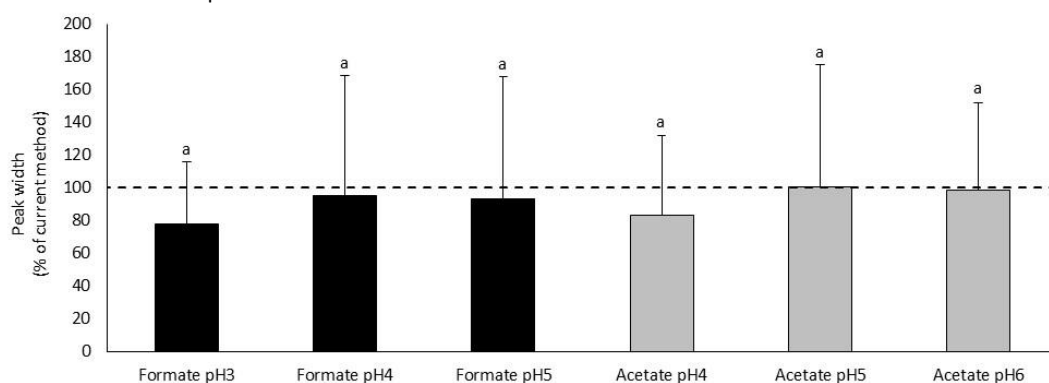
Figure 3.3 Signal-to-noise ratio observed using ammonium-buffered mobile phases compared to the current 0.1% formic acid mobile phase.



Data expressed as mean \pm SD, n=20 analytes. Significance relative to current method, *p<0.05, one-way ANOVA with LSD post-hoc test. ^aDifferent letters represent statistical differences between groups, p<0.05, one-way ANOVA with LSD post-hoc test.

None of the six alternative mobile phases tested showed a significant change in peak width compared to the current method using 0.1% formic acid mobile phase (Figure 3.4).

Figure 3.4 Peak width observed using ammonium-buffered mobile phases compared to the current 0.1% formic acid mobile phase.

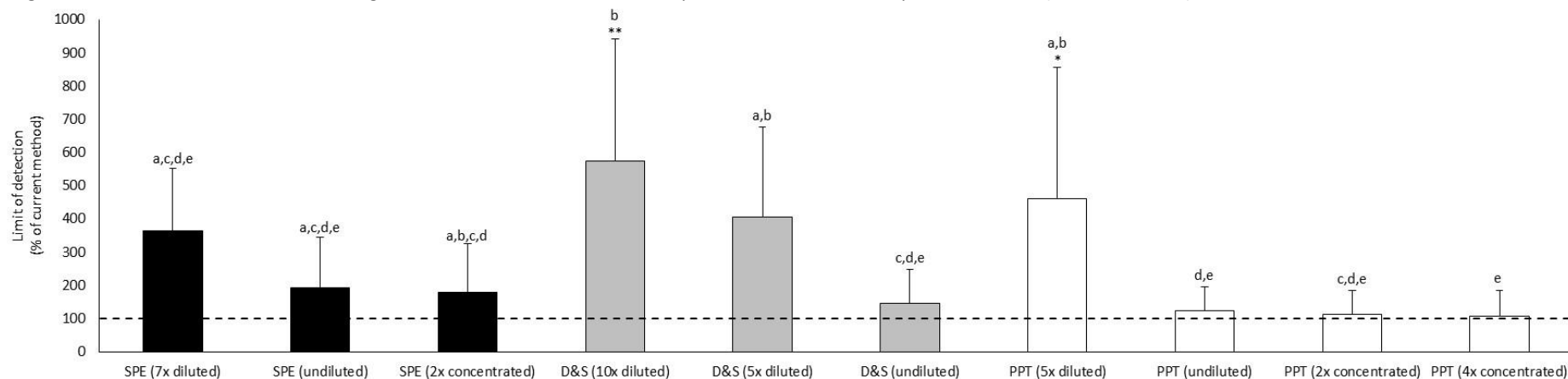


Data expressed as mean \pm SD, n=20 analytes. Significance relative to current method, * $p \leq 0.05$, one-way ANOVA with LSD post-hoc test. ^aDifferent letters represent statistical differences between groups, $p \leq 0.05$, one-way ANOVA with LSD post-hoc test.

3.3.2. Extraction method development

None of the ten alternative extraction methods (SPE 7x diluted, undiluted, 2x concentrated; D&S 10x diluted, 5x diluted, undiluted; PPT 5x diluted, undiluted, 2x concentrated, 4x concentrated) showed a significant decrease in LOD compared to the current method using SPE (4x concentrated) (**Figure 3.5**). D&S (10x diluted) ($472.9 \pm 367.9\%$) and PPT (5x diluted) ($359.6 \pm 395.7\%$) showed significant increases in LOD compared to the current method. Of the ten alternative extraction methods tested, PPT (4x concentrated) showed the lowest LOD (11.3 ± 16.0 nM).

Figure 3.5 Limit of detection observed using alternative extraction methods compared to the current solid-phase extraction (4x concentrated) method.



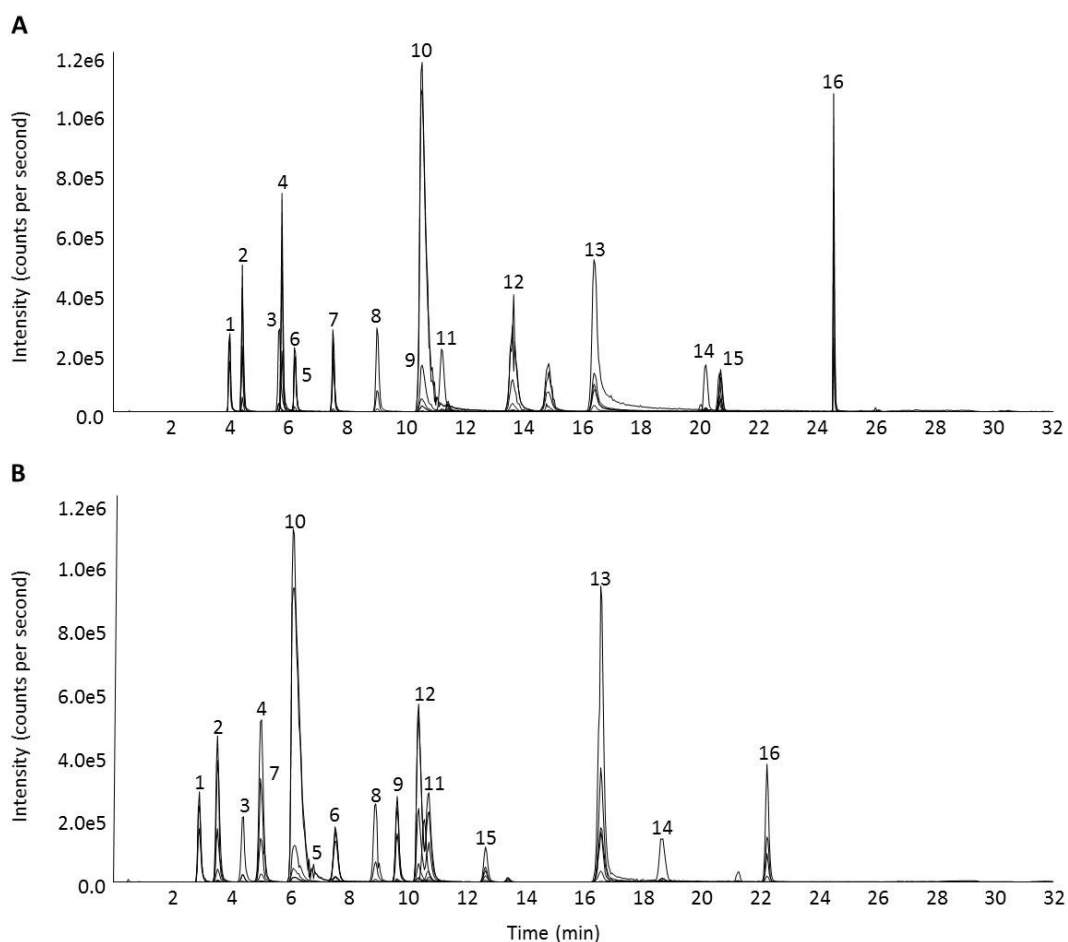
SPE, solid-phase extraction; D&S, dilute-and-shoot; PPT, protein precipitation. Data expressed as mean \pm SD, n=9 analytes. Significance relative to current method, * $p \leq 0.05$, ** $p \leq 0.01$, one-way ANOVA with LSD post-hoc test. a,b,c,d,e Different letters represent statistical differences between groups, $p \leq 0.05$, one-way ANOVA with LSD post-hoc test.

3.3.3. HPLC-ESI-MS/MS method development

The chromatographic conditions of the HPLC-ESI-MS/MS method for quantifying cyanidin-3-glucoside and its phenolic metabolites in biological samples were optimised in order to reduce sample run time from 32 minutes while maintaining the sensitivity, peak shape, and separation of the initial method.

Two column diameters were tested: 4.6 mm (as used by the initial 32 minute method) and 2.1 mm. The 2.1 mm diameter column was deemed to be preferable based upon a visual assessment of reduced elution times for all analytes (**Figure 3.6**).

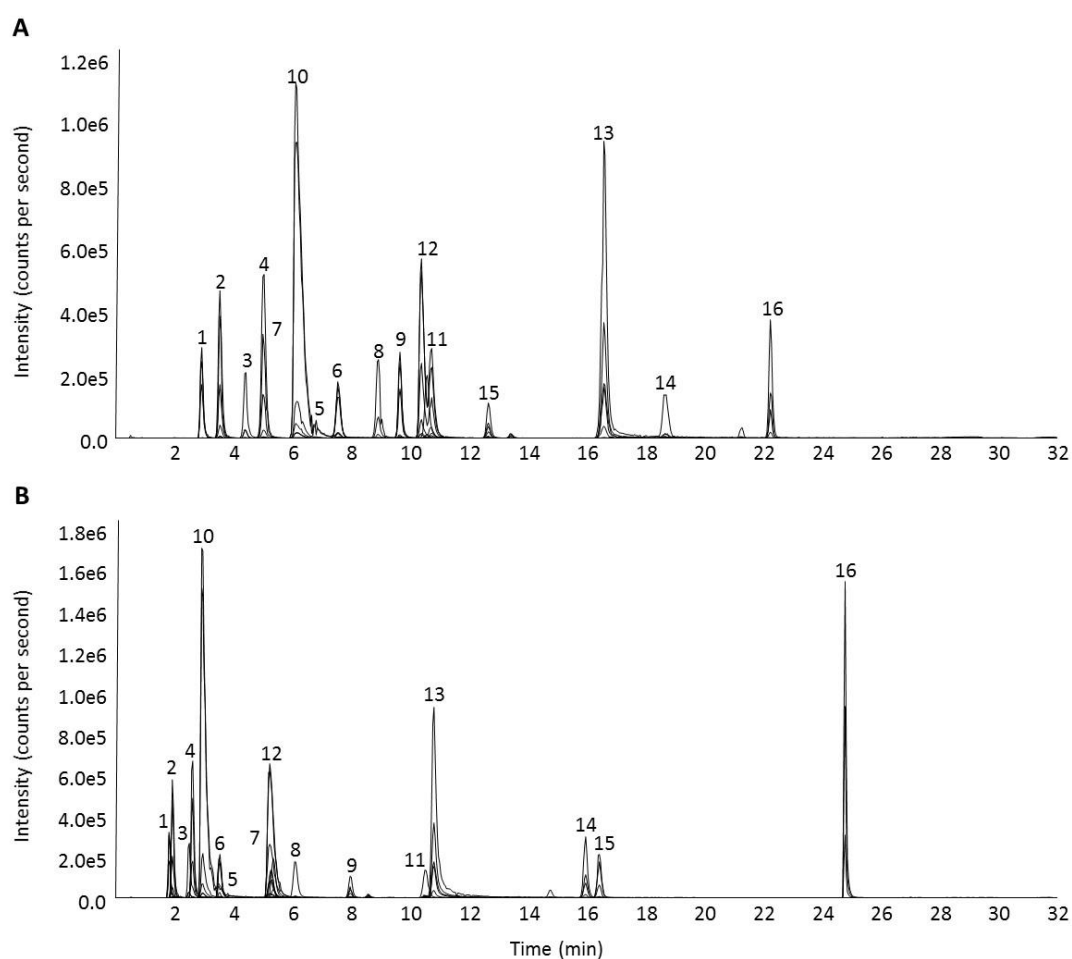
Figure 3.6 Chromatography of initial 32 minute method using column diameter of 4.6 mm (A) and following optimisation of column diameter to 2.1 mm (B) during development of an HPLC-ESI-MS/MS method with reduced run time for the quantification of cyanidin-3-glucoside and its phenolic metabolites.



1, benzoic acid-4-glucuronide; 2, protocatechuic acid-4-glucuronide; 3, protocatechuic acid; 4, protocatechuic acid-3-glucuronide; 5, vanillic acid-4-glucuronide; 6, isovanillic acid-3-glucuronide; 7, hippuric acid; 8, protocatechuic acid-3/4-sulfate; 9, 4-hydroxybenzaldehyde; 10, vanillic acid; 11, (iso)vanillic acid-3/4-sulfate; 12, methyl 3,4-dihydroxybenzoate; 13, phloroglucinaldehyde; 14, ferulic acid; 15, scopoletin; 16, phloridzin.

Five column temperatures were tested: 37°C (as used by the initial 32 minute method), 40°C, 50°C, 60°C, and 70°C. Considerable changes in chromatography were observed following relatively small changes in column temperature with 40°C deemed to be preferable based upon a visual assessment of slightly improved peak shape and reduced elution time for some analytes, particularly the analytes eluting at between 2 and 10 minutes (**Figure 3.7**).

Figure 3.7 Chromatography using column temperature of 37°C (A) and following optimisation of column temperature to 40°C (B) during development of an HPLC-ESI-MS/MS method with reduced run time for the quantification of cyanidin-3-glucoside and its phenolic metabolites.

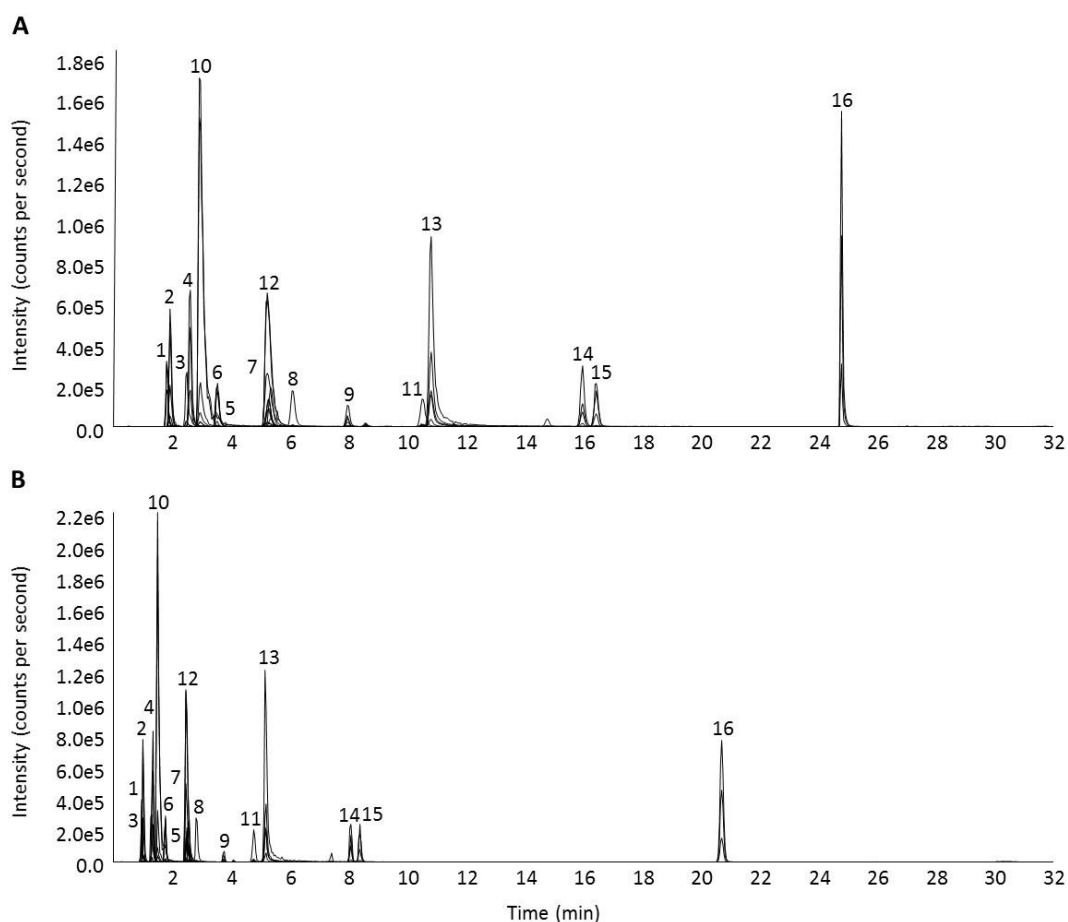


1, benzoic acid-4-glucuronide; 2, protocatechuic acid-4-glucuronide; 3, protocatechuic acid; 4, protocatechuic acid-3-glucuronide; 5, vanillic acid-4-glucuronide; 6, isovanillic acid-3-glucuronide; 7, hippuric acid; 8, protocatechuic acid-3/4-sulfate; 9, 4-hydroxybenzaldehyde; 10, vanillic acid; 11, (iso)vanillic acid-3/4-sulfate; 12, methyl 3,4-dihydroxybenzoate; 13, phloroglucinaldehyde; 14, ferulic acid; 15, scopoletin; 16, phloridzin.

Five mobile phase flow rates were tested: 1.5 mL min⁻¹ / 1.0 mL min⁻¹ (as used by the initial 32 minute method, using the 4.6 mm diameter column), 0.8 mL min⁻¹, 0.6 mL min⁻¹ / 0.4 mL min⁻¹, 0.6 mL min⁻¹, and 0.45 mL min⁻¹ / 0.3 mL min⁻¹. The four potential new flow rates were run using the 2.1 mm diameter column and compared against the original 1.5 mL min⁻¹ / 1.0 mL min⁻¹ flow rate using the 4.6 mm diameter column due to column pressure limits. The

mobile phase flow rate of 0.6 mL min^{-1} was deemed to be preferable based upon a visual assessment of slightly improved peak shape for some analytes, particularly phloroglucinaldehyde, and reduced elution time for all analytes (**Figure 3.8**).

Figure 3.8 Chromatography using mobile phase flow rate of 1.5 mL min^{-1} / 1.0 mL min^{-1} with 4.6 mm diameter column (A) and following optimisation of mobile phase flow rate to 0.6 mL min^{-1} with 2.1 mm diameter column (B) during development of an HPLC-ESI-MS/MS method with reduced run time for the quantification of cyanidin-3-glucoside and its phenolic metabolites.

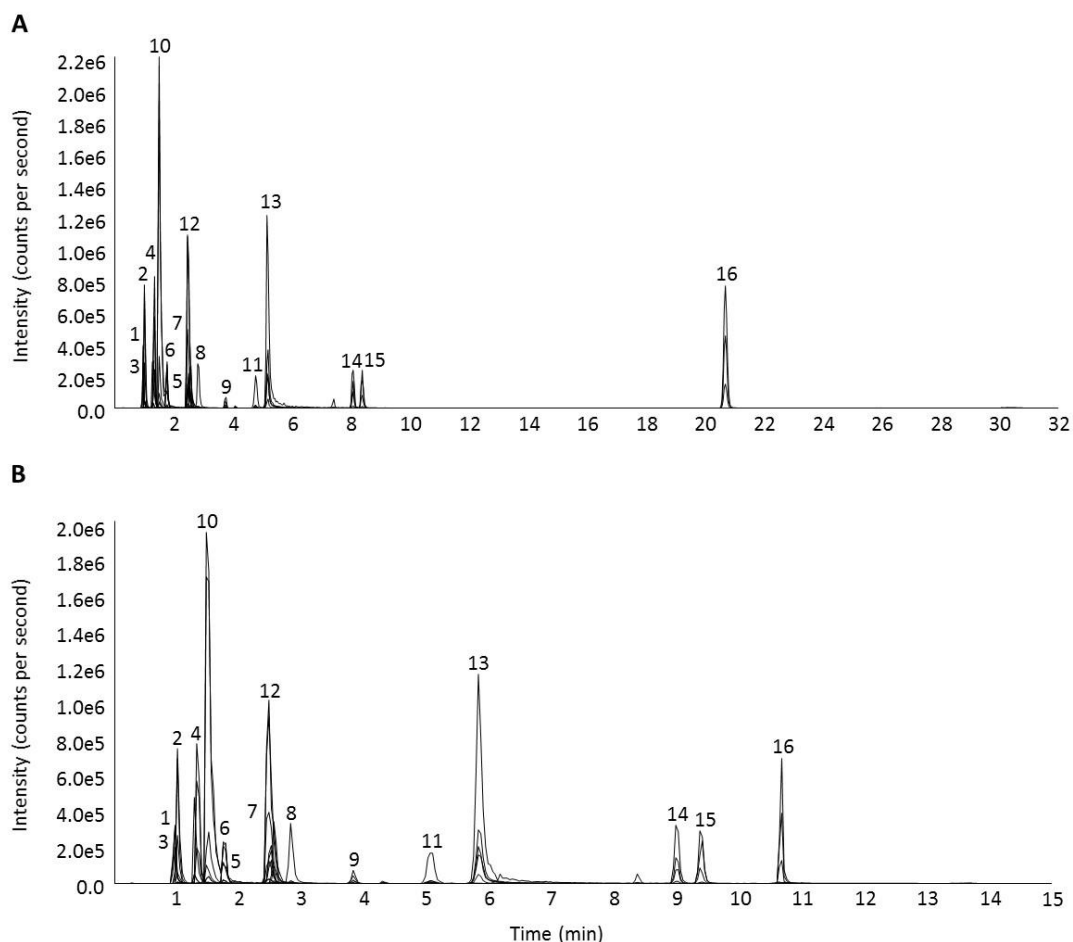


1, benzoic acid-4-glucuronide; 2, protocatechuic acid-4-glucuronide; 3, protocatechuic acid; 4, protocatechuic acid-3-glucuronide; 5, vanillic acid-4-glucuronide; 6, isovanillic acid-3-glucuronide; 7, hippuric acid; 8, protocatechuic acid-3/4-sulfate; 9, 4-hydroxybenzaldehyde; 10, vanillic acid; 11, (iso)vanillic acid-3/4-sulfate; 12, methyl 3,4-dihydroxybenzoate; 13, phloroglucinaldehyde; 14, ferulic acid; 15, scopoletin; 16, phloridzin.

Three gradient profiles were tested: 32 minutes (1% B at 0 min, 7.5% B at 7 min, 7.6% B at 14 min, 10% B at 17 min, 12% B at 18.5 min, 12.5% B at 20 min, 30% B at 24 min, 90% B at 25 to 28 min, 1% B at 29 to 32 min) (as used by the initial 32 minute method), 20 minutes (1% B at 0 min, 7.5% B at 7 min, 7.6% B at 14 min, 90% B at 14 to 17 min, 1% B at 17 to 20 min), and 15 minutes (1% B at 0 min, 7.5% B at 7 min, 7.6% B at 9 min, 90% B at 9.5 to 11.5 min, 1% B at 12 to 15 min). The 15 minute gradient profile was deemed to be preferable

based upon a visual assessment of improved peak separation, particularly the analytes eluting between 1 and 3 minutes, and reduced elution time for all analytes (**Figure 3.9**).

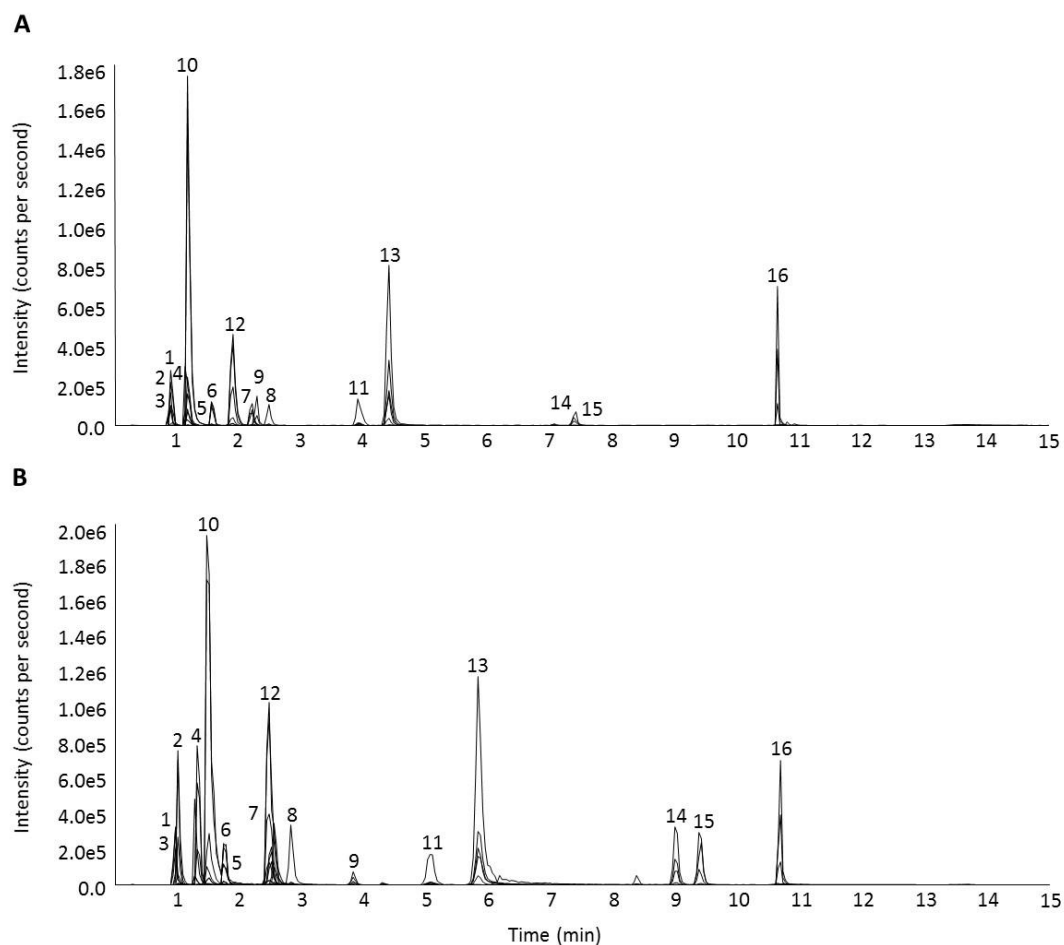
Figure 3.9 Chromatography using gradient profile of 32 minutes (1% B at 0 min, 7.5% B at 7 min, 7.6% B at 14 min, 10% B at 17 min, 12% B at 18.5 min, 12.5% B at 20 min, 30% B at 24 min, 90% B at 25 to 28 min, 1% B at 29 to 32 min) (A) and following optimisation of gradient profile to 15 minutes (1% B at 0 min, 7.5% B at 7 min, 7.6% B at 9 min, 90% B at 9.5 to 11.5 min, 1% B at 12 to 15 min) (B) during development of an HPLC-ESI-MS/MS method with reduced run time for the quantification of cyanidin-3-glucoside and its phenolic metabolites.



1, benzoic acid-4-glucuronide; 2, protocatechuic acid-4-glucuronide; 3, protocatechuic acid; 4, protocatechuic acid-3-glucuronide; 5, vanillic acid-4-glucuronide; 6, isovanillic acid-3-glucuronide; 7, hippuric acid; 8, protocatechuic acid-3/4-sulfate; 9, 4-hydroxybenzaldehyde; 10, vanillic acid; 11, (iso)vanillic acid-3/4-sulfate; 12, methyl 3,4-dihydroxybenzoate; 13, phloroglucinaldehyde; 14, ferulic acid; 15, scopoletin; 16, phloridzin.

Two mobile phase formic acid concentrations were tested: 0.1% (as used by the initial 32 minute method) and 1%. The mobile phase formic acid concentration of 0.1% was deemed to be preferable based upon a visual assessment of increased peak height for most analytes, particularly the analytes eluting at between 1 and 3 minutes, and peak separation, particularly for ferulic acid and scopoletin (**Figure 3.10**).

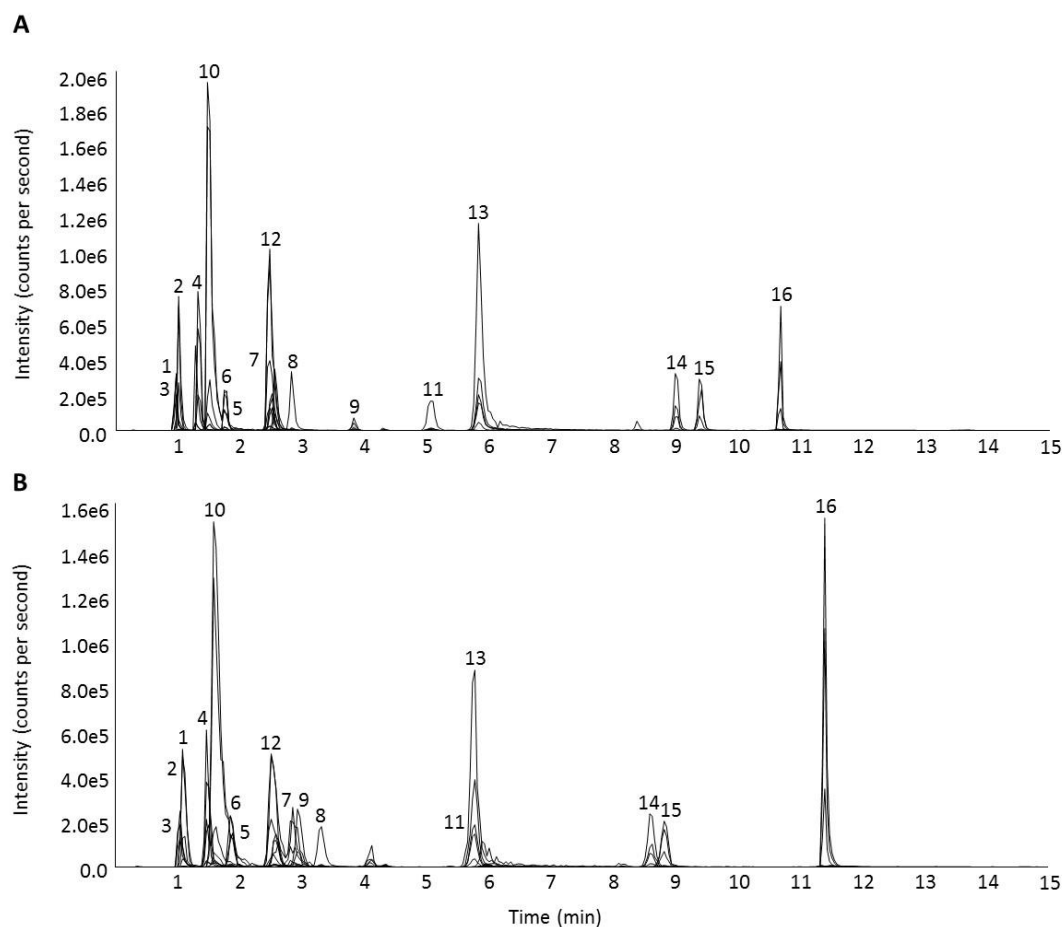
Figure 3.10 Chromatography using mobile phase formic acid concentration of 1% (A) and optimised mobile phase formic acid concentration of 0.1% (B) during development of an HPLC-ESI-MS/MS method with reduced run time for the quantification of cyanidin-3-glucoside and its phenolic metabolites.



1, benzoic acid-4-glucuronide; 2, protocatechuic acid-4-glucuronide; 3, protocatechuic acid; 4, protocatechuic acid-3-glucuronide; 5, vanillic acid-4-glucuronide; 6, isovanillic acid-3-glucuronide; 7, hippuric acid; 8, protocatechuic acid-3/4-sulfate; 9, 4-hydroxybenzaldehyde; 10, vanillic acid; 11, (iso)vanillic acid-3/4-sulfate; 12, methyl 3,4-dihydroxybenzoate; 13, phloroglucinaldehyde; 14, ferulic acid; 15, scopoletin; 16, phloridzin.

Two column lengths were tested: 100 mm (as used by the initial 32 minute method) and 50 mm. The column length of 50 mm was deemed to be preferable based upon a visual assessment of peak separation, particularly for hippuric acid and methyl 3,4-dihydroxybenzoate (**Figure 3.11**).

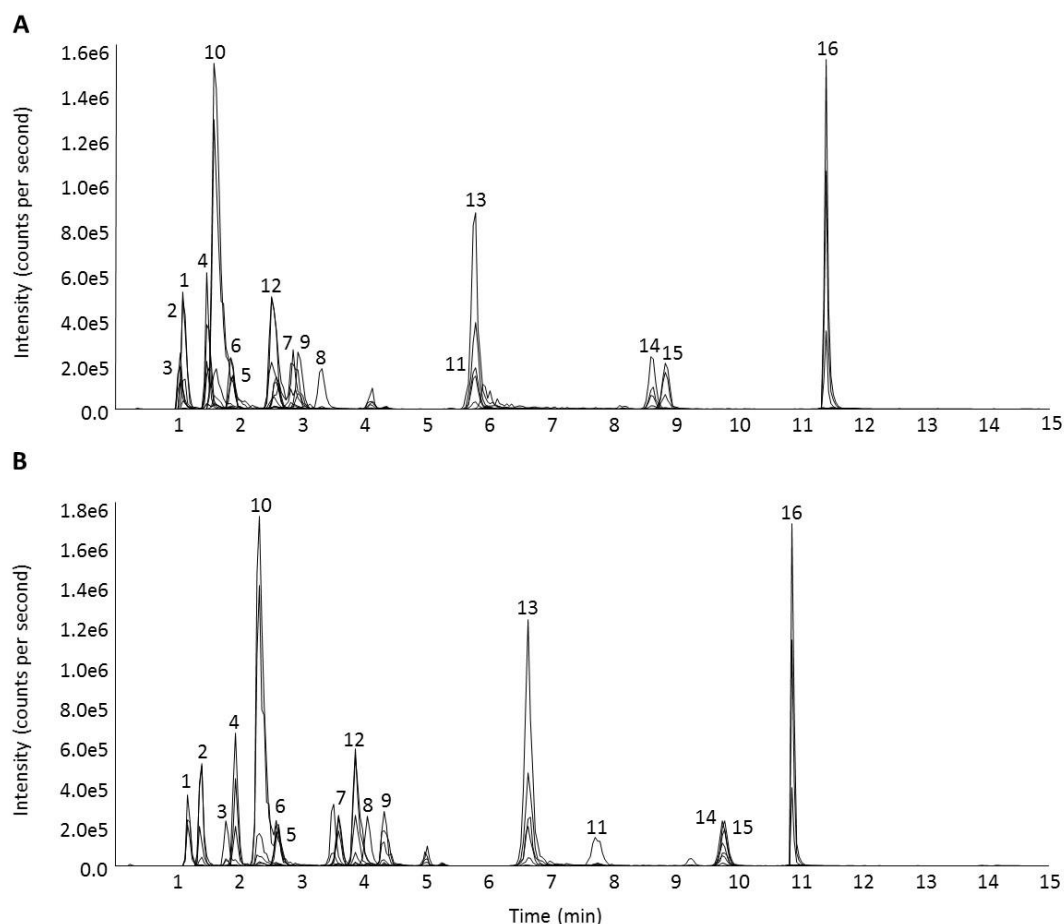
Figure 3.11 Chromatography using column length of 100 mm (A) and following optimisation of column length to 50 mm (B) during development of an HPLC-ESI-MS/MS method with reduced run time for the quantification of cyanidin-3-glucoside and its phenolic metabolites.



1, benzoic acid-4-glucuronide; 2, protocatechuic acid-4-glucuronide; 3, protocatechuic acid; 4, protocatechuic acid-3-glucuronide; 5, vanillic acid-4-glucuronide; 6, isovanillic acid-3-glucuronide; 7, hippuric acid; 8, protocatechuic acid-3/4-sulfate; 9, 4-hydroxybenzaldehyde; 10, vanillic acid; 11, (iso)vanillic acid-3/4-sulfate; 12, methyl 3,4-dihydroxybenzoate; 13, phloroglucinaldehyde; 14, ferulic acid; 15, scopoletin; 16, phloridzin.

Two injection volumes were tested: 5 μ L (as used by the initial 32 minute method) and 1 μ L. The injection volume of 5 μ L was deemed to be preferable based upon a visual assessment of improved peak separation, particularly for benzoic acid-4-glucuronide, protocatechuic acid-4-glucuronide and protocatechuic acid, and increased peak height for all analytes. This completed the development of the final optimised 15 minute method (**Figure 3.12**).

Figure 3.12 Chromatography using injection volume of 1 μ L (A) and final optimised 15 minute method with injection volume of 5 μ L (B) following development of an HPLC-ESI-MS/MS method with reduced run time for the quantification of cyanidin-3-glucoside and its phenolic metabolites.



1, benzoic acid-4-glucuronide; 2, protocatechuic acid-4-glucuronide; 3, protocatechuic acid; 4, protocatechuic acid-3-glucuronide; 5, vanillic acid-4-glucuronide; 6, isovanillic acid-3-glucuronide; 7, hippuric acid; 8, protocatechuic acid-3/4-sulfate; 9, 4-hydroxybenzaldehyde; 10, vanillic acid; 11, (iso)vanillic acid-3/4-sulfate; 12, methyl 3,4-dihydroxybenzoate; 13, phloroglucinaldehyde; 14, ferulic acid; 15, scopoletin; 16, phloridzin.

3.4. Discussion

An HPLC-ESI-MS/MS method capable of extracting, separating and quantifying over 40 phenolic metabolites of cyanidin-3-glucoside in biological samples within a 32 minute run time was developed previously by our group (Czank *et al.* 2013, de Ferrars *et al.* 2014c). The present study aimed to develop this method further by exploring the effect of ammonium-buffered mobile phases on method sensitivity, to test alternative sample extraction techniques to increase throughput during urine sample processing, and to reduce sample run time from 32 minutes via optimisation of HPLC parameters.

Six ammonium-buffered mobile phases (10 mM ammonium formate, pH 3, pH 4, pH 5; 10 mM ammonium acetate, pH 4, pH 5, pH 6) were assessed in comparison to the 0.1% formic acid solution used as the aqueous mobile phase in the current method. Ammonium formate

at pH 3 showed a decrease in signal-to-noise ratio compared to the current method while the remaining five ammonium-buffered mobile phases showed no significant change compared to the current method. None of the six ammonium-buffered mobile phases showed a significant change in peak width compared to the current method. The lack of significant change shown when using the ammonium-buffered mobile phases compared to the current method may be due to the variability in response observed from the 20 analytes tested. Whilst the mean signal-to-noise ratios as a percentage of the current method showed no significant change for five of the six ammonium-buffered mobile phases, individual analytes showed a wide variability of responses ranging from 5.8% for phloridzin (positive ionisation mode) using ammonium formate at pH 3 to 268.0% for vanillic acid-3/4-sulfate using ammonium acetate at pH 6. The difference in analyte response to change in mobile phase may be due caused by differences in the surface activity of the ammonium salts and analyte ions (Beaudry and Vachon 2006). Following droplet formation at the end of the spray needle, the charged particles with the highest surface activity will accumulate at the droplet surface, effectively blocking the evaporation into the gas phase of any ions at the centre of the droplet (Cech and Enke 2001, Zhou and Cook 2001, Henriksen *et al.* 2005). Surface activity has been linked to polarity (Henriksen *et al.* 2005) and small differences in the polarity of the metabolites may explain the difference in analyte response to change in mobile phase observed in the present study. This variation has been noted previously (Mallet *et al.* 2004) and can explain the difficulty in predicting the effect that mobile phase additives can have on the ionisation of structurally similar analytes as they compete with buffer salt ions within the ion source (Cech and Enke 2001). Despite the positive effect caused by some mobile phases on signal-to-noise ratio of some analytes, and due to prioritisation of qualitative detection and quantification of an extensive range of metabolites in the analytical method, it is necessary to compromise during method development and consider the effect that changes to the method have on analyte response as a whole. The lack of an overall significant increase in method sensitivity observed in the present study when using ammonium-buffered mobile phases means that the 0.1% formic acid mobile phase used by the current method should be considered optimal.

Ten sample extraction methods (SPE 7x diluted, undiluted, 2x concentrated; D&S 10x diluted, 5x diluted, undiluted; PPT 5x diluted, undiluted, 2x concentrated, 4x concentrated) were assessed in comparison to the SPE 4x concentrated method used in our usual method. Eight of ten methods showed no significant change in LOD from the current method with D&S (10x diluted) and PPT (5x diluted) showing significant increases in LOD compared to the

current method. Sample concentration steps are commonly included in sample extraction methods prior to LC-MS analysis in order to increase the concentration, and therefore increase the signal-to-noise ratio, of the analytes of interest (Cooke *et al.* 2006, Grace *et al.* 2007). However, it has been suggested that this approach can also result in concentration of matrix components which can lead to suppression of the analytes of interest during ionisation (Dams *et al.* 2003). Alternative sample extraction methods including a dilution step were included in the present study to investigate whether the current method was subject to this effect but no evidence was observed in this study as the four methods including dilution steps showed the highest LODs of the ten alternative methods tested. Of the eight methods that showed no significant change in LOD from the current method (SPE 7x diluted, undiluted, 2x concentrated; D&S 5x diluted, undiluted; PPT undiluted, 2x concentrated, 4x concentrated), the three SPE methods were included to explore the effect of varying the dilution/concentration step but were not considered optimal for extraction of urine samples due to the lower throughput caused by the time needed to pre-condition, run samples through, and dry SPE cartridges which could take up to 4 hours compared to approximately 2 hours for PPT and 30 minutes for D&S. Of the remaining five methods (D&S 5x diluted, undiluted; PPT undiluted, 2x concentrated, 4x concentrated), the two D&S methods, whilst showing no significant difference in LOD from the current method and the extraction method with the highest potential throughput, were not considered optimal due to the risk of accumulation of salts and impurities within the ion source resulting in loss of instrument sensitivity and increased risk of adduct formation. Of the remaining three methods (PPT undiluted, 2x concentrated, 4x concentrated), no significant difference in LOD was observed but PPT (4x concentrated) showed the lowest LOD and was therefore considered to be the optimal sample extraction method for processing urine samples.

Seven HPLC parameters (column diameter, column temperature, mobile phase flow rate, gradient profile, mobile phase formic acid concentration, column length, injection volume) were optimised with the aim of achieving similar or better levels of method sensitivity, peak shape and resolution as the initial 32 minute HPLC-ESI-MS/MS method within a reduced run time. The PFP stationary phase had been previously reported to be optimal for separation of phenolic metabolites (de Ferrars *et al.* 2014c) and so the choice of stationary phase was not reassessed in the present study. However, the column diameter and length were assessed and it was found that the 50 x 2.1 mm PFP column was capable of achieving similar sensitivity, peak shape and resolution as the 100 x 4.6 mm PFP column used in the initial 32 minute method. The use of the 50 x 2.1 mm column then facilitated a reduction in mobile

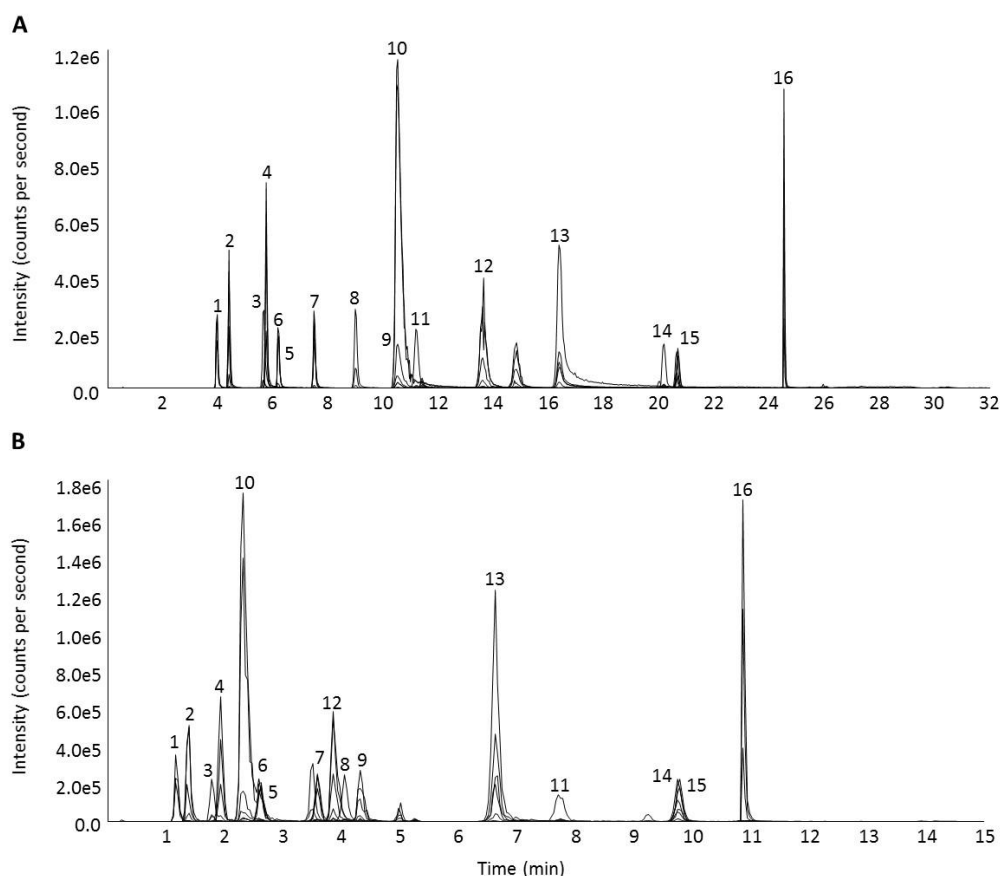
phase flow rate from 1.5 mL min⁻¹ / 1 mL min⁻¹ to 0.6 mL min⁻¹. The reduction in flow rate has two advantages over the previous method; firstly, it improves evaporation within the ion source and therefore should improve ionisation efficiency, and secondly, mobile phase usage is reduced therefore lowering the cost of using this method. The use of the 50 x 2.1 mm column also achieved acceptable peak resolution within a quicker timeframe which allowed for the HPLC gradient profile to be adjusted to reduce the overall run time. The initial ramp from 1% mobile phase B to 7.5% B at 7 min was unchanged as this was the period during which the majority of the analytes were eluted when using the 50 x 2.1 mm column. This meant that the ramp from 7.5% B to 7.6% B was less important for peak resolution in the new method compared to the initial method and so could be reduced from 7 minutes to 2 minutes. At this point in the new method, few analytes remained to be eluted therefore the ramp up to the 90% B wash phase could be reduced from 9 minutes to 30 seconds. The 90% B wash phase was also reduced from 3 minutes to 2 minutes. In total, these changes to the gradient profile reduced the run time from 32 minutes to 15 minutes per sample resulting in quicker analysis times and further reductions in method running costs. The concentration of 0.1% formic acid in the mobile phase optimised previously (de Ferrars *et al.* 2014c) was reassessed in the present study due to the change in column and conditions but the original method was again found to be optimal. The injection volume of 5 µL used in the initial method was assessed due to the reduction in column length and diameter but the original method was also deemed to be preferable. In addition to these changes, the MS source gas (curtain, nebulizer, auxiliary) flows were amended in the optimised 15 minute method. This change was made based on advice received during an AB SCIEX engineer visit which stated that the high gas flows used in the previous method were too high and should be reduced as it would not affect the chromatography or sensitivity of the method but would increase the longevity of the nitrogen gas generator. Overall, a number of changes were made to the initial 32 minute method to yield an improved 15 minute method (**Table 3.2**). The method developed in the present study is capable of detecting an equal number of phenolic metabolites with comparable levels of sensitivity, in under half the run time (**Figure 3.13**). The final optimised 15 minute method should be validated prior to use to assess the relative strengths and limitations of the method and to allow confidence in the results obtained when quantifying of anthocyanin metabolites in future studies.

Table 3.2 Comparison of initial 32 minute HPLC-ESI-MS/MS method and optimised 15 minute HPLC-ESI-MS/MS method parameters.

	Initial 32 minute method	Optimised 15 minute method
HPLC	Agilent 1200 series with DAD	Agilent 1200 series with DAD
Column stationary phase	PFP, 2.6 μm	PFP, 2.6 μm
Column length	100 mm	50 mm
Column diameter	4.6 mm	2.1 mm
Column temperature	37°C	40°C
Guard cartridge	PFP, 4.6 x 2.0 mm	PFP, 2.1 x 2.0 mm
Injector temperature	4°C	4°C
Injection volume	5 μL	5 μL
Mobile phase A	0.1 % (v/v) formic acid in water	0.1 % (v/v) formic acid in water
Mobile phase B	0.1 % (v/v) formic acid in acetonitrile	0.1 % (v/v) formic acid in acetonitrile
Flow rate	1.5 mL min ⁻¹ at 0 min 1.0 mL min ⁻¹ at 7 to 14 min 1.5 mL min ⁻¹ at 14 to 32 min	0.6 mL min ⁻¹
Gradient	1% B at 0 min 7.5% B at 7 min 7.6% B at 14 min 10% B at 17 min 12% B at 18.5 min 12.5% B at 20 min 30% B at 24 min 90% B at 25 to 28 min 1% B at 29 to 32 min	1% B at 0 min 7.5% B at 7 min 7.6% B at 9 min 90% B at 9.5 to 11.5 min 1% B at 12 to 15 min
Mass spectrometer	AB SCIEX 3200 series QTRAP	AB SCIEX 3200 series QTRAP
Ion source	Turbo V	Turbo V
Ionisation mode	ESI, negative/positive	ESI, negative/positive
Voltage	-4000 / +5500 V	-4000 / +5500 V
Temperature	700°C	700°C
Curtain gas	40 psi	35 psi
Nebuliser gas	60 psi	40 psi
Auxiliary gas	60 psi	45 psi

Column length, column diameter, column temperature, flow rate, and gradient changed based on optimisation of the method during the present study. Guard cartridge changed to match the amended column diameter. Curtain, nebulizer, and auxiliary gas flows changed following advice from an AB SCIEX engineer that the values used in the initial 32 minute method were too high.

Figure 3.13 Comparison of (A) initial 32 minute HPLC-ESI-MS/MS method and (B) optimised 15 minute HPLC-ESI-MS/MS method chromatography



1, benzoic acid-4-glucuronide; 2, protocatechuic acid-4-glucuronide; 3, protocatechuic acid; 4, protocatechuic acid-3-glucuronide; 5, vanillic acid-4-glucuronide; 6, isovanillic acid-3-glucuronide; 7, hippuric acid; 8, protocatechuic acid-3/4-sulfate; 9, 4-hydroxybenzaldehyde; 10, vanillic acid; 11, (iso)vanillic acid-3/4-sulfate; 12, methyl 3,4-dihydroxybenzoate; 13, phloroglucinaldehyde; 14, ferulic acid; 15, scopoletin; 16, phloridzin.

3.5. Conclusion

Ongoing development of methods for quantifying anthocyanins metabolites in biological samples is important for improving data quality when monitoring metabolites at nanomolar concentrations, and to allow for the detection of novel metabolites present at concentrations below the current limits of detection. The present study provides evidence that the use of ammonium-buffered mobile phase does not improve method sensitivity when quantifying anthocyanin metabolites and that the 0.1% formic acid mobile phase used by the previously reported HPLC-ESI-MS/MS method (Czank *et al.* 2013, de Ferrars *et al.* 2014c) is optimal. The present study provides evidence that PPT may be used as a suitable alternative to SPE when extracting anthocyanin metabolites from clinical urine samples. The present study also reports further optimisation of the existing 32 minute HPLC-ESI-MS/MS method to produce a method capable of achieving similar sensitivity, resolution, and peak shape within a 15 minute run time.

Chapter 4. Validation of HPLC-ESI-MS/MS Methods for Quantifying Anthocyanin Metabolites in Human Serum and Urine.

4.1. Introduction

Anthocyanins have been extensively studied due to their reported health effects (McCullough *et al.* 2012, Cassidy *et al.* 2015) but recently the focus in this area has shifted towards the phenolic metabolites of anthocyanins to explain the observed bioactivity due to the low bioavailability of the parent anthocyanins (Wu *et al.* 2002, Kay *et al.* 2005). To facilitate further study of anthocyanin metabolites, reliable methods of detecting and quantifying these compounds in biological samples are required. To this end, an analytical method was developed using high performance liquid chromatography coupled to an electrospray ionisation tandem mass spectrometer (HPLC-ESI-MS/MS) capable of separating and quantifying cyanidin-3-glucoside and 17 of its phenolic metabolites in human serum samples within a 32 minute sample run time (Czank *et al.* 2013, de Ferrars *et al.* 2014c). Further development of this method to reduce sample run time, simplify sample preparation, and expand the number of quantifiable analytes through improved ionisation efficiency yielded a second analytical method capable of separating and quantifying cyanidin-3-glucoside and 54 of its phenolic metabolites in human urine samples within a 15 minute sample run time. The present study describes the validation of these two methods. The phenolic metabolites included in the two methods were chosen based on those recently reported to be present in serum and urine following intake of cyanidin-3-glucoside (Czank *et al.* 2013, Rodriguez-Mateos *et al.* 2013, de Ferrars *et al.* 2014a, de Ferrars *et al.* 2014b). The design of the present study was based on published guidelines for bioanalytical method validation (Food and Drug Administration 2001, United Nations Office on Drugs and Crime 2009) where specificity, limit of detection (LOD), linearity, accuracy, precision, and extraction efficiency were examined. These guidelines represent the gold standard in bioanalytical method validation and are typically used by pharmacological and toxicological studies in the pursuit of FDA drug approval where very high standards of methods for routine analysis are expected. Expectations for analytical method quality in nutritional research may be lower due to inherent difficulties such as inter-participant variation (de Roos 2013) but it is important that methods for analysing clinical samples from nutritional studies are

developed with these guidelines in mind. Some nutritional studies utilise the FDA and UN guidelines to validate their analytical method but these studies typically detect and quantify either single (Zeng *et al.* 2015, Ramalingam and Ko 2016) or small numbers of analytes (Wang *et al.* 2014b, Wei *et al.* 2016). Due to the difficulties involved in optimising methods to be both qualitative and quantitative for the high number of analytes included in the methods presented here, the present study was less focused on achieving the high standards laid out in the FDA and UN guidelines and more focused on using the guidelines to assess the relative strengths and limitations of the method and to provide information on situations in which the methods may be more or less appropriate to use. The aim of the present study was to answer the following questions:

- Are the correct analytes being quantified? (Specificity)
- What are the lowest metabolite concentrations that the methods are capable of detecting? (LOD)
- Is the response linear over the relevant concentration range? (Linearity)
- Are the calculated metabolite concentrations close to the 'true' concentrations? (Accuracy)
- Are these results repeatable and reproducible? (Precision)
- Are the compounds of interest recovered from the biological samples effectively and consistently by the sample preparation method? (Extraction efficiency)

4.2. Methods

4.2.1. Materials and reagents

Acetonitrile and methanol were purchased from Fisher Scientific (Loughborough, UK). Strata-X™ 33 µm polymeric sorbent 500 mg/6 mL solid-phase extraction cartridges, Kinetex® pentafluorophenyl (PFP) high-performance liquid chromatography (HPLC) columns (2.6 µm, 100 x 4.6 mm, 100 Å and 2.6 µm, 50 x 2.1 mm, 100 Å) and SecurityGuard® cartridges (PFP, 4.6 x 2.0 mm and 2.1 x 2.0 mm) were purchased from Phenomenex (Macclesfield, UK). Cyanidin-3-glucoside (kuromanin chloride) was purchased from Extrasynthese (Genay, France). The phase II conjugates of phenolic acids (protocatechuic acid-3-glucuronide, protocatechuic acid-4-glucuronide, protocatechuic acid-3-sulfate, protocatechuic acid-4-sulfate, isovanillic acid-3-glucuronide, vanillic acid-4-glucuronide, isovanillic acid-3-sulfate, vanillic acid-4-sulfate, benzoic acid-4-glucuronide) were synthesised by the School of Chemistry and Centre for Biomolecular Sciences, University of St. Andrews (UK) using

published methods (Zhang *et al.* 2012). 3-hydroxyhippuric acid and 4-hydroxyhippuric acid were purchased from Alfa Chemistry (Stony Brook, USA). Methyl 3,4-dihydroxybenzoate (3,4-dihydroxy-benzoic acid methyl ester) was purchased from Alfa Aesar (Heysham, UK). All other materials, reagents, and standards were purchased from Sigma-Aldrich (Dorset, UK), including: Acrodisc PTFE syringe filters (13 mm, 0.45 μ m), human serum from human male AB plasma (Product No.: H4522) formic acid (FA), dimethyl sulfoxide (DMSO), 2,3-dihydroxybenzoic acid, 2,4-dihydroxybenzoic acid, 2,5-dihydroxybenzoic acid, 2-hydroxy-4-methoxybenzoic acid, 2-hydroxybenzoic acid, 2-hydroxycinnamic acid, 3-(3-hydroxyphenyl)propionic acid, 3-(4-hydroxy-3-methoxyphenyl)propionic acid, 3,4-dihydroxybenzaldehyde, 3,4-dihydroxyphenylacetic acid, 3,5-dihydroxybenzoic acid, 3-hydroxybenzoic acid, 3-hydroxyphenylacetic acid, 3-methylhippuric acid (N-[3-methylbenzoyl]glycine), 3-(4-hydroxyphenyl)propionic acid, 4-hydroxybenzaldehyde, 4-hydroxybenzoic acid, 4-hydroxybenzyl alcohol, 4-hydroxyphenylacetic acid, 4-methylhippuric acid (N-[4-methylbenzoyl]glycine), α -hydroxyhippuric acid ([benzoylamino]hydroxyacetic acid), benzoic acid, benzoylglutamic acid, caffeic acid (3,4-dihydroxycinnamic acid), chlorogenic acid (3-[3,4-dihydroxycinnamoyl]quinic acid), ferulic acid (4-hydroxy-3-methoxycinnamic acid), gallic acid (3,4,5-trihydroxybenzoic acid), hippuric acid (benzoylaminoacetic acid), homovanillic acid (4-hydroxy-3-methoxyphenylacetic acid), isoferulic acid (3-hydroxy-4-methoxycinnamic acid), isovanillic acid (3-hydroxy-4-methoxybenzoic acid), kaempferol (3,4',5,7-tetrahydroxyflavone), protocatechuic acid (PCA, 3,4-dihydroxybenzoic acid), p-coumaric acid (*trans*-4-hydroxycinnamic acid), phloroglucinaldehyde (PGA, 2,4,6-trihydroxybenzaldehyde), phenylacetic acid, phloridzin (phloridzin dihydrate), rosmarinic acid ([*R*]-*O*-[3,4-dihydroxycinnamoyl]-3-[3,4-dihydroxyphenyl]lactic acid), scopoletin (7-hydroxy-5-methoxycoumarin), sinapic acid (4-hydroxy-3,5-dimethoxy-cinnamic acid), syringic acid (4-hydroxy-3,5-dimethoxy-benzoic acid), *trans*-cinnamic acid, *trans*-3-hydroxycinnamic acid, and vanillic acid (4-hydroxy-3-methoxybenzoic acid). Water was 18M Ω /cm Milli-Q quality and all solvents were LC-MS grade.

4.2.2. Clinical intervention study design

Banked urine samples from a previously conducted anthocyanin intervention (Czank *et al.* 2013) were used for the present analysis. Briefly, samples were originally collected from healthy males (n=8; age, 27.8 \pm 8.1 y; BMI, 23.2 \pm 1.5 kg/m²) prior to (t=0 h) and after consuming a 500 mg bolus of isotopically labelled cyanidin-3-glucoside containing three ¹³C-atoms on the A-ring and two ¹³C-atoms on the B-ring (6,8,10,3',5'-¹³C₅-C3G, hereafter

referred to as $^{13}\text{C}_5\text{-C3G}$). Participants were asked to arrive on the study day in a fasted state (minimum 8 h). Individual urine samples were collected during the 6 hour study day and total urine voids were collected during the 6-24h and 24-48 hour periods. An anthocyanin-free meal was provided between 2-4 hours post-bolus. Participants were asked to maintain a low anthocyanin diet for the next 48 hours. Participants were also asked to avoid any foods containing high levels of anthocyanins and ^{13}C (Morrison *et al.* 2000) over the 7 day run-in period and during the intervention. Upon collection, the urine samples were combined with 100 mg of ascorbate per 500 mL of urine and were also acidified manually to pH 2.4 using formic acid. All samples were stored at -80°C until analysis.

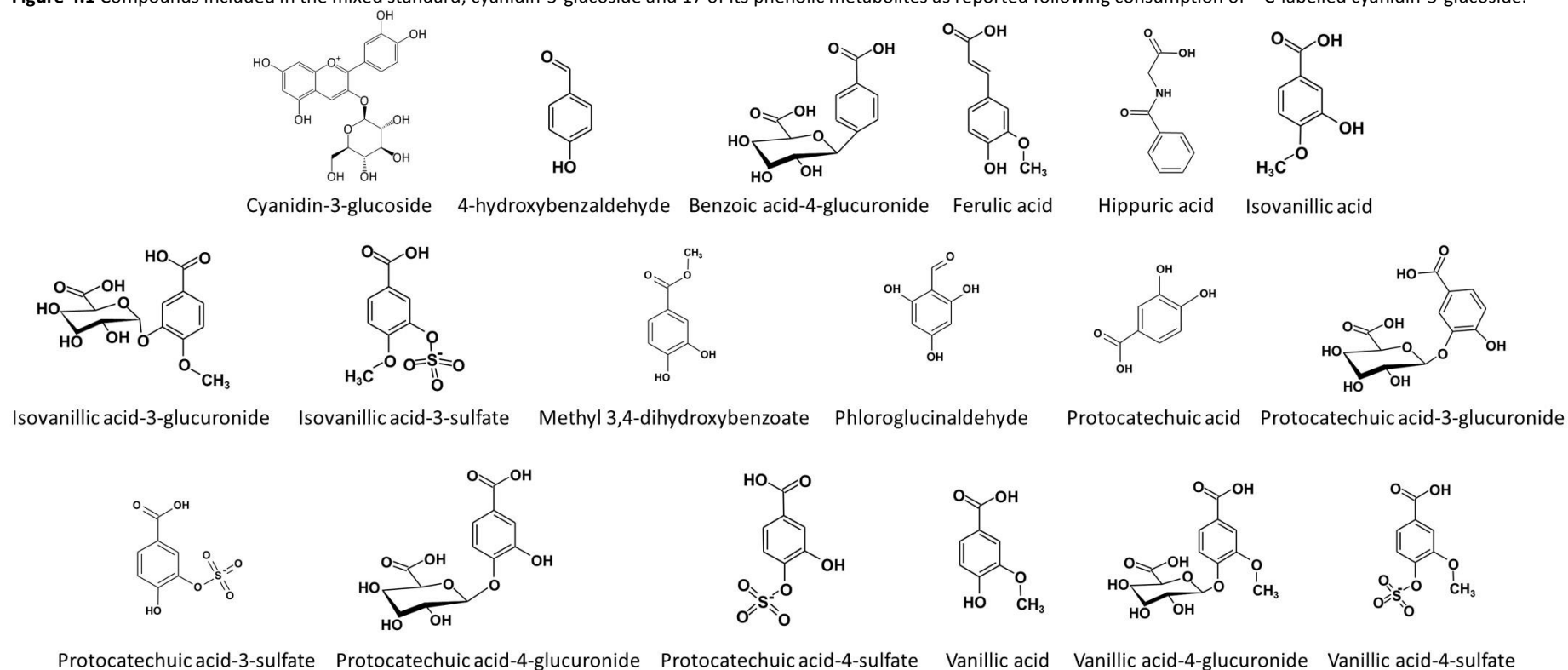
4.2.3. Serum sample preparation: solid phase extraction (SPE)

40 mL of commercially-sourced human serum was extracted via SPE following previously reported methodology (Czank *et al.* 2013, de Ferrars *et al.* 2014c). Briefly, SPE cartridges were preconditioned with 6 mL of acidified methanol (acidified to pH 2.4 using formic acid) followed by 6 mL of acidified water (acidified to pH 2.4 using formic acid). Cartridges were loaded with 1 mL acidified water followed by 1 mL of serum. Samples were eluted at a flow rate of approximately 1 drop/second. Cartridges were washed with 12 mL of acidified water before being dried under vacuum for 30 mins. 5 mL of acidified methanol was added to the cartridges and left to soak for 10 mins before the samples were eluted with a total of 7mL acidified methanol. The eluent was evaporated to approximately 50 μL on a rotary evaporator (Thermo SPD Speedvac). Following evaporation, the samples were reconstituted with 200 μL of acidified water. The samples were then sonicated for 10 mins with the ultrasonic water bath kept cool using ice, followed by vortex mixing for 10 seconds and filtration through a 0.45 μm syringe filter. Filtrates were combined to provide approximately 10 mL of extracted matrix to be used as 'blank serum' during sample preparation.

4.2.4. Matrix-matched (serum) analytical standard preparation

A mixed standard was composed of cyanidin-3-glucoside and 17 of its serum metabolites, as reported following consumption of ^{13}C -labelled cyanidin-3-glucoside (Czank *et al.* 2013, de Ferrars *et al.* 2014a). The 18 compounds included in the mixed standard were cyanidin-3-glucoside, 4-hydroxybenzaldehyde, benzoic acid-4-glucuronide, ferulic acid, hippuric acid, isovanillic acid, isovanillic acid-3-glucuronide, isovanillic acid-3-sulfate, methyl 3,4-dihydroxybenzoate, protocatechuic acid, protocatechuic acid-3-glucuronide, protocatechuic acid-3-sulfate, protocatechuic acid-4-glucuronide, protocatechuic acid-4-sulfate, phloroglucinaldehyde, vanillic acid, vanillic acid-4-glucuronide, and vanillic acid-4-sulfate (Figure 4.1).

Figure 4.1 Compounds included in the mixed standard; cyanidin-3-glucoside and 17 of its phenolic metabolites as reported following consumption of ^{13}C -labelled cyanidin-3-glucoside.



Adapted from (Czank *et al.* 2013, de Ferrars *et al.* 2014a).

The mixed standard was added to the extracted commercial serum ('blank serum'), along with scopoletin and phloridzin internal standards, to give 0.098 μM (Low), 1.56 μM (Mid) and 50 μM (High) samples. Stock solutions of each analyte were also added separately to 'blank serum' to give individual 50 μM samples of each metabolite.

4.2.5. Urine sample preparation: protein precipitation (PPT)

20 mL of pooled acidified baseline urine was extracted via PPT. 1 mL of urine was spiked with 4 mL of acetonitrile containing 0.1% v/v formic acid, mixed by vortex for 10 seconds, stored at -20°C for 30 mins and centrifuged at $4000 \times g$, 8°C for 10 mins. After centrifugation, the supernatant was removed, placed into a test tube and evaporated to dryness on a Thermo Speedvac concentrator. Samples were reconstituted in 250 μL of mobile phase diluent (0.1/5/94.9 v/v/v formic acid/methanol/water). Samples were sonicated for 10 mins with the ultrasonic water bath kept cool using ice, followed by vortex mixing for 10 seconds and filtration through a 0.45 μm syringe filter. Filtrates were combined to provide approximately 5 mL of extracted matrix to be used as 'blank urine' during sample preparation.

4.2.6. Matrix-matched (urine) analytical standard preparation

A mixed standard was composed of cyanidin-3-glucoside and 54 of its recently identified urine metabolites (Czank *et al.* 2013, Rodriguez-Mateos *et al.* 2013, de Ferrars *et al.* 2014a, de Ferrars *et al.* 2014b) (**Table 4.1**). The mixed standard was added to the 'blank urine', along with scopoletin and phloridzin internal standards, to give 0.098 μM (Low), 1.56 μM (Mid) and 50 μM (High) samples. Stock solutions of each analyte were also added separately to 'blank urine' to give individual 50 μM samples of each metabolite.

Table 4.1 Metabolite composition of urine mixed standard.

Compound		
2,3-dihydroxybenzoic acid	4-hydroxyhippuric acid	Methyl 3,4-dihydroxybenzoate
2,4-dihydroxybenzoic acid	4-hydroxyphenylacetic acid	PCA
2,5-dihydroxybenzoic acid	4-methylhippuric acid	PCA-3-glucuronide
2-hydroxy-4-methoxybenzoic acid	α -hydroxyhippuric acid	PCA-4-glucuronide
2-hydroxybenzoic acid	Benzoic acid	PCA-3-sulfate
2-hydroxycinnamic acid	Benzoic acid-4-glucuronide	PCA-4-sulfate
3-(3-hydroxyphenyl)propionic acid	Benzoylglutamic acid	p-coumaric acid
3-(4-hydroxy-3-methoxyphenyl)propionic acid	Caffeic acid	PGA
3,4-dihydroxybenzaldehyde	Chlorogenic acid	Phenylacetic acid
3,4-dihydroxyphenylacetic acid	Cyanidin-3-glucoside	Rosmarinic acid
3,5-dihydroxybenzoic acid	Ferulic acid	Sinapic acid
3-hydroxybenzoic acid	Gallic acid	Syringic acid
3-hydroxyhippuric acid	Hippuric acid	<i>trans</i> -cinnamic acid
3-hydroxyphenylacetic acid	Homovanillic acid	<i>trans</i> -3-hydroxycinnamic acid
3-methylhippuric acid	Isoferulic acid	Vanillic acid
3-(4-hydroxyphenyl)propionic acid	Isovanillic acid	Vanillic acid-4-glucuronide
4-hydroxybenzaldehyde	Isovanillic acid-3-glucuronide	Vanillic acid-4-sulfate
4-hydroxybenzoic acid	Isovanillic acid-3-sulfate	
4-hydroxybenzyl alcohol	Kaempferol	

In order to test the extraction efficiency of the PPT sample preparation method, additional samples were prepared by spiking pooled acidified baseline urine with the mixed standard and internal standards (phloridzin and scopoletin) to give 0.098 μM (Low), 1.56 μM (Mid), and 50 μM (High) samples. The samples were then processed using the PPT method and metabolite concentrations quantified against a calibration curve.

4.2.7. Chromatography (32 minute run)

HPLC-ESI-MS/MS analysis was carried out using an Agilent (Stockport, UK) 1200 series HPLC equipped with a Diode Array Detector (DAD) coupled to an AB SCIEX (Warrington, UK) 3200 series QTRAP® MS/MS system with Turbo V™ electrospray ionisation source using previously established methods (Czank *et al.* 2013, de Ferrars *et al.* 2014c). Briefly, a Kinetex® pentafluorophenyl (PFP) (2.6 μm , 100 x 4.6 mm) RP-HPLC column was used with a PFP SecurityGuard® cartridge (4.6 x 2.0 mm). The column temperature was set at 37°C, injector temperature of 4°C and injection volume of 5 μL . Mobile Phase A was 0.1% (v/v) formic acid in water and Mobile Phase B was 0.1% (v/v) formic acid in acetonitrile at a flow rate of 1.5 mL min^{-1} at 0 min, 1 mL min^{-1} at 7 to 14 min and 1.5 mL min^{-1} at 14 to 32 min. The gradient consisted of 1% B at 0 min, 7.5% B at 7 min, 7.6% B at 14 min, 10% B at 17 min, 12% B at 18.5 min, 12.5% B at 20 min, 30% B at 24 min, 90% B at 25 to 28 min, 1% B at 29 to 32 min. MS/MS source parameters included ionspray voltage, -4000 V / +5500 V; temperature, 700°C; curtain gas, 40 psi; nebulizer gas and auxiliary gas, 60 psi. Scheduled multiple reaction monitoring (sMRM) scans were performed using parameters optimised for the detection of the analytical standards (**Table 4.2**).

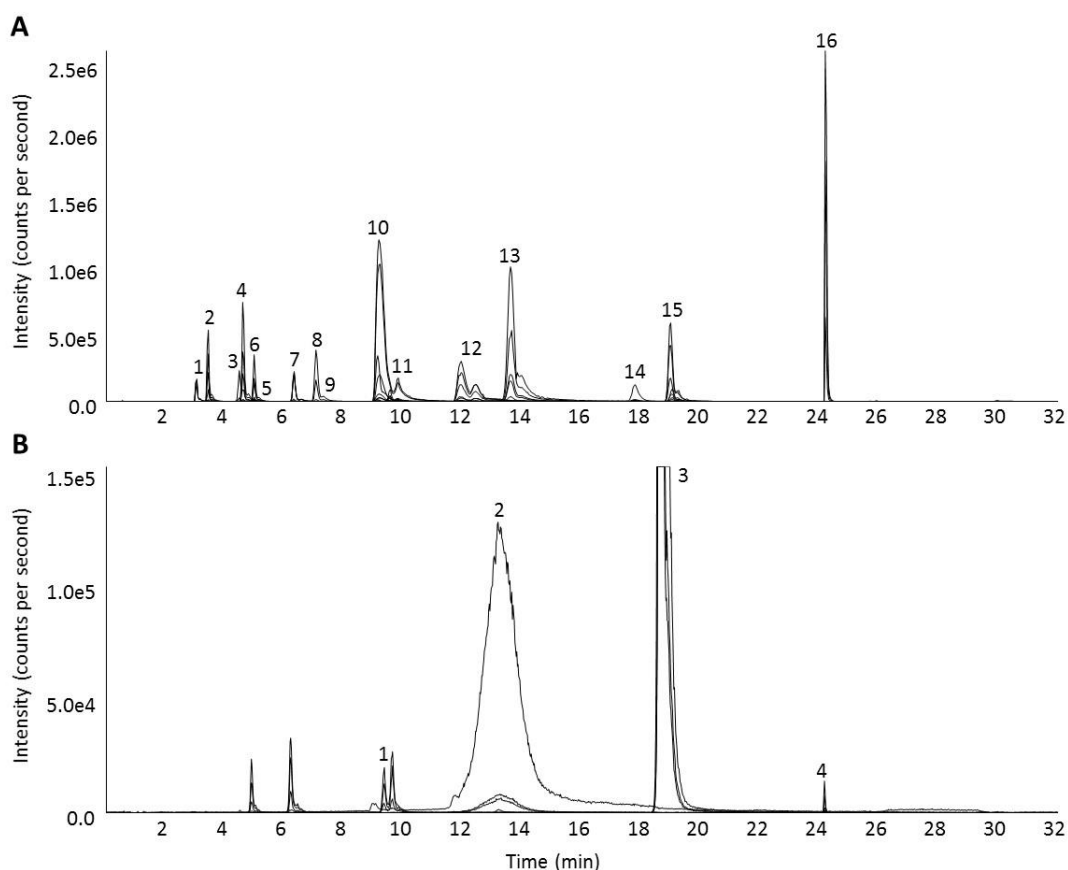
Table 4.2 sMRM schedule used to analyse serum samples on the AB SCIEX 3200 QTRAP® instrument.

Compound	Transitions (m/z) precursor/product ion	Scan time range (min)	Scan mode
Benzoic acid-4-glucuronide	313/175,113,93*	2.0 – 4.0	-
Protocatechuic acid-4-glucuronide	329.01/153*,113,109	2.4 – 4.4	-
Protocatechuic acid	153.01/108*,91,81	3.2 – 5.2	-
Protocatechuic acid-3-glucuronide	329.01/153*,113,109	3.4 – 5.4	-
Vanillic acid-4-glucuronide	343.01/167,152,113*	4.6 – 6.6	-
Isovanillic acid-3-glucuronide	343.01/167,152,113*	4.6 – 6.6	-
Hippuric acid	177.9/133.9*,77.1,131.8	5.0 – 7.0	-
Protocatechuic acid-3/4-sulfate ^a	233.01/153,109*,189	6.3 – 8.3	-
4-hydroxybenzaldehyde	121.2/107.8,92*,65.1	7.0 – 9.0	-
Isovanillic acid	169.01/151.1,125,93*	7.3 – 11.3	+
Vanillic acid	167.03/152*,123,108	8.8 – 10.8	-
(Iso)vanillic acid-3/4-sulfate ^a	247/167*,152,108	8.9 – 10.9	-
Methyl 3,4-dihydroxybenzoate	167/107.8*,107.1,91.2	11.5 – 13.5	-
Cyanidin-3-glucoside	449/287*,213,137	11.9 – 15.9	+
Phloroglucinaldehyde	153/151*,125,107	13.7 – 15.7	-
Ferulic acid	193/178,149,134*	17.8 – 19.8	-
Scopoletin	193/133.2*,122,94.1	17.1 – 21.1	+
Scopoletin	191/104*,147.9,120	18.1 – 20.1	-
Phloridzin	437/275, 169, 107*	22.1 – 26.1	+
Phloridzin	435/273*,167,123	23.1 – 25.1	-

*Transition used for quantitation. ^aIsomers of this metabolite were unresolvable using this HPLC-ESI-MS/MS method so were quantified as a single analyte.

Samples were analysed in negative ionisation mode and in positive ionisation mode, with internal standards included in both methods (**Figure 4.2**). Retention time and the detection of three or more of the relevant ion transitions were used to confirm the identity of the metabolites. For quantification, the peak area of the most intense ion transition was used. A ten-point calibration (0 – 25 µM) curve was prepared by spiking a standard mixture of the compounds into a matched-matrix (blank serum) and coefficients of determination (R^2) were established as linear (0.996 ± 0.003).

Figure 4.2 sMRM chromatograms showing the separation of cyanidin-3-glucoside and its phenolic metabolites in serum using optimised negative (A) and positive (B) 32 minute HPLC-ESI-MS/MS methods.



(A) 1, benzoic acid-4-glucuronide; 2, protocatechuic acid-4-glucuronide; 3, protocatechuic acid; 4, protocatechuic acid-3-glucuronide; 5, vanillic acid-4-glucuronide; 6, isovanillic acid-3-glucuronide; 7, hippuric acid; 8, protocatechuic acid-3/4-sulfate; 9, 4-hydroxybenzaldehyde; 10, vanillic acid; 11, (iso)vanillic acid-3/4-sulfate; 12, methyl 3,4-dihydroxybenzoate; 13, phloroglucinaldehyde; 14, ferulic acid; 15, scopoletin; 16, phloridzin. (B) 1, isovanillic acid; 2, cyanidin-3-glucoside; 3, scopoletin; 4, phloridzin.

4.2.8. Chromatography (15 minute run)

HPLC-ESI-MS/MS analysis was carried out as described above with the following exceptions: a Kinetex® PFP (2.6 μm , 50 x 2.1 mm) RP-HPLC column was used with a PFP SecurityGuard® cartridge (2.1 x 2.0 mm), column temperature was set at 40°C, and mobile phase flow rate of 0.6 mL min⁻¹ was used. The gradient consisted of 1% B at 0 min, 7.5% B at 7 min, 7.6% B at 9 min, 90% B at 9.5 to 11.5 min, 1% B at 12 to 15 min. MS/MS source curtain gas, 35 psi; nebulizer gas, 40 psi; auxiliary gas, 45 psi were used. sMRM scans were performed using parameters optimised for the detection of analytical standards (Table 4.3).

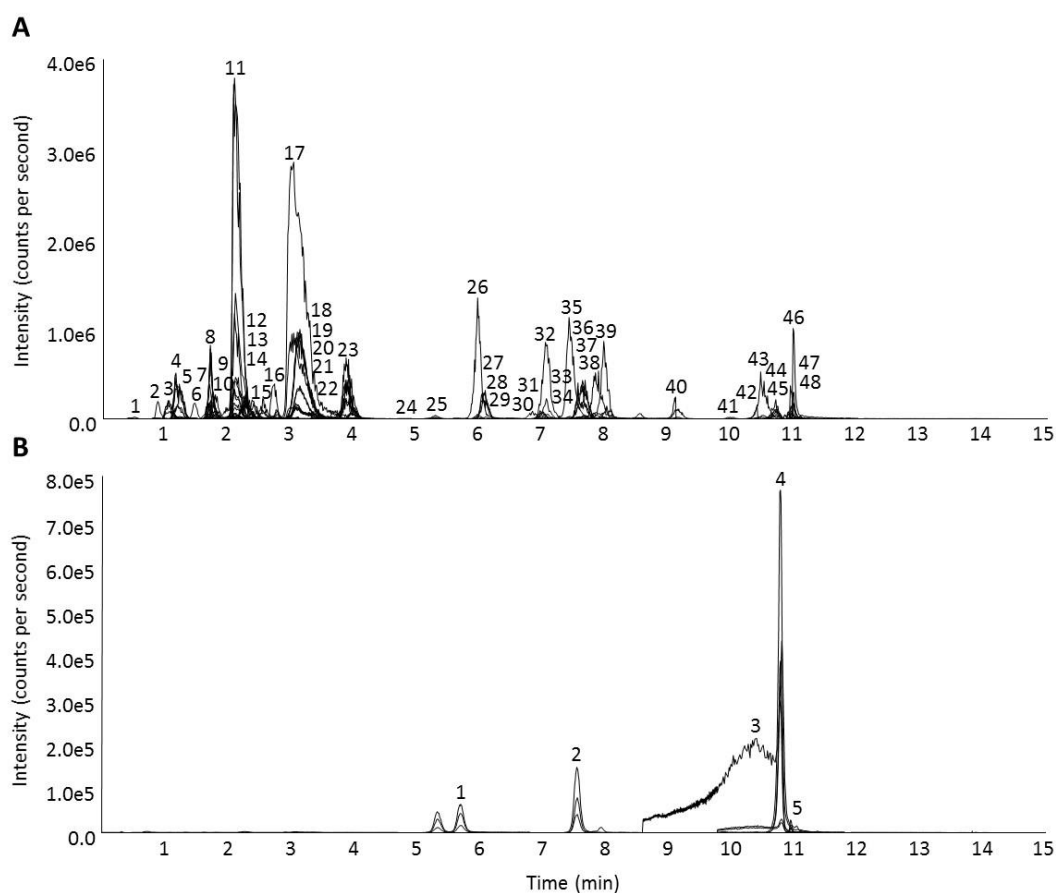
Table 4.3 sMRM schedule used to analyse urine samples on the AB SCIEX 3200 QTRAP® instrument.

Compound	Transitions (m/z) precursor/product ion	Scan time range (min)	Scan mode
<i>trans</i> -Cinnamic acid	147/103*,79,64	0.0 – 1.5	-
Gallic acid	169.2/125.1*,106.7,78.8	0.0 – 1.9	-
Benzoic acid-4-glucuronide	313.1/175.1,113.1*,93.1	0.1 – 2.1	-
Protocatechuic acid-4-glucuronide	329/153*,113,109	0.2 – 2.2	-
α -hydroxyhippuric acid	194.3/176.3,148.3,73.3*	0.4 – 2.4	-
Protocatechuic acid	153.1/108.1*,91.1,81.1	0.7 – 2.7	-
Protocatechuic acid-3-glucuronide	329.1/153.1*,113.1,109.1	0.7 – 2.7	-
4-hydroxyhippuric acid	194.2/150.2,100.2*,93.2	0.8 – 2.8	-
2,3/2,4/2,5/3,5-dihydroxybenzoic acid ^a	152.8/109*,107.8,90.8	1.1 – 3.1	-
3,4-dihydroxyphenylacetic acid	167.2/123.2*,108.2,95.2	1.1 – 3.1	-
3-hydroxyhippuric acid	194.1/150.1*,148.1,93.1	1.1 – 3.1	-
4-hydroxybenzyl alcohol	123/121*,105,77	1.1 – 3.1	-
Protocatechuic acid-3/4-sulfate	233.1/189.1,153.1,109.1*	1.1 – 3.1	-
Vanillic acid-4-glucuronide	343.2/167.2,152.2,113.2*	1.3 – 3.3	-
3,4-dihydroxybenzaldehyde	136.9/107.9*,92,81	1.6 – 3.6	-
3/4-hydroxybenzoic acid	137.1/93.1*,75.1,65.1	1.8 – 3.8	-
Hippuric acid	177.9/133.9*,131.8,77.1	2.0 – 4.0	-
Isovanillic acid-3-glucuronide	343.1/167.1,152.1,113.1*	2.1 – 4.1	-
Isovanillic acid-3-sulfate	247/167*,152,108	2.1 – 4.1	-
4-hydroxyphenylacetic acid	151.2/123.2,107.2*,93.2	2.5 – 4.5	-
Vanillic acid-4-sulfate	247.1/167.1*,152.1,108.1	2.9 – 4.9	-
3-hydroxyphenylacetic acid	151.1/136.1,121.1,107.1*	3.0 – 5.0	-
4-hydroxybenzaldehyde	121.2/107.8,92.2*,65.2	3.1 – 5.1	-
Isovanillic acid	169.01/151.1,125,93*	3.8 – 7.8	+
Vanillic acid	167.3/152.3*,123.3,108.3	4.4 – 6.4	-
Caffeic acid	179/135*,106,89	5.1 – 7.1	-
Benzoylglutamic acid	250/206*,162,121	5.2 – 7.2	-
Homovanillic acid	181.1/166.1,137.1*,79.1	5.2 – 7.2	-
Benzoic acid	121/93,92,77*	5.4 – 7.4	-
Phenylacetic acid	135/119,91*,64	5.6 – 7.6	-
Syringic acid	199/155.2,140*,125	5.6 – 9.6	+
3-(4-hydroxyphenyl)propionic acid	165.1/121.1*,97.1,93.1	5.7 – 7.7	-
3-(3-hydroxyphenyl)propionic acid	165/121*,119,106	6.2 – 8.2	-
Methyl 3,4-dihydroxybenzoate	167/107.8*,107.1,91.2	6.2 – 8.2	-
Chlorogenic acid	353/191*,161,127	6.6 – 8.6	-
4-methylhippuric acid	192.2/148.2,146.2,91.2*	6.7 – 8.7	-
3-methylhippuric acid	192.1/148.1,146.1,90.9*	6.8 – 8.8	-
2-hydroxybenzoic acid	137/93*,75,65	7.0 – 9.0	-
p-Coumaric acid	163/118.9*,116.9,92.9	7.1 – 9.1	-
Phloroglucinaldehyde	153/151*,125,107	7.2 – 9.2	-
3-(4-hydroxy-3-methoxyphenyl)propionic acid	195/136*,121,119	7.8 – 9.8	-
<i>trans</i> -3-hydroxycinnamic acid	163.2/119.2*,93.2,91.2	8.4 – 10.4	-
Cyanidin-3-glucoside	449/287*,213,137	8.8 – 12.8	+
Scopoletin	193/133.2*,122,94.1	8.8 – 12.8	+
Phloridzin	437/275,169,107*	8.9 – 12.9	+
2-hydroxycinnamic acid	163/119*,117,93	9.8 – 11.8	-
(Iso)ferulic acid ^a	193.1/178.1,149.1,134.1*	9.8 – 11.8	-
Scopoletin	191/147.9*,120,104	9.8 – 11.8	-
Rosmarinic acid	359.1/197.1,179.1,161.1*	9.9 – 11.9	-
Sinapic acid	223/208*,193,164	9.9 – 11.9	-
Phloridzin	435.1/273.1,167.1*,123.1	9.9 – 11.9	-
2-hydroxy-4-methoxybenzoic acid	167.1/123.1,108.1*,80.1	10.0 – 12.0	-
Kaempferol	285/239*,229,211	10.1 – 12.1	-

*Transition used for quantitation. ^aIsomers of this metabolite were unresolvable using this HPLC-ESI-MS/MS method so were quantified as a single analyte.

Samples were analysed in negative ionisation mode and in positive ionisation mode, with internal standards included in both methods (**Figure 4.3**). Retention time and the detection of three or more of the relevant ion transitions were used to confirm the identity of the metabolites. For quantification, the peak area of the most intense ion transition was used. An eleven-point calibration curve (0 – 50 μ M) was prepared by spiking a standard mixture of the compounds into a matched-matrix (blank urine) and coefficients of determination (R^2) were established as linear (0.995 ± 0.003).

Figure 4.3 sMRM chromatograms showing the separation of cyanidin-3-glucoside and its phenolic metabolites in urine using optimised negative (A) and positive (B) 15 minute HPLC-ESI-MS/MS methods.



(A) 1, *trans*-cinnamic acid; 2, gallic acid; 3, benzoic acid-4-glucuronide; 4, protocatechuic acid-4-glucuronide; 5, α -hydroxyhippuric acid; 6, protocatechuic acid; 7, protocatechuic-3-glucuronide; 8, 4-hydroxyhippuric acid; 9, 2,3/2,4/2,5/3,5-dihydroxybenzoic acid; 10, 3,4-dihydroxyphenylacetic acid; 11, 3-hydroxyhippuric acid; 12, 4-hydroxybenzyl alcohol; 13, protocatechuic acid-3/4-sulfate; 14, vanillic acid-4-glucuronide; 15, 3,4-dihydroxybenzaldehyde; 16, 3/4-hydroxybenzoic acid; 17, hippuric acid; 18, isovanillic acid-3-glucuronide; 19, isovanillic acid-3-sulfate; 20, 4-hydroxyphenylacetic acid; 21, vanillic acid-4-sulfate; 22, 3-hydroxyphenylacetic acid; 23, 4-hydroxybenzaldehyde; 24, vanillic acid; 25, caffeic acid; 26, benzoylglutamic acid; 27, homovanillic acid; 28, benzoic acid; 29, phenylacetic acid; 30, 3-(4-hydroxyphenyl)propionic acid; 31, 3-(3-hydroxyphenyl)propionic acid; 32, methyl 3,4-dihydroxybenzoate; 33, chlorogenic acid; 34, 4-methylhippuric acid; 35, 3-methylhippuric acid; 36, 2-hydroxybenzoic acid; 37, *p*-coumaric acid; 38, phloroglucinaldehyde; 39, 3-(4-hydroxy-3-methoxyphenyl)propionic acid; 40, *trans*-3-hydroxycinnamic acid; 41, 2-hydroxycinnamic acid; 42, (iso)ferulic acid; 43, scopoletin; 44, rosmarinic acid; 45, sinapic acid; 46, phloridzin; 47, 2-hydroxy-4-methoxybenzoic acid; 48, kaempferol. (B) 1, isovanillic acid; 2, syringic acid; 3, cyanidin-3-glucoside; 4, scopoletin; 5, phloridzin.

4.2.9. Validation criteria

The validation criteria (specificity, limit of detection, linearity, accuracy, precision and extraction efficiency) (**Table 4.4**) and acceptable limits were selected based on published bioanalytical method validation guidelines (Food and Drug Administration 2001, United Nations Office on Drugs and Crime 2009).

Table 4.4 Validation criteria and acceptable limits.

Validation criteria	Acceptable limit, n
Specificity (Retention time)	≤2%, n=5
Specificity (MRM transitions)	≤20%, n=5
Limit of detection	N/A
Linearity	≥0.99, n=2
Accuracy	Low, 80 – 120%; Mid/High, 85 – 115%, n=5
Precision (Intra-day)	Low, ≤20%; Mid/High, ≤15%, n=5
Precision (Inter-day)	Low, ≤20%; Mid/High, ≤15%, n=10
Extraction efficiency	Recovery ≤115% and CV ≤15%, n=5

MRM, multiple reaction monitoring; Low, 0.098 µM; Mid, 1.56 µM; High, 50 µM. Adapted from (Food and Drug Administration 2001, United Nations Office on Drugs and Crime 2009)

Specificity is a measure of the selectivity of the method in identifying and quantifying the correct peaks (Božović and Kulasingam 2013). Specificity was measured by comparison between a mixed sample and individual standard in terms of peak retention time and variance in the proportions of the three MRM transitions used for identification. The limit of detection (LOD) is a calculation of the lowest analyte concentration the method is able to detect and was based on the concentration required to produce a signal-to-noise ratio of 3-to-1 (Božović and Kulasingam 2013). Linearity is a measure of the analyte response and specifies the range over which the response is defined as linear. Accuracy is a measure of the variation between the known concentration of a sample and the concentration calculated by the method (Božović and Kulasingam 2013). Precision is a measure of the variation between the calculated concentrations of samples (Božović and Kulasingam 2013). Precision can be split into measuring the variation between samples in the same analysis run (intra-day) or between samples run on separate occasions (inter-day). Extraction efficiency is a measure of the percentage of analyte that is recovered using the sample extraction procedure (United Nations Office on Drugs and Crime 2009).

4.3. Results

4.3.1. Matrix-matched (serum) analytical standard (32 minute run)

Specificity. 16 of 20 analytes were within the validation limits for retention time variance ($\leq 2\%$) (Table 4.5). Mean retention time variance was $1.0 \pm 1.0\%$ and ranged from 0.0 – 3.0%. 19 of 20 analytes were within validation limits for MRM transition variance ($\leq 20\%$). Mean MRM transition variance was $4.8 \pm 6.9\%$ and ranged between 0.0 – 42.7%.

Limit of detection. Mean limit of detection was 9.5 ± 13.0 nM and ranged between 0.2 nM for phloridzin (negative ionisation mode) and 59.2 nM for isovanillic acid (Table 4.5).

Linearity. 17 of 20 analytes were found to produce a linear response across the complete range tested (0 – 50 μM) (Table 4.5). Mean coefficient of determination (R^2) was 0.996 ± 0.003 and ranged between 0.990 – 1.000.

Accuracy. 4 of 20 analytes were within validation limits for recovery (80 – 120%) at the low concentration (0.098 μM) (Table 4.6). Mean recovery at the low concentration was $157.1 \pm 80.9\%$ and ranged between 76.1 – 460.4%. 7 of 20 analytes were within validation limits for recovery (85 – 115%) at the mid concentration (1.56 μM). Mean recovery at the mid concentration was $116.7 \pm 19.7\%$ and ranged between 50.5 – 146.6%. 16 of 20 analytes were within the validation limits for recovery (85 – 115%) at the high concentration (50 μM). Mean recovery at the high concentration was $91.6 \pm 16.5\%$ and ranged between 46.7 – 108.5%.

Precision. 14 of 20 analytes were within validation limits for intra-day coefficient of variation (CV) ($\leq 20\%$) at the low concentration (0.098 μM) (Table 4.6). Mean intra-day CV at the low concentration was $16.3 \pm 10.8\%$ and ranged between 5.1 – 45.3%. 19 of 20 analytes were within validation limits for intra-day CV ($\leq 15\%$) at the mid concentration (1.56 μM). Mean intra-day CV at the mid concentration was $6.2 \pm 3.2\%$ and ranged between 1.3 – 12.3%. 20 of 20 analytes were within validation limits for intra-day CV ($\leq 15\%$) at the high concentration (50 μM). Mean intra-day CV at the high concentration was $4.6 \pm 2.7\%$ and ranged between 0.9 – 13.5%.

13 of 20 analytes were within validation limits for inter-day CV ($\leq 20\%$) at the low concentration (Table 4.6). Mean inter-day CV at the low concentration was $18.3 \pm 8.2\%$ and ranged between 7.9 – 40.8%. 16 of 20 analytes were within validation limits for inter-day CV ($\leq 15\%$) at the mid concentration. Mean inter-day CV at the mid concentration was $9.7 \pm 5.0\%$ and ranged between 1.9 – 21.9%. 20 of 20 analytes were within validation limits for inter-day CV ($\leq 15\%$) at the high concentration. Mean inter-day CV at the high concentration was $6.0 \pm 3.1\%$ and ranged between 2.9 – 14.3%.

Table 4.5 Validation of specificity, limit of detection, and linearity of a 32 minute HPLC-ESI-MS/MS method for quantifying cyanidin-3-glucoside, its phenolic metabolites, and two internal standards in serum.

Compound	Specificity				LOD (nM)	Linearity	
	Difference between R _t ^a (%)	Difference between transition proportions ^b (%)				Range	R ² value ^c
		MRM 1	MRM 2	MRM 3			
Cyanidin-3-glucoside	0.5	0.1	1.9	0.7	18.0	0 – 50 μM	0.995
4-hydroxybenzaldehyde	2.8 [†]	0.1	1.5	8.2	7.9	0 – 12.5 μM	0.993
Benzoic acid-4-glucuronide	1.5	0.1	1.9	2.4	5.9	0 – 50 μM	0.998
Ferulic acid	1.1	13.6	12.5	42.7 [†]	8.9	0 – 50 μM	0.991
Hippuric acid	3.0 [†]	0.3	2.1	12.9	0.5	0 – 50 μM	0.998
Isovanillic acid	0.0	1.2	1.7	0.0	59.2	0 – 50 μM	0.999
Isovanillic acid-3-glucuronide	0.1	1.7	2.2	0.2	7.5	0 – 50 μM	0.998
(Iso)vanillic acid-3/4-sulfate	2.7 [†]	15.4	16.3	5.7	7.1	0 – 50 μM	1.000
Methyl 3,4-dihydroxybenzoate	2.1 [†]	0.7	4.9	3.1	3.6	0 – 50 μM	0.994
Phloroglucinaldehyde	0.0	0.7	7.0	0.3	8.4	0 – 6.25 μM	0.997
Protocatechuic acid	0.6	1.4	2.8	9.0	5.0	0 – 50 μM	0.998
Protocatechuic acid-3-glucuronide	0.0	3.7	5.5	0.5	3.9	0 – 50 μM	1.000
Protocatechuic acid-3/4-sulfate	1.7	2.2	2.4	2.8	0.7	0 – 50 μM	0.995
Protocatechuic acid-4-glucuronide	0.4	2.7	4.2	3.0	5.1	0 – 50 μM	0.999
Vanillic acid	0.3	5.5	12.8	3.2	23.2	0 – 50 μM	0.998
Vanillic acid-4-glucuronide	0.2	0.5	3.2	1.5	7.9	0 – 50 μM	0.998
Phloridzin (-)	0.2	1.8	1.5	4.5	0.2	0 – 12.5 μM	0.996
Phloridzin (+)	0.0	2.2	18.2	0.7	10.8	0 – 50 μM	0.990
Scopoletin (-)	1.8	11.4	16.6	1.0	3.9	0 – 50 μM	0.995
Scopoletin (+)	0.1	0.5	1.3	0.3	1.5	0 – 50 μM	0.991

R_t , retention time; MRM, multiple reaction monitoring; LOD, limit of detection; R^2 , coefficient of determination; (-), negative ionisation mode; (+), positive ionisation mode. Low, 0.098 μ M; Mid, 1.56 μ M; High, 50 μ M. ^aUN guideline, $\leq 2\%$, $n=5$. ^bUN guideline, $\leq 20\%$, $n=5$. ^cFDA guideline, ≥ 0.99 , $n=2$. [†]Outside FDA/UN bioanalytical method validation guidelines.

Table 4.6 Validation of accuracy and precision of a 32 minute HPLC-ESI-MS/MS method for quantifying cyanidin-3-glucoside, its phenolic metabolites, and two internal standards in serum.

Compound	Accuracy			Precision					
	Recovery (%)			Intra-day CV (%)			Inter-day CV (%)		
	Low ^a	Mid ^b	High ^b	Low ^c	Mid ^d	High ^d	Low ^e	Mid ^f	High ^f
Cyanidin-3-glucoside	76.1 [†]	50.5 [†]	81.4 [†]	32.3 [†]	11.1	13.5	30.2 [†]	15.2 [†]	14.3
4-hydroxybenzaldehyde	118.5	123.1 [†]	61.6 [†]	17.0	1.3	3.5	19.8	3.0	9.8
Benzoic acid-4-glucuronide	125.8 [†]	112.8	106.2	16.4	7.9	5.0	19.9	11.1	4.0
Ferulic acid	135.2 [†]	132.2 [†]	90.7	11.4	4.4	3.6	10.0	9.0	5.6
Hippuric acid	ND [†]	ND [†]	99.7	ND [†]	ND [†]	0.9	ND [†]	ND [†]	4.2
Isovanillic acid	197.6 [†]	102.8	90.2	32.9 [†]	5.3	5.7	22.5 [†]	7.5	9.4
Isovanillic acid-3-glucuronide	136.8 [†]	111.6	98.7	11.5	8.7	4.3	26.1 [†]	6.7	6.9
(Iso)vanillic acid-3/4-sulfate	134.3 [†]	120.2 [†]	108.5	7.3	8.7	6.6	19.1	18.7 [†]	6.2
Methyl 3,4-dihydroxybenzoate	169.8 [†]	146.6 [†]	93.5	5.5	2.7	3.3	13.4	8.5	3.3
Phloroglucinaldehyde	101.1	110.2	46.7 [†]	22.1 [†]	6.2	2.3	19.2	8.1	11.6
Protocatechuic acid	144.4 [†]	113.7	101.9	8.8	6.8	3.1	11.0	6.4	2.9
Protocatechuic acid-3-glucuronide	127.6 [†]	119.2 [†]	105.2	6.9	7.7	6.2	12.7	9.9	4.7
Protocatechuic acid-3/4-sulfate	139.8 [†]	123.5 [†]	104.0	10.5	11.4	4.4	17.0	14.7	4.2
Protocatechuic acid-4-glucuronide	114.3	110.8	103.5	19.8	4.4	2.1	14.3	11.4	3.5
Vanillic acid	184.2 [†]	120.4 [†]	93.7	23.5 [†]	3.7	3.3	23.1 [†]	6.1	7.3
Vanillic acid-4-glucuronide	195.7 [†]	127.7 [†]	104.5	13.9	3.9	3.7	40.8 [†]	8.6	3.0
Phloridzin (-)	96.7	103.6	64.5 [†]	11.6	5.0	5.8	10.9	9.8	5.1
Phloridzin (+)	460.4 [†]	122.9 [†]	94.6	45.3 [†]	12.3	8.0	ND [†]	21.9 [†]	6.2
Scopoletin (-)	138.0 [†]	123.1 [†]	92.3	8.1	4.4	3.7	7.9	5.9	5.2
Scopoletin (+)	189.2 [†]	142.2 [†]	91.4	5.1	2.3	2.9	12.1	1.9	3.2

CV, coefficient of variation; (-), negative ionisation mode; (+), positive ionisation mode. ND, not detected. Low, 0.098 µM; Mid, 1.56 µM; High, 50 µM. ^aFDA guideline, 80 – 120%, n=5. ^bFDA guideline, 85 – 115%, n=5. ^cFDA guideline, ≤20%, n=5. ^dFDA guideline, ≤15%, n=5. ^eFDA guideline, ≤20%, n=10. ^fFDA guideline, ≤15%, n=10. [†]Outside FDA/UN bioanalytical method validation guidelines.

4.3.2. Matrix-matched (urine) analytical standard (15 minute run)

Specificity. 53 of 53 analytes were within the validation limits for retention time variance ($\leq 2\%$) (Table 4.7). Mean retention time variance was $0.7 \pm 0.6\%$ and ranged from 0.0 – 2.0%. 51 of 53 analytes were within validation limits for MRM transition variance ($\leq 20\%$). Mean MRM transition variance was $6.0 \pm 6.6\%$ and ranged between 0.0 – 52.3%.

Limit of detection. Mean limit of detection was 96.7 ± 541.7 nM and ranged between 0.3 nM for 4-hydroxyhippuric acid and 3954.7 nM for phenylacetic acid (Table 4.7).

Linearity. 53 of 53 analytes were found to produce a linear response across the complete range tested (0 – 50 μM) (Table 4.7). Mean coefficient of determination (R^2) was 0.995 ± 0.003 and ranged between 0.990 – 1.000.

Accuracy. 15 of 53 analytes were within validation limits for recovery (80 – 120%) at the low concentration (0.098 μM) (Table 4.7). Mean recovery at the low concentration was $203.6 \pm 195.8\%$ and ranged between 2.0 – 956.8%. 37 of 53 analytes were within validation limits for recovery (85 – 115%) at the mid concentration (1.56 μM). Mean recovery at the mid concentration was $115.0 \pm 62.0\%$ and ranged between 15.0 – 366.7%. 48 of 53 analytes were within the validation limits for recovery (85 – 115%) at the high concentration (50 μM). Mean recovery at the high concentration was $99.8 \pm 40.5\%$ and ranged between 21.5 – 364.3%.

Table 4.7 Validation of specificity, limit of detection, linearity, and accuracy of a 15 minute HPLC-ESI-MS/MS method for quantifying cyanidin-3-glucoside, its phenolic metabolites, and two internal standards in urine.

Compound	Specificity				LOD (nM)	Linearity		Accuracy		
	Difference between R _t ^a (%)	Difference between transition proportions ^b (%)				Range	R ² value ^c	Recovery (%)		
		MRM 1	MRM 2	MRM 3				Low ^d	Mid ^e	High ^e
2,3/2,4/2,5/3,5-dihydroxybenzoic acid	2.0	0.9	2.4	17.6	2.0	0 - 50 μM	0.997	207.6 [†]	88.6	92.2
2-hydroxy-4-methoxybenzoic acid	0.0	2.6	2.0	8.0	18.5	0 - 50 μM	0.998	83.1	87.9	95.4
2-hydroxybenzoic acid	1.4	0.1	0.4	0.9	47.9	0 - 50 μM	0.998	136.4 [†]	85.5	99.4
2-hydroxycinnamic acid	1.5	1.7	16.9	13.9	22.6	0 - 50 μM	0.995	93.8	98.6	93.2
3-(3-hydroxyphenyl)propionic acid	1.2	1.4	6.8	17.6	8.1	0 - 50 μM	0.993	331.8 [†]	92.2	86.4
3-(4-hydroxy-3-methoxyphenyl)propionic acid	0.8	1.4	3.8	6.4	6.4	0 - 50 μM	0.995	294.5 [†]	98.3	97.5
3-(4-hydroxyphenyl)propionic acid	0.8	11.4	3.6	10.4	9.1	0 - 50 μM	0.992	331.8 [†]	95.5	86.0
3,4-dihydroxybenzaldehyde	1.2	1.4	4.5	0.7	37.6	0 - 50 μM	0.993	92.3	104.7	89.9
3,4-dihydroxyphenylacetic acid	1.4	8.9	9.2	16.1	29.2	0 - 50 μM	0.990	271.0 [†]	215.8 [†]	98.6
3/4-hydroxybenzoic acid	1.0	0.6	18.7	6.0	3.4	0 - 50 μM	0.996	796.4 [†]	80.3 [†]	94.5
3-hydroxyhippuric acid	1.3	2.5	9.4	6.5	0.4	0 - 50 μM	0.991	283.3 [†]	302.2 [†]	77.0 [†]
3-hydroxyphenylacetic acid	0.2	4.2	9.5	0.1	0.4	0 - 50 μM	0.990	227.4 [†]	132.3 [†]	87.6
3-methylhippuric acid	1.4	1.3	2.5	3.0	9.5	0 - 50 μM	0.994	114.1	104.9	89.8
4-hydroxybenzaldehyde	0.2	11.3	0.2	6.8	32.6	0 - 50 μM	0.997	158.9 [†]	85.9	92.1
4-hydroxybenzyl alcohol	1.6	3.3	17.1	6.0	29.8	0 - 50 μM	0.992	398.2 [†]	366.7 [†]	111.6
4-hydroxyhippuric acid	0.0	19.3	10.6	12.2	0.3	0 - 50 μM	0.991	140.1 [†]	125.8 [†]	152.6 [†]
4-hydroxyphenylacetic acid	0.4	10.2	2.5	17.3	6.2	0 - 50 μM	0.991	578.3 [†]	261.5 [†]	364.3 [†]
4-methylhippuric acid	0.7	1.8	52.3 [†]	9.4	9.4	0 - 50 μM	0.997	148.0 [†]	103.3	86.6
α-hydroxyhippuric acid	0.8	17.4	0.5	0.1	16.1	0 - 50 μM	0.997	65.7 [†]	86.3	92.5
Benzoic acid	0.8	5.3	7.8	15.4	54.3	0 - 50 μM	0.992	956.8 [†]	91.2	87.0
Benzoic acid-4-glucuronide	0.6	2.8	4.8	3.3	19.3	0 - 50 μM	0.997	19.1 [†]	88.7	90.1
Benzoylglutamic acid	0.1	2.4	2.2	0.7	1.1	0 - 50 μM	0.995	183.9 [†]	95.6	92.5
Caffeic acid	0.9	0.2	6.9	1.0	10.3	0 - 50 μM	0.994	208.1 [†]	111.1	85.5
Chlorogenic acid	0.4	0.8	29.8 [†]	7.6	2.4	0 - 50 μM	0.997	98.2	102.1	95.1
Cyanidin-3-glucoside	0.0	0.5	10.5	16.9	7.5	0 - 50 μM	0.997	56.3 [†]	65.1 [†]	94.7
Gallic acid	0.3	0.1	14.4	7.7	116.4	0 - 50 μM	0.999	25.3 [†]	98.3	91.8
Hippuric acid	0.7	1.5	3.2	4.9	0.4	0 - 50 μM	0.990	245.2 [†]	184.4 [†]	21.5 [†]
Homovanillic acid	0.7	16.0	10.0	8.5	9.1	0 - 50 μM	0.991	54.1 [†]	15.0 [†]	114.8 [†]

Table 4.7 (Continued)

Compound	Specificity				LOD (nM)	Linearity		Accuracy		
	Difference between R _t ^a (%)	Difference between transition proportions ^b (%)				Range	R ² value ^c	Recovery (%)		
		MRM 1	MRM 2	MRM 3				Low ^d	Mid ^e	High ^e
Isovanillic acid	0.1	1.8	0.7	0.0	45.8	0 - 50 µM	0.996	160.7 [†]	96.2	90.1
Isovanillic acid-3-glucuronide	2.0	7.2	4.0	5.1	5.7	0 - 50 µM	0.995	398.5 [†]	113.4	96.4
Isovanillic acid-3-sulfate	0.6	0.8	0.0	2.2	30.7	0 - 50 µM	0.999	4.1 [†]	91.9	109.0
(Iso)ferulic acid	0.6	6.4	9.5	1.7	9.4	0 - 50 µM	0.997	94.8	90.6	114.4
Kaempferol	0.0	0.3	0.5	0.2	26.7	0 - 50 µM	0.997	105.1	90.0	90.1
Methyl 3,4-dihydroxybenzoate	1.0	1.4	4.2	13.2	17.1	0 - 50 µM	0.993	117.7	96.6	89.6
p-Coumaric acid	0.1	0.4	0.5	3.8	3.9	0 - 50 µM	0.993	2.0 [†]	105.8	93.1
Phenylacetic acid	0.6	3.2	3.9	8.2	3954.7	0 - 50 µM	0.992	ND	ND	92.4
Phloroglucinaldehyde	0.9	1.4	18.2	17.2	23.3	0 - 50 µM	0.994	116.5	102.0	88.1
Protocatechuic acid	0.5	0.7	2.2	4.0	12.8	0 - 50 µM	0.994	97.0	93.9	99.1
Protocatechuic acid-3-glucuronide	0.5	3.5	1.0	3.6	26.6	0 - 50 µM	0.994	93.1	98.1	87.6
Protocatechuic acid-3/4-sulfate	0.6	3.8	9.3	9.7	1.0	0 - 50 µM	0.994	529.4 [†]	112.2	90.4
Protocatechuic acid-4-glucuronide	1.4	3.7	4.2	5.8	16.7	0 - 50 µM	0.996	86.8	92.4	89.8
Rosmarinic acid	0.0	1.9	5.6	0.0	15.2	0 - 50 µM	1.000	89.3	86.0	92.8
Sinapic acid	0.0	1.0	1.6	2.8	11.1	0 - 50 µM	0.998	121.7 [†]	95.5	93.0
Syringic acid	0.1	1.0	0.0	1.7	4.9	0 - 50 µM	0.995	155.2 [†]	101.7	89.1
<i>trans</i> -3-hydroxycinnamic acid	0.2	8.3	8.3	6.5	21.7	0 - 50 µM	0.998	260.3 [†]	106.8	92.4
<i>trans</i> -Cinnamic acid	1.6	1.1	10.6	13.1	3.4	0 - 50 µM	0.990	109.5	267.9 [†]	142.2 [†]
Vanillic acid	0.1	2.9	7.8	9.7	14.2	0 - 50 µM	0.998	263.9 [†]	100.9	96.1
Vanillic acid-4-glucuronide	0.1	7.8	8.0	3.8	3.0	0 - 50 µM	0.995	110.2	134.4 [†]	98.4
Vanillic acid-4-sulfate	1.7	2.1	4.4	3.6	1.0	0 - 50 µM	0.996	151.7 [†]	138.2 [†]	103.9
Phloridzin (-)	0.5	0.2	1.3	2.8	19.6	0 - 50 µM	0.999	38.7 [†]	88.0	86.9
Phloridzin (+)	0.4	2.8	2.3	0.6	14.9	0 - 50 µM	0.992	659.4 [†]	31.7 [†]	88.8
Scopoletin (-)	0.6	14.8	13.8	6.6	283.7	0 - 50 µM	0.995	78.6 [†]	91.6	111.0
Scopoletin (+)	0.2	1.4	1.4	1.9	49.8	0 - 50 µM	0.993	142.1 [†]	84.7 [†]	102.2

R_t, retention time; MRM, multiple reaction monitoring; LOD, limit of detection; R₂, coefficient of determination; (-), negative ionisation mode; (+), positive ionisation mode; ND, not detected. Low, 0.098 µM; Mid, 1.56 µM; High, 50 µM. ^aUN guideline, ≤2%, n=5. ^bUN guideline, ≤20%, n=5. ^cFDA guideline, ≥0.99, n=2. ^dFDA guideline, 80 – 120%, n=5. ^eFDA guideline, 85 – 115%, n=5. [†]Outside FDA/UN bioanalytical method validation guidelines.

Precision. 12 of 53 analytes were within validation limits for intra-day coefficient of variation (CV) ($\leq 20\%$) at the low concentration ($0.098\ \mu\text{M}$) (Table 4.8). Mean intra-day CV at the low concentration was $106.8 \pm 133.7\%$ and ranged between $5.3 - 710.3\%$. 38 of 53 analytes were within validation limits for intra-day CV ($\leq 15\%$) at the mid concentration ($1.56\ \mu\text{M}$). Mean intra-day CV at the mid concentration was $26.3 \pm 35.4\%$ and ranged between $4.4 - 158.3\%$. 48 of 53 analytes were within validation limits for intra-day CV ($\leq 15\%$) at the high concentration ($50\ \mu\text{M}$). Mean intra-day CV at the high concentration was $16.0 \pm 35.7\%$ and ranged between $2.5 - 204.5\%$.

7 of 53 analytes were within validation limits for inter-day CV ($\leq 20\%$) at the low concentration (Table 4.8). Mean inter-day CV at the low concentration was $139.9 \pm 170.4\%$ and ranged between $11.7 - 918.9\%$. 33 of 53 analytes were within validation limits for inter-day CV ($\leq 15\%$) at the mid concentration. Mean inter-day CV at the mid concentration was $62.1 \pm 135.1\%$ and ranged between $4.9 - 806.8\%$. 44 of 53 analytes were within validation limits for inter-day CV ($\leq 15\%$) at the high concentration. Mean inter-day CV at the high concentration was $21.4 \pm 39.3\%$ and ranged between $3.6 - 174.8\%$.

Extraction efficiency. 9 of 53 analytes were within validation limits for recovery ($\leq 115\%$) and CV ($\leq 15\%$) at the low concentration ($0.098\ \mu\text{M}$) (Table 4.8). Mean recovery at the low concentration was $267.3 \pm 219.3\%$ and ranged between $13.0 - 972.3\%$. Mean CV at the low concentration was $46.6 \pm 84.3\%$ and ranged between $6.4 - 516.2\%$. 34 of 53 analytes were within validation limits for recovery ($\leq 115\%$) and CV ($\leq 15\%$) at the mid concentration ($1.56\ \mu\text{M}$). Mean recovery at the mid concentration was $140.9 \pm 131.6\%$ and ranged between $36.2 - 601.5\%$. Mean CV at the mid concentration was $19.1 \pm 18.3\%$ and ranged between $6.7 - 115.0\%$. 45 of 53 analytes were within validation limits for recovery ($\leq 115\%$) and CV ($\leq 15\%$) at the high concentration ($50\ \mu\text{M}$). Mean recovery at the high concentration was $75.4 \pm 59.7\%$ and ranged between $23.0 - 462.3\%$. Mean CV at the high concentration was $20.3 \pm 24.4\%$ and ranged between $4.5 - 107.1\%$.

Table 4.8 Validation of precision and extraction efficiency of a 15 minute HPLC-ESI-MS/MS method for quantifying cyanidin-3-glucoside, its phenolic metabolites, and two internal standards in urine.

Compound	Precision						Extraction Efficiency					
	Intra-day CV (%)			Inter-day CV (%)			Low ^e		Mid ^e		High ^e	
	Low ^a	Mid ^b	High ^b	Low ^c	Mid ^d	High ^d	Recovery (%)	CV (%)	Recovery (%)	CV (%)	Recovery (%)	CV (%)
2,3/2,4/2,5/3,5-dihydroxybenzoic acid	64.8 [†]	14.6	4.7	118.6 [†]	12.0	4.5	818.8 [†]	12.9 [†]	135.8 [†]	27.4 [†]	32.0	13.7
2-hydroxy-4-methoxybenzoic acid	10.7	7.1	4.7	13.3	8.8	4.6	57.4	14.8	67.8	14.0	59.5	9.9
2-hydroxybenzoic acid	44.0 [†]	6.0	5.6	85.3 [†]	8.2	5.0	188.9 [†]	18.9 [†]	101.6	13.5	66.8	10.8
2-hydroxycinnamic acid	8.2	6.0	4.4	15.7	7.9	5.7	66.0	13.0	87.1	13.6	62.8	10.4
3-(3-hydroxyphenyl)propionic acid	148.6 [†]	8.7	10.7	188.5 [†]	10.1	10.6	371.2 [†]	31.4 [†]	101.5	10.8	54.4	13.0
3-(4-hydroxy-3-methoxyphenyl)propionic acid	62.3 [†]	13.0	6.3	70.4 [†]	26.5 [†]	5.2	182.8 [†]	10.6 [†]	202.8 [†]	14.3 [†]	74.8	8.9
3-(4-hydroxyphenyl)propionic acid	148.6 [†]	14.8	11.0	185.7 [†]	136.3 [†]	73.2 [†]	308.5 [†]	37.0 [†]	104.6	7.6	54.4	13.0
3,4-dihydroxybenzaldehyde	9.7	4.8	5.3	46.7 [†]	4.9	5.4	177.2 [†]	23.0 [†]	67.1	10.3	59.3	14.7
3,4-dihydroxyphenylacetic acid	62.3 [†]	63.9 [†]	4.0	54.2 [†]	46.6 [†]	12.9	609.5 [†]	47.4 [†]	502.2 [†]	39.9 [†]	58.3	12.3
3/4-hydroxybenzoic acid	113.7 [†]	7.3	5.1	110.2 [†]	41.2 [†]	4.7	675.1 [†]	19.8 [†]	496.0 [†]	15.4 [†]	74.7	13.6
3-hydroxyhippuric acid	73.2 [†]	50.0 [†]	51.7 [†]	115.9 [†]	164.0 [†]	35.1 [†]	364.9 [†]	38.6 [†]	242.6 [†]	15.4 [†]	111.0 [†]	67.4 [†]
3-hydroxyphenylacetic acid	24.1 [†]	34.1 [†]	11.5	390.7 [†]	107.3 [†]	145.9 [†]	358.1 [†]	6.4 [†]	252.7 [†]	19.3 [†]	30.8	7.4
3-methylhippuric acid	11.7	7.6	6.5	11.7	8.1	9.0	464.5 [†]	12.9 [†]	101.0	12.5	54.4	14.1
4-hydroxybenzaldehyde	68.5 [†]	10.7	3.9	529.2 [†]	9.6	6.6	173.4 [†]	18.2 [†]	56.6	9.1	73.5	13.6
4-hydroxybenzyl alcohol	190.4 [†]	111.7 [†]	13.7	133.3 [†]	497.7 [†]	24.4 [†]	694.7 [†]	56.7 [†]	601.5 [†]	35.8 [†]	82.8	10.6
4-hydroxyhippuric acid	80.5 [†]	43.6 [†]	171.3 [†]	137.2 [†]	123.7 [†]	133.8 [†]	197.8 [†]	325.9 [†]	311.2 [†]	115.0 [†]	462.3 [†]	56.4 [†]
4-hydroxyphenylacetic acid	70.4 [†]	158.3 [†]	47.4 [†]	161.1 [†]	299.8 [†]	86.6 [†]	136.0 [†]	166.7 [†]	234.6 [†]	29.6 [†]	131.7 [†]	107.1 [†]
4-methylhippuric acid	39.8 [†]	8.3	8.7	45.4 [†]	7.7	7.7	451.1 [†]	14.8 [†]	101.3	13.4	53.6	10.4
α-hydroxyhippuric acid	13.3	6.1	5.4	69.6 [†]	8.0	6.2	13.0 [†]	39.1 [†]	47.2	10.5	65.5	11.3
Benzoic acid	108.4 [†]	50.8 [†]	7.7	736.7 [†]	95.1 [†]	8.4	105.2 [†]	135.6 [†]	72.8	6.9	77.4	8.9
Benzoic acid-4-glucuronide	199.6 [†]	5.9	7.8	132.6 [†]	6.9	8.7	64.1 [†]	29.4 [†]	53.4	11.5	56.3	9.0
Benzoylglutamic acid	80.4 [†]	4.4	2.5	83.2 [†]	6.6	6.0	105.6 [†]	54.4 [†]	84.4	11.1	60.7	10.4
Caffeic acid	16.9	11.1	7.2	64.4 [†]	10.4	6.3	214.9 [†]	17.2 [†]	87.1	14.4	46.2	9.6
Chlorogenic acid	18.2	5.4	2.7	59.3 [†]	5.5	3.6	233.1 [†]	13.0 [†]	92.5	11.9	61.3	11.5
Cyanidin-3-glucoside	76.2 [†]	11.4	10.6	50.2 [†]	14.6	11.9	43.4	9.4	43.6	7.8	71.8	10.5
Gallic acid	317.9 [†]	6.0	6.0	148.8 [†]	10.4	6.0	144.8 [†]	46.8 [†]	76.0	6.7	60.9	14.4
Hippuric acid	50.9 [†]	118.0 [†]	204.5 [†]	110.9 [†]	806.8 [†]	132.4 [†]	332.5 [†]	33.1 [†]	123.3 [†]	42.8 [†]	192.7 [†]	78.4 [†]
Homovanillic acid	710.3 [†]	139.2 [†]	14.5	161.8 [†]	131.2 [†]	17.4 [†]	542.7 [†]	32.2 [†]	541.7 [†]	20.3 [†]	75.2 [†]	18.5 [†]

Table 4.8 (Continued)

Compound	Precision						Extraction Efficiency					
	Intra-day CV (%)			Inter-day CV (%)			Low ^e		Mid ^e		High ^e	
	Low ^a	Mid ^b	High ^b	Low ^c	Mid ^d	High ^d	Recovery (%)	CV (%)	Recovery (%)	CV (%)	Recovery (%)	CV (%)
Isovanillic acid	38.3 [†]	5.0	11.1	45.5 [†]	11.2	12.4	135.5 [†]	39.8 [†]	72.4	13.2	88.0	13.3
Isovanillic acid-3-glucuronide	93.6 [†]	60.7 [†]	4.4	65.0 [†]	64.7 [†]	4.3	217.3 [†]	9.8 [†]	163.2 [†]	28.1 [†]	76.4	9.9
Isovanillic acid-3-sulfate	345.2 [†]	9.4	6.3	144.9 [†]	8.6	6.6	25.9 [†]	516.2 [†]	71.8	8.6	37.3 [†]	92.9 [†]
(Iso)ferulic acid	96.3 [†]	13.7	9.0	63.9 [†]	11.5	8.6	972.3 [†]	9.8 [†]	162.7 [†]	18.0 [†]	86.4	7.8
Kaempferol	101.6 [†]	6.9	7.0	918.9 [†]	10.2	6.9	305.0 [†]	32.9 [†]	56.1	8.9	71.6	12.2
Methyl 3,4-dihydroxybenzoate	6.2	15.0	7.9	17.7	14.8	8.4	90.5	9.8	86.8	11.9	53.1	13.5
p-Coumaric acid	515.8 [†]	8.9	4.1	145.0 [†]	7.5	4.0	95.6	10.7	96.9	13.1	56.4	12.6
Phenylacetic acid	ND	ND	5.4	ND	ND	6.9	ND	ND	41.7 [†]	39.0 [†]	64.6	8.8
Phloroglucinaldehyde	5.3	9.7	6.2	19.2	10.5	7.5	55.3	8.0	46.7	10.0	58.3	10.8
Protocatechuic acid	88.8 [†]	14.8	5.9	71.9 [†]	11.5	5.4	88.2	13.2	77.2	12.7	64.7	12.8
Protocatechuic acid-3-glucuronide	13.1	9.0	8.6	14.4	8.9	8.3	222.2 [†]	14.3 [†]	56.5	12.7	62.1	13.9
Protocatechuic acid-3/4-sulfate	66.0 [†]	12.6	4.2	72.2 [†]	13.0	7.5	107.4 [†]	19.6 [†]	186.9 [†]	19.1 [†]	44.6	4.5
Protocatechuic acid-4-glucuronide	44.1 [†]	13.1	5.7	85.5 [†]	11.1	6.7	85.4	8.3	73.1	11.0	60.8	15.0
Rosmarinic acid	16.3	6.4	4.9	19.4	6.1	4.5	55.3	8.5	50.2	11.2	70.3	12.6
Sinapic acid	62.6 [†]	9.6	6.9	48.3 [†]	9.9	5.8	470.4 [†]	16.7 [†]	92.9	7.3	70.2	11.9
Syringic acid	12.0	5.1	11.1	44.0 [†]	6.2	10.1	265.9 [†]	9.3 [†]	87.7	13.9	69.7	14.3
<i>trans</i> -3-hydroxycinnamic acid	34.6 [†]	6.9	6.7	50.6 [†]	5.7	7.4	22.8 [†]	137.8 [†]	65.6	11.2	69.3	9.4
<i>trans</i> -Cinnamic acid	134.3 [†]	52.0 [†]	33.5 [†]	235.8 [†]	141.3 [†]	174.8 [†]	264.0 [†]	30.3 [†]	127.9 [†]	42.0 [†]	93.6 [†]	98.9 [†]
Vanillic acid	119.0 [†]	12.6	5.3	144.7 [†]	32.0 [†]	4.5	207.0 [†]	15.3 [†]	208.8 [†]	15.0 [†]	68.9	8.9
Vanillic acid-4-glucuronide	286.9 [†]	11.5	4.5	201.9 [†]	32.2 [†]	4.3	585.6 [†]	28.6 [†]	103.3	10.5	55.0	10.5
Vanillic acid-4-sulfate	117.3 [†]	27.0 [†]	6.1	110.2	42.9 [†]	6.4	486.6 [†]	22.9 [†]	298.1 [†]	16.6 [†]	23.0 [†]	52.9 [†]
Phloridzin (-)	354.5 [†]	7.2	9.3	152.1 [†]	7.2	8.3	75.8 [†]	46.8 [†]	36.2	9.7	55.0	11.4
Phloridzin (+)	56.8 [†]	39.4 [†]	13.5	364.7 [†]	55.3 [†]	11.3	418.6 [†]	53.8 [†]	59.6	15.0	70.3	14.5
Scopoletin (-)	32.9 [†]	12.8	5.8	108.5 [†]	12.3	8.4	251.6 [†]	30.7	89.6	12.8 [†]	67.1	7.9
Scopoletin (+)	89.4 [†]	67.6 [†]	9.8	98.6 [†]	78.4 [†]	7.0	301.0 [†]	48.9 [†]	67.9	77.2 [†]	91.4 [†]	6.5

CV, coefficient of variation; (-), negative ionisation mode; (+), positive ionisation mode; ND, not detected. Low, 0.098 µM; Mid, 1.56 µM; High, 50 µM. ^aFDA guideline, ≤20%, n=5. ^bFDA guideline, ≤15%, n=5. ^cFDA guideline, ≤20%, n=10. ^dFDA guideline, ≤15%, n=10. ^eUN guideline, recovery ≤115% and CV ≤15%, n=5.

4.4. Discussion

Studies requiring the detection and quantification of anthocyanins in food products (Merken and Beecher 2000) or clinical samples (Cooke *et al.* 2006) have successfully utilised HPLC methods and ultraviolet/visible wavelength (UV-Vis) detection for many years and continue to do so whilst updating the methods to include recent advances in HPLC technology such as ultra-high performance liquid chromatography (UPLC) (Kalili and de Villiers 2011) and hydrophilic interaction chromatography (HILIC) (Willemse *et al.* 2013). The UV absorbance of anthocyanins is caused by the delocalised electrons present within the phenolic ring structure (Dearden and Forbes 1959), a trait shared by the phenolic metabolites of anthocyanins. However, whilst UV-Vis detection of phenolic acids has been used by many studies (Robbins 2003), the difficulty in chromatographically separating high numbers of structurally similar phenolic compounds and the poor availability of analytical standards has created the need for methods combining the separation of HPLC with the compound identification of mass spectrometry in order to study the *in vivo* metabolism of anthocyanins. The present study describes the validation of two LC-MS methods developed for this purpose. Validation of analytical methods is important in providing information to users about the relative strengths and limitations of the method as well as establishing confidence in the reliability of the results obtained (Božović and Kulasingam 2013). The present study sought to answer the following questions:

Are the correct analytes being quantified?

80% of the analytes tested were within guideline limits for retention time variance using the 32 minute method with 100% of analytes within guidelines using the 15 minute method. The analytes that fell outside the guideline limits (4-hydroxybenzaldehyde, hippuric acid, (iso)vanillic acid-3/4-sulfate, methyl 3,4 dihydroxybenzoate) may have been caused by slight variations in mobile phase preparation or build-up of impurities within the HPLC guard column affecting mobile phase flow. 95% of analytes were within guidelines for MRM transition variance using the 32 minute method with 96% of analytes within guidelines using the 15 minute method. The analytes that fell outside the guideline limits may have been caused by differences in ionisation between the individual reference sample that contained only the analyte of interest and the sample spiked with mixed standard containing all the tested analytes. Overall, the present study suggests that both methods have acceptable levels of specificity and users can be confident that the correct analytes are being quantified.

What are the lowest metabolite concentrations that the methods are capable of detecting?

The mean limits of detection were 9.5 nM with a range of 0.2 – 59.2 nM for the 32 minute method and 96.7 nM with a range of 0.3 – 3954.7 nM for the 15 minute method. The higher limit of detection for the 15 minute method is likely a result of the increased number of analytes included in this method compared to the 32 minute method. Overall, the present study suggests that both methods are sensitive enough to detect the levels of metabolites reported in clinical samples (Czank *et al.* 2013, Rodriguez-Mateos *et al.* 2013, de Ferrars *et al.* 2014a, de Ferrars *et al.* 2014b).

Is the response linear over the relevant concentration range?

85% of analytes were within guidelines for linear response over the full range of concentrations tested (0 – 50 μ M) using the 32 minute method with 100% of analytes within guidelines using the 15 minute method. The analytes that fell outside of the guideline limits (4-hydroxybenzaldehyde, phloroglucinaldehyde, phloridzin [-]) were caused by a lack of linearity above 6.25 μ M. However, the range over which a linear response was observed for these analytes is still adequate for quantification of the reported concentrations in clinical samples. It should be noted that two aldehyde compounds exhibited a non-linear response at the higher concentrations. Non-linear responses in LC-MS analysis can be caused by a number of factors including saturation during ionisation, detector saturation, and clustering of analyte ions at high concentrations (Bakhtiar and Majumdar 2007, Yuan *et al.* 2012). Formation of aldehyde cluster ions has been reported previously (Ostrowski *et al.* 2014) but further study is required to establish if the non-linear response of the aldehyde metabolites at high concentrations persists as previous studies have observed that analytes may exhibit linear and non-linear characteristics on the same instrument on different days (Yuan *et al.* 2012). Overall, the present study suggests that both methods have acceptable levels of linearity and users can be confident that the tested analytes will respond linearly over the tested concentration range.

Are the calculated metabolite concentrations close to the 'true' concentrations?

Using the 32 minute method, 20%, 35% and 80% of analytes were within guidelines for accuracy at the low, mid and high concentrations, respectively. Using the 15 minute method, 28%, 70% and 91% of analytes were within guidelines at the low, mid and high concentrations, respectively. The levels of accuracy observed at the low concentration (0.098 μ M) were likely to be caused by proximity to the limits of detection resulting in greater levels of variation within the analyte response. However, recoveries were largely

within a factor of 10 of 100% recovery which equates to the difference between 1 nM and 10 nM when quantifying metabolite concentrations. Within the wider context of nutrition research, which is subject to large degrees of inter-participant variation (de Roos 2013), this level of variation at low concentrations can be considered acceptable. The FDA and UN guidelines on which the current validation experiment was designed (Food and Drug Administration 2001, United Nations Office on Drugs and Crime 2009) are primarily used in pharmacological and toxicological analyses which routinely detect xenobiotics in genetically homogenous laboratory animals resulting in reduced inter-participant variation and are therefore capable of accuracy levels currently not possible in nutritional analysis (Gibney *et al.* 2005). Overall, the present study suggests that accuracy at low and mid concentrations ($\leq 1.56 \mu\text{M}$) is currently a limitation for both methods and users should be cautious about the quantification of phenolic metabolites at this level using these methods.

Are these results consistently repeatable and reproducible?

Using the 32 minute method, 70%, 95% and 100% of analytes were within guidelines for intra-day precision whilst 65%, 80% and 100% of analytes were within guidelines for inter-day precision at the low, mid and high concentrations, respectively. Using the 15 minute method, 23%, 72% and 91% of analytes were within guidelines for intra-day precision whilst 13%, 62% and 83% of analytes were within guidelines for inter-day precision at the low, mid and high concentrations, respectively. The 32 minute method showed improved levels of precision compared to the 15 minute method, however, this is likely to be a result of the increased number of analytes included in the 15 minute method resulting in reduced dwell time per analyte and therefore greater levels of variation as each peak is made up of fewer data points (AB SCIEX 2011). Development of new methods often requires compromise between the quality of the method and the number of quantifiable analytes. Qualitative detection of an extensive list of metabolites was prioritised in the development of these methods. For these methods to be suitable for use in nutritional research, a high level of precision can be deemed more important than a high level of accuracy. The high level of inter-participant variation in nutritional studies places an emphasis on analysing the relative changes in metabolite concentrations within participants, which needs good analytical precision, rather than quantifying absolute concentration values for which a high level of accuracy would be required. Overall, the present study suggests that precision may be a limitation of the 15 minute method at lower concentrations ($\leq 1.56 \mu\text{M}$) and users should be cautious about the quantification of phenolic metabolites at this level using this method.

Are the compounds of interest recovered from the biological samples effectively and consistently by the sample preparation method?

Using the PPT method for extraction of urine samples, 17%, 64% and 85% of analytes were within guidelines for extraction efficiency at the low, mid and high concentrations, respectively. The poor extraction efficiency observed at the lower concentrations ($\leq 1.56 \mu\text{M}$) may be due to endogenous matrix components not removed during the extraction process causing suppression of the analyte ions (Polson *et al.* 2003). It is also possible that the results may be due to the poor accuracy and precision of the 15 minute method at the lower concentrations resulting in high CV values. The advantages of low cost and high throughput of PPT compared to SPE suggest that future studies aiming to quantify phenolic metabolites in urine may wish to consider PPT as a suitable sample preparation method. PPT is unlikely to be the most appropriate option for extraction of serum or plasma samples due to the greater presence of ion-suppressing proteins and phospholipids in these matrices that are only partially removed by PPT (Chang *et al.* 2007, Bylda *et al.* 2014). SPE remains the optimal sample preparation method for extraction of serum or plasma samples prior to LC-MS analysis (Bylda *et al.* 2014). Overall, the present study suggests that PPT may have limited value as a urine sample preparation technique for recovery of metabolites at lower concentrations ($\leq 1.56 \mu\text{M}$) although this may be difficult to evaluate due to the poor accuracy and precision of the method.

The use of extracted human serum and urine as a matched matrix in sample preparation is likely to increase the level of baseline noise compared to samples prepared using mobile phase due to matrix effects caused by salts, proteins, or phospholipids present in the extracted serum and urine matrices that were not removed during the extraction process (Dams *et al.* 2003). However, while it may have been possible to report improved validation results using a mobile phase matrix (de Ferrars *et al.* 2014c), the use of the extracted serum and urine matrices is an advantage of the present study as it provides a more realistic representation of the results that can be expected when analysing clinical serum and urine samples (Food and Drug Administration 2001, Božović and Kulasingam 2013). These matrix effects may have been eliminated via the use of stable-isotope-labelled internal standards (Matuszewski *et al.* 2003) but due to the number of analytes included in the present analysis, this was not feasible and analogue internal standards were used.

The present study highlighted the strengths (specificity, limits of detection, linearity) and limitations (accuracy and precision at lower concentrations) of the developed methods. These results demonstrate the effect of prioritising qualitative detection of a wide range of

anthocyanin metabolites over the focused quantification of a few select metabolites. The large number of analytes included in the methods meant that some instrument parameters, such as the ion source temperature and gases, had to be chosen based on their suitability for the range of metabolites instead of being optimised for a single analyte which may have affected detection limits. Whilst acknowledging the limitations of the methods, it should be noted that the developed methods are capable of detection and quantification of a greater number of phenolic metabolites within a shorter run time than previously published methods (Rodriguez-Mateos *et al.* 2013, Pimpão *et al.* 2015).

Whilst the accuracy and precision of the methods may be considered acceptable for qualitative analysis and quantifying relative concentrations of anthocyanin metabolites for nutritional research, efforts should be made to improve the sensitivity of the HPLC-ESI-MS/MS methods as a way of improving these aspects of the methods. By increasing sensitivity, and therefore improving the limits of detection, the accuracy and precision of the methods should be improved (Božović and Kulasingam 2013). Future work should investigate potential methods for increasing the sensitivity of the current methods such as via the use of hydrophilic interaction chromatography (HILIC) or the use of more sensitive instrumentation.

The use of HILIC in conjunction with electrospray ionisation mass spectrometry has been increasing recently with a number of reported bioanalytical applications (Jian *et al.* 2010) including quantification of anthocyanins in fruit and vegetables (Willemse *et al.* 2013). HILIC provides potential advantages over traditional reverse-phase (RP)-HPLC methods due to the differences in stationary phases and solvents. In traditional RP-HPLC, water acts as the weak solvent and polar organic solvents such as methanol or acetonitrile act as the strong solvent. In RP-HPLC, most compounds are eluted in high aqueous/low organic mobile phase conditions which are difficult to evaporate within the ESI ion source and therefore can lead to poor ionisation. In HILIC, the roles of strong and weak solvents are switched so that organic solvents are weak and water is strong. Most compounds are eluted in high organic/low aqueous conditions which improves evaporation within the ion source resulting in improved ionisation and greater method sensitivity (Nguyen and Schug 2008).

The use of higher specification, more sensitive instrumentation would also help to improve the reliability of the current method by improving the signal-to-noise ratio, lowering the limits of detection and therefore improving accuracy and precision of the method at the metabolite concentrations reported in clinical samples. By upgrading from the AB SCIEX 3200 series QTRAP® instrument used in the present study to the next model from the same

supplier, the AB SCIEX 4000 series, a factor of 8-10 increase in overall sensitivity could be expected with another factor of 8 increase possible via the use of the AB SCIEX 5000 series (Impey 2005) and a further factor of 4-5 increase possible via the use of the AB SCIEX 6500 series (Romanelli *et al.* 2012). Whilst there will be areas for improvement in all methods, the present study demonstrates that the methods developed by our group are capable of qualitative detection and quantification of anthocyanin metabolites for the purposes of relative concentration comparisons in clinical samples.

4.5. Conclusion

Validation of analytical methods capable of quantifying phenolic metabolites of anthocyanins in clinical samples is crucial for the confident study of *in vivo* anthocyanin metabolism. The present study provides information on the strengths and limitations of HPLC-ESI-MS/MS methods for detection and quantification of a wide range of anthocyanin metabolites in both human serum and urine. Whilst poor accuracy and precision at low concentrations limits the use of these methods in quantifying absolute metabolite concentrations in clinical samples, the methods may be considered acceptable for qualitative detection and quantification of phenolic metabolites of anthocyanins for the purposes of comparing relative concentrations in nutritional studies.

Chapter 5. Establishing Robust Metabolic Biomarkers of Anthocyanin Consumption.

5.1. Introduction

Epidemiological studies have suggested that diets high in anthocyanins could reduce the risk of cardiovascular disease (Mink *et al.* 2007, Cassidy *et al.* 2011, Dohadwala *et al.* 2011, Rodriguez-Mateos *et al.* 2013). Studies investigating the effects of anthocyanin intake use standard methods to establish intake and monitor adherence to dietary restrictions such as food frequency questionnaires and food diaries (Jennings *et al.* 2012, Rodriguez-Mateos *et al.* 2013). However, these methods of estimating and monitoring intake have many drawbacks such as misreporting of consumption data and limitations associated with food composition databases (Beaton 1994, Thompson *et al.* 2010) and this can lead to significant under or overestimation of intake (Rodriguez-Mateos *et al.* 2014). A more accurate method for monitoring food intake is to measure biomarkers of intake, which are specific compounds in the blood that are known to be reliable indicators of consumption (Hedrick *et al.* 2012). Suitable biomarker candidates can be identified via two approaches; discovery-driven and hypothesis-driven (Kuhnle 2012). A discovery-driven approach requires little prior understanding of the bioavailability or metabolism of the food/compound of interest and involves utilising metabolomics analysis to identify all possible metabolites and using multivariate analysis to identify suitable biomarker candidates. A hypothesis-driven approach starts from an understanding of the metabolism of the food/compound of interest and uses this information to create a list of possible candidate biomarkers before analysing clinical samples to test the suitability of these candidates. Whichever approach is used, ideal biomarkers of intake should satisfy the following criteria: robust, validated methods of quantification should exist; biomarker concentration should be sensitive to changes in intake of the dietary component of interest; the biomarker should be specific to the dietary component of interest, i.e. found in limited quantities within the background diet; and finally, a clear understanding of the absorption, distribution, metabolism and excretion (ADME) of the biomarker and how this process is affected by factors such as genetics and diet composition should exist. (Potischman 2003, Spencer *et al.* 2008, Jenab *et al.* 2009, Kuhnle 2012).

A number of biomarkers for measuring the intake of flavonoid-rich foods have been proposed. These include using urinary flavonoid levels as a measure of fruit and vegetable

intake (Nielsen *et al.* 2002, Krogholm 2011) and urinary excretion of hippuric acid as a measure of flavonoid intake from fruit and vegetables (Penczynski *et al.* 2015). A discovery-driven approach has also been used to identify metabolic profiles associated with intake of polyphenol-rich foods (Edmands *et al.* 2015). Biomarkers of intake for specific phenolic compounds have also been proposed such as urinary excretion of isoferulic acid as a biomarker of chlorogenic acid intake from coffee (Hodgson *et al.* 2004) and urinary levels of phenolic metabolites such as benzoic acid and gallic acid as biomarkers of quercetin and epigallocatechin gallate intake respectively (Loke *et al.* 2009). A number of metabolites, such as syringic acid (van Dorsten *et al.* 2010) and gallic acid (Urpi-Sarda *et al.* 2015), have also been proposed as suitable urinary biomarkers of intake for anthocyanin-rich foods such as wine and grape juice. To the author's knowledge, none of these biomarkers have been accepted as robust and sensitive intake biomarkers and there have been no metabolic biomarkers for specific anthocyanin intake proposed to date.

The present study aimed to use a hypothesis-driven approach to identify metabolites that could be used as biomarkers of anthocyanin intake through the use of ^{13}C -labelling to improve the accuracy of future clinical intervention studies exploring the bioactivity of anthocyanins. Anthocyanins have been demonstrated to be present in low concentrations in the blood and urine following intake (Wu *et al.* 2002, Kay *et al.* 2005) but they have been reported to be extensively metabolised in the body (Czank *et al.* 2013, de Ferrars *et al.* 2014b). Stable isotope labelling has been used in nutritional metabolic research since the 1930s (Schoenheimer and Rittenberg 1935) but has been used more extensively since the late 1970s/early 1980s (Schwartz and Giesecke 1979, Smith 1983) after improvements in mass spectrometric techniques simplified the detection of stable isotopes (Turnlund 1989). The use of stable isotope labelling is important for the identification of suitable biomarker candidates as it allows for mass spectrometry to distinguish between the metabolites resulting from a dietary intervention and metabolites resulting from the background diet by the change in mass/charge ratio (m/z) which would not be possible with other methods using unlabelled interventions. This allows for metabolites only present within the body at high concentrations following consumption of foods/compounds of interest, i.e. good biomarkers of intake, to be identified. The present study used serum and urine samples from a recently conducted ^{13}C -labelled cyanidin-3-glucoside (C3G) intervention (Czank *et al.* 2013) to compare concentrations of ^{13}C -labelled C3G and its ^{13}C -labelled phenolic metabolites in the blood and urine following intake, relative to levels present in the blood and urine resulting from the background diet composed of naturally abundant ^{12}C . The use of ^{13}C -labelled C3G

enabled mass spectrometric discrimination between metabolites resulting from the intervention (as they will contain heavy carbon 13) and those originating from the background diet (as they will contain molecules comprising naturally abundant carbon 12). The present study scanned for ^{13}C and ^{12}C analytes of C3G and 17 recently identified metabolites in serum (Czank *et al.* 2013, de Ferrars *et al.* 2014a) and 58 metabolites in urine (Czank *et al.* 2013, Rodriguez-Mateos *et al.* 2013, de Ferrars *et al.* 2014b, de Ferrars *et al.* 2014c) for their potential utility as biomarkers of C3G intake.

5.2. Methods

5.2.1. Materials and reagents

Acetonitrile and methanol were purchased from Fisher Scientific (Loughborough, UK). Strata-X™ 33 μm polymeric sorbent 500 mg/6 mL solid-phase extraction cartridges, Kinetex® pentafluorophenyl (PFP) high-performance liquid chromatography (HPLC) columns (2.6 μm , 100 x 4.6 mm, 100 Å and 2.6 μm , 50 x 2.1 mm, 100 Å) and SecurityGuard® cartridges (PFP, 4.6 x 2.0 mm and 2.1 x 2.0 mm) were purchased from Phenomenex (Macclesfield, UK). Cyanidin-3-glucoside (kuromanin chloride) was purchased from Extrasynthese (Genay, France). The phase II conjugates of phenolic acids (protocatechuic acid-3-glucuronide, protocatechuic acid-4-glucuronide, protocatechuic acid-3-sulfate, protocatechuic acid-4-sulfate, isovanillic acid-3-glucuronide, vanillic acid-4-glucuronide, isovanillic acid-3-sulfate, vanillic acid-4-sulfate, benzoic acid-4-glucuronide) were synthesised by the School of Chemistry and Centre for Biomolecular Sciences, University of St. Andrews (UK) using published methods (Zhang *et al.* 2012). 3-hydroxyhippuric acid and 4-hydroxyhippuric acid were purchased from Alfa Chemistry (Stony Brook, USA). Methyl 3,4-dihydroxybenzoate (3,4-dihydroxy-benzoic acid methyl ester) was purchased from Alfa Aesar (Heysham, UK). All other materials, reagents, and standards were purchased from Sigma-Aldrich (Dorset, UK), including: Acrodisc PTFE syringe filters (13 mm, 0.45 μm), formic acid (FA), dimethyl sulfoxide (DMSO), 2,3-dihydroxybenzoic acid, 2,4-dihydroxybenzoic acid, 2,5-dihydroxybenzoic acid, 2-hydroxy-4-methoxybenzoic acid, 2-hydroxybenzoic acid, 2-hydroxycinnamic acid, 3-(3-hydroxyphenyl)propionic acid, 3-(4-hydroxy-3-methoxyphenyl)propionic acid, 3,4-dihydroxybenzaldehyde, 3,4-dihydroxyphenylacetic acid, 3,5-dihydroxybenzoic acid, 3-hydroxybenzoic acid, 3-hydroxyphenylacetic acid, 3-methylhippuric acid (N-[3-methylbenzoyl]glycine), 3-(4-hydroxyphenyl)propionic acid, 4-hydroxybenzaldehyde, 4-hydroxybenzoic acid, 4-hydroxybenzyl alcohol, 4-hydroxyphenylacetic acid, 4-methylhippuric acid (N-[4-methylbenzoyl]glycine), α -hydroxyhippuric acid

([benzoylamino]hydroxyacetic acid), benzoic acid, benzoylglutamic acid, caffeic acid (3,4-dihydroxycinnamic acid), chlorogenic acid (3-[3,4-dihydroxycinnamoyl]quinic acid), ferulic acid (4-hydroxy-3-methoxycinnamic acid), gallic acid (3,4,5-trihydroxybenzoic acid), hippuric acid (benzoylaminoacetic acid), homovanillic acid (4-hydroxy-3-methoxyphenylacetic acid), isoferulic acid (3-hydroxy-4-methoxycinnamic acid), isovanillic acid (3-hydroxy-4-methoxybenzoic acid), kaempferol (3,4',5,7-tetrahydroxyflavone), protocatechuic acid (PCA, 3,4-dihydroxybenzoic acid), p-coumaric acid (*trans*-4-hydroxycinnamic acid), phloroglucinaldehyde (PGA, 2,4,6-trihydroxybenzaldehyde), phenylacetic acid, phloridzin (phloridzin dihydrate), rosmarinic acid ([*R*]-*O*-[3,4-dihydroxycinnamoyl]-3-[3,4-dihydroxyphenyl]lactic acid), scopoletin (7-hydroxy-5-methoxycoumarin), sinapic acid (4-hydroxy-3,5-dimethoxy-cinnamic acid), syringic acid (4-hydroxy-3,5-dimethoxy-benzoic acid), *trans*-cinnamic acid, *trans*-3-hydroxycinnamic acid, and vanillic acid (4-hydroxy-3-methoxybenzoic acid). Water was 18M Ω /cm Milli-Q quality and all solvents were LC-MS grade.

5.2.2. Clinical intervention study design

Banked serum and urine samples from a previously conducted anthocyanin intervention (Czank *et al.* 2013) were used for the present analysis. Briefly, samples were originally collected from healthy males ($n=8$; age, 27.8 ± 8.1 y; BMI, 23.2 ± 1.5 kg/m²) prior to ($t=0$ h) and after consuming a 500 mg bolus of isotopically labelled cyanidin-3-glucoside containing three ¹³C-atoms on the A-ring and two ¹³C-atoms on the B-ring (6,8,10,3',5'-¹³C₅-C3G, hereafter referred to as ¹³C₅-C3G). Participants were asked to arrive on the study day in a fasted state (minimum 8 h). Blood samples were collected at regular intervals ($t=0.5$ h, $t=1$ h, $t=2$ h, $t=4$ h, $t=6$ h, $t=24$ h and $t=48$ h) following consumption. Individual urine samples were collected during the 6 hour study day and total urine voids were collected during the 6-24h and 24-48 hour periods. An anthocyanin-free meal was provided between 2-4 hours post-bolus. Participants were asked to maintain a low anthocyanin diet for the next 48 hours. Participants were also asked to avoid any foods containing high levels of anthocyanins and ¹³C (Morrison *et al.* 2000) over the 7 day run-in period and during the intervention. Upon collection, the blood samples were left to clot for 1 hour before being centrifuged at 3000 x *g* for 10 min. The serum was then removed and 7 mL were acidified manually to pH 2.4 with formic acid using a pH meter. Urine samples were combined with 100 mg of ascorbate per 500 mL of urine and were also acidified manually to pH 2.4 using formic acid. All samples were stored at -80°C until analysis.

5.2.3. Serum sample preparation: solid-phase extraction (SPE)

48 acidified serum samples were extracted via SPE, following previously reported methodology (Czank *et al.* 2013, de Ferrars *et al.* 2014c). Briefly, SPE cartridges were preconditioned with 6 mL of acidified methanol (acidified to pH 2.4 using formic acid) followed by 6 mL of acidified water (acidified to pH 2.4 using formic acid). Cartridges were loaded with 1 mL acidified water followed by 1 mL of serum spiked with 4 µL of internal standard (1 mg/mL phloridzin) and sample tubes were rinsed with a further 1 mL of acidified water and loaded onto the cartridge. Samples were eluted at a flow rate of approximately 1 drop/second. Extraction cartridges were washed with 12 mL of acidified water before being dried under vacuum for 30 mins. 5 mL of acidified methanol was added to the cartridges and left to soak for 10 mins before the samples were eluted, including a final 2 mL of acidified methanol. The eluent was evaporated to approximately 50 µL on a rotary evaporator (Thermo SPD Speedvac). Following evaporation, the samples were reconstituted with 200 µL acidified water and 2.5 µL of a volume indicator (volume control standard; 1 mg/mL scopoletin) to allow determination of accurate volume. The samples were then sonicated for 10 mins with the ultrasonic water bath kept cool using ice, followed by vortex mixing for 10 seconds, filtration through a 0.45 µm syringe filter and were finally stored at -80°C until analysis.

5.2.4. Urine sample preparation: protein precipitation (PPT)

Acidified urine samples were pooled to create three time-points for each of the eight participants; Baseline (BL), 6-24 hours and 24-48 hours. The 24 pooled urine samples were extracted via PPT. Samples were spiked with 4.36 µL of internal standard (1 mg/mL phloridzin) and 4 mL of acetonitrile containing 0.1% v/v formic acid, mixed by vortex for 10 seconds, stored at -20°C for 30 mins and centrifuged at 4000 x *g*, 8°C for 10 mins. After centrifugation, the supernatant was removed, placed into a test tube and evaporated to dryness on a Thermo Speedvac concentrator. Samples were reconstituted in 247.6 µL of mobile phase diluent (0.1/5/94.9 v/v/v formic acid/methanol/water) and 2.4 µL of scopoletin (0.1 mg/mL) added to samples to give a 5 µM internal standard. Samples were sonicated for 10 mins with the ultrasonic water bath kept cool using ice, mixed by vortex for 10 seconds, filtered through a 0.45 µm syringe filter and finally stored at -80°C until analysis.

5.2.5. Serum chromatography

HPLC-ESI-MS/MS analysis was carried out using an Agilent (Stockport, UK) 1200 series HPLC equipped with a Diode Array Detector (DAD) coupled to an AB SCIEX (Warrington, UK) 3200 series QTRAP® MS/MS system with Turbo V™ electrospray ionisation source using

previously established methods (Czank *et al.* 2013, de Ferrars *et al.* 2014c). Briefly, a Kinetex® pentafluorophenyl (PFP) (2.6 µm, 100 x 4.6 mm) RP-HPLC column was used with a PFP SecurityGuard® cartridge (4.6 x 2.0 mm). The column temperature was set at 37°C, injector temperature of 4°C and injection volume of 5 µL. Mobile Phase A was 0.1% (v/v) formic acid in water and Mobile Phase B was 0.1% (v/v) formic acid in acetonitrile at a flow rate of 1.5 mL min⁻¹ at 0 min, 1 mL min⁻¹ at 7 to 14 min and 1.5 mL min⁻¹ at 14 to 32 min. The gradient consisted of 1% B at 0 min, 7.5% B at 7 min, 7.6% B at 14 min, 10% B at 17 min, 12% B at 18.5 min, 12.5% B at 20 min, 30% B at 24 min, 90% B at 25 to 28 min, 1% B at 29 to 32 min. MS/MS source parameters included ionspray voltage, -4000 V / +5500 V; temperature, 700°C; curtain gas, 40 psi; nebulizer gas and auxiliary gas, 60 psi. Scheduled multiple reaction monitoring (sMRM) scans were performed using parameters optimised for the detection of analytical standards (**Table 5.1**). Samples were analysed in negative and positive ionisation modes at *m/z* to detect metabolites from the background diet that contained only the naturally abundant ¹²C carbon atoms. Samples were also analysed at *m/z* +2, for all compounds except cyanidin-3-glucoside, scopoletin and phloridzin, to detect B-ring-derived ¹³C-labelled metabolites that contained two ¹³C carbon atoms. Additionally, methyl 3,4-dihydroxybenzoate and ferulic acid were analysed at *m/z* +3 to detect A-ring-derived ¹³C-labelled metabolites that contained three ¹³C carbon atoms. Cyanidin-3-glucoside was analysed at *m/z* +5 due to the compound containing all five ¹³C carbon atoms.

Retention time and the detection of three or more of the relevant ion transitions were used to confirm the identity of the metabolites. For quantification, the peak area of the most intense ion transition was used. An eleven-point calibration (0 – 12.5 µM) curve was prepared by spiking a standard mixture of the compounds into a matched-matrix (blank serum) and coefficients of determination (*R*²) were established as linear (0.991 ± 0.007).

Table 5.1 sMRM schedule used to analyse the extracted serum samples on the AB SCIEX 3200 QTRAP® instrument.

Compound	¹² C Transitions (m/z) precursor/product ions	¹³ C Transitions (m/z +2) precursor/product ions	¹³ C Transitions (m/z +3) precursor/product ions	¹³ C Transitions (m/z +5) precursor/product ions	Scan time range (min)	Scan mode
Benzoic acid-4-glucuronide	313/175,113,93*	315/177,115,95*	N/A	N/A	2.0 – 4.0	-
Protocatechuic acid-4-glucuronide	329.01/153*,113,109	331.01/155*,115,111	N/A	N/A	2.4 – 4.4	-
Protocatechuic acid	153.01/108*,91,81	155.01/110*,93,83	N/A	N/A	3.2 – 5.2	-
Protocatechuic acid-3-glucuronide	329.01/153*,113,109	331.01/155*,115,111	N/A	N/A	3.4 – 5.4	-
Vanillic acid-4-glucuronide	343.01/167,152,113*	345.01/169,154,115*	N/A	N/A	4.6 – 6.6	-
Isovanillic acid-3-glucuronide	343.01/167,152,113*	345.01/169,154,115*	N/A	N/A	4.6 – 6.6	-
Hippuric acid	177.9/133.9*,77.1,131.8	179.9/135.9*,79.1,133.8	N/A	N/A	5.0 – 7.0	-
Protocatechuic acid-3/4-sulfate ^a	233.01/153,109*,189	235.01/155,111*,191	N/A	N/A	6.3 – 8.3	-
4-hydroxybenzaldehyde	121.2/107.8,92*,65.1	123.2/109.8,94*,67.1	N/A	N/A	7.0 – 9.0	-
Isovanillic acid	169.01/151.1,125,93*	171.01/153.1,127,95*	N/A	N/A	7.3 – 11.3	+
Vanillic acid	167.03/152*,123,108	169.03/154*,125,110	N/A	N/A	8.8 – 10.8	-
(Iso)vanillic acid-3/4-sulfate ^a	247/167*,152,108	249/169*,154,110	N/A	N/A	8.9 – 10.9	-
Methyl 3,4-dihydroxybenzoate	167/107.8*,107.1,91.2	169/109.8*,109.1,93.2	170/110.8*,110.1,94.2	N/A	11.5 – 13.5	-
Cyanidin-3-glucoside	449/287*,213,137	N/A	N/A	454/292*,218,142	11.9 – 15.9	+
Phloroglucinaldehyde	153/151*,125,107	155/153*,127,109	N/A	N/A	13.7 – 15.7	-
Ferulic acid	193/178,149,134*	195/180,151,136*	196/181,152,137*	N/A	17.8 – 19.8	-
Scopoletin	193/133.2*,122,94.1	N/A	N/A	N/A	17.1 – 21.1	+
Scopoletin	191/104*,147.9,120	N/A	N/A	N/A	18.1 – 20.1	-
Phloridzin	437/275,169,107*	N/A	N/A	N/A	22.1 – 26.1	+
Phloridzin	435/273*,167,123,81	N/A	N/A	N/A	23.1 – 25.1	-

*Transition used for quantitation. N/A, compound not analysed using this m/z. ^aIsomers of this metabolite were unresolvable using this HPLC-ESI-MS/MS method so were quantified as a single analyte

5.2.6. Urine chromatography

HPLC-ESI-MS/MS analysis was carried out using an Agilent 1200 series HPLC equipped with a DAD coupled to an AB SCIEX 3200 series QTRAP® MS/MS system with Turbo V™ electrospray ionisation source using methods adapted from previously established methods (Czank *et al.* 2013, de Ferrars *et al.* 2014c). Briefly, a Kinetex® PFP (2.6 µm, 50 x 2.1 mm) RP-HPLC column was used with a PFP SecurityGuard® cartridge (2.1 x 2.0 mm). The column temperature was set at 40°C, injector temperature of 4°C and injection volume of 5 µL. Mobile Phase A was 0.1% (v/v) formic acid in water and Mobile Phase B was 0.1% (v/v) formic acid in acetonitrile at a flow rate of 0.6 mL min⁻¹. The gradient consisted of 1% B at 0 min, 7.5% B at 7 min, 7.6% B at 9 min, 90% B at 9.5 to 11.5 min, 1% B at 12 to 15 min. MS/MS source parameters included ionspray voltage, -4000 V / +5500 V; temperature, 700°C; curtain gas, 35 psi; nebulizer gas, 40 psi; auxiliary gas, 45 psi. sMRM scans were performed using parameters optimised for the detection of analytical standards (**Table 5.2**). Samples were analysed in negative and positive ionisation modes at *m/z* to detect metabolites from the background diet that contained only the naturally abundant ¹²C carbon atoms. Samples were also analysed at *m/z* +2, for all compounds except cyanidin-3-glucoside, scopoletin and phloridzin, to detect B-ring-derived ¹³C-labelled metabolites that contained two ¹³C carbon atoms. Additionally, samples were analysed at *m/z* +3 to detect A-ring-derived ¹³C-labelled metabolites that contained three ¹³C carbon atoms. Cyanidin-3-glucoside was analysed at *m/z* +5 due to the compound containing all five ¹³C carbon atoms.

Retention time and the detection of three or more of the relevant ion transitions were used to confirm the identity of the metabolites. For quantification, the peak area of the most intense ion transition was used. A nine-point calibration curve (0 – 25 µM) was prepared by spiking a standard mixture of the compounds into a matched-matrix (blank urine) and coefficients of determination (*R*²) were established as linear (0.995 ± 0.005).

Table 5.2 sMRM schedule used to analyse the extracted urine samples on the AB SCIEX 3200 QTRAP® instrument.

Compound	¹² C Transitions (m/z) precursor/product ion	¹³ C Transitions (m/z +2) precursor/product ion	¹³ C Transitions (m/z +3) precursor/product ion	¹³ C Transitions (m/z +5) precursor/product ion	Scan time range (min)	Scan mode
<i>trans</i> -Cinnamic acid	147/103*,79,64	149/105*,81,66	150/106*,82,67	N/A	0.0 – 1.5	-
Gallic acid	169.2/125.1*,106.7,78.8	171.2/127.1*,108.7,80.8	172.2/128.1*,109.7,81.8	N/A	0.0 – 1.9	-
Benzoic acid-4-glucuronide	313.1/175.1,113.1*,93.1	315.1/177.1,115.1*,95.1	316.1/178.1,116.1*,96.1	N/A	0.1 – 2.1	-
Protocatechuic acid-4-glucuronide	329/153*,113,109	331/155*,115,111	332/156*,116,112	N/A	0.2 – 2.2	-
α-hydroxyhippuric acid	194.3/176.3,148.3,73.3*	196.3/178.3,150.3,75.3*	197.3/179.3,151.3,76.3*	N/A	0.4 – 2.4	-
Protocatechuic acid	153.1/108.1*,91.1,81.1	155.1/110.1*,93.1,83.1	156.1/111.1*,94.1,84.1	N/A	0.7 – 2.7	-
Protocatechuic acid-3-glucuronide	329.1/153.1*,113.1,109.1	331.1/155.1*,115.1,111.1	332.1/156.1*,116.1,112.1	N/A	0.7 – 2.7	-
4-hydroxyhippuric acid	194.2/150.2,100.2*,93.2	196.2/152.2,102.2*,95.2	197.2/153.2,103.2*,96.2	N/A	0.8 – 2.8	-
Dihydroxycinnamic acid-glucuronide ^a	355/179,135*,111	357/181,137*,113	358/182,138*,114	N/A	1.0 – 3.0	-
2,3/2,4/2,5/3,5-dihydroxybenzoic acid ^d	152.8/109*,107.8,90.8	154.8/111*,109.8,92.8	155.8/112*,110.8,93.8	N/A	1.1 – 3.1	-
3,4-dihydroxyphenylacetic acid	167.2/123.2*,108.2,95.2	169.2/125.2*,110.2,97.2	170.2/126.2*,111.2,98.2	N/A	1.1 – 3.1	-
3-hydroxyhippuric acid	194.1/150.1*,148.1,93.1	196.1/152.1*,150.1,95.1	197.1/153.1*,151.1,96.1	N/A	1.1 – 3.1	-
4-hydroxybenzyl alcohol	123/121*,105,77	125/123*,107,79	126/124*,108,80	N/A	1.1 – 3.1	-
Protocatechuic acid-3/4-sulfate ^d	233.1/189.1,153.1,109.1*	235.1/191.1,155.1,111.1*	236.1/192.1,156.1,112.1*	N/A	1.1 – 3.1	-
Vanillic acid-4-glucuronide	343.2/167.2,152.2,113.2*	345.2/169.2,154.2,115.2*	346.2/170.2,155.2,116.2*	N/A	1.3 – 3.3	-
3,4-dihydroxybenzaldehyde	136.9/107.9*,92,81	138.9/109.9*,94,83	139.9/110.9*,95,84	N/A	1.6 – 3.6	-
3/4-hydroxybenzoic acid ^d	137.1/93.1*,75.1,65.1	139.1/95.1*,77.1,67.1	140.1/96.1*,78.1,68.1	N/A	1.8 – 3.8	-
Methyl dihydroxybenzoate-sulfate ^b	247/167,152*,137	249/169,154*,139	250/170,155,140	N/A	1.9 – 3.9	-
Hippuric acid	177.9/133.9*,131.8,77.1	179.9/135.9*,133.8,79.1	180.9/136.9*,134.8,80.1	N/A	2.0 – 4.0	-
Isovanillic acid-3-glucuronide	343.1/167.1,152.1,113.1*	345.1/169.1,154.1,115.1*	346.1/170.1,155.1,116.1*	N/A	2.1 – 4.1	-
Isovanillic acid-3-sulfate	247/167*,152,108	249/169*,154,110	250/170*,155,111	N/A	2.1 – 4.1	-
4-hydroxyphenylacetic acid	151.2/123.2,107.2*,93.2	153.2/125.2,109.2*,95.2	154.2/126.2,110.2*,96.2	N/A	2.5 – 4.5	-
Vanillic acid-4-sulfate	247.1/167.1*,152.1,108.1	249.1/169.1*,154.1,110.1	250.1/170.1*,155.1,111.1	N/A	2.9 – 4.9	-
3-hydroxyphenylacetic acid	151.1/136.1,121.1,107.1*	153.1/138.1,123.1,109.1*	154.1/139.1,124.1,110.1*	N/A	3.0 – 5.0	-
4-hydroxybenzaldehyde	121.2/107.8,92.2*,65.2	123.2/109.8,94.2*,67.2	124.2/110.8,95.2*,68.2	N/A	3.1 – 5.1	-
Dihydroxyphenylacetic acid-sulfate ^c	247/167*,152,123	249/169*,154,125	250/170*,155,126	N/A	3.3 – 5.3	-
Isovanillic acid	169.01/151.1,125,93*	171.01/153.1,127,95*	172.01/154.1,128,96*	N/A	3.8 – 7.8	+
Vanillic acid	167.3/152.3*,123.3,108.3	169.3/154.3*,125.3,110.3	170.3/155.3*,126.3,111.3	N/A	4.4 – 6.4	-
Caffeic acid	179/135*,106,89	181/137*,108,91	182/138*,109,92	N/A	5.1 – 7.1	-
Benzoylglutamic acid	250/206*,162,121	252/208*,164,123	253/209*,165,124	N/A	5.2 – 7.2	-
Homovanillic acid	181.1/166.1,137.1*,79.1	183.1/168.1,139.1*,81.1	184.1/169.1,140.1*,82.1	N/A	5.2 – 7.2	-
Benzoic acid	121/93,92,77*	123/95,94,79*	124/96,95,80*	N/A	5.4 – 7.4	-
Phenylacetic acid	135/119,91*,64	137/121,93*,66	138/122,94*,67	N/A	5.6 – 7.6	-
Syringic acid	199/155.2,140*,125	201/157.2,142*,127	202/158.2,143*,128	N/A	5.6 – 9.6	+

Table 5.2 (Continued)

Compound	¹² C Transitions (m/z) precursor/product ion	¹³ C Transitions (m/z +2) precursor/product ion	¹³ C Transitions (m/z +3) precursor/product ion	¹³ C Transitions (m/z +5) precursor/product ion	Scan time range (min)	Scan mode
3-(4-hydroxyphenyl)propionic acid	165.1/121.1*,97.1,93.1	167.1/123.1*,99.1,95.1	168.1/124.1*,100.1,96.1	N/A	5.7 – 7.7	-
Hydroxy-methoxycinnamic acid-glucuronide ^a	369/193,173,111*	371/195,175,113*	372/196,176,114	N/A	6.0 – 8.0	-
3-(3-hydroxyphenyl)propionic acid	165/121*,119,106	167/123*,121,108	168/124*,122,109	N/A	6.2 – 8.2	-
Methyl 3,4-dihydroxybenzoate	167/107.8*,107.1,91.2	169/109.8*,109.1,93.2	170/110.8*,110.1,94.2	N/A	6.2 – 8.2	-
Chlorogenic acid	353/191*,161,127	355/193*,163,129	356/194*,164,130	N/A	6.6 – 8.6	-
4-methylhippuric acid	192.2/148.2,146.2,91.2*	194.2/150.2,148.2,93.2*	195.2/151.2,149.2,94.2*	N/A	6.7 – 8.7	-
3-methylhippuric acid	192.1/148.1,146.1,90.9*	194.1/150.1,148.1,92.9*	195.1/151.1,149.1,93.9*	N/A	6.8 – 8.8	-
2-hydroxybenzoic acid	137/93*,75,65	139/95*,77,67	140/96*,78,68	N/A	7.0 – 9.0	-
p-Coumaric acid	163/118.9*,116.9,92.9	165/120.9*,118.9,94.9	166/121.9*,119.9,95.9	N/A	7.1 – 9.1	-
Phloroglucinaldehyde	153/151*,125,107	155/153*,127,109	156/154*,128,110	N/A	7.2 – 9.2	-
3-(4-hydroxy-3-methoxyphenyl)propionic acid	195/136*,121,119	197/138*,123,121	198/139*,124,122	N/A	7.8 – 9.8	-
<i>trans</i> -3-hydroxycinnamic acid	163.2/119.2*,93.2,91.2	165.2/121.2*,95.2,93.2	166.2/122.2*,96.2,94.2	N/A	8.4 – 10.4	-
Cyanidin-3-glucoside	449/287*,213,137	N/A	N/A	454/292*,218,142	8.8 – 12.8	+
Scopoletin	193/133.2*,122,94.1	N/A	N/A	N/A	8.8 – 12.8	+
Phloridzin	437/275,169,107*	N/A	N/A	N/A	8.9 – 12.9	+
2-hydroxycinnamic acid	163/119*,117,93	165/121*,119,95	166/122*,120,96	N/A	9.8 – 11.8	-
(<i>Iso</i>)ferulic acid ^d	193.1/178.1,149.1,134.1*	195.1/180.1,151.1,136.1*	196.1/181.1,152.1,137.1*	N/A	9.8 – 11.8	-
Scopoletin	191/147.9*,120,104	N/A	N/A	N/A	9.8 – 11.8	-
Rosmarinic acid	359.1/197.1,179.1,161.1*	361.1/199.1,181.1,163.1*	362.1/200.1,182.1,164.1*	N/A	9.9 – 11.9	-
Sinapic acid	223/208*,193,164	225/210*,195,166	226/211*,196,167	N/A	9.9 – 11.9	-
Phloridzin	435.1/273.1,167.1*,123.1	N/A	N/A	N/A	9.9 – 11.9	-
Dimethoxy-hydroxycinnamic acid-glucuronide ^a	399/355,223*,173	401/357,225*,175	402/358,226*,176	N/A	9.9 – 11.9	-
2-hydroxy-4-methoxybenzoic acid	167.1/123.1,108.1*,80.1	169.1/125.1,110.1*,82.1	170.1/126.1,111.1*,83.1	N/A	10.0 – 12.0	-
Kaempferol	285/239*,229,211	287/241*,231,213	288/242*,232,214	N/A	10.1 – 12.1	-

*Transition used for quantitation. N/A, compound not analysed using this m/z. ^aPutative metabolite therefore analytical standard not available, 2-hydroxycinnamic acid standard curve used for quantitation. ^bPutative metabolite therefore analytical standard not available, methyl 3,4-dihydroxybenzoate standard curve used for quantitation. ^cPutative metabolite therefore analytical standard not available, 3-(4-hydroxyphenyl)propionic acid standard curve used for quantitation. ^dIsomers of this metabolite were unresolvable using this HPLC-ESI-MS/MS method so were quantified as a single analyte.

5.3. Results

5.3.1. Serum biomarkers

18 analytes were included in the analysis method to quantify the concentrations present in the serum from either the ^{13}C -labelled cyanidin-3-glucoside intervention or from the background diet in eight participants across eight time-points (0 – 48 h). Six analytes were detected from the ^{13}C -labelled cyanidin-3-glucoside intervention in at least one participant (**Table 5.3**) with concentrations ranging from 0.9 – 146.3 nM. Concentrations of the same analytes from the background diet ranged from 0.0 – 3743.5 nM. Hippuric acid was also detected at high concentration (1595.9 ± 987.6 nM) from the background diet in all participants. Cyanidin-3-glucoside was the analyte from the ^{13}C -labelled cyanidin-3-glucoside intervention found at the highest concentration (76.9 ± 47.6 nM). PCA-3/4-sulfate and hippuric acid were detected in all eight participants and PCA-3-glucuronide was detected at the same time-point (1 h) for each of the four participants in which it was detected.

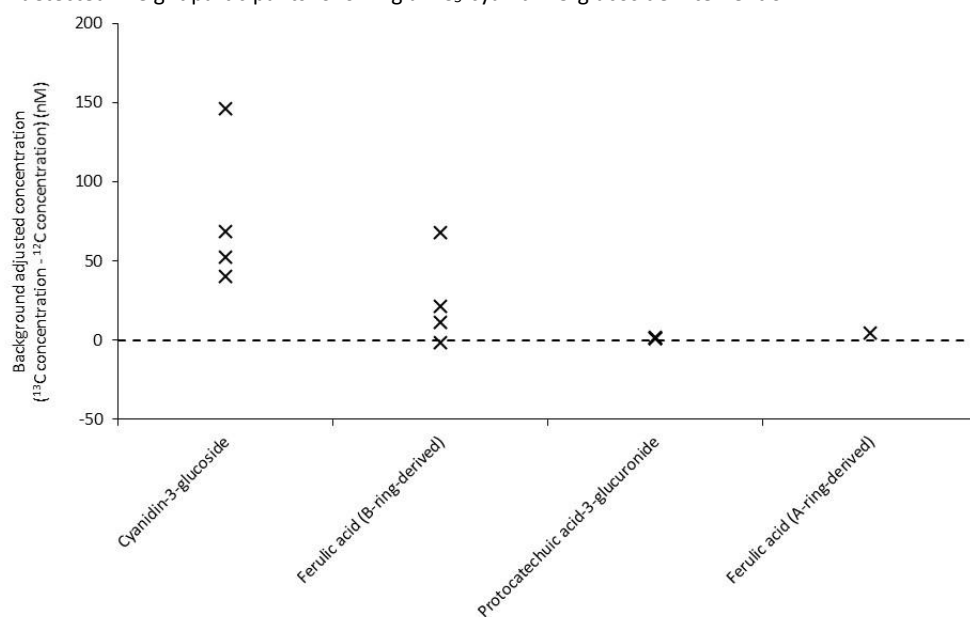
Table 5.3 Anthocyanin metabolite concentrations from $^{13}\text{C}_5$ -cyanidin-3-glucoside intervention compared to ^{12}C background levels in serum samples.

Compound	n=	^{13}C T _{max} (h) (mean \pm SD)	^{12}C background concentration (nM) (mean \pm SD)	^{13}C C _{max} (nM) (mean \pm SD)	Background adjusted concentration (nM) (mean \pm SD)
Cyanidin-3-glucoside	4	0.9 \pm 0.3	0.0 \pm 0.0	76.9 \pm 47.6	76.9 \pm 47.6
B-ring-derived					
4-hydroxybenzaldehyde	ND	ND	ND	ND	ND
Benzoic acid-4-glucuronide	ND	ND	ND	ND	ND
Ferulic acid	4	25.0 \pm 18.0	3.7 \pm 7.4	28.4 \pm 26.5	24.7 \pm 30.2
Hippuric acid	8	15.3 \pm 12.1	1595.9 \pm 987.6	25.1 \pm 14.9	-1570.8 \pm 993.4
Isovanillic acid	ND	ND	ND	ND	ND
IVA-3-glucuronide	ND	ND	ND	ND	ND
(I)VA-3/4-sulfate	ND	ND	ND	ND	ND
Methyl 3,4-DHB	ND	ND	ND	ND	ND
Phloroglucinaldehyde	ND	ND	ND	ND	ND
Protocatechuic acid	ND	ND	ND	ND	ND
PCA-3/4-sulfate	8	20.6 \pm 22.7	16.1 \pm 10.9	12.4 \pm 9.6	-3.6 \pm 16.2
PCA-3-glucuronide	4	1.0 \pm 0.0	0.0 \pm 0.0	1.2 \pm 0.4	1.2 \pm 0.4
PCA-4-glucuronide	ND	ND	ND	ND	ND
Vanillic acid	ND	ND	ND	ND	ND
Vanillic acid-4-glucuronide	ND	ND	ND	ND	ND
A-ring-derived					
Ferulic acid	1	48.0 \pm 0.0	0.0 \pm 0.0	4.7 \pm 0.0	4.7 \pm 0.0
Methyl 3,4-DHB	ND	ND	ND	ND	ND

IVA, isovanillic acid; Methyl 3,4-DHB, methyl 3,4-dihydroxybenzoate; PCA, protocatechuic acid. n=, number of participants in which metabolite was detected. ^{13}C T_{max}, time-point at which the maximum concentration of ^{13}C metabolites from the C3G intervention was observed. ^{12}C background concentration is the concentration of ^{12}C metabolites detected from the background diet at the ^{13}C T_{max} time-point. ^{13}C C_{max}, maximum concentration of ^{13}C metabolites from the C3G intervention observed amongst the eight participants. Background adjusted concentration is the ^{13}C C_{max} concentration minus the ^{12}C background concentration. ND, not detected.

Comparing the levels of metabolites derived from the ^{13}C -labelled cyanidin-3-glucoside intervention against those derived from the ^{12}C background diet, cyanidin-3-glucoside itself was detected in ^{13}C scans but not in ^{12}C scans indicating there was none in the background diet. Four out of the six analytes detected as derived from the ^{13}C -labelled intervention were found at concentrations above those derived from the ^{12}C background diet. Hippuric acid was detected at much greater concentrations from the background diet than from the ^{13}C -labelled intervention diet. PCA-3-glucuronide displayed the lowest variation (33.9%) between concentrations across all time-points for the four participants in which it was detected. Amongst all detected analytes, cyanidin-3-glucoside was found at the highest concentration within the ^{13}C -labelled metabolites and was also found at the lowest concentrations within the metabolites from the ^{12}C background diet meaning that cyanidin-3-glucoside had the highest background adjusted concentration (**Figure 5.1**).

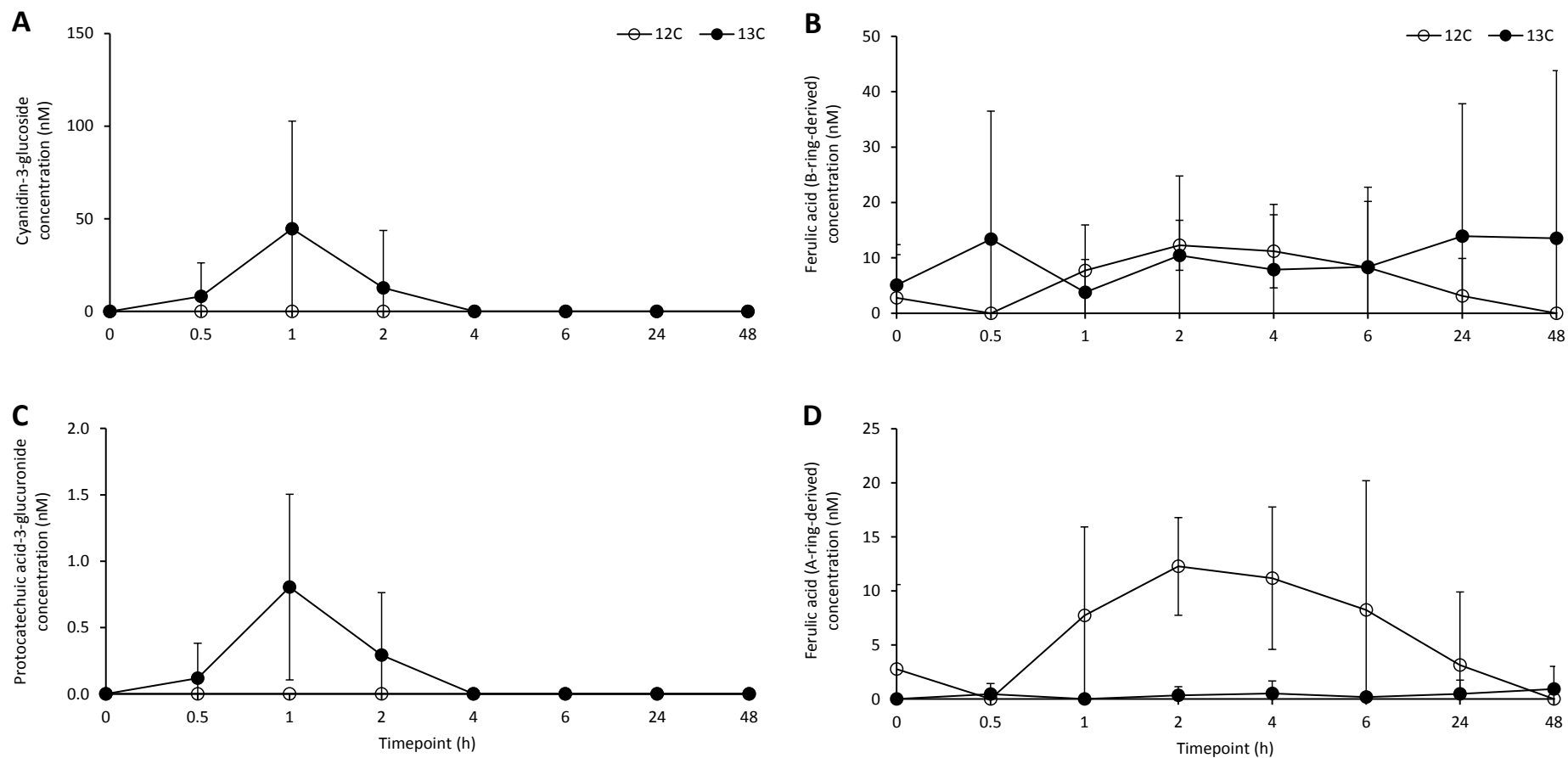
Figure 5.1 Background adjusted concentrations of cyanidin-3-glucoside and its serum metabolites detected in eight participants following a $^{13}\text{C}_5$ -cyanidin-3-glucoside intervention.



n=8 study participants. Each cross represents data from a single participant in which a ^{13}C -labelled analyte was detected and the maximum background adjusted analyte concentration (^{13}C concentration minus ^{12}C concentration) calculated to be present in that participant. Dotted line represents the point at which the analyte concentration from the ^{13}C -labelled cyanidin-3-glucoside intervention is equal to the concentration found in the background diet.

Analysis of the metabolite concentration from the ^{13}C -labelled cyanidin-3-glucoside intervention compared to the level from the background diet shows that cyanidin-3-glucoside and PCA-3-glucuronide both peak in concentration at 1 h following intake, while B-ring-derived ferulic acid reached concentrations elevated above background first at 0.5 h and again at 24 and 48 h following ^{13}C -labelled cyanidin-3-glucoside intake (**Figure 5.2**).

Figure 5.2 ^{13}C -labelled serum metabolite concentration compared to ^{12}C background concentration throughout 48 hours following $^{13}\text{C}_5$ -cyanidin-3-glucoside intervention.



(A) Cyanidin-3-glucoside. (B) Ferulic acid (B-ring-derived). (C) Protocatechuic acid-3-glucuronide. (D) Ferulic acid (A-ring-derived). 12C, background concentration; 13C, ^{13}C -labelled metabolite concentration. Results expressed as mean \pm SD.

5.3.2. Urine biomarkers

107 analytes were included in the analysis method to quantify the concentrations present in the urine from either detection of the ^{13}C -labelled cyanidin-3-glucoside from the intervention bolus or naturally abundant ^{12}C analytes, reflecting compounds derived from the background diet in eight participants across eight time-points (0 – 48 h). 36 analytes were detected from the ^{13}C -labelled cyanidin-3-glucoside intervention in at least one participant (**Table 5.4**) with concentrations ranging from 0.1 – 217.3 nM. Concentrations of the same analytes from the background diet ranged from 0.0 – 4127.1 nM. 3-methylhippuric acid was the analyte from the ^{13}C -labelled cyanidin-3-glucoside intervention found at the highest concentration (77.3 ± 61.4 nM). 17 analytes were detected in all eight participants. Maximal concentrations of A-ring-derived gallic acid and isovanillic acid were detected in 6-24 hour samples of all eight participants. 11 analytes were detected from the background diet at every time-point in all participants; 3/4-hydroxybenzoic acid, 3-hydroxyhippuric acid, 3-hydroxyphenylacetic acid, 4-hydroxyhippuric acid, 4-hydroxyphenylacetic acid, dihydroxycinnamic acid-glucuronide, dimethoxy-hydroxycinnamic acid-glucuronide, hippuric acid, homovanillic acid, hydroxy-methoxycinnamic acid-glucuronide, and *trans*-cinnamic acid.

Table 5.4 Anthocyanin metabolite concentrations from $^{13}\text{C}_5$ -cyanidin-3-glucoside intervention compared to ^{12}C background levels in urine samples.

Compound	n=	^{12}C background concentration (nM) (mean \pm SD)	^{13}C C _{max} (nM) (mean \pm SD)	Background adjusted concentration (nM) (mean \pm SD)
Cyanidin-3-glucoside	ND	ND	ND	ND
B-ring-derived				
2,3/2,4/2,5/3,5-dihydroxybenzoic acid	ND	ND	ND	ND
2-hydroxy-4-methoxybenzoic acid	ND	ND	ND	ND
2-hydroxybenzoic acid	ND	ND	ND	ND
2-hydroxycinnamic acid	ND	ND	ND	ND
3-(3-hydroxyphenyl)propionic acid	ND	ND	ND	ND
3-(4-hydroxy-3-methoxyphenyl)propionic acid	ND	ND	ND	ND
3-(4-hydroxyphenyl)propionic acid	1	0.0 \pm 0.0	0.6 \pm 0.0	0.6 \pm 0.0
3,4-dihydroxybenzaldehyde	ND	ND	ND	ND
3,4-dihydroxyphenylacetic acid	3	3.1 \pm 5.4	24.4 \pm 13.5	21.2 \pm 17.8
3/4-hydroxybenzoic acid	2	1.9 \pm 0.0	0.6 \pm 0.8	-1.3 \pm 0.8
3-hydroxyhippuric acid	8	203.5 \pm 249.5	14.9 \pm 12.7	-188.5 \pm 253.1
3-hydroxyphenylacetic acid	ND	ND	ND	ND
3-methylhippuric acid	8	0.2 \pm 0.3	77.3 \pm 61.4	77.1 \pm 61.4
4-hydroxybenzaldehyde	ND	ND	ND	ND
4-hydroxybenzyl alcohol	ND	ND	ND	ND
4-hydroxyhippuric acid	2	155.4 \pm 57.4	0.4 \pm 0.4	-154.9 \pm 57.1
4-hydroxyphenylacetic acid	2	59.3 \pm 24.1	1.7 \pm 0.5	-57.6 \pm 23.6
4-methylhippuric acid	8	0.3 \pm 0.3	75.1 \pm 62.3	74.8 \pm 62.2
α -hydroxyhippuric acid	ND	ND	ND	ND
Benzoic acid	ND	ND	ND	ND
Benzoic acid-4-glucuronide	ND	ND	ND	ND
Benzoylglutamic acid	ND	ND	ND	ND
Caffeic acid	2	0.0 \pm 0.0	0.2 \pm 0.2	0.2 \pm 0.2
Chlorogenic acid	ND	ND	ND	ND
Dihydroxycinnamic acid-glucuronide	8	2.3 \pm 1.5	0.8 \pm 0.7	-1.5 \pm 1.9
Dihydroxyphenylacetic acid-sulfate	2	4.0 \pm 5.7	12.9 \pm 16.8	8.8 \pm 22.5
Dimethoxy-hydroxycinnamic acid-glucuronide	8	5.6 \pm 9.9	1.8 \pm 1.0	-3.8 \pm 9.6
(Iso)ferulic acid	ND	ND	ND	ND
Gallic acid	8	0.8 \pm 0.8	1.2 \pm 0.6	0.4 \pm 0.7
Hippuric acid	8	1810.7 \pm 1296.9	28.5 \pm 18.6	-1782.2 \pm 1302.2
Homovanillic acid	1	58.5 \pm 0.0	1.8 \pm 0.0	-56.7 \pm 0.0
Hydroxy-methoxycinnamic acid-glucuronide	8	12.9 \pm 8.5	4.0 \pm 3.8	-8.9 \pm 7.6
Isovanillic acid	8	0.0 \pm 0.0	0.0 \pm 0.0	0.0 \pm 0.0
Isovanillic acid-3-glucuronide	ND	ND	ND	ND
Isovanillic acid-3-sulfate	3	0.0 \pm 0.0	1.0 \pm 0.6	1.0 \pm 0.6
Kaempferol	4	0.3 \pm 0.6	0.3 \pm 0.4	0.0 \pm 0.2
Methyl 3,4-dihydroxybenzoate	ND	ND	ND	ND
Methyl dihydroxybenzoate-sulfate	8	2.0 \pm 4.5	1.6 \pm 1.0	-0.5 \pm 5.1
Protocatechuic acid	ND	ND	ND	ND
Protocatechuic acid-3-glucuronide	ND	ND	ND	ND
Protocatechuic acid-3/4-sulfate	ND	ND	ND	ND
Protocatechuic acid-4-glucuronide	ND	ND	ND	ND
p-Coumaric acid	ND	ND	ND	ND
Phloroglucinaldehyde	ND	ND	ND	ND
Phenylacetic acid	ND	ND	ND	ND
Rosmarinic acid	5	0.0 \pm 0.1	0.1 \pm 0.1	0.0 \pm 0.1
Sinapic acid	ND	ND	ND	ND
Syringic acid	ND	ND	ND	ND
<i>trans</i> -3-hydroxycinnamic acid	1	0.0 \pm 0.0	3.0 \pm 0.0	3.0 \pm 0.0
<i>trans</i> -Cinnamic acid	8	3.9 \pm 3.6	1.5 \pm 0.6	-2.4 \pm 3.5

Table 5.4 (Continued)

Compound	n=	¹² C background concentration (nM) (mean ± SD)	¹³ C C _{max} (nM) (mean ± SD)	Background adjusted concentration (nM) (mean ± SD)
Vanillic acid	ND	ND	ND	ND
Vanillic acid-4-glucuronide	ND	ND	ND	ND
Vanillic acid-4-sulfate	ND	ND	ND	ND
A-ring-derived				
2,3/2,4/2,5/3,5-dihydroxybenzoic acid	ND	ND	ND	ND
2-hydroxy-4-methoxybenzoic acid	ND	ND	ND	ND
2-hydroxybenzoic acid	ND	ND	ND	ND
2-hydroxycinnamic acid	ND	ND	ND	ND
3-(3-hydroxyphenyl)propionic acid	ND	ND	ND	ND
3-(4-hydroxy-3-methoxyphenyl)propionic acid	ND	ND	ND	ND
3-(4-hydroxyphenyl)propionic acid	ND	ND	ND	ND
3,4-dihydroxybenzaldehyde	ND	ND	ND	ND
3,4-dihydroxyphenylacetic acid	ND	ND	ND	ND
3/4-hydroxybenzoic acid	ND	ND	ND	ND
3-hydroxyhippuric acid	6	133.3 ± 98.3	1.0 ± 0.9	-132.3 ± 98.6
3-hydroxyphenylacetic acid	ND	ND	ND	ND
3-methylhippuric acid	8	0.2 ± 0.3	4.6 ± 4.2	4.4 ± 4.2
4-hydroxybenzaldehyde	ND	ND	ND	ND
4-hydroxybenzyl alcohol	ND	ND	ND	ND
4-hydroxyhippuric acid	ND	ND	ND	ND
4-hydroxyphenylacetic acid	1	40.1 ± 0.0	4.4 ± 0.0	-35.7 ± 0.0
4-methylhippuric acid	8	0.3 ± 0.3	4.6 ± 4.0	4.3 ± 3.9
α-hydroxyhippuric acid	ND	ND	ND	ND
Benzoic acid	ND	ND	ND	ND
Benzoic acid-4-glucuronide	ND	ND	ND	ND
Benzoylglutamic acid	ND	ND	ND	ND
Caffeic acid	7	0.4 ± 0.8	1.6 ± 1.9	1.2 ± 1.4
Chlorogenic acid	ND	ND	ND	ND
Dihydroxycinnamic acid-glucuronide	3	0.8 ± 0.4	0.0 ± 0.0	-0.7 ± 0.4
Dihydroxyphenylacetic acid-sulfate	ND	ND	ND	ND
Dimethoxy-hydroxycinnamic acid-glucuronide	3	4.7 ± 3.5	0.1 ± 0.1	-4.6 ± 3.6
(Iso)ferulic acid	ND	ND	ND	ND
Gallic acid	8	0.6 ± 0.6	55.3 ± 16.8	54.7 ± 16.2
Hippuric acid	8	1640.4 ± 1446.7	13.4 ± 11.6	-1627.1 ± 1436.7
Homovanillic acid	2	73.0 ± 26.5	1.8 ± 1.3	-71.1 ± 25.2
Hydroxy-methoxycinnamic acid-glucuronide	5	13.0 ± 7.9	0.5 ± 0.4	-12.5 ± 7.7
Isovanillic acid	8	0.0 ± 0.0	0.3 ± 0.2	0.3 ± 0.2
Isovanillic acid-3-glucuronide	ND	ND	ND	ND
Isovanillic acid-3-sulfate	ND	ND	ND	ND
Kaempferol	ND	ND	ND	ND
Methyl 3,4-dihydroxybenzoate	ND	ND	ND	ND
Methyl dihydroxybenzoate-sulfate	8	2.0 ± 4.5	0.2 ± 0.1	-1.9 ± 4.5
Protocatechuic acid	ND	ND	ND	ND
Protocatechuic acid-3-glucuronide	ND	ND	ND	ND
Protocatechuic acid-3/4-sulfate	ND	ND	ND	ND
Protocatechuic acid-4-glucuronide	ND	ND	ND	ND
p-Coumaric acid	ND	ND	ND	ND
Phloroglucinaldehyde	ND	ND	ND	ND
Phenylacetic acid	ND	ND	ND	ND
Rosmarinic acid	ND	ND	ND	ND
Sinapic acid	ND	ND	ND	ND
Syringic acid	ND	ND	ND	ND
trans-3-hydroxycinnamic acid	ND	ND	ND	ND

Table 5.4 (Continued)

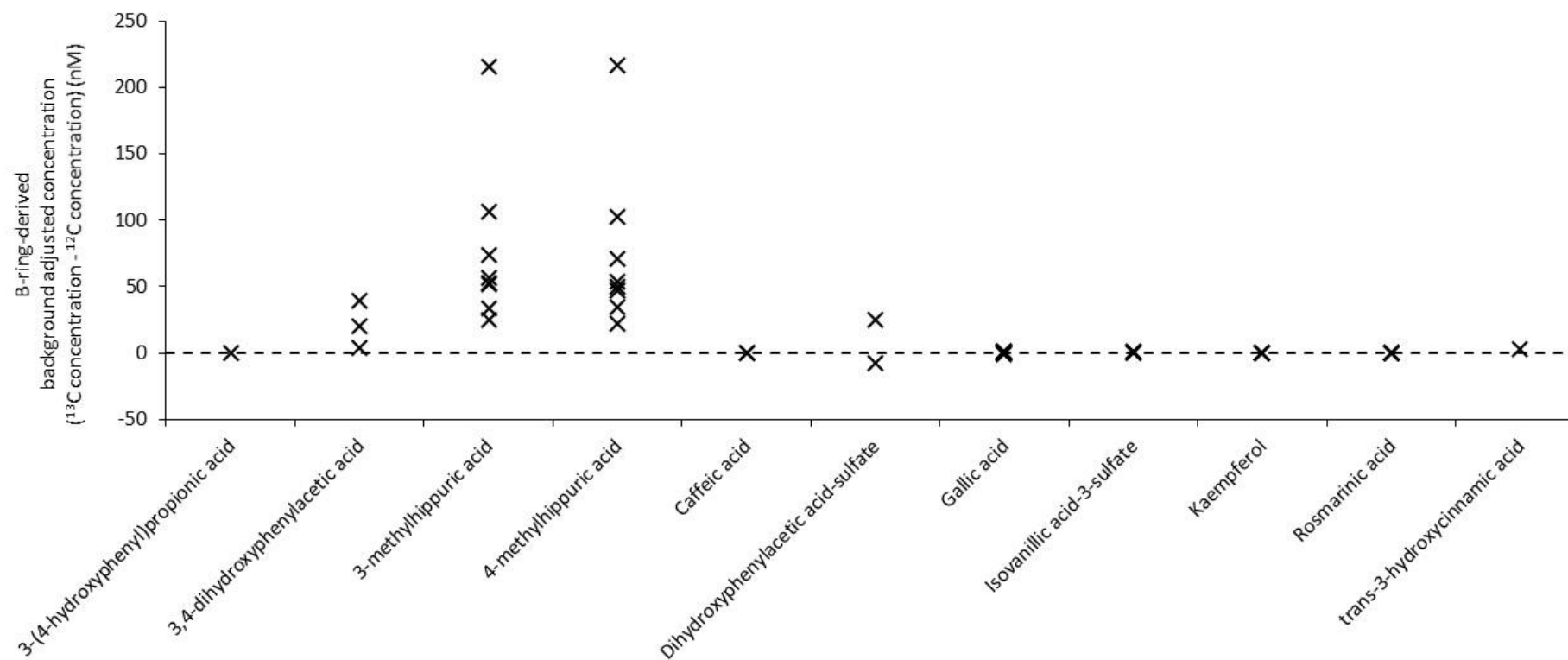
Compound	n=	¹² C background concentration (nM) (mean ± SD)	¹³ C C _{max} (nM) (mean ± SD)	Background adjusted concentration (nM) (mean ± SD)
<i>trans</i> -Cinnamic acid	ND	ND	ND	ND
Vanillic acid	ND	ND	ND	ND
Vanillic acid-4-glucuronide	ND	ND	ND	ND
Vanillic acid-4-sulfate	ND	ND	ND	ND

n=, number of participants in which metabolite was detected. ¹²C background concentration is the concentration of ¹²C metabolites detected from the background diet at the ¹³C T_{max} time-point (time-point at which the maximum concentration of ¹³C metabolites from the C3G intervention was observed). ¹³C C_{max}, maximum concentration of ¹³C metabolites from the C3G intervention observed amongst the eight participants. Background adjusted concentration is the ¹³C C_{max} concentration minus the ¹²C background concentration. ND, not detected.

16 analytes showed concentrations of ¹³C-labelled metabolites above those present in baseline samples (reflecting background concentrations) (**Figure 5.3 & Figure 5.4**). Hippuric acid was detected at much greater concentrations from the background diet than from the ¹³C-labelled cyanidin-3-glucoside intervention. A-ring-derived gallic acid displayed the lowest variation (29.6%) between concentrations for the participants in which it was detected.

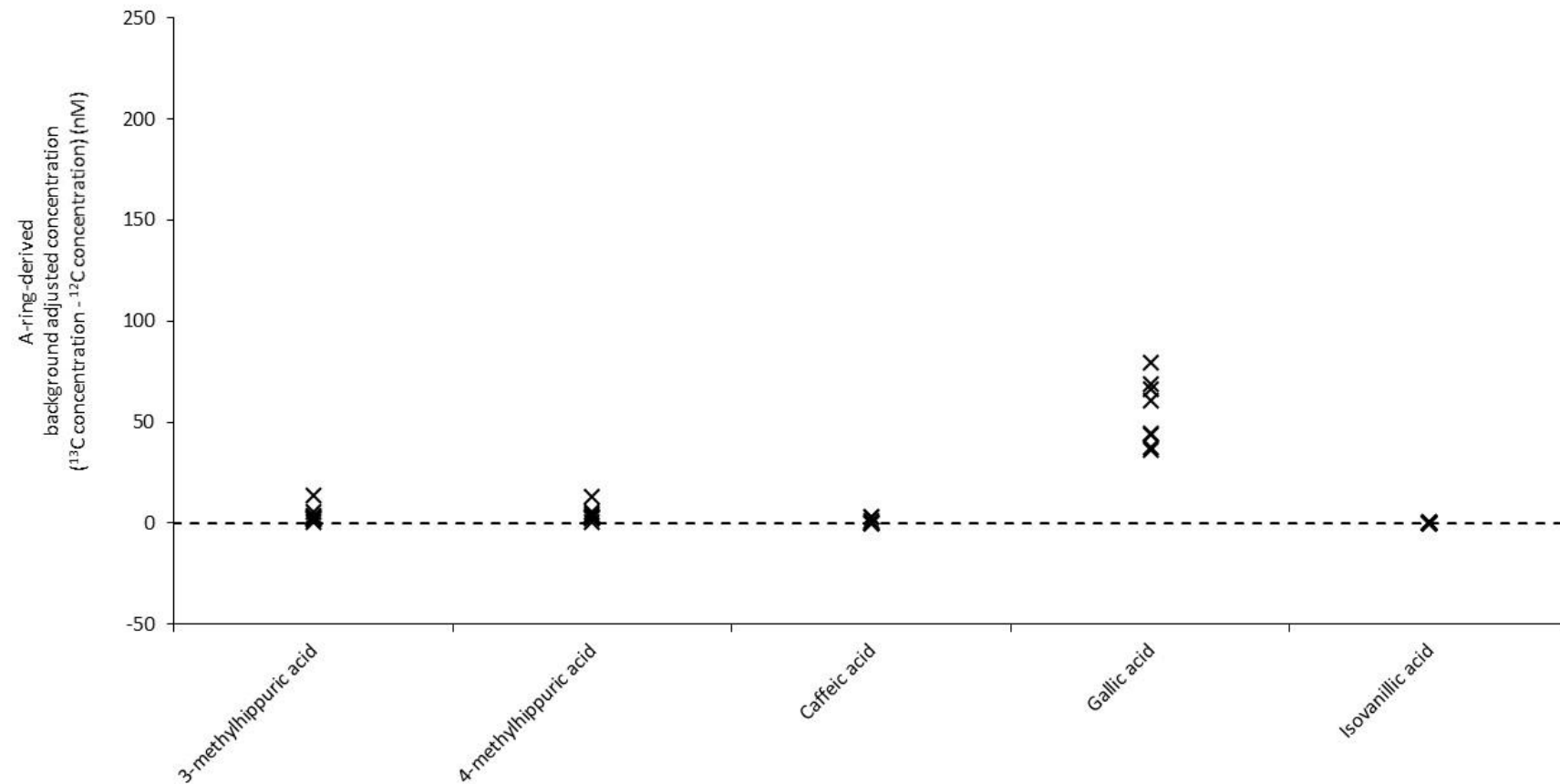
Analysis of the metabolite concentrations following the ¹³C-labelled cyanidin-3-glucoside intervention compared to the level from the ¹²C background diet (**Figure 5.5 & Figure 5.6**) shows that most analytes increase marginally from baseline to 24-48 hours post-intervention.

Figure 5.3 Background adjusted concentrations of urinary B-ring-derived metabolites detected in eight participants following a $^{13}\text{C}_5$ -cyanidin-3-glucoside intervention.



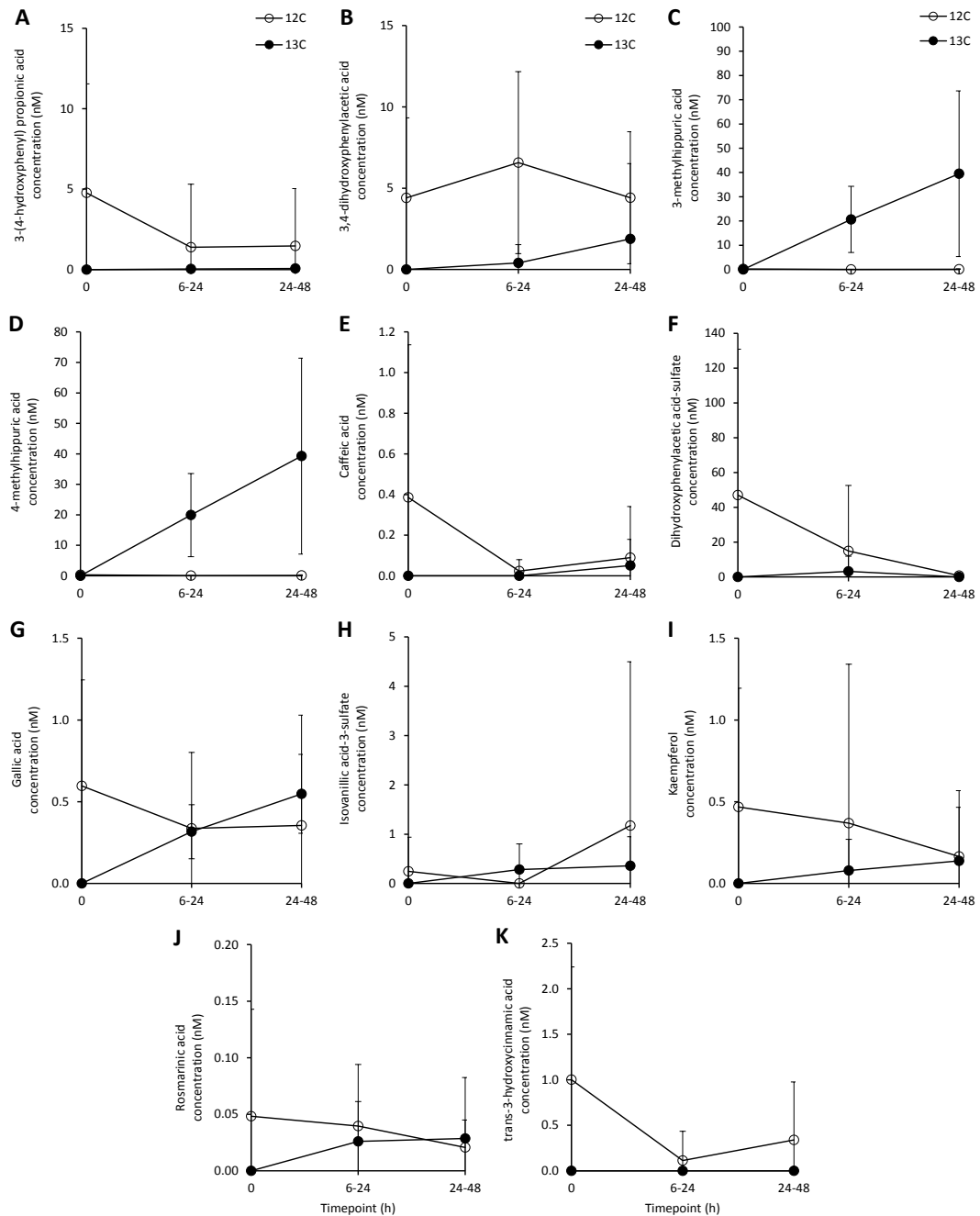
n=8 study participants. Each cross represents data from a single participant in which a ^{13}C -labelled analyte was detected and the maximum background adjusted analyte concentration (^{13}C concentration minus ^{12}C concentration) calculated to be present in that participant. Dotted line represents the point at which the analyte concentration from the ^{13}C -labelled cyanidin-3-glucoside intervention is equal to the concentration found in the background diet.

Figure 5.4 Background adjusted concentrations of urinary A-ring-derived metabolites detected in eight participants following a $^{13}\text{C}_5$ -cyanidin-3-glucoside intervention.



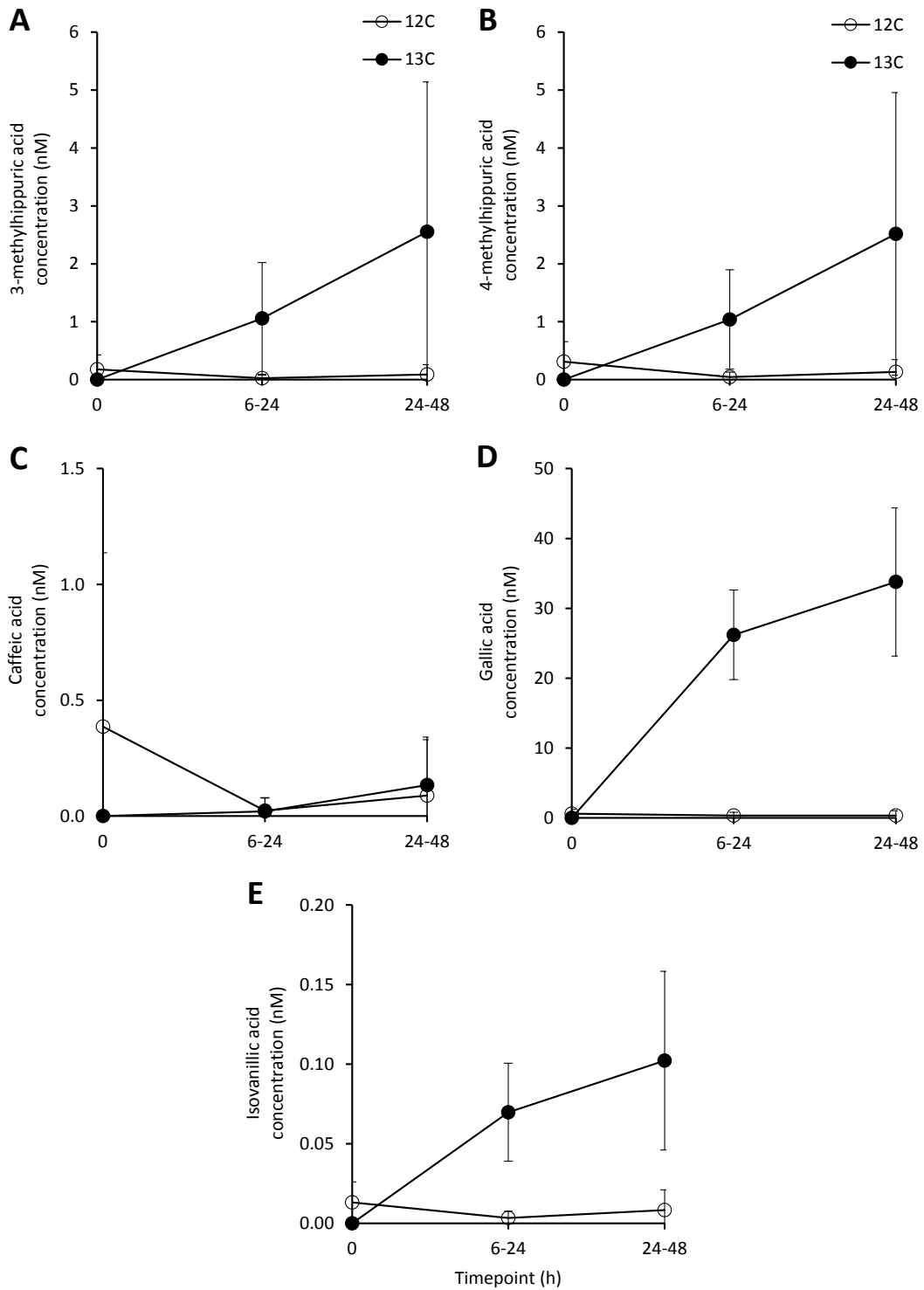
n=8 study participants. Each cross represents data from a single participant in which a ^{13}C -labelled analyte was detected and the maximum background adjusted analyte concentration (^{13}C concentration minus ^{12}C concentration) calculated to be present in that participant. Dotted line represents the point at which the analyte concentration from the ^{13}C -labelled cyanidin-3-glucoside intervention is equal to the concentration found in the background diet.

Figure 5.5 ^{13}C -labelled B-ring-derived urinary metabolite concentration compared to ^{12}C background concentration throughout 48 hours following $^{13}\text{C}_5$ -cyanidin-3-glucoside intervention.



(A) 3-(4-hydroxyphenyl)propionic acid. (B) 3,4-dihydroxyphenylacetic acid. (C) 3-methylhippuric acid. (D) 4-methylhippuric acid. (E) Caffeic acid. (F) Dihydroxyphenylacetic acid-sulfate. (G) Gallic acid. (H) Isovanillic acid-3-sulfate. (I) Kaempferol. (J) Rosmarinic acid. (K) *trans*-3-hydroxycinnamic acid. ^{12}C , background concentration; ^{13}C , ^{13}C -labelled metabolite concentration. Results expressed as mean \pm SD.

Figure 5.6 ^{13}C -labelled A-ring-derived urinary metabolite concentration compared to ^{12}C background concentration throughout 48 hours following $^{13}\text{C}_5$ -cyanidin-3-glucoside intervention.



(A) 3-methylhippuric acid. (B) 4-methylhippuric acid. (C) Caffeic acid. (D) Gallic acid. (E) Isovanillic acid. ^{12}C , background concentration; ^{13}C , ^{13}C -labelled metabolite concentration. Results expressed as mean \pm SD.

5.4. Discussion

Epidemiological studies and human trials investigating the bioactivity of anthocyanins currently use tools such as food frequency questionnaires to record subjects' food consumption and then use this to estimate flavonoid intake. The present study investigated the possibility of monitoring anthocyanin intake through quantifying characteristic metabolites as biomarkers of intake.

Four serum metabolites were detected from the $^{13}\text{C}_5$ -C3G intervention at concentrations exceeding those seen in the background diet. The parent anthocyanin, cyanidin-3-glucoside, and ferulic acid were detected at the highest concentrations above background levels but were only detected in four out of eight participants and showed high inter-participant variability making these analytes poor biomarker candidates. PCA-3-glucuronide showed little variation in terms of the time-point and concentration at which it was detected; however, it was only detected in half of the participants and at concentrations only slightly above background levels, therefore ruling out this metabolite as a potential biomarker. Hippuric acid and sulfate conjugates of PCA were detected in all eight of the study participants; however, the concentrations detected from the $^{13}\text{C}_5$ -C3G intervention were typically lower than those detected in the background. Hippuric acid was detected at very high concentrations from the background diet, making it difficult to isolate specific changes in labelled metabolite concentration and therefore is a particularly poor candidate as an anthocyanin biomarker of intake. The results of this study do not present any suitable serum biomarkers of anthocyanin intake. Further study may identify possible biomarker candidates within the serum but urine may represent a more promising source of biomarkers and should be the focus of future research.

16 urinary metabolites were detected from the $^{13}\text{C}_5$ -C3G intervention at concentrations exceeding those seen in the background diet. The four metabolites with the highest levels above the background diet were the B-ring-derived 3,4-dihydroxyphenylacetic acid, 3-methylhippuric acid, 4-methylhippuric acid and A-ring-derived gallic acid. However, 3,4-dihydroxyphenylacetic acid was only detected in three out of eight participants and is therefore not a suitable biomarker candidate. The other three metabolites were all detected in each of the eight participants. 3-methylhippuric acid (77.1 ± 61.4 nM) and 4-methylhippuric acid (74.8 ± 62.2 nM) were both found at higher concentrations above background than gallic acid (54.7 ± 16.2 nM) but they also showed greater levels of inter-individual variation amongst the participants (79.6% & 83.2% vs 29.6%, respectively). This suggests that gallic acid may be the best candidate for a urinary biomarker of anthocyanin

intake as it meets the criteria of being found in all participants, at levels above those found in the background diet and with little inter-individual variation. However, while gallic acid was found to be present above background levels in this study, the $^{13}\text{C}_5$ -C3G trial was conducted by asking volunteers to limit their intake of black tea which is one of the main sources of gallic acid in the diet (Neveu *et al.* 2010). Previous studies have shown that 24 hours after intake of 500 mL of black tea, levels of gallic acid in the urine can reach up to 2.6 μM (Del Rio *et al.* 2010b) which is well in excess of the nanomolar concentrations detected in the present study. An increase in the background level of gallic acid present in the urine to micromolar concentrations following regular consumption of black tea may limit the utility of gallic acid to be used as a biomarker of intake in studies of free-living individuals. Previous studies, however, have also reported gallic acid as a possible biomarker of anthocyanin intake in 24 h urine samples (Ito *et al.* 2005, Urpi-Sarda *et al.* 2015) suggesting that gallic acid may be a useful biomarker of anthocyanin intake in studies that control the diet of participants and therefore limit the contribution of background sources. Further research is required to establish the viability of gallic acid as a urinary biomarker of anthocyanin intake.

A potentially more promising approach may be to look for a characteristic metabolite profile of anthocyanin intake rather than a single representative metabolite. A number of studies have used a metabolomics approach to identify metabolic signatures present following intake of anthocyanin-rich foods or beverages (van Dorsten *et al.* 2010, Khymenets *et al.* 2015). In isolation, gallic acid may be a suitable biomarker of anthocyanin intake. However, it seems likely that a panel of metabolites combining gallic acid with other metabolites that were present following the C3G intervention at concentrations in excess of those resulting from the background diet such as 3,4-dihydroxyphenylacetic acid, 3-methylhippuric acid, and 4-methylhippuric acid may represent an improved biomarker of anthocyanin intake. Future studies should investigate the utility of this approach.

One limitation of the present analysis was, of the 18 serum metabolites and 23 urine metabolites previously reported (Czank *et al.* 2013), only six serum metabolites and seven urine metabolites were detected in this study. Analysis of the extraction efficiency of the internal standard, phloridzin, shows that the mean recoveries in serum ($104.8 \pm 23.6\%$) and urine ($72.0 \pm 27.6\%$) were acceptable, which suggests that there were no issues with the sample preparation methods that could have affected the recovery of the anthocyanin metabolites in the present study.

Analysis of the peak areas obtained from the QC samples that were included in this sample run show that the response for both QC standards, scopoletin and phloridzin, were within the normal limits for both ionisation modes (**Table 5.5**) which suggests that there were no issues with instrument response that could have affected the detection of anthocyanin metabolites in the present study.

Table 5.5 QC sample response obtained in the present study compared to expected response based on previous QC samples.

Compound	Peak area (counts per second) (mean \pm SD)	Expected range (counts per second)
Scopoletin (-)	$1.02 \times 10^6 \pm 4.08 \times 10^4$	$8.38 \times 10^5 - 1.53 \times 10^6$
Phloridzin (-)	$1.42 \times 10^7 \pm 5.76 \times 10^5$	$7.79 \times 10^6 - 1.52 \times 10^7$
Scopoletin (+)	$2.86 \times 10^6 \pm 1.13 \times 10^5$	$2.62 \times 10^6 - 5.02 \times 10^6$
Phloridzin (+)	$1.90 \times 10^5 \pm 1.27 \times 10^4$	$3.61 \times 10^4 - 2.02 \times 10^5$

(-), negative ionisation mode; (+), positive ionisation mode.

A possible explanation for the lower number of metabolites detected in this study compared to those reported previously (Czank *et al.* 2013) is the difference in sensitivity between the instruments used in the two studies. The previously reported method (Czank *et al.* 2013) used an AB SCIEX 4000 QTRAP® mass spectrometer which is capable of sensitivity that is eight to ten times greater than is possible with the AB SCIEX 3200 QTRAP® instrument used in the present study (Impey 2005). The concentrations detected in the present study are close to the limit of detection for the current method and so this difference in sensitivity between the two instruments could explain why some metabolites could not be detected in this investigation.

The difficulty in identifying suitable biomarkers in this investigation (as well as any dietary flavonoid intervention) is largely due to the high level of inter-participant variation in terms of metabolites detected, their concentrations and the time of their maximal plasma concentration. High levels of inter-participant variation are common in nutrition research (de Roos 2013) due to genetic differences between study participants causing differences in the way nutrients are metabolised (Minihane 2010, Wakeling and Ford 2012). This presents a challenge when attempting to identify reliable biomarkers of intake as an ideal biomarker should be applicable across the general population. Flavonoids pose an additional problem due to the apparent role of gut microbiota in their metabolism (Forester and Waterhouse

2008, Selma *et al.* 2009) which creates the potential for further variation amongst the population via differences in individuals' microbiomes (Arumugam *et al.* 2011). However, these problems should not deter future research into suitable biomarkers of anthocyanin intake as these biomarkers have the potential to greatly increase the accuracy of future anthocyanin clinical interventions. The use of a signature panel of metabolites as a biomarker of anthocyanin intake may help to mitigate some of these issues by removing the reliance on a single metabolite and reducing the effect of inter-individual variation.

The present study investigated both serum and urine samples as sources of metabolic biomarkers. Future work should focus on urinary biomarkers as a greater number of anthocyanin metabolites are present at much higher concentrations (Czank *et al.* 2013, de Ferrars *et al.* 2014a) making them easier to detect and quantify compared to serum metabolites. There are also practical considerations given that the goal of identifying biomarkers of intake is to improve accuracy of intake data/background diet and compliance in studies. Collection of urine samples can be done at home by untrained volunteers whereas collection of blood samples requires the volunteers to visit the study centre in order to have their blood taken by a trained professional (Spencer *et al.* 2008). Based on these limitations, establishing urinary biomarkers of anthocyanin intake should be a priority.

5.5. Conclusion

The present study suggests gallic acid is the most suitable urinary biomarker of anthocyanin intake, provided the background diet is stable in tea intake. Further studies are needed in order to establish the sensitivity of this metabolite in response to changing levels of anthocyanin consumption before it can be considered an acceptable biomarker of intake to be used in future epidemiological study of anthocyanins. Alternatively, gallic acid may be used, alongside a number of other metabolites identified in the present study, as part of a signature panel of metabolites characteristic of anthocyanin intake.

Chapter 6. The Effects of Different Metabolite Profiles on sVCAM-1 and IL-6 Expression in TNF- α and CD40L-stimulated HUVEC.

6.1. Introduction

Cardiovascular disease is responsible for over a quarter of all deaths in the UK every year (British Heart Foundation 2015). Epidemiological studies have reported that anthocyanin-rich diets can reduce the risk of cardiovascular disease (McCullough *et al.* 2012, Cassidy *et al.* 2013). This finding has been supported by clinical trials that have observed positive effects on vascular measures such as blood pressure (Erlund *et al.* 2008) and flow-mediated dilation (Rodriguez-Mateos *et al.* 2013) and also by *in vitro* studies that have shown positive effects on expression of relevant cytokines following consumption of anthocyanins (Speciale *et al.* 2013, Huang *et al.* 2014). However, bioavailability studies have reported very low concentrations of anthocyanins in the blood following consumption (Mazza *et al.* 2002, Milbury *et al.* 2002). Recent studies have demonstrated that anthocyanins are extensively metabolised within the body (Czank *et al.* 2013) suggesting that the metabolites may be responsible for the observed vascular bioactivity of anthocyanins.

One of the main drivers of cardiovascular disease is the process of atherosclerosis whereby blood vessels become stiffened and occluded by formation of plaques within the vasculature leading to outcomes such as hypertension and myocardial infarction (Vogel 1997). The initial stages of atherosclerosis are characterised by chronic inflammation within the vascular endothelium (Libby *et al.* 2002). This process is initiated by the reaction of endothelial cells to increase expression of proinflammatory cytokines such as cell adhesion molecules and selectins in response to insults such as smoking and high oxidised LDL (oxLDL) levels (Tedgui and Mallat 2006). These cytokines attract monocytes, trigger their transformation into activated macrophages and facilitate their adhesion to and passage through the endothelium into the intima (Granger *et al.* 2004). Once through the endothelial layer, the macrophages are able to differentiate into foam cells leading to the formation of fatty streaks that can progress to form the atherosclerotic plaques that ultimately lead to the pathologies associated with cardiovascular disease (Granger *et al.* 2004).

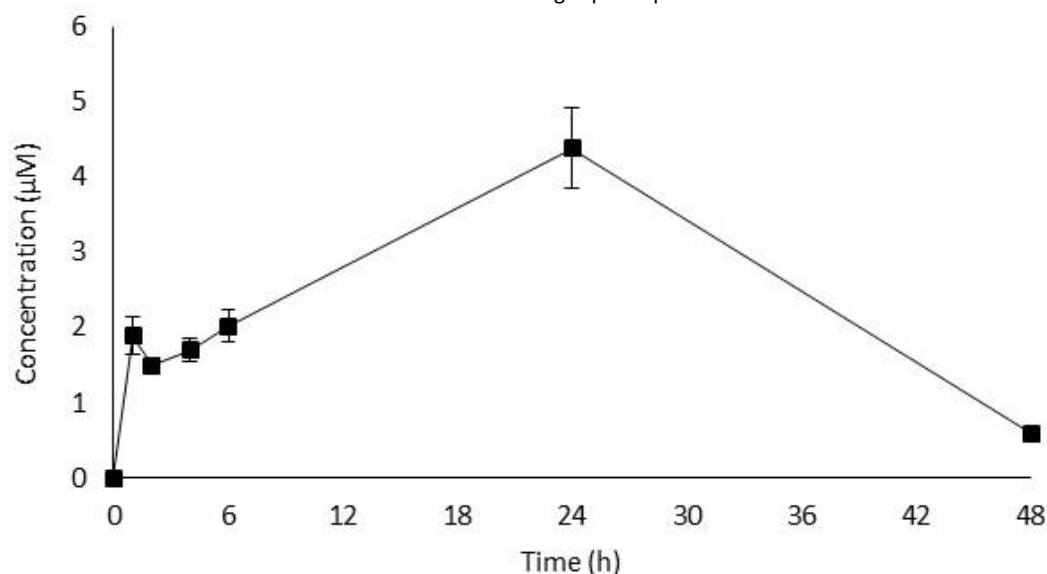
Tumour necrosis factor- α (TNF- α) and cluster of differentiation 40 ligand (CD40L) are signalling molecules produced by a number of cell types including activated macrophages

and endothelial cells in response to proinflammatory stimuli. TNF- α is released by activated cells in the vasculature and activates endothelial cells to upregulate adhesion molecules and other proinflammatory mediators via the nuclear factor- κ B (NF- κ B) and mitogen-activated protein kinase (MAPK) signalling pathways (Baud and Karin 2001). CD40L is a transmembrane protein expressed in activated T-cells that when bound with CD40 receptor can trigger a cascade of proinflammatory cytokines within endothelial cells (Déchanet *et al.* 1997). As such, TNF- α and CD40L are commonly used to stimulate an inflammatory response within endothelial cell types *in vitro* (Xia *et al.* 2009, Wu *et al.* 2012). VCAM-1 is a cell adhesion molecule expressed in endothelial cells involved in the attachment and migration of monocytes across the endothelium (Carter and Wicks 2001). VCAM-1 acts through interactions with integrin α 4 β 1 and activation of NOX leading to production of reactive oxygen species and further inflammatory progression (Blankenberg *et al.* 2003). IL-6 is produced in response to infection and following binding with its receptor, IL-6R, acts via downstream signal transducer and activator of transcription (STAT), and janus kinase (JAK) signalling pathways to induce inflammatory gene expression (Schuett *et al.* 2009, Brasier 2010). VCAM-1 and IL-6 are both downstream signalling molecules within the TNF- α /CD40L-stimulated inflammatory response and are commonly used as *in vitro* biomarkers of inflammation in endothelial cells (Hidalgo *et al.* 2012, Wang *et al.* 2012), therefore embodying a vascular model of initiation of inflammation.

Recently the focus of research into the vascular bioactivity of anthocyanins has shifted away from the parent compounds (as found in the diet) and towards studying their phenolic metabolites (as found in the circulation). Recent work published by our group has investigated the effect of anthocyanin metabolites, both individually (Amin *et al.* 2015, Edwards *et al.* 2015) and as simple combinations (di Gesso *et al.* 2015, Warner *et al.* 2016), on the expression of proinflammatory cytokines such as VCAM-1 and IL-6 in HUVEC. However, neither of these approaches accurately reflects the *in vivo* metabolite profiles with respect to diversity and complexity of mixtures reported following consumption. The present study aimed to address this by investigating the effect of treatments composed of the metabolite profiles reported in the serum following an anthocyanin feeding trial (Czank *et al.* 2013, de Ferrars *et al.* 2014a) on VCAM-1 and IL-6 expression in HUVEC. The pharmacokinetic data (**Figure 6.1**) was used to create three different metabolite mixtures that reflect the metabolites present (profile and concentration) within the blood at three distinct peaks/time-points post-consumption (1, 6 and 24 hours) (de Ferrars *et al.* 2014a).

The aim of the present study was to establish the impact of distinct metabolite profiles on vascular inflammation following consumption of anthocyanins.

Figure 6.1 Pharmacokinetic data from a ^{13}C -labelled cyanidin-3-glucoside feeding trial showing total ^{13}C metabolite concentration in serum across 48 hours in eight participants.



Results displayed as mean \pm SD, $n=8$. Serum kinetic data was used to establish three treatments that reflect the metabolite composition at three distinct peak concentrations observed at 1, 6 and 24 hours post-consumption. The effect of the three treatments on expression of VCAM-1 and IL-6 in TNF- α and CD40L-stimulated HUVEC was investigated. Adapted from (Czank *et al.* 2013, de Ferrars *et al.* 2014a).

6.2. Methods

6.2.1. Materials and reagents

Cyanidin-3-glucoside was obtained from Extrasynthese (Genay, France) and prepared at a concentration of 40 mM in 100% dimethyl sulfoxide (DMSO, molecular biology grade; Sigma-Aldrich, Dorset, UK). Phase II conjugates of phenolic acids (benzoic acid-4-glucuronide, PCA-4-glucuronide, PCA-3-sulfate, PCA-4-sulfate, vanillic acid-4-glucuronide, isovanillic acid-3-glucuronide, vanillic acid-4-sulfate, and isovanillic acid-3-sulfate) were synthesised at the School of Chemistry and Centre for Biomolecular Sciences, University of St. Andrews (UK) via recently published methods (Zhang *et al.* 2012). Primary stock solution of synthetic treatments were made at a concentration of 200 mM in 100% DMSO with the exception of PCA-3-sulfate, PCA-4-sulfate, and isovanillic acid-3-sulfate which were prepared at 25 mM concentrations (in 50:50 DMSO:MilliQ water), while vanillic acid-4-sulfate was prepared at 50 mM concentrations (in 50:50 DMSO:MilliQ water). Commercial standards, PCA, PGA, vanillic acid, isovanillic acid, 4-hydroxybenzaldehyde, ferulic acid, and hippuric acid were purchased from Sigma-Aldrich (Dorset, UK) and prepared at a concentration of 5 mg/mL in

100% DMSO. Cryo-preserved, early passage HUVEC from pooled donors, human large vessel endothelial cell basal media, human large vessel endothelial cell growth media supplement, antibiotic supplement, and trypsin were purchased from Caltag Medsystems (Buckingham, UK). Trypsin neutralising solution was purchased from Lonza (Slough, UK). Cryo-preserved D1.1 Jurkat cells were obtained from the American Type Culture Collection (ATCC, LGC Standards, Teddington, UK). DuoSet® human VCAM-1 enzyme-linked immunosorbent assay (ELISA) kit, DuoSet® human IL-6 ELISA kit, 96-well microplates, reagent diluent, substrate solution, and plate sealers were purchased from R & D Systems (Abingdon, UK). CD40L monoclonal antibody was purchased from Enzo Life Sciences (Exeter, UK). 96-well microplates were purchased from BD Falcon (Oxford, UK). Fetal bovine serum, RPMI-1640 media, penicillin/streptomycin, and L-glutamine were purchased from PAA (Pasching, Austria). Water-soluble tetrazolium salt-1 reagent [WST-1, (4-[3-(4-Iodophenyl)-2-(4-nitrophenyl)-2H-5-tetrazolio]-1,3-benzene disulfonate)] was purchased from Roche Applied Science (Burgess Hill, UK). Lyophilised recombinant human TNF- α was purchased from Invitrogen (Paisley, UK). Ethanol was purchased from Fisher Scientific (Loughborough, UK). Nunclon™ 75 cm² flasks, Nunclon™ 24-well plates, DMSO, trypan blue, fibronectin, and BAY11-7085 were purchased from Sigma-Aldrich, (Dorset, UK).

6.2.2. Treatment preparation

Stock solutions of the metabolites were prepared in DMSO and used to prepare 250 μ M working solutions in human large vessel endothelial cell basal media. The working solutions were then used to prepare treatments (**Table 6.1**) to replicate previously reported metabolite profiles identified at 1, 6 and 24 hours post-consumption (P-1, P-6, P-24; respectively) of 500mg ¹³C₅-labelled C3G (Czank *et al.* 2013, de Ferrars *et al.* 2014a) (Figure 6.1).

Concentration response was established by treatment with the mixtures at concentrations 10 fold above and below the peak concentration identified previously in the human study (Czank *et al.* 2013, de Ferrars *et al.* 2014a) [P-1 (0.19, 1.9, 19 μ M), P-6 (0.2, 2.0, 20 μ M), and P-24 (0.4, 4.4, 44 μ M)].

Table 6.1 Composition of treatments P-1, P-6, and P-24.

Compound	Concentration (μM)		
	P-1	P-6	P-24
4-hydroxybenzaldehyde	0.01	0.01	0.01
Benzoic acid-4-glucuronide	0.01	0.04	0.04
Cyanidin-3-glucoside	0.05	-	-
Ferulic acid	0.29	0.21	0.59
Hippuric acid	0.07	0.23	1.94
Isovanillic acid	0.12	-	-
Isovanillic acid-3-glucuronide	0.01	0.02	-
Isovanillic acid-3-sulfate	-	-	0.17
Phloroglucinaldehyde	0.03	0.55	0.05
Protocatechuic acid	0.04	0.08	0.01
Protocatechuic acid-3-sulfate	0.07	0.02	0.02
Protocatechuic acid-4-glucuronide	0.02	0.03	-
Protocatechuic acid-4-sulfate	0.07	0.02	0.02
Vanillic acid	1.10	0.80	1.36
Vanillic acid-4-glucuronide	0.01	0.02	-
Vanillic acid-4-sulfate	-	-	0.17
Total	1.90	2.03	4.38

P-1, P-6, P-24 are treatments designed to replicate previously reported metabolite profiles identified at 1, 6, and 24 hours respectively, post-consumption of 500 mg of $^{13}\text{C}_5$ -labelled C3G (Czank *et al.* 2013, de Ferrars *et al.* 2014a). A dash represents a metabolite that is not found in that particular treatment.

6.2.3. HUVEC culture

HUVEC were maintained in human large vessel endothelial cell basal media supplemented with antibiotics and growth factors at 37°C with 5% CO_2 in 75 cm^2 flasks coated with fibronectin (0.26 $\mu\text{g}/\text{cm}^2$). HUVEC were cultured to 90-95% confluence prior to being split using 0.025% trypsin and all experiments were conducted using HUVEC at passage two to four.

6.2.4. D1.1 Jurkat cell culture

D1.1 Jurkat cells were cultured in RPMI-1640 media supplemented with 1% penicillin/streptomycin, 10% FBS, and 2 mM L-glutamine was used to culture at 37°C with 5% CO_2 in 75 cm^2 flasks. Cell density was maintained between 2.5×10^5 and 1×10^6 cells/mL and density was calculated using a haemocytometer and trypan blue staining.

6.2.5. Cytotoxicity assay

The effect of treatments on cell viability was measured using the WST-1 cell proliferation assay. HUVEC were seeded in a fibronectin-coated (0.41 $\mu\text{g}/\text{cm}^2$) 96-well plate at ~20,000 cells/well and grown to confluence at 37°C, 5% CO_2 . The culture media was then removed and replaced with 100 μL of each treatment prepared in human large vessel endothelial cell basal media at the highest concentration used in the activity assays. Controls consisted of 0.07% DMSO in media with no HUVEC (blank), media (control), 0.07% DMSO in media

(vehicle control), and PBS (WST-1 negative control). The quintuplicate samples were incubated for 24 hours at 37°C, 5% CO₂ before 10 µL of WST-1 reagent was added to each well. The plate was incubated at 37°C, 5% CO₂ for a further 2 hours before absorbance readings were taken at 450 nm with a reference wavelength of 650 nm using a BMG microplate reader (FLUOstar Omega, BMG Labtech, Aylesbury, UK).

6.2.6. TNF-α induced sVCAM-1 and IL-6 expression in HUVEC: Time-course assay

HUVEC were cultured using the procedure outlined previously and seeded into triplicate 24-well, fibronectin-coated (0.25 µg/cm²) plates at a density of ~80,000 cells/well. The plates were incubated at 37°C, 5% CO₂ until the cells reached 90-95% confluence. The culture media was removed and HUVEC were pre-incubated with control samples in 600 µl human large vessel endothelial cell basal media for 30 minutes prior to the addition of TNF-α (10 ng/mL). Control samples consisted of unstimulated HUVEC in media (basal), TNF-α only (positive control), 0.07% DMSO in media (vehicle control), and BAY11-7085 (1 µM, 1 hour pre-incubation, negative control). The plates were incubated for either 6, 18 or 24 hours at 37°C, 5% CO₂ before the media was removed and stored at -80°C until analysis.

6.2.7. TNF-α stimulation of sVCAM-1 and IL-6 expression in HUVEC

HUVEC were cultured and seeded into 24-well plates using the procedure outlined previously. Upon reaching 90-95% confluence, the culture media was removed and HUVEC were pre-incubated with treatments in 600 µl human large vessel endothelial cell basal media for 30 minutes prior to the addition of TNF-α (10 ng/mL). Control samples consisted of unstimulated HUVEC in media (basal), TNF-α only (positive control), 0.07% DMSO in media (vehicle control), and BAY11-7085 (1 µM, 1 hour pre-incubation, negative control). The plates were incubated for 24 hours at 37°C, 5% CO₂ before the media was removed and stored at -80°C until analysis.

6.2.8. CD40L stimulation of sVCAM-1 and IL-6 expression in HUVEC

HUVEC were cultured and seeded into 24-well plates using the procedure outlined previously. Upon reaching 90-95% confluence, the culture media was removed and HUVEC were pre-incubated with treatments in 600 µl human large vessel endothelial cell basal media for 30 minutes prior to the addition of D1.1 Jurkat cells (1 x 10⁶ cells/well). Control samples consisted of unstimulated HUVEC in media (basal), D1.1 Jurkat cells only (positive control), 0.07% DMSO in media (vehicle control), and D1.1 Jurkat cells pre-incubated for 1 hour with 10 µg/mL CD40L monoclonal antibody (negative control). The plates were incubated for 24 hours at 37°C, 5% CO₂ before the media was removed and stored at -80°C until analysis.

6.2.9. sVCAM-1 ELISA

Expression of sVCAM-1 was measured using a DuoSet® ELISA kit according to the manufacturer's instructions. Prior to analysis, samples were centrifuged at 4°C, 13000 rpm for 10 mins to remove D1.1 Jurkat cells and cell debris. TNF- α -stimulated HUVEC media was diluted 1:2 and CD40L-stimulated HUVEC media was diluted 1:4 with reagent diluent. The kit used a mouse anti-human VCAM-1 capture antibody (2 μ g/mL in PBS) and biotinylated sheep anti-human VCAM-1 detection antibody (200 ng/mL in reagent diluent). Colorimetric assay was used to quantify sVCAM-1 expression by measuring absorbance at 450 nm with a reference wavelength of 570 nm using a BMG microplate reader.

6.2.10. IL-6 ELISA

Expression of IL-6 was measured using a DuoSet® ELISA kit according to the manufacturer's instructions. Prior to analysis, samples were centrifuged at 4°C, 13000 rpm for 10 mins to remove D1.1 Jurkat cells and cell debris. TNF- α -stimulated HUVEC media was diluted 1:4 and CD40L-stimulated HUVEC media was diluted 1:1 with reagent diluent. The kit used a mouse anti-human IL-6 capture antibody (2 μ g/mL in PBS) and biotinylated goat anti-human IL-6 detection antibody (50 ng/mL in reagent diluent). Colorimetric assay was used to quantify IL-6 expression by measuring absorbance at 450 nm with a reference wavelength of 570 nm using a BMG microplate reader.

6.2.11. Statistical analysis

For cytotoxicity and ELISA data, one-way analysis of variance (ANOVA) with LSD post-hoc test was performed on either three (ELISA) or five (cytotoxicity) biological replicates (with each biological replicate representing the mean of two technical replicates) using SPSS for Windows statistical software package (version 22, IBM, New York, USA). Significance was determined at the 5% confidence level. Statistical analysis was conducted on raw data with mean values graphed as either percentage of positive control (cytotoxicity and activity assays) or fold change from basal (time-course assays) with error bars representing standard deviation.

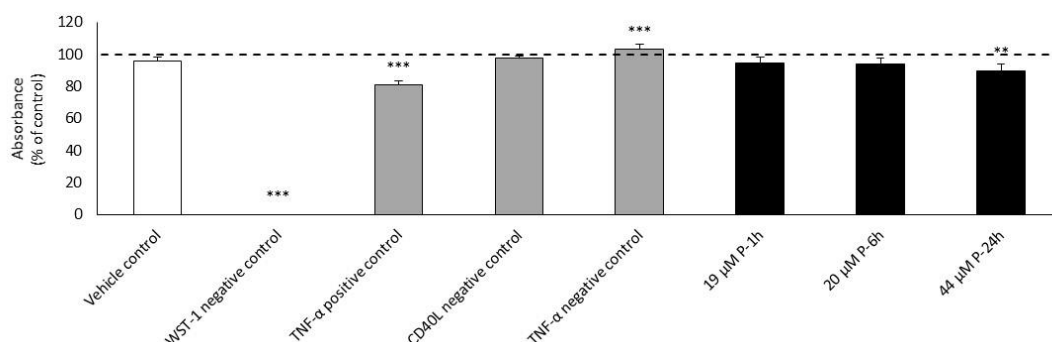
6.3. Results

6.3.1. Cytotoxicity assay

Three treatments (19 μ M P-1, 20 μ M P-6, and 44 μ M P-24) were utilised in the sVCAM-1 and IL-6 activity assays, reflecting concentrations that are tenfold higher than peak concentrations identified previously (Czank *et al.* 2013, de Ferrars *et al.* 2014a). 19 μ M P-1,

20 μ M P-6, 44 μ M P-24, TNF- α positive control, CD40L negative control and TNF- α negative control were screened for cytotoxicity (**Figure 6.2**). No significant reduction in HUVEC viability was observed, with the exception of TNF- α positive control and the maximum concentration 44 μ M P-24 treatment. TNF- α negative control showed a significant increase in viability.

Figure 6.2 Cytotoxicity of treatment compounds in HUVEC as measured by WST-1 assay following 24 hour incubation.

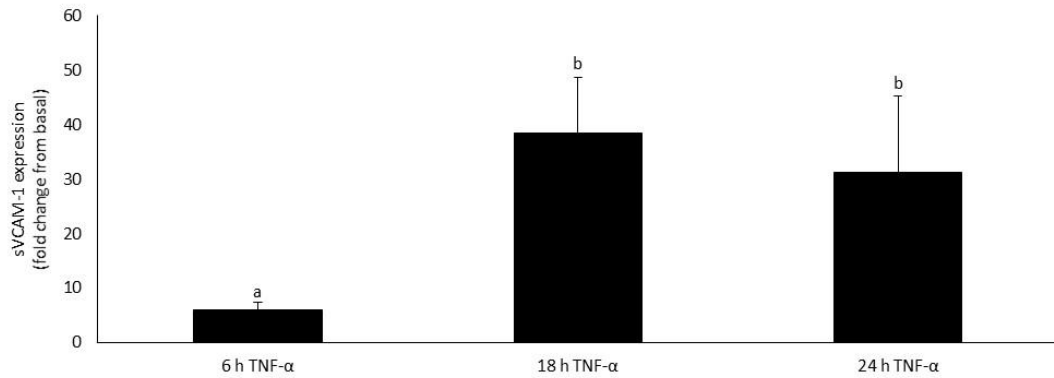


Cell viability (mean absorbance as percentage of control absorbance) for control (media), vehicle control (0.07% DMSO in media), WST-1 negative control (PBS), TNF- α positive control (10 ng/mL TNF- α), CD40L negative control (10 μ g/mL CD40L monoclonal antibody), TNF- α negative control (1 μ M BAY11-7085 antibody), 19 μ M P-1, 20 μ M P-6, and 44 μ M P-24. Data shown as mean \pm SD, n=5. Significance relative to vehicle control, **p \leq 0.01, ***p \leq 0.001, one-way ANOVA with LSD post-hoc test.

6.3.2. TNF- α induced sVCAM-1 expression time-course validation

Expression of sVCAM-1 in HUVEC was measured following incubation with TNF- α positive control for 6, 18 or 24 hours to establish optimal incubation time (**Figure 6.3**). Both the 18 hour (38.4 fold increase from basal) and 24 hour (31.2 fold increase from basal) time-points showed a significantly higher response compared to the 6 hour time-point (5.9 fold increase from basal). There was no significant difference between the response at 18 and 24 hours.

Figure 6.3 sVCAM-1 production in TNF- α -stimulated HUVEC.

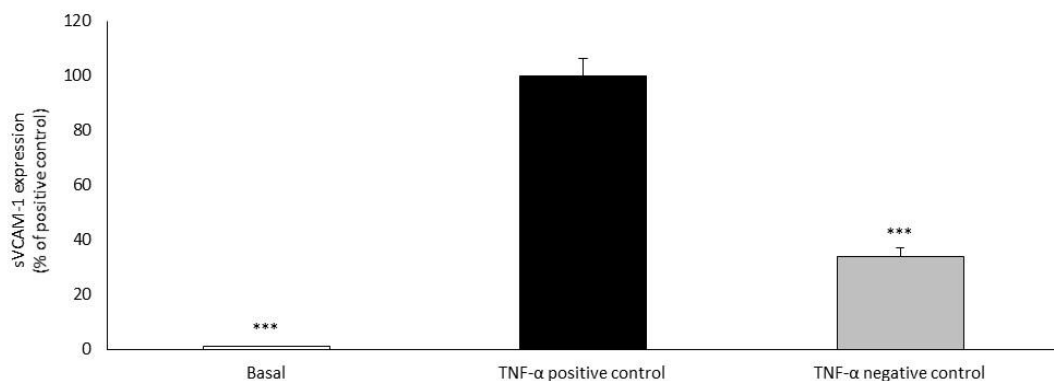


HUVEC were incubated with TNF- α positive control (10 ng/mL TNF- α) for 6, 18 or 24 hours before cell supernatant quantitation of sVCAM-1 expression via ELISA. Data expressed as mean \pm SD, n=3. ^{a,b}Different letters represent statistical differences between groups, $p < 0.05$, one-way ANOVA with LSD post-hoc test.

6.3.3. TNF- α induced sVCAM-1 expression

Compared to unstimulated HUVEC, incubation with TNF- α positive control led to a 95.4 fold increase in sVCAM-1 expression which was significantly inhibited ($66.2 \pm 3.3\%$) when HUVEC were pre-treated with BAY11-7085 as a TNF- α negative control to inhibit phosphorylation of I κ B α and block the NF- κ B signalling pathway, therefore reducing expression of sVCAM-1. (Figure 6.4).

Figure 6.4 sVCAM-1 production in TNF- α -stimulated HUVEC.

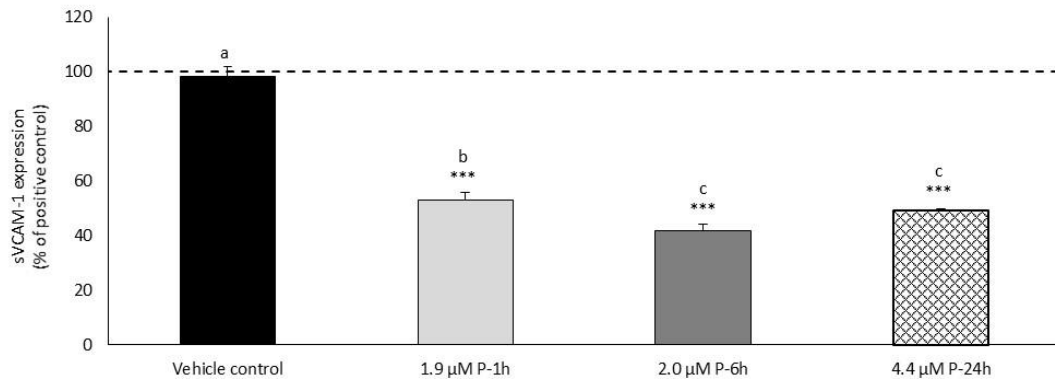


HUVEC were incubated with TNF- α positive control (10 ng/mL TNF- α) for 24 hours before cell supernatant quantitation of sVCAM-1 expression via ELISA. TNF- α negative control was pre-treated with 1 μ M BAY11-7085 antibody for 1 hour prior to TNF- α stimulation. Data expressed as mean \pm SD, n=3. Significance relative to positive control, *** $p < 0.001$, one-way ANOVA with LSD post-hoc test.

The effect of three previously reported metabolite profiles (Czank *et al.* 2013, de Ferrars *et al.* 2014a) (1.9 μ M P-1, 2.0 μ M P-6, and 4.4 μ M P-24) on expression of sVCAM-1 in TNF- α -stimulated HUVEC was investigated in HUVEC following 24 hours. After 24 hours, all three treatments showed a significant reduction in sVCAM-1 expression compared to vehicle

control (**Figure 6.5**). 2.0 μM P-6 ($58.4 \pm 2.5\%$) and 4.4 μM P-24 ($50.7 \pm 0.6\%$) both showed a greater reduction in sVCAM-1 expression than 1.9 μM P-1 ($46.9 \pm 2.9\%$).

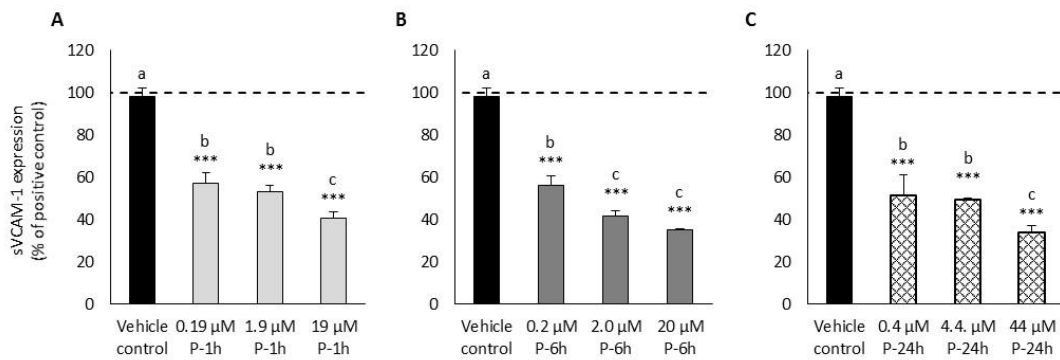
Figure 6.5 sVCAM-1 production following treatment with anthocyanin metabolites in TNF- α -stimulated HUVEC.



HUVEC were incubated with TNF- α positive control (10 ng/mL TNF- α) and vehicle control (0.07% DMSO in media) or treatments (1.9 μM P-1, 2.0 μM P-6, 4.4 μM P-24) for 24 hours before cell supernatant quantitation of sVCAM-1 expression via ELISA. Data expressed as mean \pm SD, $n=3$. Significance relative to vehicle control, *** $p<0.001$, one-way ANOVA with LSD post-hoc test. ^{a,b,c}Different letters represent statistical differences between groups, $p\leq 0.05$, one-way ANOVA with LSD post-hoc test.

Concentration response was established by incubating HUVEC with the metabolite profiles at cumulative concentrations 10 fold above and below the peak concentration identified previously in the human study (Czank *et al.* 2013, de Ferrars *et al.* 2014a) [P-1 (0.19, 1.9, 19 μM), P-6 (0.2, 2.0, 20 μM), and P-24 (0.4, 4.4, 44 μM)]. All treatments showed significant reductions in sVCAM-1 expression relative to vehicle control (**Figure 6.6**) with the greatest response observed at the highest concentrations tested (19 μM P-1, $59.3 \pm 2.8\%$; 20 μM P-6, $65.1 \pm 0.5\%$; 44 μM P-24, $66.2 \pm 3.5\%$).

Figure 6.6 sVCAM-1 production following treatment with anthocyanin metabolites in TNF- α -stimulated HUVEC.

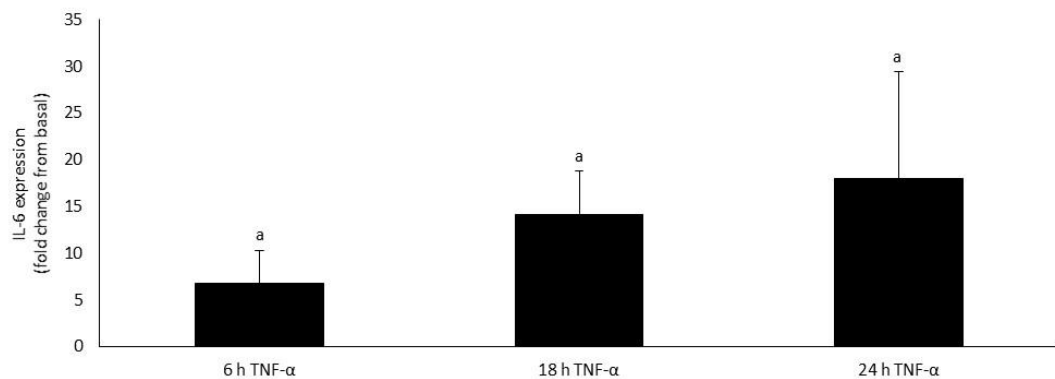


HUVEC were incubated with TNF- α positive control (10 ng/mL TNF- α) and vehicle control (0.07% DMSO in media) or treatments (0.19 μ M P-1, 1.9 μ M P-1, 19 μ M P-1; 0.2 μ M P-6, 2.0 μ M P-6, 20 μ M P-6; 0.4 μ M P-24, 4.4 μ M P-24, 44 μ M P-24) for 24 hours before cell supernatant quantitation of sVCAM-1 expression via ELISA. Data expressed as mean \pm SD, n=3. Significance relative to vehicle control, ***p<0.001, one-way ANOVA with LSD post-hoc test. ^{a,b,c}Different letters represent statistical differences between groups, p \leq 0.05, one-way ANOVA with LSD post-hoc test.

6.3.4. TNF- α induced IL-6 expression time-course assay validation

Expression of IL-6 in HUVEC was measured following incubation with TNF- α positive control for 6, 18 or 24 hours to establish optimal incubation time (**Figure 6.7**). No significant difference was observed between the various incubation periods.

Figure 6.7 IL-6 production in TNF- α -stimulated HUVEC.

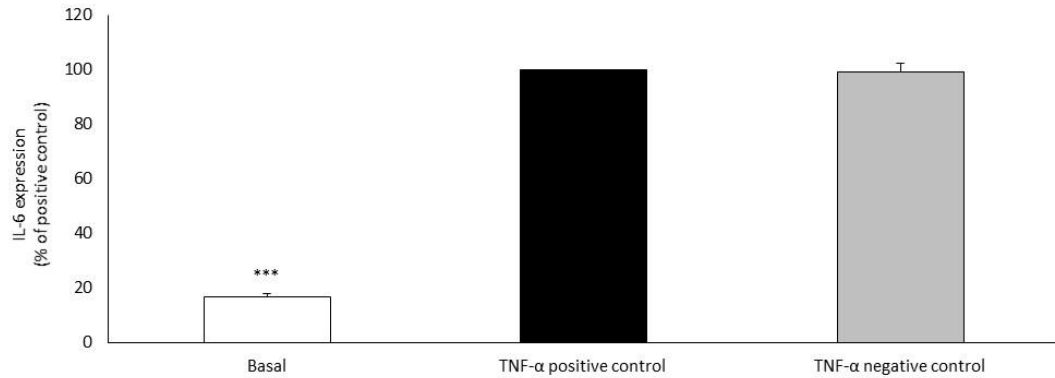


HUVEC were incubated with TNF- α positive control (10 ng/mL TNF- α) for 6, 18 or 24 hours before cell supernatant quantitation of IL-6 expression via ELISA. Data expressed as mean \pm SD, n=3. ^aDifferent letters represent statistical differences between groups, p \leq 0.05, one-way ANOVA with LSD post-hoc test.

6.3.5. TNF- α induced IL-6 expression

Compared to unstimulated HUVEC, incubation with TNF- α positive control led to a 6.0 fold increase in IL-6 expression which was not significantly inhibited (0.9 \pm 3.2%) by pre-treatment of HUVEC with TNF- α negative control (**Figure 6.8**).

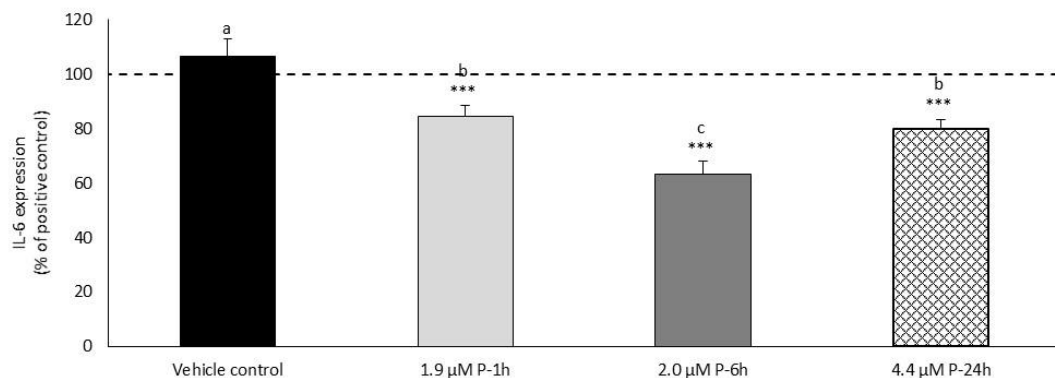
Figure 6.8 IL-6 production in TNF- α -stimulated HUVEC.



HUVEC were incubated with TNF- α positive control (10 ng/mL TNF- α) for 24 hours before cell supernatant quantitation of IL-6 expression via ELISA. TNF- α negative control was pre-treated with 1 μ M BAY11-7085 antibody for 1 hour prior to TNF- α stimulation. Data expressed as mean \pm SD, n=3. Significance relative to positive control, ***p<0.001, one-way ANOVA with LSD post-hoc test.

The effect of three previously reported metabolite profiles (Czank *et al.* 2013, de Ferrars *et al.* 2014a) (1.9 μ M P-1, 2.0 μ M P-6, and 4.4 μ M P-24) on expression of IL-6 in TNF- α -stimulated HUVEC was investigated in HUVEC following 24 hours. After 24 hours, all three treatments showed a significant reduction in IL-6 expression compared to vehicle control (**Figure 6.9**). The metabolite profile identified at 6h post-consumption (2.0 μ M P-6; 36.6 \pm 4.6%) showed the greatest activity on IL-6 expression (1.9 μ M P-1; 15.6 \pm 4.1% and 4.4 μ M P-24; 20.3 \pm 3.7%).

Figure 6.9 IL-6 production following treatment with anthocyanin metabolites in TNF- α -stimulated HUVEC.

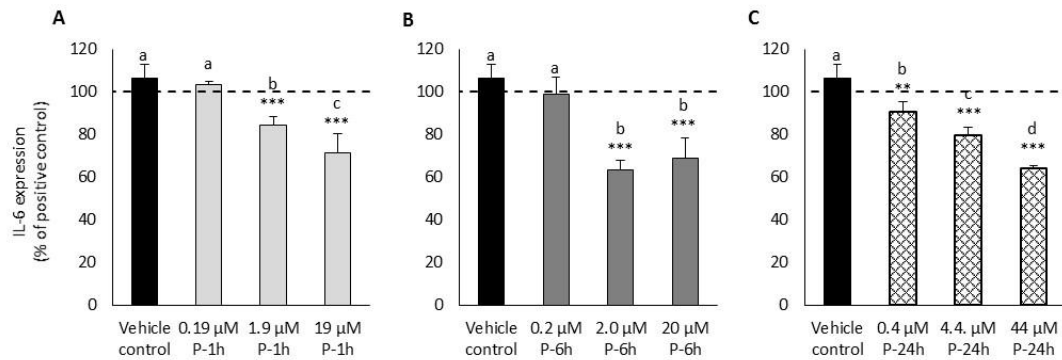


HUVEC were incubated with TNF- α positive control (10 ng/mL TNF- α) and vehicle control (0.07% DMSO in media) or treatments (1.9 μ M P-1, 2.0 μ M P-6, 4.4 μ M P-24) for 24 hours before cell supernatant quantitation of IL-6 expression via ELISA. Data expressed as mean \pm SD, n=3. Significance relative to vehicle control, ***p<0.001, one-way ANOVA with LSD post-hoc test. ^{a,b,c} Different letters represent statistical differences between groups, p \leq 0.05, one-way ANOVA with LSD post-hoc test.

Concentration response was established by incubating HUVEC with the metabolite profiles at cumulative concentrations 10 fold above and below the peak concentration identified previously in the human study (Czank *et al.* 2013, de Ferrars *et al.* 2014a) [P-1 (0.19, 1.9, 19 μ M), P-6 (0.2, 2.0, 20 μ M), and P-24 (0.4, 4.4, 44 μ M)]. All treatments showed a significant

reduction in IL-6 expression compared to vehicle control except for 0.19 μM P-1 and 0.2 μM P-6 (**Figure 6.10**). The greatest reductions were observed from 19 μM P-1 ($28.5 \pm 8.9\%$), 2.0 μM P-6 ($36.6 \pm 4.6\%$), and 44 μM P-24 ($35.6 \pm 0.9\%$).

Figure 6.10 IL-6 production following treatment with anthocyanin metabolites in TNF- α -stimulated HUVEC.

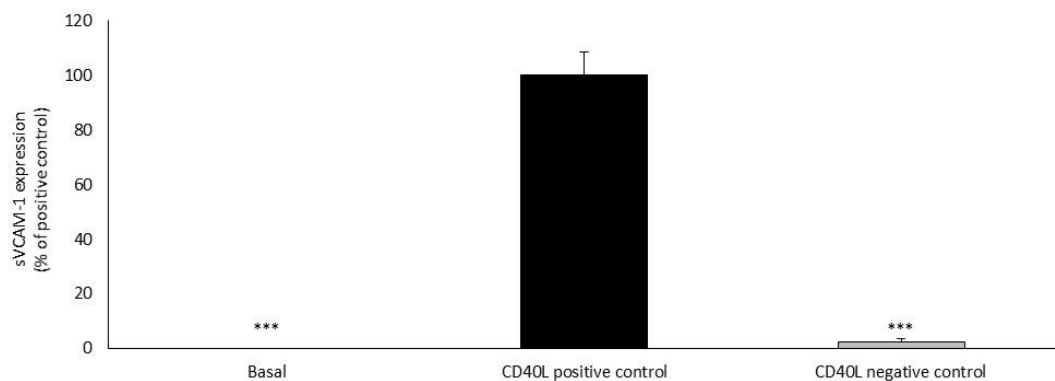


HUVEC were incubated with TNF- α positive control (10 ng/mL TNF- α) and vehicle control (0.07% DMSO in media) or treatments (0.19 μM P-1, 1.9 μM P-1, 19 μM P-1; 0.2 μM P-6, 2.0 μM P-6, 20 μM P-6; 0.4 μM P-24, 4.4 μM P-24, 44 μM P-24) for 24 hours before cell supernatant quantitation of IL-6 expression via ELISA. Data expressed as mean \pm SD, n=3. Significance relative to vehicle control, **p \leq 0.01, ***p \leq 0.001, one-way ANOVA with LSD post-hoc test. ^{a,b,c,d}Different letters represent statistical differences between groups, p \leq 0.05, one-way ANOVA with LSD post-hoc test.

6.3.6. CD40L induced sVCAM-1 expression

Compared to unstimulated HUVEC, incubation with CD40L positive control led to a significant increase in sVCAM-1 expression which was significantly inhibited ($97.8 \pm 1.4\%$) via pre-treatment of HUVEC with CD40L negative control (**Figure 6.11**).

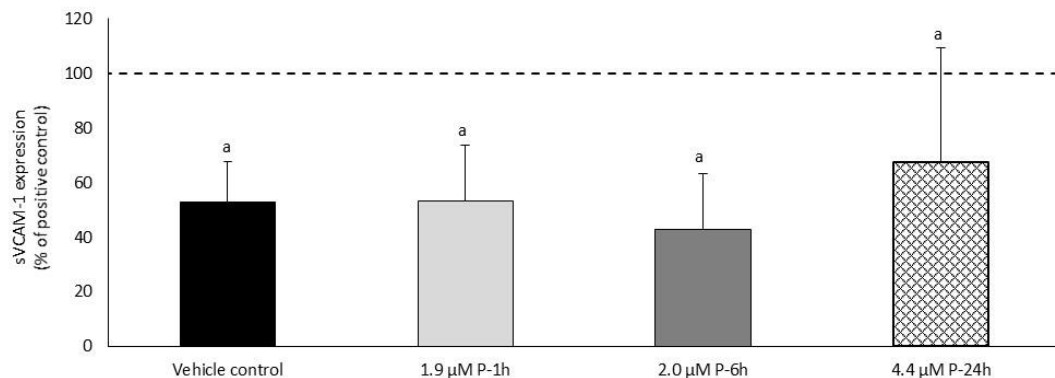
Figure 6.11 sVCAM-1 production in CD40L-stimulated HUVEC.



HUVEC were incubated with CD40L positive control (1×10^6 CD40L-expressing D1.1 Jurkat cells/well) for 24 hours before cell supernatant quantitation of sVCAM-1 expression via ELISA. CD40L negative control was pre-treated with 10 $\mu\text{g/mL}$ CD40L monoclonal antibody for 1 hour prior to CD40L stimulation. Data expressed as mean \pm SD, n=3. Significance relative to positive control, ***p \leq 0.001, one-way ANOVA with LSD post-hoc test.

The effect of three previously reported metabolite profiles (Czank *et al.* 2013, de Ferrars *et al.* 2014a) (1.9 μ M P-1, 2.0 μ M P-6, and 4.4 μ M P-24) on expression of sVCAM-1 in CD40L-stimulated HUVEC was investigated in HUVEC following 24 hours. After 24 hours incubation, none of the three treatments showed significant reduction in sVCAM-1 expression compared to vehicle control (**Figure 6.12**).

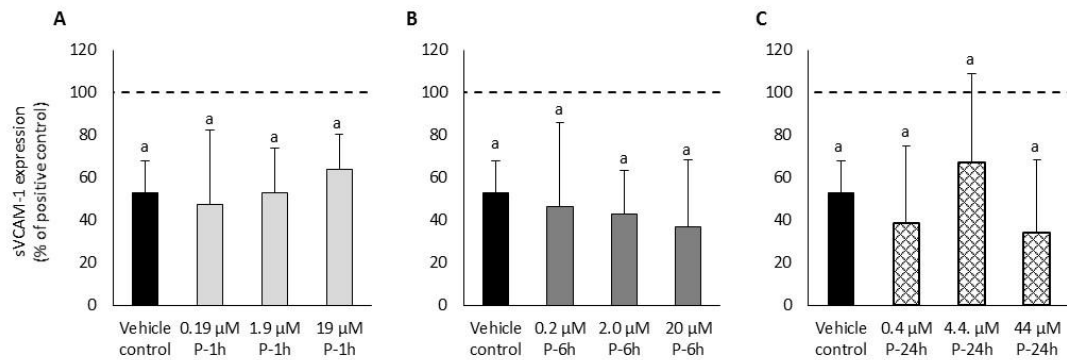
Figure 6.12 sVCAM-1 production following treatment with anthocyanin metabolites in CD40L-stimulated HUVEC.



HUVEC were incubated with CD40L positive control (1×10^5 CD40L-expressing D1.1 Jurkat cells/well) and vehicle control (0.07% DMSO in media) or treatments (1.9 μ M P-1, 2.0 μ M P-6, and 4.4 μ M P-24) for 24 hours before cell supernatant quantitation of sVCAM-1 expression via ELISA. Data expressed as mean \pm SD, n=3. Significance relative to vehicle control, * $p \leq 0.05$, one-way ANOVA with LSD post-hoc test. ^aDifferent letters represent statistical differences between groups, $p \leq 0.05$, one-way ANOVA with LSD post-hoc test.

Concentration response was established by incubating HUVEC with the metabolite profiles at cumulative concentrations 10 fold above and below the peak concentration identified previously in the human study (Czank *et al.* 2013, de Ferrars *et al.* 2014a) [P-1 (0.19, 1.9, 19 μ M), P-6 (0.2, 2.0, 20 μ M), and P-24 (0.4, 4.4, 44 μ M)]. None of the treatments showed a significant reduction in sVCAM-1 expression compared to vehicle control (**Figure 6.13**).

Figure 6.13 sVCAM-1 production following treatment with anthocyanin metabolites in CD40L-stimulated HUVEC.

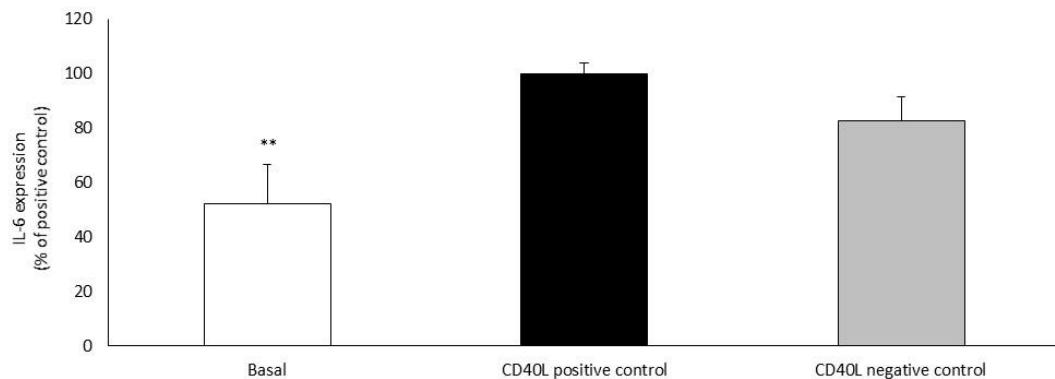


HUVEC were incubated with CD40L positive control (1×10^5 CD40L-expressing D1.1 Jurkat cells/well) and vehicle control (0.07% DMSO in media) or treatments (0.19 μM P-1, 1.9 μM P-1, 19 μM P-1; 0.2 μM P-6, 2.0 μM P-6, 20 μM P-6; 0.4 μM P-24, 4.4 μM P-24, 44 μM P-24) for 24 hours before cell supernatant quantitation of sVCAM-1 expression via ELISA. Data expressed as mean \pm SD, $n=3$. Significance relative to vehicle control, * $p \leq 0.05$, one-way ANOVA with LSD post-hoc test. ^aDifferent letters represent statistical differences between groups, $p \leq 0.05$, one-way ANOVA with LSD post-hoc test.

6.3.7. CD40L induced IL-6 expression

Compared to unstimulated HUVEC, incubation with CD40L positive control led to a 2.0 fold increase in IL-6 expression which was not significantly inhibited ($17.4 \pm 8.8\%$) via pre-treatment of HUVEC with CD40L negative control (**Figure 6.14**).

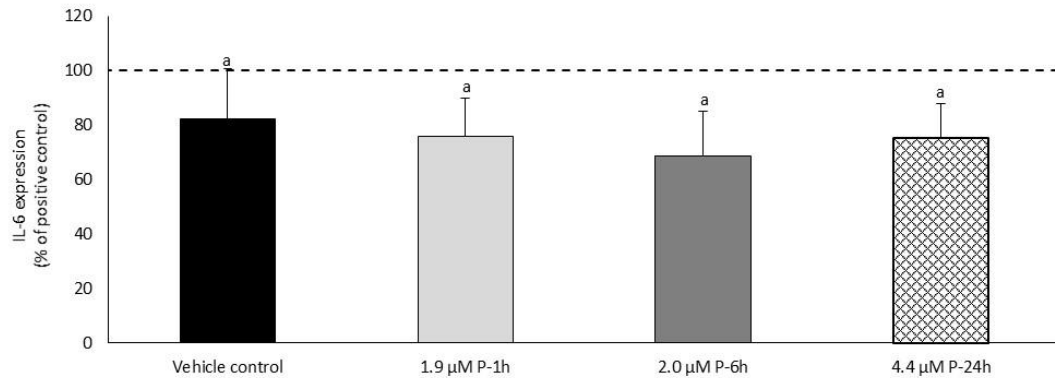
Figure 6.14 IL-6 production in CD40L-stimulated HUVEC.



HUVEC were incubated with CD40L positive control (1×10^5 CD40L-expressing D1.1 Jurkat cells/well) for 24 hours before cell supernatant quantitation of IL-6 expression via ELISA. CD40L negative control was pre-treated with 10 μg/mL CD40L monoclonal antibody for 1 hour prior to CD40L stimulation. Data expressed as mean \pm SD, $n=3$. Significance relative to positive control, ** $p \leq 0.01$, one-way ANOVA with LSD post-hoc test.

The effect of three previously reported metabolite profiles (Czank *et al.* 2013, de Ferrars *et al.* 2014a) (1.9 μM P-1, 2.0 μM P-6, and 4.4 μM P-24) on expression of IL-6 in CD40L-stimulated HUVEC was investigated in HUVEC following 24 hours. After 24 hours, none of the three treatments showed a significant reduction in IL-6 expression compared to vehicle control (**Figure 6.15**).

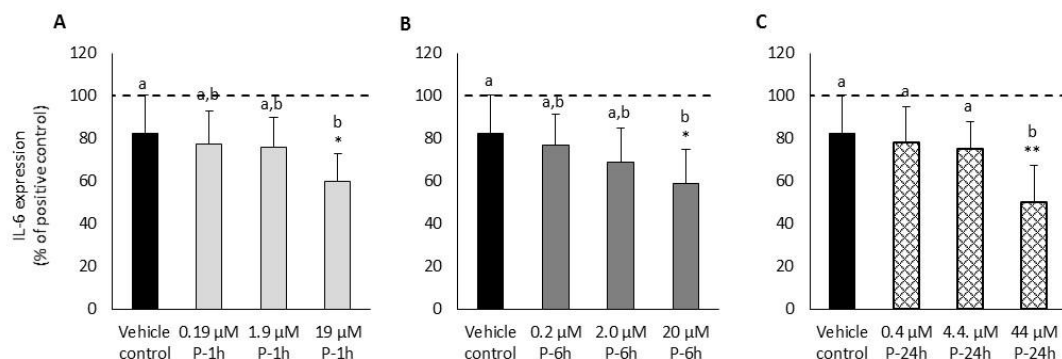
Figure 6.15 IL-6 production following treatment with anthocyanin metabolites in CD40L-stimulated HUVEC.



HUVEC were incubated with CD40L positive control (1×10^6 CD40L-expressing D1.1 Jurkat cells/well) and vehicle control (0.07% DMSO in media) or treatments (1.9 μM P-1, 2.0 μM P-6, and 4.4 μM P-24) for 24 hours before cell supernatant quantitation of IL-6 expression via ELISA. Data expressed as mean \pm SD, $n=3$. Significance relative to vehicle control, * $p \leq 0.05$, one-way ANOVA with LSD post-hoc test. ^aDifferent letters represent statistical differences between groups, $p \leq 0.05$, one-way ANOVA with LSD post-hoc test.

Concentration response was established by incubating HUVEC with the metabolite profiles at cumulative concentrations 10 fold above and below the peak concentration identified previously in the human study (Czank *et al.* 2013, de Ferrars *et al.* 2014a) [P-1 (0.19, 1.9, 19 μM), P-6 (0.2, 2.0, 20 μM), and P-24 (0.4, 4.4, 44 μM)]. Significant reductions in IL-6 expression relative to vehicle control (**Figure 6.16**) were observed at the highest concentrations tested (19 μM P-1, $40.2 \pm 12.9\%$; 20 μM P-6, $41.2 \pm 16.1\%$; 44 μM P-24, $49.8 \pm 17.3\%$).

Figure 6.16 IL-6 production following treatment with anthocyanin metabolites in CD40L-stimulated HUVEC.



HUVEC were incubated with CD40L positive control (1×10^6 CD40L-expressing D1.1 Jurkat cells/well) and vehicle control (0.07% DMSO in media) or treatments (0.19 μM P-1, 1.9 μM P-1, 19 μM P-1; 0.2 μM P-6, 2.0 μM P-6, 20 μM P-6; 0.4 μM P-24, 4.4 μM P-24, 44 μM P-24) for 24 hours before cell supernatant quantitation of IL-6 expression via ELISA. Data expressed as mean \pm SD, $n=3$. Significance relative to vehicle control, * $p \leq 0.05$, ** $p \leq 0.01$, one-way ANOVA with LSD post-hoc test. ^{a,b}Different letters represent statistical differences between groups, $p \leq 0.05$, one-way ANOVA with LSD post-hoc test.

6.4. Discussion

Initial studies into the bioactivity of anthocyanins *in vitro* used parent compounds at supraphysiological concentrations (Xu *et al.* 2004, Xia *et al.* 2007). More recently, work in our lab and elsewhere has begun to use individual phenolic metabolites at physiological concentrations (Amin *et al.* 2015, Edwards *et al.* 2015, Krga *et al.* 2016) in order to better represent the compounds present in the body following anthocyanin consumption. Limited studies have been conducted in our lab using mixtures of metabolites (di Gesso *et al.* 2015, Warner *et al.* 2016) providing information on the additive effects of metabolites in combination whilst still not perfectly representing the metabolic profiles observed following anthocyanin consumption. Some studies have used extracted serum containing phenolic metabolites of proanthocyanidins (Guerrero *et al.* 2013) to investigate bioactivity, however, this approach comes with limitations such as the high level of proteins and other serum components present that cannot be controlled for. To the author's knowledge, the present study is the first to study the bioactivity of anthocyanin metabolites using metabolite profiles, under controlled conditions and at physiologically appropriate concentrations, as reported in serum following the consumption of anthocyanins (Czank *et al.* 2013, de Ferrars *et al.* 2014a). Concentration response was also investigated by the inclusion of metabolite profiles at cumulative concentrations 10 fold above and below the peak concentration, and within the range reported amongst eight participants post-consumption of 500 mg of ¹³C-labelled cyanidin-3-glucoside (Czank *et al.* 2013, de Ferrars *et al.* 2014a).

In the present study, significant reductions in sVCAM-1 and IL-6 expression were observed when HUVEC were treated with three previously reported anthocyanin metabolite profiles (Czank *et al.* 2013, de Ferrars *et al.* 2014a) in an experimental model of inflammation involving TNF- α -stimulation (Figure 6.5 & Figure 6.9). This demonstrates that relatively low concentrations (average, 0.22 μ M; range 0.01 μ M to 1.94 μ M; **Table 6.2**) of individual component metabolites can have significant bioactive effects when in combination.

The treatments showed reductions in TNF- α and CD40L-stimulated VCAM-1 expression of greater than $46.9 \pm 5.8\%$ and $32.7 \pm 12.2\%$ respectively, which compares to similar studies reporting greater than 40% reduction of TNF- α -stimulated VCAM-1 expression by treatment with 2.4 μ M of parent un-metabolised flavonoids (Wu *et al.* 2012) and greater than 10% reduction of CD40L-stimulated VCAM-1 expression by 1 μ M cyanidin-3-glucoside (Xia *et al.* 2009) in HUVEC.

The present study also showed reductions in TNF- α and CD40L-stimulated IL-6 expression of greater than $15.6 \pm 11.0\%$ and $24.0 \pm 4.0\%$ respectively.

Table 6.2 Composition of treatments.

1.9 μ M P-1			2.0 μ M P-6			4.4 μ M P-24		
Compound	μ M	%	Compound	μ M	%	Compound	μ M	%
4-hydroxybenzaldehyde	0.01	0.5	4-hydroxybenzaldehyde	0.01	0.5	4-hydroxybenzaldehyde	0.01	0.2
Benzoic acid-4-glucuronide	0.01	0.5	Benzoic acid-4-glucuronide	0.04	2.0	Benzoic acid-4-glucuronide	0.04	0.9
Cyanidin-3-glucoside	0.05	2.6	Cyanidin-3-glucoside	-	-	Cyanidin-3-glucoside	-	-
Ferulic acid	0.29	15.3	Ferulic acid	0.21	10.3	Ferulic acid	0.59	13.5
Hippuric acid	0.07	3.7	Hippuric acid	0.23	11.3	Hippuric acid	1.94	44.3
Isovanillic acid	0.12	6.3	Isovanillic acid	-	-	Isovanillic acid	-	-
Isovanillic acid-3-glucuronide	0.01	0.5	Isovanillic acid-3-glucuronide	0.02	1.0	Isovanillic acid-3-glucuronide	-	-
Isovanillic acid-3-sulfate	-	-	Isovanillic acid-3-sulfate	-	-	Isovanillic acid-3-sulfate	0.17	3.9
PCA	0.04	2.1	PCA	0.08	3.9	PCA	0.01	0.2
PCA-3-sulfate	0.07	3.7	PCA-3-sulfate	0.02	1.0	PCA-3-sulfate	0.02	0.5
PCA-4-glucuronide	0.02	1.1	PCA-4-glucuronide	0.03	1.5	PCA-4-glucuronide	-	-
PCA-4-sulfate	0.07	3.7	PCA-4-sulfate	0.02	1.0	PCA-4-sulfate	0.02	0.5
PGA	0.03	1.6	PGA	0.55	27.1	PGA	0.05	1.1
Vanillic acid	1.10	57.9	Vanillic acid	0.80	39.4	Vanillic acid	1.36	31.1
Vanillic acid-4-glucuronide	0.01	0.5	Vanillic acid-4-glucuronide	0.02	1.0	Vanillic acid-4-glucuronide	-	-
Vanillic acid-4-sulfate	-	-	Vanillic acid-4-sulfate	-	-	Vanillic acid-4-sulfate	0.17	3.9
Total	1.90	100.0	Total	2.03	100.0	Total	4.38	100.0
Mean	0.14		Mean	0.17		Mean	0.40	
Minimum	0.01		Minimum	0.01		Minimum	0.01	
Maximum	1.10		Maximum	0.80		Maximum	1.94	

PCA, protocatechuic acid; PGA, phloroglucinaldehyde. A dash represents a metabolite that is not found in that particular treatment.

This compares to previous studies reporting greater than 10% reduction of TNF- α -stimulated IL-6 expression by 5 μ M apigenin (Gerritsen *et al.* 1995) and greater than 12% reduction of CD40L-stimulated IL-6 expression by 1 μ M cyanidin-3-glucoside (Xia *et al.* 2007) in HUVEC.

The present study suggests that bioactivity of anthocyanin metabolites is sustained across changing metabolic profiles during a 24 hour period and provides an explanation for the effects on cardiovascular function seen beyond 1-2 hours in anthocyanin feeding studies (Kropat *et al.* 2013, Rodriguez-Mateos *et al.* 2013) as different metabolite profiles exert differential effects across time. It also suggests that bioactivity of anthocyanins is not reduced following microbial catabolism and subsequent phase II metabolism (methylation, glucuronidation, and sulfation), which are processes generally considered to detoxify and increase rates of elimination in the body (Zamek-Gliszczynski *et al.* 2006).

Vanillic acid makes up a large proportion (>31%) of the metabolites within each treatment profile (Table 6.2), which suggests that this metabolite, a methylated form of PCA produced from the anthocyanin B-ring, may be an important factor in the observed bioactivity of anthocyanins. Indeed, previous *in vitro* studies using vanillic acid in isolation have demonstrated significant bioactivity in reducing expression of VCAM-1 and IL-6 in CD40L/oxLDL-stimulated HUVEC (Amin *et al.* 2015), reducing IL-6 expression in LPS-stimulated mouse peritoneal macrophages (Kim *et al.* 2011) and reducing superoxide production in angiotensin II-stimulated HUVEC (Edwards *et al.* 2015). However, the concentrations of vanillic acid used in this study (1-2 μ M) are relatively low which suggests that it is unlikely that vanillic acid alone is responsible for the observed bioactivity. This is supported by recent *in vitro* analysis of TNF- α production in LPS-stimulated THP-1 monocytes which indicated additive effects when vanillic acid is combined with other phenolic metabolites such as PCA and 4-hydroxybenzoic acid (di Gesso *et al.* 2015). Future work should focus on investigating the nature of this additive effect.

Examination of the structural composition of the P-1, P-6, and P-24 treatments (**Table 6.3 & Table 6.4**) highlights some interesting elements in relation to the observed bioactivity in this study. In terms of structural groups, there is a shift away from contributions by benzoic acids in early metabolite profiles observed at 1 hour post-consumption towards greater contribution by hippuric acid in later metabolite profiles observed at 6 and 24 hours post-consumption. Hippuric acid can be found in the blood at mM concentrations in healthy individuals (Vanholder *et al.* 2003) which suggests that the maintenance of bioactivity seen across the P-1, P-6, and P-24 treatments is unlikely to be due to the μ M increases reported following anthocyanin consumption. There is also a decrease in contribution from early

metabolite profiles observed at 1 hour to later profiles observed at 24 hours post-consumption of compounds containing hydroxyl and methoxy groups relative to an increase in sulfate and glycine conjugates, suggesting that the presence of sulfate and glycine conjugates may be important in maintaining bioactivity in relation to inflammatory response. This is supported by previous work in our lab looking at the structure-activity relationship of anthocyanin phase II-metabolites affecting expression of VCAM-1 and IL-6 in HUVEC which observed maximal reductions in cytokine expression following treatment with sulfate conjugates of PCA (Amin *et al.* 2015). Further research is required in order to fully understand the nature of the relationship between metabolite structure and bioactivity.

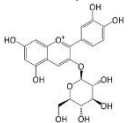
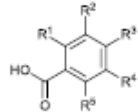
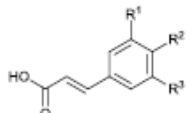
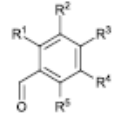
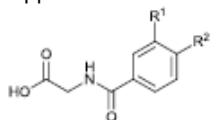
Table 6.3 Structural composition of treatments.

P-1		P-6		P-24	
Structural group	% ^a	Structural group	% ^a	Structural group	% ^a
Anthocyanins	2.6	Anthocyanins	0.0	Anthocyanins	0.0
Benzaldehydes	2.1	Benzaldehydes	27.6	Benzaldehydes	1.4
Benzoic acids	76.3	Benzoic acids	50.7	Benzoic acids	40.9
Hippuric acids	3.7	Hippuric acids	11.3	Hippuric acids	44.3
Phenylpropanoic acids	15.3	Phenylpropanoic acids	10.3	Phenylpropanoic acids	13.5
Structural group	% ^b	Structural group	% ^b	Structural group	% ^b
Hydroxyl	94.7	Hydroxyl	84.7	Hydroxyl	47.0
Glucuronide	2.6	Glucuronide	5.4	Glucuronide	0.9
Glycine	3.7	Glycine	11.3	Glycine	44.3
Methoxy	80.5	Methoxy	51.7	Methoxy	52.3
Sulfate	7.4	Sulfate	2.0	Sulfate	8.7

^aSum of percentage contributions towards total treatment composition by compounds in each respective structural group. ^bSum of percentage contributions towards total treatment contribution by compounds containing each respective functional group.

Concentration response was established by incubating HUVEC with the metabolite profiles at cumulative concentrations 10 fold above and below the peak concentration identified previously in the human study (Czank *et al.* 2013, de Ferrars *et al.* 2014a). In many cases a non-linear concentration response was observed with maximal bioactivity at the mean concentrations (1.9-4.4 μ M) suggesting no increased bioactivity would be conferred by increasing anthocyanin intake beyond the 500 mg used in the ¹³C-labelled cyanidin-3-glucoside study (Czank *et al.* 2013). Previous studies in our lab have also reported non-linear, bimodal concentration responses in relation to flavonoid bioactivity (Kay *et al.* 2012, Amin *et al.* 2015, di Gesso *et al.* 2015) with maximal bioactivity often observed at the 1 μ M level. Previous studies investigating concentration response of blueberry flavonoids in relation to *in vivo* biomarkers such as flow-mediated dilation have also observed a bimodal response with a maximal response seen following intake of 766 mg of blueberry flavonoids (Rodriguez-Mateos *et al.* 2013).

Table 6.4 Structural information on metabolites included in treatments.

Structure	Common Name	IUPAC Name	Configuration ^a
	Cyanidin-3-glucoside	(2 <i>S</i> ,3 <i>R</i> ,4 <i>S</i> ,5 <i>R</i> ,6 <i>R</i>)-2-[2-(3,4-Dihydroxyphenyl)-5,7-dihydroxy-chromen-3-yl]oxy-6-(hydroxymethyl)oxane-3,4,5-triol	R ¹ ,R ² = OH
	Protocatechuic acid Benzoic acid-4-glucuronide Protocatechuic acid-4-glucuronide Protocatechuic acid-3-sulfate Protocatechuic acid-4-sulfate Vanillic acid Isovanillic acid Vanillic acid-4-glucuronide Isovanillic acid-3-glucuronide Vanillic acid-4-sulfate Isovanillic acid-3-sulfate	3,4-Dihydroxybenzoic acid 6-(4-Carboxyphenoxy)-3,4,5-trihydroxytetrahydro-2 <i>H</i> -pyran-2-carboxylic acid 6-(4-Carboxy-2-hydroxyphenoxy)-3,4,5-trihydroxytetrahydro-2 <i>H</i> -pyran-2-carboxylic acid 5-Carboxy-2-hydroxyphenyl sulfate 4-Carboxy-2-hydroxyphenyl sulfate 4-Hydroxy-3-methoxybenzoic acid 3-Hydroxy-4-methoxybenzoic acid 6-(4-Carboxy-2-methoxyphenoxy)-3,4,5-trihydroxytetrahydro-2 <i>H</i> -pyran-2-carboxylic acid 6-(5-Carboxy-2-methoxyphenoxy)-3,4,5-trihydroxytetrahydro-2 <i>H</i> -pyran-2-carboxylic acid 4-Carboxy-2-methoxyphenyl sulfate 5-Carboxy-2-methoxyphenyl sulfate	R ² ,R ³ = OH R ³ = O-GlcA R ² = OH, R ³ = O-GlcA R ² = OSO ₃ ⁻ , R ³ = OH R ² = OH, R ³ = OSO ₃ ⁻ R ² = OCH ₃ , R ³ = OH R ² = OH, R ³ = OCH ₃ R ² = OCH ₃ , R ³ = O-GlcA R ² = O-GlcA, R ³ = OCH ₃ R ² = OCH ₃ , R ³ = OSO ₃ ⁻ R ² = OSO ₃ ⁻ , R ³ = OCH ₃
	Phenylpropanoic acids Ferulic acid	3-(4-Hydroxy-3-methoxyphenyl)-prop-2-anoic acid	R ¹ = OCH ₃ , R ² = OH
	Benzaldehydes Phloroglucinaldehyde 4-hydroxybenzaldehyde	2,4,6-Trihydroxybenzaldehyde 4-hydroxybenzaldehyde	R ¹ ,R ³ ,R ⁵ = OH R ³ = OH
	Hippuric acids Hippuric acid	2-Benzamidoacetic acid	R ¹ ,R ² = H

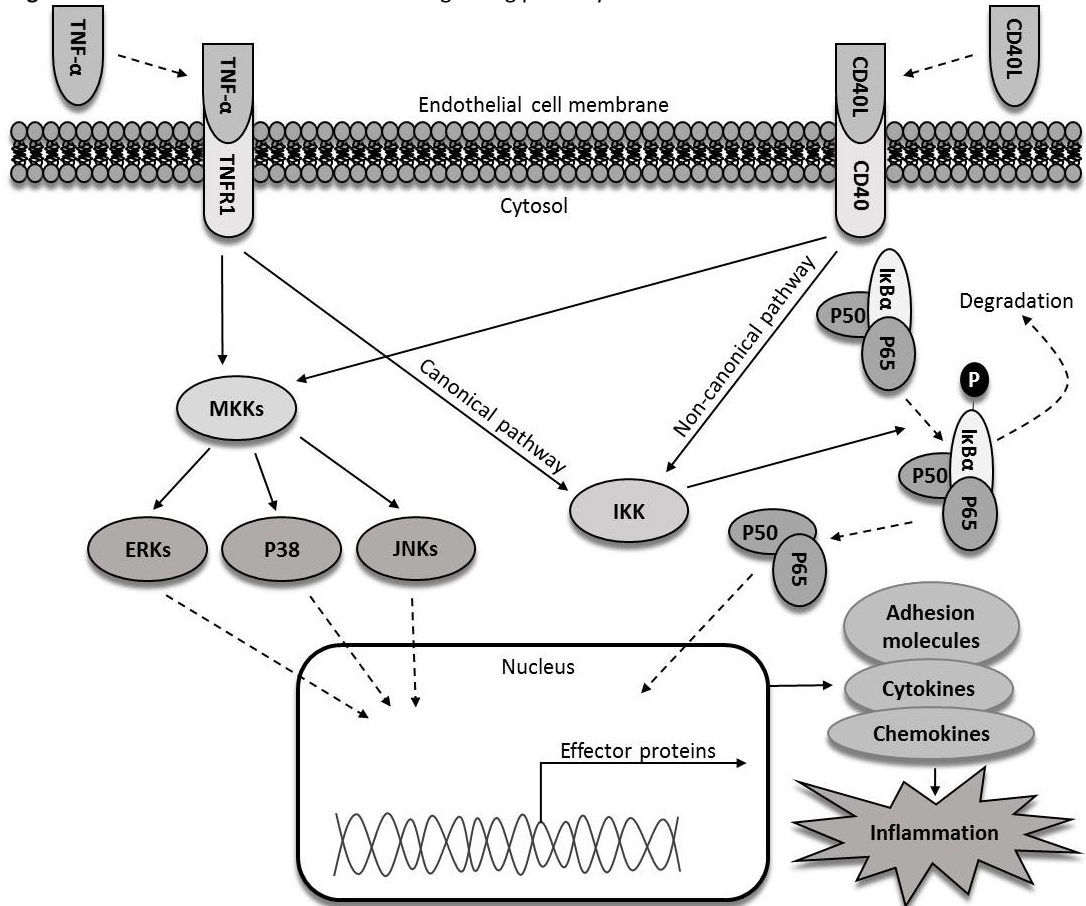
^aR¹-R⁵ represents hydrogen (H) or position of a functional group such as: OH, hydroxyl; OCH₃, methoxy; O-GlcA, O-glucuronide; SO₃⁻, sulfate. Adapted from (de Ferrars *et al.* 2014c).

However, in the present study, a number of cases (**Figure 6.10A, Figure 6.10C, Figure 6.16**) did show a linear concentration response with increased bioactivity at the highest treatment concentrations. Recent studies within our lab investigating the effect of metabolite combinations on inflammatory biomarkers have also observed linear concentration responses (Warner *et al.* 2016). The high vanillic acid content of the treatments in the present study may provide an explanation for the observed linear response as previous studies have noted linear concentration responses in relation to this particular metabolite (Amin *et al.* 2015). Further investigation is required in order to establish the concentration response relationship of serum anthocyanin metabolite profiles in inflammation.

The significant reductions in sVCAM-1 and IL-6 associated with the 1.9 μ M P-1, 2.0 μ M P-6, and 4.4 μ M P-24 treatments that were seen in TNF- α -stimulated HUVEC were not replicated following CD40L stimulation. This suggests that the phenolic metabolites are not acting upon the MAPK signalling pathway which is activated following both TNF- α and CD40L stimulation (Pamukcu *et al.* 2011, Hayden and Ghosh 2014) as we would expect to observe similar results following both TNF- α and CD40L stimulation if the phenolic metabolites affected this pathway. The possibility remains that anthocyanin metabolites exert their effect through interaction with the TNF receptor as a number of studies have reported the ability of anthocyanins and their metabolites to inhibit the effect of TNF- α stimulation (Krga *et al.* 2016, Warner *et al.* 2016). However, inhibition of proinflammatory cytokine expression by anthocyanin metabolites following CD40L stimulation has also been reported (Amin *et al.* 2015) suggesting that the phenolic metabolites are likely to be acting downstream of the TNF and CD40 receptors. Future studies may wish to investigate the effect of anthocyanin metabolite profiles on the MAPK and NF- κ B pathways in more detail by exploring their effect on expression of transcription factors such as AP-1 and c-JUN via phosphorylation of P38 and JNK, as has been demonstrated previously using anthocyanins (Oak *et al.* 2006) and PCA (Lin *et al.* 2007), and thus represents a possible upstream target for anthocyanin metabolites. Future study of the effect of anthocyanin metabolite profiles on p38 and JNK phosphorylation may provide more information on the mechanism behind their observed bioactivity.

The results of the present study suggest that the phenolic metabolites may be exerting their effect via the canonical pathway of TNF- α signalling, upstream of the IKK and NF- κ B proteins which are common to both the canonical TNF- α and non-canonical CD40L signalling pathways (**Figure 6.17**) (Hayden and Ghosh 2014).

Figure 6.17 Activation of MAPK and NF- κ B signalling pathways via TNF- α and CD40L stimulation.



CD40(L), cluster of differentiation 40 (ligand); ERK, extracellular signal-regulated kinases; I κ B α , NF- κ B inhibitory protein; IKK, inhibitory- κ B kinase; JNK, c-Jun N-terminal kinases; MKK, mitogen-activated protein kinase kinases; P, phosphate; p38, mitogen-activated protein kinase; p50, nuclear factor- κ B p50 subunit; p65, NF- κ B p65 subunit; TNF- α , tumour necrosis factor- α ; TNFR1, TNF receptor 1. Adapted from (Pamukcu *et al.* 2011, Hayden and Ghosh 2014, Sabio and Davis 2014).

In comparison to the non-canonical, CD40L-stimulated pathway of NF- κ B signalling, a number of signalling molecules are unique to the canonical pathway such as TNFR1-associated death domain protein (TRADD), transforming growth factor- β activated kinase (TAK1), and NF- κ B essential modulator (NEMO) (Hayden and Ghosh 2014, Sabio and Davis 2014) but further work is required to identify the mechanism by which the phenolic metabolites exert their bioactive effect. The results of the present study may also indicate the potential for phenolic metabolites to have an additive effect if acting across multiple signalling pathways. This is supported by recent studies demonstrating that flavonoids and phenolic acids can affect the expression of many microRNAs (Milenkovic *et al.* 2013), both *in vitro* and *in vivo*, and anthocyanins can modulate the expression of over 1200 genes in the aorta of apoE-deficient mice, including many genes involved in oxidative stress, monocyte infiltration, and the progression of atherosclerosis such as chemokines and cell adhesion molecules (Mauray *et al.* 2012). Further research using additional stimuli associated with

atherosclerosis development such as angiotensin II, peroxynitrite (ONOO⁻), and oxidised low-density lipoprotein (oxLDL), and exploring alternative signalling pathways such as the PI3K/Akt pathway is needed to explore the possible additive effects of anthocyanin metabolites.

Another possibility is that the lack of significant reductions in sVCAM-1 seen in the CD40L-stimulated HUVEC is due to increased variability caused by the co-incubation of HUVEC with CD40L-expressing D1.1 Jurkat cells. The significant reduction in CD40L-stimulated VCAM-1 expression caused by the vehicle control was not replicated in the TNF- α -stimulated VCAM-1 expression. A possible explanation for this observation is cytotoxicity of DMSO towards the D1.1 Jurkat cells resulting in reduced sVCAM-1 expression, however, further investigation would be required to validate this hypothesis. Future studies could mitigate these issues via the use of soluble CD40L protein. This method was considered cost-prohibitive in the present study. The P-1 and P-6 metabolite composition treatments had no effect on cell viability, while a modest effect was observed for the P-24 composition treatment (90% viability) when incubated with tenfold higher concentration than the reported mean (43.8 μ M). The TNF- α positive control reduced viability by 19.2% which is similar to previous studies that have shown 20 – 25% reduction in HUVEC viability following 24 hour incubation with TNF- α (Louise and Obrig 1991, Ramana *et al.* 2004). The TNF- α negative control, BAY11-7085, mildly increased cell viability and was used as an inhibitor of both sVCAM-1 and IL-6 expression for the negative control in this study. However, despite BAY11-7085 being commonly used in this context (Dumont *et al.* 2012, Lee *et al.* 2012), it did not significantly reduce IL-6 expression following either TNF- α or CD40L stimulation in this study. BAY11-7085 exerts its effect on IL-6 expression via inhibition of I κ B α phosphorylation therefore blocking activation and nuclear translocation of NF- κ B (Pierce *et al.* 1997). A possible explanation for the lack of IL-6 inhibition compared to sVCAM-1 observed in this study is that while BAY11-7085 was able to inhibit the NF- κ B pathway and therefore inhibit expression of sVCAM-1 which relies on binding of NF- κ B to its promoter region for transcription (Carter and Wicks 2001), BAY11-7085 has been shown to be unable to inhibit activation of the MAPK pathway by TNF- α (Pierce *et al.* 1997) and therefore was unable to prevent downstream expression of IL-6 (Sabio and Davis 2014). Future studies should consider alternative compounds that have shown the ability to inhibit IL-6 such as cardamonin (Yu *et al.* 2014) and nobiletin (Sawa *et al.* 2008).

Future work should aim to expand upon the work presented here in a number of ways. Firstly, via the use of primary vascular cell lines to validate the observations made using HUVEC in the present study. HUVEC are widely used in vascular research due to the fact they

are relatively inexpensive and easy to culture but there is evidence to suggest that alternative cell lines such as human aortic endothelial cells (HAEC) or human coronary artery endothelial cells (HCAEC) may provide results that are more relevant to *in vivo* situation when studying inflammatory cytokines such as VCAM-1 and IL-6 (Bouïs *et al.* 2001). Time course studies revealed optimal assay incubations of 24h for sVCAM-1 and IL-6 expression. A 30 minute pre-treatment time was used in the present study but future work may also benefit from an investigation into the effect of different pre-treatment times on the bioactivity of the metabolites and metabolite profiles. Another possible area for future study is to investigate the expression of membrane-bound instead of soluble VCAM-1. The soluble form of VCAM-1 was measured in the present study as it simpler to quantify (Vastag *et al.* 1999), is a valid biomarker of inflammation (Carter and Wicks 2001) and is commonly used as an endpoint for flavonoid bioactivity studies in HUVEC (Xia *et al.* 2009, Jia *et al.* 2013). Additional analysis of the effect on membrane-bound VCAM-1 would provide further insight into the pathways through which anthocyanin metabolites exert their bioactivity. Finally, future research should aim to include analysis of mRNA production to accompany the analysis of sVCAM-1 and IL-6 protein expression. Analysis of mRNA production would provide information on whether the observed effects on sVCAM-1 and IL-6 protein expression were due to pre- or post-translational effects. This information would help to establish the mechanism and pathway through which the anthocyanin metabolites are having their effect. Analysis of mRNA would also help to show whether there were any effects on sVCAM-1 and IL-6 mRNA production caused by the anthocyanin metabolites in CD40L-stimulated HUVEC that were not seen in the protein expression results.

6.5. Conclusion

In summary, the present study utilised a novel treatment design to mimic time-specific metabolite profiles in order to demonstrate that low concentrations of anthocyanin metabolites, in combination, can reduce TNF- α -stimulated expression of sVCAM-1 and IL-6, two important biomarkers of inflammation associated with atherosclerosis and CVD. Furthermore, the active concentrations are achievable following consumption of 500 mg of cyanidin-3-glucoside and therefore achievable through the diet. The increased bioactivity of the 6 and 24 hour post-consumption profiles suggests that bioactive compounds are maintained within the blood for many hours after consumption of the parent compound. These findings provide valuable insight into the role of anthocyanins in promoting good health.

Chapter 7. General Discussion and Future Perspectives

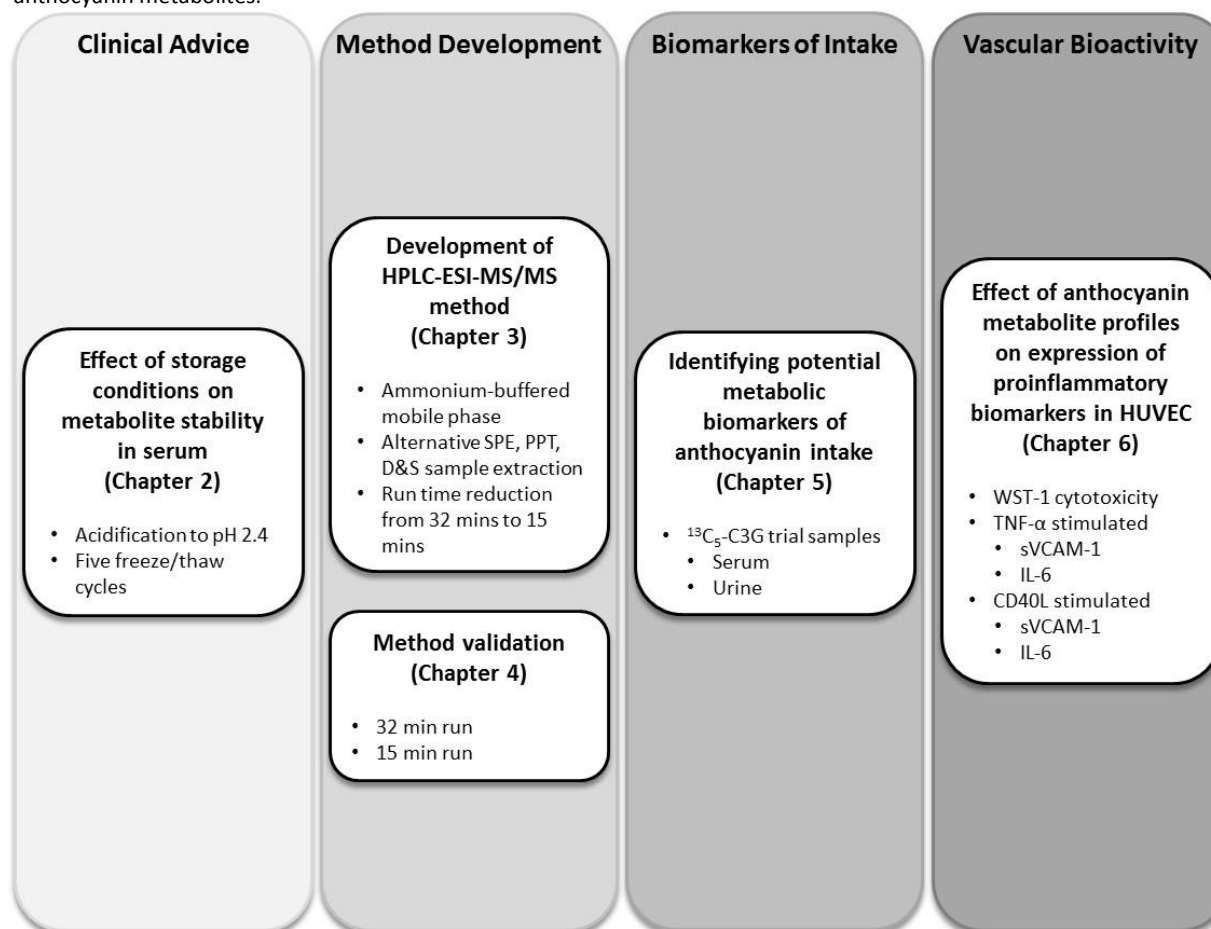
7.1. General Discussion

Anthocyanins are polyphenol pigments found in many commonly consumed fruits and vegetables such as berries, grapes, and red cabbage (Crozier *et al.* 2010, Del Rio *et al.* 2010a). Evidence from epidemiological studies (Jennings *et al.* 2012, Cassidy *et al.* 2015) and randomised controlled trials (Dohadwala *et al.* 2011, Rodriguez-Mateos *et al.* 2013) suggests that diets high in anthocyanins are associated with a reduced risk of cardiovascular disease. Instability at neutral pH (Rein 2005) and the poor bioavailability of anthocyanins observed in feeding trials (Manach *et al.* 2005) suggested that the parent compounds were likely not responsible for the observed bioactivity of anthocyanins and that the metabolites of anthocyanins may be key to their bioactivity. Recent studies have confirmed that anthocyanins are metabolised to produce a wide range of phenolic compounds (Czank *et al.* 2013, de Ferrars *et al.* 2014b) and that these metabolites can have positive effects on inflammatory and vascular function, which are known biomarkers of cardiovascular disease (Rodriguez-Mateos *et al.* 2013, Amin *et al.* 2015, di Gesso *et al.* 2015, Warner *et al.* 2016).

The present thesis aimed to contribute to our understanding of anthocyanin metabolism and its importance in cardiovascular health via four approaches (**Figure 7.1**): providing information on the stability of phenolic metabolites in biological matrices for future clinical studies; improving current LC-MS methods for quantifying anthocyanin metabolites in serum and urine samples to increase throughput and afford lower limits of detection; investigating phenolic metabolites as biomarkers of anthocyanin intake with the goal of improving accuracy of consumption monitoring; and investigating the effect of physiologically relevant anthocyanin metabolite profiles on expression of proinflammatory biomarkers.

The shift away from studying the parent anthocyanins and towards their phenolic metabolites has required the development of methods capable of detecting and quantifying large numbers of metabolites at nanomolar concentrations in biological matrices. Due to their absorption within both the visible spectrum at 465 – 550 nm and UV spectrum at 270 – 280 nm, anthocyanins have typically been detected and quantified using HPLC with DAD detector methodology (Hong and Wrolstad 1990, Cao and Prior 1999). DAD detection of phenolic acids is also possible (Robbins 2003) but can be restrictive in terms of detection limits, and the number of metabolites that can be quantified within the same method due to the need for chromatographic separation.

Figure 7.1 Experimental scheme for the assessment of stability, quantification methods, biomarker utility, and bioactivity of anthocyanin metabolites.



HPLC, high-performance liquid chromatography; ESI, electrospray ionisation; MS, mass spectrometry; SPE, solid-phase extraction; PPT, protein precipitation; D&S, dilute-and-shoot; $^{13}\text{C}_5\text{-C3G}$, ^{13}C -labelled cyanidin-3-glucoside; HUVEC, human umbilical vein endothelial cells; WST-1, water-soluble tetrazolium salt-1; TNF- α , tumour necrosis factor- α ; sVCAM-1, soluble vascular cell adhesion molecule-1; IL-6, interleukin-6; CD40L, cluster of differentiation 40 ligand.

By combining HPLC separation with mass spectrometry detection, highly specific and sensitive methods for the quantification of phenolic metabolites of anthocyanins in biological samples have been developed (Rodriguez-Mateos *et al.* 2013, Pimpão *et al.* 2014, McKay *et al.* 2015, Xie *et al.* 2016), including an HPLC-ESI-MS/MS method with a 32 minute run time developed by our group that was used for the detection and quantification of 45 phenolic metabolites in serum and urine samples from a ¹³C-labelled C3G intervention (Czank *et al.* 2013, de Ferrars *et al.* 2014c). In chapters 3 and 4, the present thesis describes the development and validation of this method. Improvements to the method were deemed necessary in order to allow detection of novel metabolites potentially below the LOD of the current method, to improve the accuracy and precision of metabolite quantification via increased signal-to-noise ratios within the *in vivo* concentration range, and to increase throughput to facilitate the analysis of large sample sets in future clinical studies.

Addition of ammonium buffers to the mobile phase was investigated as a means of improving ionisation efficiency and increasing sensitivity. Alternative methods of improving ionisation efficiency such as flow splitting were also considered. Flow splitting involves post-column splitting of the mobile phase flow to send the majority direct to the waste while a small proportion enters the ion source. This has the effect of greatly reducing the volume of solvent within the ion source which speeds up evaporation and therefore improves ionisation. Ultimately, it was decided that this approach would be complicated to set up and similar results could be achieved through optimisation of HPLC parameters. Addition of ammonium buffers to the mobile phase was considered the best option for increasing method sensitivity in the present study. Ionisation of analytes in ESI-MS is a complex process affected by many factors but it has been suggested that small amounts (≤ 10 mM) of volatile buffer salts such as ammonium acetate or ammonium formate can lead to improved ionisation efficiency of analytes due to the increased presence of ions within the mobile phase (Banerjee and Mazumdar 2012, Hua and Jenke 2012) and previous studies have reported optimal sensitivity for the detection of flavonoids when using ammonium-buffered mobile phases (Rauha *et al.* 2001, de Rijke *et al.* 2003) but no studies have explored the effect on ionisation of phenolic acids. The present study provides data that suggests that both 10 mM ammonium acetate and 10 mM ammonium formate have a negative effect on phenolic acid ionisation across a range of pH values and that their use should be avoided.

Switching to a shorter HPLC column (50 mm vs 100 mm) with a smaller internal diameter (2.1 mm x 4.6 mm), reducing the mobile phase flow rate to 0.6 mL min⁻¹, and optimising various HPLC parameters, including column temperature and mobile phase gradient, yielded

a method that was able to detect and quantify a greater number of metabolites (53 vs 45) in less than half the run time (15 min vs 32 min) compared to the previous method (de Ferrars *et al.* 2014c). The new 15 minute method also compares favourably in terms of quantifiable metabolites and/or run time against methods previously reported in the literature for quantification of phenolic metabolites in biological samples (Rodriguez-Mateos *et al.* 2013, Pimpão *et al.* 2014, McKay *et al.* 2015, Xie *et al.* 2016). The present thesis describes the validation of both the new 15 minute method and the previous 32 minute method. Validation of the 32 minute method has been reported previously (de Ferrars *et al.* 2014c) but the decision was taken to re-validate in the present study as the previous validation was conducted at only one concentration and used a spiked mobile phase matrix. Validation at three concentrations in a matched-matrix (extracted serum), as recommended in the FDA guidelines for bioanalytical method validation (Food and Drug Administration 2001), provided a more realistic understanding of the relative strengths and limitations of the method. Validation of both methods revealed good specificity, linearity, and LODs but limitations in terms of accuracy and precision at the lower concentrations (0.098 μM and 1.56 μM). This may limit the future use of these methods in the quantification of absolute metabolite concentrations in clinical samples but, due to the high levels of inter-participant variation that exist in clinical nutrition research and low metabolite concentrations detected, both methods can be utilised for detection of metabolite profiles and quantification of relative concentrations. Validation of the new 15 minute method highlights the need for continued development of the method in order to further reduce LODs and improve accuracy and precision at the lower concentrations. The validation of analytical methods following FDA guidelines as described in the present thesis is crucial to provide confidence in the results obtained using them. Whilst a number of anthocyanin feeding studies report validation results for their analytical methods (Cooke *et al.* 2006, Giordano *et al.* 2007, Nakamura *et al.* 2009), there are still many that do not which makes it difficult to compare the quality of analytical methods within the field. The lack of published validation data should be addressed if the standard of clinical analysis in nutrition is to be improved.

Assessment of the health effects associated with anthocyanin consumption relies upon accurate estimations of dietary intake. It has been suggested that, due to problems with misreporting of intake and inaccurate or incomplete database values for anthocyanin content in dietary sources associated with traditional methods of estimating dietary intake such as food frequency questionnaires (Beaton 1994, Thompson *et al.* 2010), quantifying the levels of characteristic metabolites in the body may offer an improved method of monitoring

anthocyanin consumption (Hedrick *et al.* 2012). In chapter 5, the present thesis aimed to use serum and urine samples from a recently conducted ^{13}C -labelled cyanidin-3-glucoside trial (Czank *et al.* 2013) to identify metabolites present in all participants at concentrations above those resulting from the background diet as potential biomarkers of anthocyanin intake. Gallic acid in urine was found to be the best candidate in the present study based upon its detection at similar concentrations above background levels across all eight participants. Previous studies have also suggested a role for gallic acid in determining anthocyanin consumption (Ito *et al.* 2005, Urpi-Sarda *et al.* 2015) but the present study is the first to use ^{13}C -labelling to identify potential metabolic biomarkers of anthocyanin intake. The detection of ^{13}C -labelled metabolites is an important advantage of the present study as it allowed a distinction to be made between metabolites present within the background diet and metabolites present due to the consumption of the labelled anthocyanin. A limitation of the present study is the non-detection of a number of metabolites that had been observed within the same serum and urine samples by a previous study (Czank *et al.* 2013). The differences in observed metabolites between the two studies may be due to a decrease in method sensitivity in the present study, possibly caused by the change in MS instrumentation or by the increase in the number of metabolites analysed by the method used in the present study. The poor accuracy and precision of the analytical method at lower concentrations may also have negatively affected the quantification of metabolites in the present study resulting in possible metabolite biomarkers being ruled out incorrectly. Future studies may wish to reinvestigate potential biomarkers of anthocyanin intake using more sensitive analytical methods. Following the identification of any additional candidate metabolites as biomarkers of anthocyanin intake, the next step towards their use in monitoring anthocyanin intake in clinical studies would be to assess the responsiveness of the metabolites to changes in anthocyanin intake. This could be achieved by asking volunteers to consume varying amounts of cyanidin-3-glucoside on separate days, with a one week washout period in between each occasion, and collect urine samples to monitor the concentration of the metabolite biomarker candidates and assess how urine metabolite levels are affected by the changes in anthocyanin intake. Once this concentration response has been established, any potential biomarkers of anthocyanin intake should be validated using samples from large clinical trials to evaluate their effectiveness within the wider population as biomarkers of anthocyanin intake, how this is affected by differences in genetics and gut microbiota, and how this analytical approach compares against traditional diet monitoring methods.

The present thesis investigated the bioactivity of anthocyanin metabolite profiles at physiological concentrations in a vascular cell model. Recent *in vitro* studies have reported positive effects on vascular and inflammatory biomarkers in a range of cell types following incubation with anthocyanin metabolites but these studies have typically used metabolites either in isolation (Amin *et al.* 2015, Edwards *et al.* 2015) or in equimolar combinations (di Gesso *et al.* 2015, Warner *et al.* 2016) with neither approach accurately representing the *in vivo* situation following anthocyanin consumption. These studies provide information regarding additive effects of metabolites in combination and how bioactivity is affected by methylation/sulfation/glucuronidation. This data is important to our understanding of the mechanisms behind the bioactivity of anthocyanins but is perhaps more relevant to a pharmaceutical approach in which the most active metabolites or metabolite combinations can be isolated and provided to consumers at an optimal dose to improve cardiovascular health. In order to provide better nutritional advice about the types of foods to eat, when to eat them, and how much to eat, it is necessary to have data on the bioactivity of physiologically relevant metabolite profiles. To the author's knowledge, the present study is the first to study the bioactivity of anthocyanin metabolite profiles *in vitro* in the combinations and concentrations at which they were observed *in vivo* and therefore provides more physiologically relevant information regarding the bioactivity of anthocyanins. The effect on expression of two proinflammatory cytokines, sVCAM-1 and IL-6, was investigated in CD40L and TNF- α -stimulated HUVEC. It was found that the metabolite profiles were capable of inhibiting the expression of sVCAM-1 and IL-6 following TNF- α stimulation and that the 6 h and 24 h metabolite profiles were more active than the 1 h profile suggesting that bioactive compounds are produced during anthocyanin metabolism and remain active for at least 24 hours following consumption. This is an important finding of the present study and suggests a role for gut microbiota in the production of bioactive metabolites. A recent study investigated the effect of blueberry polyphenols on vascular function *in vivo* and reported a correlation between peaks in total metabolite concentration at 1-2 h and 6 h following consumption, and improvements in FMD (Rodriguez-Mateos *et al.* 2013) but the present study is the first to investigate the effect of a physiologically relevant 24 h anthocyanin metabolite profile on expression of proinflammatory cytokines *in vitro*.

In summary, the key outcomes of the present thesis are:

- Unlike the parent anthocyanin, the stability of phenolic metabolites within a serum matrix over 240 hours was unaffected by either pH or up to five freeze/thaw cycles.
- Use of 10 mM ammonium formate (pH 3-5) or 10 mM ammonium acetate (pH 4-6) buffer solutions as aqueous mobile phase did not increase the sensitivity of an HPLC-ESI-MS/MS method for quantifying anthocyanin metabolites in biological samples.
- As a urine sample preparation technique, protein precipitation was capable of delivering limits of detection for anthocyanin metabolites equal to those obtained using solid-phase extraction, with reduced cost and increased throughput.
- Compared to an existing 32 minute HPLC-ESI-MS/MS method, similar chromatographic separation and method sensitivity was achieved in 15 minutes by changing the following method parameters:
 - Column length: 100 mm to 50 mm
 - Column diameter: 4.6 mm to 2.1 mm
 - Column temperature: 37°C to 40°C
 - Flow rate: 1.5 mL min⁻¹/1.0 mL min⁻¹ to 0.6 mL min⁻¹
 - Gradient:

1% B at 0 min	to	1% B at 0 min
7.5% B at 7 min		7.5% B at 7 min
7.6% B at 14 min		7.6% B at 9 min
10% B at 17 min		90% B at 9.5 to 11.5 min
12% B at 18.5 min		1% B at 12 to 15 min
12.5% B at 20 min		
30% B at 24 min		
90% B at 25 to 28 min		
1% B at 29 to 32 min		
- According to FDA and UN guidelines on bioanalytical method validation, both the existing 32 minute and developed 15 minute HPLC-ESI-MS/MS methods had acceptable linearity, specificity and sensitivity with limits of detection in the nanomolar range. Accuracy and precision were acceptable at 50 µM but outside guidelines at 1.56 µM and 0.098 µM for both methods.
- Urine represents the most likely source of anthocyanin intake biomarkers with gallic acid identified as the most promising metabolite candidate in this study.
- Anthocyanin metabolite profiles observed in serum at 1, 6 and 24 hours post-consumption of ¹³C-labelled cyanidin-3-glucoside were able to significantly reduce expression of the proinflammatory cytokines sVCAM-1 and IL-6 in TNF-α-stimulated HUVEC.

7.2. Future Perspectives

The present thesis describes the development of an HPLC-ESI-MS/MS method for the quantification of anthocyanin metabolites in biological matrices. A range of approaches were evaluated for improving the existing method such as the addition of ammonium salts to the mobile phase, alternative sample extraction methods, and optimisation of HPLC parameters. Future work should aim to continue the development of this method in a number of key areas. In chapter 3, a PPT method was suggested as an alternative sample extraction method for urine samples but due to the high level of ion-suppressing matrix components present in serum, SPE is still necessary for these samples. At present, the analytical method uses individual SPE cartridges in an offline process which is time-consuming and expensive. Sample processing throughput could be increased via the use of an automated online SPE system or by switching to a 96-well plate SPE format. Future development of this method should also focus on improving method sensitivity and reducing LODs. One possible route for improving sensitivity is via the use of HILIC HPLC columns. HILIC columns are well-suited to ESI mass spectrometry applications due to the nature of the stationary phases and solvents used (Nguyen and Schug 2008). In traditional RP-HPLC gradient methods, mobile phases are initially mostly aqueous with increasing amounts of organic solvents added gradually to elute the analytes of interest from the stationary phase. In HILIC, the opposite is the case with predominantly organic mobile phases and water acting as the strong solvent (Hemström and Irgum 2006). This means that when using traditional RP-HPLC methods, high volumes of aqueous solvent enter the ion source which can lead to poor evaporation and ionisation efficiency. HILIC can deliver improved ionisation efficiency, and therefore increased method sensitivity, due to the higher volumes of organic solvent resulting in faster evaporation within the ion source (Jandera 2011). Due to the potential for improved ionisation and sensitivity, the use of HILIC in combination with ESI mass spectrometry has increased in recent years (Jian *et al.* 2010) and a number of recent studies have reported the use of HILIC in the quantification of anthocyanins (Willemse *et al.* 2013, Sun *et al.* 2015, Deineka *et al.* 2016) suggesting that the technique may also be suitable for analysis of phenolic metabolites. Switching from RP-HPLC to HILIC would require further method development but has the potential to deliver improvements in method sensitivity that are necessary to deliver high quality quantification of anthocyanin metabolites.

The short-term effect of acidification and freeze/thaw cycling on the stability of anthocyanin metabolites in biological samples was investigated in the present thesis. However, the long-term storage stability of phenolic metabolites in biological matrices is still unknown. This is

relevant as the time between collection of biological samples from the first participants and sample analysis in a large clinical study can be considerable, often up to 12 months. The long-term storage stability of anthocyanins in juice matrices has been extensively studied due to the commercial need for storage of juices prior to consumption. These studies typically follow FDA guidance for accelerated storage stability studies (Food and Drug Administration 2003) and store juices at 25°C for six months to mimic the effect of 12 months storage at ambient temperature and under these conditions, anthocyanins have been shown to be unstable with losses of up to 90% during storage (Hager *et al.* 2008, Wilkes *et al.* 2013, Mäkilä *et al.* 2016). Long-term stability of phenolic acids, such as hydroxycinnamic acids, in juice matrices has also been studied and found to result in losses of 20 – 40% following storage (Wilkes *et al.* 2013, Mäkilä *et al.* 2016). To the author's knowledge, no studies have been conducted that explore the stability of anthocyanins or their metabolites in biological matrices over a similar timescale. Future studies may wish to fill this gap in our knowledge by conducting a 12 month storage stability study in which serum and/or urine aliquots are spiked with anthocyanins and phenolic acids at a known concentration and then stored at -80°C for 12 months to mimic the storage of clinical samples prior to analysis. Analysis at 1, 3, 6 and 12 months by LC-MS to monitor the anthocyanin and phenolic acid concentrations against an external standard at each timepoint would provide valuable information on the stability of clinical samples from anthocyanin interventions. Whilst there is evidence to suggest that the temperatures of -20°C or -80°C at which clinical samples are typically stored may protect anthocyanins and their phenolic metabolites from degradation during storage (de Ancos *et al.* 2000), due to the time and money invested in the collection of clinical samples it would surely be useful to confirm their stability during long-term storage.

The extensive list of phenolic anthocyanin metabolites quantified in the present thesis is based upon reported metabolites from recent studies (Rodriguez-Mateos *et al.* 2013, de Ferrars *et al.* 2014a, de Ferrars *et al.* 2014b), particularly those observed in a recent ¹³C-labelled C3G feeding trial (Czank *et al.* 2013). However, whilst a large number of metabolites were detected in the biological samples collected during this trial, only 43.9% of the ¹³C isotope tracer was recovered suggesting that either the labelled compound was retained within the tissues, eliminated outside the 48 hour sampling window of the study, or that there are more metabolite compounds still to be identified. Future studies should explore the formation of glutathione conjugates of anthocyanins and their phenolic metabolites. Glutathione is present at millimolar concentrations in cells with particularly high concentrations found in the liver, and has a role in the conjugation and detoxification of

xenobiotics (Arrick and Nathan 1984, Pompella *et al.* 2003). MSⁿ techniques were not used in the present thesis but could be used by future studies to identify glutathione conjugates via analysis of fragmentation patterns. Glutathione conjugates of quercetin (Galati *et al.* 2001, Hong and Mitchell 2006) and catechin (Moridani *et al.* 2001) flavonoids have been reported suggesting that conjugates of anthocyanins and their phenolic metabolites to glutathione or its constituent glutamic acid, cysteine, and glycine residues may also exist.

Along with the identification of novel metabolites, future work should also seek to improve the availability of analytical standards via synthesis of compounds not currently commercially available such as phase II sulfate and glucuronide conjugates. Greater availability of analytical standards would simplify the optimisation of methods to confirm detection and accurately quantify novel metabolites such as glutathione conjugates. Currently, many novel metabolites can only be tentatively identified based upon analysis of their fragmentation pattern using MSⁿ techniques and while synthesis of analytical standards can be an expensive and slow process, it is important for the confirmation of metabolite detection. Synthesis of stable isotopically-labelled analytical standards could also provide the opportunity to improve the accuracy and precision of analytical methods via their use as internal standards (Stokvis *et al.* 2005). Analytical standards that are structurally identical to their metabolite counterparts apart from the presence of a stable isotope label can be used as internal standards that elute at the same time as the metabolite of interest meaning they are subject to the same matrix effects resulting in greater accuracy and precision when comparing metabolite response against internal standard response to quantify metabolite concentrations (Stokvis *et al.* 2005). Due to the current unavailability of stable isotopically-labelled analytical standards, the present thesis used phloridzin and scopoletin as internal standards due to their structural similarity to the metabolites of interest. If available, and feasible due to the number of metabolites included in the method, future studies should consider the use of stable isotopically-labelled analytical standards as internal standards to minimise matrix effects and improve the accuracy and precision of the method.

The 1 h, 6 h, and 24 h timepoints used in the analysis of anthocyanin metabolite bioactivity in the present thesis were chosen as they represented peaks in total metabolite concentration observed in the previously conducted ¹³C₅-C3G trial (Czank *et al.* 2013, de Ferrars *et al.* 2014a) but anthocyanin metabolites were still detected at 48 hours following consumption. Few previous studies had collected samples beyond 24 hours as it was believed that anthocyanins were quickly eliminated within the first few hours following consumption. Now that it has been observed that anthocyanins are in fact metabolised

extensively and that these metabolites are present in the circulation for at least 48 hours following consumption, it would be useful to understand how long anthocyanin metabolites remain in circulation and how long the metabolite profile retains bioactivity. In the short term, the effect of the reported 48 h metabolite profile on IL-6 and sVCAM-1 protein expression should be explored to compare against the results obtained for the 1 h, 6 h, and 24 h profiles in the present study. In the long term, it would be informative to conduct a similar ¹³C-labelled anthocyanin feeding trial with sample collection extended beyond 48 hours, perhaps to 72 or 96 hours, to capture the full extent of anthocyanin metabolism as this is currently unknown. Characterisation of the metabolite profiles present at 48 hours and beyond and investigation of their bioactivity would inform future nutritional advice by providing data relating to how often anthocyanins should be consumed to maintain the optimal levels of bioactive metabolites within the circulation.

The present thesis investigated the effect of physiologically relevant anthocyanin metabolite profiles on levels of proinflammatory cytokines in HUVEC. The next step for this work would be to analyse the effect on mRNA levels to see if the observed effect on sVCAM-1 and IL-6 protein expression in TNF- α -stimulated HUVEC is replicated by a corresponding reduction in mRNA. No effect was observed in the present study on sVCAM-1 or IL-6 expression following CD40L stimulation so analysis of mRNA levels would also provide information on possible post-transcriptional regulation of this pathway. HUVEC were used in the present study due to their ease of use and low cost but alternative cell types such as human coronary artery endothelial cells (HCAEC) or THP-1 monocytes have also been used previously (di Gesso *et al.* 2015, Edwards *et al.* 2015) and future studies should look to replicate this analysis in these cell types to fully understand the effect of anthocyanin metabolites on vascular function. Anthocyanins have been shown to act upon a number of proinflammatory signalling pathways including MAPK (Xie *et al.* 2011, Jeong *et al.* 2013) and NF- κ B (Paixão *et al.* 2012, Lee *et al.* 2014) and the effect of anthocyanin metabolite profiles on these pathways should also be explored to elucidate the mechanism responsible for their observed bioactivity. In the future it may even be possible to monitor the real-time effect of anthocyanin metabolites on protein expression in live cells using a novel technique that pulls magnetised carbon nanotubes through cell membranes, collecting specific proteins as they pass through the cell that can be quantified without the need for cell lysis (Yang *et al.* 2014). This technique will require further development before it becomes a viable alternative to current protein analysis methods but has already been demonstrated to have no effect on cell viability or MAPK signalling pathway activity (Cai *et al.* 2007, Yang *et al.* 2014). This approach to

quantifying protein expression could enable an experiment in which vascular cells could be incubated with media containing an anthocyanin metabolite profile and the effect on proinflammatory cytokine expression over 24 hours could be monitored. This technique would negate the issue of heterogeneity between cell populations affecting results that is possible with the current approach that requires culture and treatment of multiple cell populations with lysing at various timepoints to compare levels of protein expression.

In addition to *in vitro* work, *in vivo* analysis of anthocyanin metabolite profile bioactivity could be attempted via an approach similar to that used in a recent study (Rodriguez-Mateos *et al.* 2013). Participants could be fed a 500 mg dose of cyanidin-3-glucoside with metabolite profiles established over 96 hours in addition to monitoring of vascular measures such as FMD and blood pressure, and levels of proinflammatory cytokines such as sVCAM-1 and IL-6 in circulation to investigate the bioactivity of different metabolite profiles *in vivo*. Characterisation of each participant's microbiome could also be undertaken to try and identify any microbial profiles that could be characterised as producing more or less active metabolite profiles based on the analysis of vascular biomarkers. The long-term goal of this work should be to produce an 'interactome-like' analysis of how anthocyanins, microbiota, and pro-inflammatory cytokines interact with each other to establish whether there may be a microbiotic profile that produces more active metabolites than others, and if so, whether there is a particular anthocyanin or group of anthocyanins that promote the growth of this microbiotic profile. Understanding how the relationship between anthocyanins and gut microbiota can be exploited to maximise the effect of anthocyanin consumption on cardiovascular disease may be an important area of future research in this field.

Studies investigating the metabolism of anthocyanins have observed large variation in the metabolites detected and their concentrations (Czank *et al.* 2013, de Ferrars *et al.* 2014b). Alongside genetic variations within the population leading to differences in absorption and metabolism (Minihane 2010, Wakeling and Ford 2012), differences in gut microbiota are also believed to play a role in inter-participant variability (Selma *et al.* 2009). Recent studies have suggested that changes in the microbiotic profile can affect the metabolism of anthocyanins (Sánchez-Patán *et al.* 2012, Boto-Ordóñez *et al.* 2014) whilst consumption of anthocyanins can lead to changes in microbiota populations (Queipo-Ortuño *et al.* 2012, Jiménez-Girón *et al.* 2014). Future studies should investigate this relationship with two aims: identifying microbiota profiles that produce particularly bioactive metabolites; and investigating anthocyanin consumption as a probiotic promoter of beneficial microbiota. In the long term, technological developments in mass spectrometry may enable much lower limits of

detection leading to detection of metabolites below current limits and improved accuracy and precision when quantifying metabolites in biological samples at the concentrations used in the present thesis. A recent study demonstrated the application of an advanced microarray for mass spectrometry (MAMS) technique using matrix-assisted laser desorption/ionisation-mass spectrometry (MALDI-MS) to quantify metabolite concentrations in single yeast cells and identify metabolically distinct phenotypes within the cell population (Ibáñez *et al.* 2013). To date, *in vitro* analysis of anthocyanin metabolism has been limited to cell types such as caco-2 endothelial cells that can be cultured in volumes large enough to produce detectable metabolite concentrations (Kay *et al.* 2009, Kamiloglu *et al.* 2015) or, due to the difficulty of culturing isolated colonic bacteria (Allen-Vercoe 2013), simulated gut fermentation systems that provide limited information on the metabolic variation between different bacterial species (Aura *et al.* 2005, Sánchez-Patán *et al.* 2012). Future studies may be able to combine improvements in colonic bacteria culture (Sommer 2015) with advanced mass spectrometry techniques (Ibáñez *et al.* 2013) to compare the metabolite profiles produced by different bacterial species following incubation with anthocyanins and improve our understanding of role of the gut microbiota in the positive health effects related to consumption of anthocyanins.

In conclusion, this thesis contributes to the current literature on anthocyanin metabolism by providing practical advice on metabolite stability to future clinical studies, further developing analytical methods for the detection and quantification of phenolic metabolites in biological samples, investigating potential candidates as biomarkers of anthocyanin intake, and by assessing the vascular bioactivity of novel physiologically relevant anthocyanin metabolite profiles. Additional work is required to further refine the analytical methods discussed in the present thesis and to fully elucidate the role of anthocyanin metabolites in maintaining cardiovascular health.

Glossary

ADME	Absorption, distribution, metabolism, and excretion
ANOVA	Analysis of variance
BL	Baseline
BMI	Body mass index
C3G	Cyanidin-3-glucoside
C β G	Cytosolic β -glucosidase
CD40	Cluster of differentiation 40
CD40L	Cluster of differentiation 40 ligand
C _{max}	Maximum concentration
COMT	Catechol- <i>O</i> -methyltransferase
CV	Coefficient of variation
CVD	Cardiovascular disease
Cy	Cyanidin
D&S	Dilute-and-shoot
DAD	Diode array detector
DMSO	Dimethyl sulfoxide
Dp	Delphinidin
ELISA	Enzyme-linked immunosorbent assay
eNOS	Endothelial nitric oxide synthase
ERK	Extracellular signal-regulated kinase
ESI	Electrospray ionisation
FDA	Food and Drug Administration
FGF2	Fibroblast growth factor 2
FMD	Flow-mediated dilation
GLUT	Glucose transporter
H ₂ O ₂	Hydrogen peroxide
HAEC	Human aortic endothelial cells
HCAEC	Human coronary artery endothelial cells
HILIC	Hydrophilic interaction chromatography

HPLC	High-performance liquid chromatography
HUVEC	Human umbilical vein endothelial cells
ICAM	Intercellular adhesion molecule
IFN- γ	Interferon- γ
IKK	Inhibitory- κ B kinase
IL	Interleukin
iNOS	Inducible nitric oxide synthase
JAK	Janus kinase
JNK	c-Jun N-terminal kinase
LC	Liquid chromatography
LDL	Low-density lipoprotein
LOD	Limit of detection
LPH	Lactase phloridzin hydrolase
LPS	Lipopolysaccharide
LSD	Least significant difference
MALDI	Matrix-assisted laser desorption/ionisation
MAMS	Microarray mass spectrometry
MAPK	Mitogen-activated protein kinase
MCP-1	Monocyte chemoattractant protein-1
M-CSF	Macrophage colony-stimulating factor
MKK	Mitogen-activated protein kinase kinase
mRNA	Messenger ribonucleic acid
MRM	Multiple reaction monitoring
MRP	Multidrug resistance protein
MS	Mass Spectrometry
Mv	Malvidin
m/z	Mass to charge ratio.
NADPH	Nicotinamide adenine dinucleotide phosphate
ND	Not detected
NF- κ B	Nuclear factor- κ B
NO	Nitric oxide

NOX	NADPH oxidase
O ₂ ⁻	Superoxide
ONOO ⁻	Peroxynitrite
oxLDL	Oxidised low-density lipoprotein
p38	Mitogen-activated protein kinase p38 subunit
p50	NF-κB p50 subunit
p65	NF-κB p65 subunit
PCA	Protocatechuic acid
PECAM-1	Platelet endothelial cellular adhesion molecule-1
PFP	Pentafluorophenyl
Pg	Pelargonidin
PGA	Phloroglucinaldehyde
Pn	Peonidin
PPT	Protein precipitation
Pt	Petunidin
R ²	Coefficient of determination
ROS	Reactive oxygen species
RP	Reverse-phase
R _t	Retention time
SD	Standard deviation
SGLT-1	Sodium-dependent glucose transporter-1
sMRM	Scheduled multiple reaction monitoring
SOD	Superoxide dismutase
SPE	Solid-phase extraction
STAT	Signal transducer and activator of transcription
SULT	Sulfotransferase
sVCAM-1	Soluble vascular cell adhesion molecule-1
T _{max}	Time of maximum concentration
TNF-α	Tumour necrosis factor-α
TNFR1	TNF receptor 1
TOF	Time-of-flight

TRADD	TNFR1-associated death domain protein
UDPGT	Uridine 5'-diphospho-glucuronosyltransferase
UN	United Nations
UPLC	Ultra-high performance liquid chromatography
UV	Ultraviolet
VCAM-1	Vascular cell adhesion molecule-1

Bibliography

AB SCIEX. (2011). "Scheduled MRM algorithm tutorial." from <http://sciex.com/documents/downloads/literature/scheduled-MRM-algorithm-tutorial.pdf>.

Adachi, J., C. Kumar, Y. Zhang, J. V. Olsen and M. Mann (2006). "The human urinary proteome contains more than 1500 proteins, including a large proportion of membrane proteins." Genome Biology **7**(9): R80.

Aktan, F. (2004). "iNOS-mediated nitric oxide production and its regulation." Life Sciences **75**(6): 639-653.

Allen-Vercoe, E. (2013). "Bringing the gut microbiota into focus through microbial culture: Recent progress and future perspective." Current Opinion in Microbiology **16**(5): 625-629.

Amarowicz, R., R. Carle, G. Dongowski, A. Durazzo, R. Galensa, D. Kammerer, G. Maiani and M. K. Piskula (2009). "Influence of postharvest processing and storage on the content of phenolic acids and flavonoids in foods." Molecular Nutrition & Food Research **53**(S2): S151-S183.

Amin, H. P., C. Czank, S. Raheem, Q. Zhang, N. P. Botting, A. Cassidy and C. D. Kay (2015). "Anthocyanins and their physiologically relevant metabolites alter the expression of IL-6 and VCAM-1 in CD40L and oxidized LDL challenged vascular endothelial cells." Molecular Nutrition & Food Research **59**(6): 1095-1106.

Anttonen, M. J. and R. O. Karjalainen (2005). "Environmental and genetic variation of phenolic compounds in red raspberry." Journal of Food Composition and Analysis **18**(8): 759-769.

Arrick, B. A. and C. F. Nathan (1984). "Glutathione metabolism as a determinant of therapeutic efficacy: A review." Cancer Research **44**(10): 4224-4232.

Arumugam, M., J. Raes, E. Pelletier, D. Le Paslier, T. Yamada, D. R. Mende, G. R. Fernandes, J. Tap, T. Bruls and J.-M. Batto (2011). "Enterotypes of the human gut microbiome." Nature **473**(7346): 174-180.

Aura, A. M., P. Martin-Lopez, K. A. O'Leary, G. Williamson, K. M. Oksman-Caldentey, K. Poutanen and C. Santos-Buelga (2005). "In vitro metabolism of anthocyanins by human gut microflora." European Journal of Nutrition **44**(3): 133-142.

Bakhtiar, R. and T. K. Majumdar (2007). "Tracking problems and possible solutions in the quantitative determination of small molecule drugs and metabolites in biological fluids using liquid chromatography-mass spectrometry." Journal of Pharmacological and Toxicological Methods **55**(3): 227-243.

Banerjee, S. and S. Mazumdar (2012). "Electrospray ionization mass spectrometry: A technique to access the information beyond the molecular weight of the analyte." International Journal of Analytical Chemistry **2012**.

Baud, V. and M. Karin (2001). "Signal transduction by tumor necrosis factor and its relatives." Trends in Cell Biology **11**(9): 372-377.

Beaton, G. H. (1994). "Approaches to analysis of dietary data: Relationship between planned analyses and choice of methodology." The American Journal of Clinical Nutrition **59**(1): 253S-261S.

Beaudry, F. and P. Vachon (2006). "Electrospray ionization suppression, a physical or a chemical phenomenon?" Biomedical Chromatography **20**(2): 200-205.

Bhagwat, S., D. B. Haytowitz and J. M. Holden (2011). "Usda database for the flavonoid content of selected foods, release 3.1." Beltsville: US Department of Agriculture: 03-01.

Bitsch, I., M. Janssen, M. Netzel, G. Strass and T. Frank (2004a). "Bioavailability of anthocyanidin-3-glycosides following consumption of elderberry extract and blackcurrant juice." International Journal of Clinical Pharmacology and Therapeutics **42**(5): 293-300.

Bitsch, R., M. Netzel, S. Sonntag, G. Strass, T. Frank and I. Bitsch (2004b). "Urinary excretion of cyanidin glucosides and glucuronides in healthy humans after elderberry juice ingestion." BioMed Research International **2004**(5): 343-345.

Blanco-Colio, L. M., M. Valderrama, L. A. Alvarez-Sala, C. Bustos, M. Ortego, M. A. Hernández-Presa, P. Cancelas, J. Gómez-Gerique, J. Millán and J. Egido (2000). "Red wine intake prevents nuclear factor- κ B activation in peripheral blood mononuclear cells of healthy volunteers during postprandial lipemia." Circulation **102**(9): 1020-1026.

Blankenberg, S., S. Barbaux and L. Tiret (2003). "Adhesion molecules and atherosclerosis." Atherosclerosis **170**(2): 191-203.

Boto-Ordóñez, M., M. Urpi-Sarda, M. I. Queipo-Ortuño, S. Tulipani, F. J. Tinahones and C. Andres-Lacueva (2014). "High levels of bifidobacteria are associated with increased levels of anthocyanin microbial metabolites: A randomized clinical trial." Food & Function **5**(8): 1932-1938.

Bouïs, D., G. A. Hospers, C. Meijer, G. Molema and N. H. Mulder (2001). "Endothelium in vitro: A review of human vascular endothelial cell lines for blood vessel-related research." Angiogenesis **4**(2): 91-102.

Božović, A. and V. Kulasingam (2013). "Quantitative mass spectrometry-based assay development and validation: From small molecules to proteins." Clinical Biochemistry **46**(6): 444-455.

Brasier, A. R. (2010). "The nuclear factor- κ B–interleukin-6 signalling pathway mediating vascular inflammation." Cardiovascular Research **86**(2): 211-218.

British Heart Foundation. (2015). "Cardiovascular disease statistics." from <https://www.bhf.org.uk/~media/files/research/heart-statistics/cardiovascular-disease-statistics---headline-statistics.docx>.

Bub, A., B. Watzl, D. Heeb, G. Rechkemmer and K. Briviba (2001). "Malvidin-3-glucoside bioavailability in humans after ingestion of red wine, dealcoholized red wine and red grape juice." European Journal of Nutrition **40**(3): 113-120.

Bylda, C., R. Thiele, U. Kobold and D. A. Volmer (2014). "Recent advances in sample preparation techniques to overcome difficulties encountered during quantitative analysis of small molecules from biofluids using LC-MS/MS." Analyst **139**(10): 2265-2276.

Cai, D., C. A. Doughty, T. B. Potocky, F. J. Dufort, Z. Huang, D. Blair, K. Kempa, Z. Ren and T. C. Chiles (2007). "Carbon nanotube-mediated delivery of nucleic acids does not result in non-specific activation of B lymphocytes." Nanotechnology **18**(36): 365101.

Cai, H. (2005). "Hydrogen peroxide regulation of endothelial function: Origins, mechanisms, and consequences." Cardiovascular Research **68**(1): 26-36.

Cao, G. and R. L. Prior (1999). "Anthocyanins are detected in human plasma after oral administration of an elderberry extract." Clinical Chemistry **45**(4): 574-576.

Carter, R. A. and I. P. Wicks (2001). "Vascular cell adhesion molecule 1 (CD106): A multifaceted regulator of joint inflammation." Arthritis & Rheumatism **44**(5): 985-994.

Cassidy, A., K. J. Mukamal, L. Liu, M. Franz, A. H. Eliassen and E. B. Rimm (2013). "High anthocyanin intake is associated with a reduced risk of myocardial infarction in young and middle-aged women." Circulation **127**(2): 188-196.

Cassidy, A., É. J. O'Reilly, C. Kay, L. Sampson, M. Franz, J. Forman, G. Curhan and E. B. Rimm (2011). "Habitual intake of flavonoid subclasses and incident hypertension in adults." The American Journal of Clinical Nutrition **93**(2): 338-347.

Cassidy, A., G. Rogers, J. J. Peterson, J. T. Dwyer, H. Lin and P. F. Jacques (2015). "Higher dietary anthocyanin and flavonol intakes are associated with anti-inflammatory effects in a population of US adults." The American Journal of Clinical Nutrition **102**(1): 172-181.

Castañeda-Ovando, A., M. d. L. Pacheco-Hernández, M. E. Páez-Hernández, J. A. Rodríguez and C. A. Galán-Vidal (2009). "Chemical studies of anthocyanins: A review." Food Chemistry **113**(4): 859-871.

Cech, N. B. and C. G. Enke (2001). "Practical implications of some recent studies in electrospray ionization fundamentals." Mass Spectrometry Reviews **20**(6): 362-387.

Chalker-Scott, L. (1999). "Environmental significance of anthocyanins in plant stress responses." Photochemistry and Photobiology **70**(1): 1-9.

Chang, M. S., Q. Ji, J. Zhang and T. A. El-Shourbagy (2007). "Historical review of sample preparation for chromatographic bioanalysis: Pros and cons." Drug Development Research **68**(3): 107-133.

Chao, P.-Y., Y.-P. Huang and W.-B. Hsieh (2013). "Inhibitive effect of purple sweet potato leaf extract and its components on cell adhesion and inflammatory response in human aortic endothelial cells." Cell Adhesion & Migration **7**(2): 237-245.

Charepalli, V., L. Reddivari, S. Radhakrishnan, R. Vadde, R. Agarwal and J. K. P. Vanamala (2015). "Anthocyanin-containing purple-fleshed potatoes suppress colon tumorigenesis via elimination of colon cancer stem cells." The Journal of Nutritional Biochemistry **26**(12): 1641-1649.

Chun, O. K., S. J. Chung and W. O. Song (2007). "Estimated dietary flavonoid intake and major food sources of US adults." The Journal of Nutrition **137**(5): 1244-1252.

Cooke, D. N., S. Thomasset, D. J. Boocock, M. Schwarz, P. Winterhalter, W. P. Steward, A. J. Gescher and T. H. Marczylo (2006). "Development of analyses by high-performance liquid chromatography and liquid chromatography/tandem mass spectrometry of bilberry (*Vaccinium myrtillus*) anthocyanins in human plasma and urine." Journal of Agricultural and Food Chemistry **54**(19): 7009-7013.

Crozier, A., D. Del Rio and M. N. Clifford (2010). "Bioavailability of dietary flavonoids and phenolic compounds." Molecular Aspects of Medicine **31**(6): 446-467.

Crozier, A., I. B. Jaganath and M. N. Clifford (2009). "Dietary phenolics: Chemistry, bioavailability and effects on health." Natural Product Reports **26**(8): 1001-1043.

Czank, C., A. Cassidy, Q. Zhang, D. J. Morrison, T. Preston, P. A. Kroon, N. P. Botting and C. D. Kay (2013). "Human metabolism and elimination of the anthocyanin, cyanidin-3-glucoside: A ¹³C-tracer study." The American Journal of Clinical Nutrition **97**(5): 995-1003.

Dams, R., M. A. Huestis, W. E. Lambert and C. M. Murphy (2003). "Matrix effect in bioanalysis of illicit drugs with LC-MS/MS: Influence of ionization type, sample preparation, and biofluid." Journal of the American Society for Mass Spectrometry **14**(11): 1290-1294.

Day, A. J., F. J. Cañada, J. C. Díaz, P. A. Kroon, R. McLauchlan, C. B. Faulds, G. W. Plumb, M. R. A. Morgan and G. Williamson (2000). "Dietary flavonoid and isoflavone glycosides are hydrolysed by the lactase site of lactase phlorizin hydrolase." FEBS Letters **468**(2-3): 166-170.

Day, A. J., M. S. DuPont, S. Ridley, M. Rhodes, M. J. C. Rhodes, M. R. A. Morgan and G. Williamson (1998). "Deglycosylation of flavonoid and isoflavonoid glycosides by human small intestine and liver β -glucosidase activity." FEBS Letters **436**(1): 71-75.

Day, A. J., J. M. Gee, M. S. DuPont, I. T. Johnson and G. Williamson (2003). "Absorption of quercetin-3-glucoside and quercetin-4'-glucoside in the rat small intestine: The role of lactase phlorizin hydrolase and the sodium-dependent glucose transporter." Biochemical Pharmacology **65**(7): 1199-1206.

de Ancos, B., E. Ibanez, G. Reglero and M. P. Cano (2000). "Frozen storage effects on anthocyanins and volatile compounds of raspberry fruit." Journal of Agricultural and Food Chemistry **48**(3): 873-879.

de Ferrars, R., C. Czank, Q. Zhang, N. Botting, P. Kroon, A. Cassidy and C. Kay (2014a). "The pharmacokinetics of anthocyanins and their metabolites in humans." British Journal of Pharmacology **171**(13): 3268-3282.

de Ferrars, R. M., A. Cassidy, P. Curtis and C. D. Kay (2014b). "Phenolic metabolites of anthocyanins following a dietary intervention study in post-menopausal women." Molecular Nutrition & Food Research **58**(3): 490-502.

de Ferrars, R. M., C. Czank, S. Saha, P. W. Needs, Q. Zhang, K. S. Raheem, N. P. Botting, P. A. Kroon and C. D. Kay (2014c). "Methods for isolating, identifying, and quantifying anthocyanin metabolites in clinical samples." Analytical Chemistry **86**(20): 10052-10058.

de Pascual-Teresa, S., D. A. Moreno and C. García-Viguera (2010). "Flavanols and anthocyanins in cardiovascular health: A review of current evidence." International Journal of Molecular Sciences **11**(4): 1679-1703.

de Rijke, E., H. Zappey, F. Ariese, C. Gooijer and U. A. T. Brinkman (2003). "Liquid chromatography with atmospheric pressure chemical ionization and electrospray ionization mass spectrometry of flavonoids with triple-quadrupole and ion-trap instruments." Journal of Chromatography A **984**(1): 45-58.

de Roos, B. (2013). "Personalised nutrition: Ready for practice?" Proceedings of the Nutrition Society **72**(01): 48-52.

Dearden, J. and W. Forbes (1959). "Light absorption studies: Part xiv. The ultraviolet absorption spectra of phenols." Canadian Journal of Chemistry **37**(8): 1294-1304.

Déchanet, J., C. Grosset, J. L. Taupin, P. Merville, J. Banchereau, J. Ripoche and J. F. Moreau (1997). "CD40 ligand stimulates proinflammatory cytokine production by human endothelial cells." The Journal of Immunology **159**(11): 5640-5647.

Deineka, V., I. Saenko, L. Deineka and I. Blinova (2016). "Hydrophilic interaction chromatography as an alternative to reversed-phase HPLC in determining anthocyanins and betacyanins." Journal of Analytical Chemistry **71**(3): 297-301.

Del Rio, D., G. Borges and A. Crozier (2010a). "Berry flavonoids and phenolics: Bioavailability and evidence of protective effects." British Journal of Nutrition **104** Suppl 3: S67-90.

Del Rio, D., L. Calani, F. Scazzina, L. Jechiu, C. Cordero and F. Brighenti (2010b). "Bioavailability of catechins from ready-to-drink tea." Nutrition **26**(5): 528-533.

di Gesso, J. L., J. S. Kerr, Q. Zhang, S. Raheem, S. K. Yalamanchili, D. O'Hagan, C. D. Kay and M. A. O'Connell (2015). "Flavonoid metabolites reduce tumor necrosis factor- α secretion to a greater extent than their precursor compounds in human THP-1 monocytes." Molecular Nutrition & Food Research **59**(6): 1143-1154.

Dohadwala, M. M., M. Holbrook, N. M. Hamburg, S. M. Shenouda, W. B. Chung, M. Titas, M. A. Kluge, N. Wang, J. Palmisano, P. E. Milbury, J. B. Blumberg and J. A. Vita (2011). "Effects of cranberry juice consumption on vascular function in patients with coronary artery disease." The American Journal of Clinical Nutrition **93**(5): 934-940.

Dumont, O., H. Mylroie, A. Sperone, A. Bauer, S. Hamdulay, N. Ali, J. Boyle, A. Samarel, D. Haskard and A. Randi (2012). "Protein kinase C ϵ activity induces anti-inflammatory and anti-apoptotic genes via an ERK1/2 and NF- κ B-dependent pathway to enhance vascular protection." Biochemical Journal **447**: 193-204.

Edmands, W. M., P. Ferrari, J. A. Rothwell, S. Rinaldi, N. Slimani, D. K. Barupal, C. Biessy, M. Jenab, F. Clavel-Chapelon, G. Fagherazzi, M.-C. Boutron-Ruault, V. A. Katzke, T. Kühn, H. Boeing, A. Trichopoulou, P. Lagiou, D. Trichopoulos, D. Palli, S. Grioni, R. Tumino, P. Vineis, A. Mattiello, I. Romieu and A. Scalbert (2015). "Polyphenol metabolome in human urine and its association with intake of polyphenol-rich foods across European countries." The American Journal of Clinical Nutrition **102**(4): 905-913.

Edwards, M., C. Czank, G. M. Woodward, A. Cassidy and C. D. Kay (2015). "Phenolic metabolites of anthocyanins modulate mechanisms of endothelial function." Journal of Agricultural and Food Chemistry **63**(9): 2423-2431.

Epstein, F. H. and R. Ross (1999). "Atherosclerosis—an inflammatory disease." New England Journal of Medicine **340**(2): 115-126.

Erlund, I., R. Koli, G. Alfthan, J. Marniemi, P. Puukka, P. Mustonen, P. Mattila and A. Jula (2008). "Favorable effects of berry consumption on platelet function, blood pressure, and HDL cholesterol." The American Journal of Clinical Nutrition **87**(2): 323-331.

Fang, J. (2014). "Some anthocyanins could be efficiently absorbed across the gastrointestinal mucosa: Extensive presystemic metabolism reduces apparent bioavailability." Journal of Agricultural and Food Chemistry **62**(18): 3904-3911.

Feild, T. S., D. W. Lee and N. M. Holbrook (2001). "Why leaves turn red in autumn. The role of anthocyanins in senescing leaves of red-osier dogwood." Plant Physiology **127**(2): 566-574.

Felgines, C., S. Talavéra, M.-P. Gonthier, O. Texier, A. Scalbert, J.-L. Lamaison and C. Rémésy (2003). "Strawberry anthocyanins are recovered in urine as glucuro- and sulfoconjugates in humans." The Journal of Nutrition **133**(5): 1296-1301.

Felgines, C., S. Talavera, O. Texier, A. Gil-Izquierdo, J.-L. Lamaison and C. Remesy (2005). "Blackberry anthocyanins are mainly recovered from urine as methylated and glucuronidated conjugates in humans." Journal of Agricultural and Food Chemistry **53**(20): 7721-7727.

Fernandes, I., J. Azevedo, A. Faria, C. a. o. Calhau, V. de Freitas and N. Mateus (2009). "Enzymatic hemisynthesis of metabolites and conjugates of anthocyanins." Journal of Agricultural and Food Chemistry **57**(2): 735-745.

Fernandes, I., V. de Freitas, C. Reis and N. Mateus (2012). "A new approach on the gastric absorption of anthocyanins." Food & Function **3**(5): 508-516.

Fernandes, I., A. Faria, V. de Freitas, C. Calhau and N. Mateus (2015). "Multiple-approach studies to assess anthocyanin bioavailability." Phytochemistry Reviews **14**(6): 899-919.

Fernández-Peralbo, M. A. and M. D. Luque de Castro (2012). "Preparation of urine samples prior to targeted or untargeted metabolomics mass-spectrometry analysis." Trends in Analytical Chemistry **41**: 75-85.

Fitzgerald, R. L., T. L. Griffin, Y.-M. Yun, R. A. Godfrey, R. West, A. J. Pesce and D. A. Herold (2012). "Dilute and shoot: Analysis of drugs of abuse using selected reaction monitoring for quantification and full scan product ion spectra for identification." Journal of Analytical Toxicology **36**(2): 106-111.

Fleschhut, J., F. Kratzer, G. Rechkemmer and S. E. Kulling (2006). "Stability and biotransformation of various dietary anthocyanins in vitro." European Journal of Nutrition **45**(1): 7-18.

Food and Drug Administration (2001). "Guidance for industry: Bioanalytical method validation."

Food and Drug Administration (2003). "Guidance for industry: Stability testing of new drug substances and products."

Forester, S. C. and A. L. Waterhouse (2008). "Identification of cabernet sauvignon anthocyanin gut microflora metabolites." Journal of Agricultural and Food Chemistry **56**(19): 9299-9304.

Fossen, T., R. Slimestad and Ø. M. Andersen (2003). "Anthocyanins with 4'-glucosidation from red onion, *Allium cepa*." Phytochemistry **64**(8): 1367-1374.

Frank, T., M. Janßen, M. Netzel, G. Straß, A. Kler, E. Kriesl and I. Bitsch (2005). "Pharmacokinetics of anthocyanidin-3-glycosides following consumption of *Hibiscus sabdariffa* L. Extract." The Journal of Clinical Pharmacology **45**(2): 203-210.

Frank, T., M. Netzel, G. Strass, R. Bitsch and I. Bitsch (2003). "Bioavailability of anthocyanidin-3-glucosides following consumption of red wine and red grape juice." Canadian Journal of Physiology and Pharmacology **81**(5): 423-435.

Galati, G., M. Y. Moridani, T. S. Chan and P. J. O'Brien (2001). "Peroxidative metabolism of apigenin and naringenin versus luteolin and quercetin: Glutathione oxidation and conjugation." Free Radical Biology and Medicine **30**(4): 370-382.

Gerritsen, M. E., W. W. Carley, G. E. Ranges, C.-P. Shen, S. A. Phan, G. F. Ligon and C. A. Perry (1995). "Flavonoids inhibit cytokine-induced endothelial cell adhesion protein gene expression." The American Journal of Pathology **147**(2): 278.

Gibney, M. J., M. Walsh, L. Brennan, H. M. Roche, B. German and B. van Ommen (2005). "Metabolomics in human nutrition: Opportunities and challenges." The American Journal of Clinical Nutrition **82**(3): 497-503.

Giordano, L., W. Coletta, P. Rapisarda, M. B. Donati and D. Rotilio (2007). "Development and validation of an LC-MS/MS analysis for simultaneous determination of delphinidin-3-glucoside, cyanidin-3-glucoside and cyanidin-3-(6-malonylglucoside) in human plasma and urine after blood orange juice administration." Journal of Separation Science **30**(18): 3127-3136.

Gould, K. S. (2004). "Nature's swiss army knife: The diverse protective roles of anthocyanins in leaves." Journal of Biomedicine and Biotechnology **2004**(5): 314-320.

Grace, P. B., N. S. Mistry, M. H. Carter, A. J. C. Leathem and P. Teale (2007). "High throughput quantification of phytoestrogens in human urine and serum using liquid chromatography/tandem mass spectrometry (LC-MS/MS)." Journal of Chromatography B **853**(1-2): 138-146.

Graham, A., N. Hogg, B. Kalyanaraman, V. O'Leary, V. Darley-Usmar and S. Moncada (1993). "Peroxynitrite modification of low-density lipoprotein leads to recognition by the macrophage scavenger receptor." FEBS Letters **330**(2): 181-185.

Granger, D. N., T. Vowinkel and T. Petnehazy (2004). "Modulation of the inflammatory response in cardiovascular disease." Hypertension **43**(5): 924-931.

Guerrero, L., M. Margalef, Z. Pons, M. Quiñones, L. Arola, A. Arola-Arnal and B. Muguerza (2013). "Serum metabolites of proanthocyanidin-administered rats decrease lipid synthesis in HepG2 cells." The Journal of Nutritional Biochemistry **24**(12): 2092-2099.

Gustavsson, E., M. Andersson, N. Stephanson and O. Beck (2007). "Validation of direct injection electrospray LC-MS/MS for confirmation of opiates in urine drug testing." Journal of Mass Spectrometry **42**(7): 881-889.

Hager, A., L. Howard, R. Prior and C. Brownmiller (2008). "Processing and storage effects on monomeric anthocyanins, percent polymeric color, and antioxidant capacity of processed black raspberry products." Journal of Food Science **73**(6): H134-H140.

Hansson, G. K. (2005). "Inflammation, atherosclerosis, and coronary artery disease." New England Journal of Medicine **352**(16): 1685-1695.

Harborne, J. (1958). "Spectral methods of characterizing anthocyanins." Biochemical Journal **70**(1): 22.

Harborne, J. B. and C. A. Williams (2000). "Advances in flavonoid research since 1992." Phytochemistry **55**(6): 481-504.

Hayden, M. S. and S. Ghosh (2014). "Regulation of NF- κ B by TNF family cytokines." Seminars in Immunology **26**(3): 253-266.

Hedrick, V., A. Dietrich, P. Estabrooks, J. Savla, E. Serrano and B. Davy (2012). "Dietary biomarkers: Advances, limitations and future directions." Nutrition Journal **11**(1): 109.

Hemström, P. and K. Irgum (2006). "Hydrophilic interaction chromatography." Journal of Separation Science **29**(12): 1784-1821.

Henriksen, T., R. K. Juhler, B. Svensmark and N. B. Cech (2005). "The relative influences of acidity and polarity on responsiveness of small organic molecules to analysis with negative ion electrospray ionization mass spectrometry (ESI-MS)." Journal of the American Society for Mass Spectrometry **16**(4): 446-455.

Hertog, M. G., E. J. Feskens, P. C. Hollman, M. B. Katan and D. Kromhout (1994). "Dietary flavonoids and cancer risk in the Zutphen Elderly Study." Nutrition and Cancer **22**(2): 175-184.

Hertog, M. G., E. J. Feskens, D. Kromhout, P. Hollman and M. Katan (1993). "Dietary antioxidant flavonoids and risk of coronary heart disease: The Zutphen Elderly Study." The Lancet **342**(8878): 1007-1011.

Hidalgo, M., S. Martin-Santamaria, I. Recio, C. Sanchez-Moreno, B. de Pascual-Teresa, G. Rimbach and S. de Pascual-Teresa (2012). "Potential anti-inflammatory, anti-adhesive, anti/estrogenic, and angiotensin-converting enzyme inhibitory activities of anthocyanins and their gut metabolites." Genes & Nutrition **7**(2): 295-306.

Hodgson, J. M., S. Yee Chan, I. B. Puddey, A. Devine, N. Wattanapenpaiboon, M. L. Wahlqvist, W. Lukito, V. Burke, N. C. Ward, R. L. Prince and K. D. Croft (2004). "Phenolic acid metabolites as biomarkers for tea- and coffee-derived polyphenol exposure in human subjects." British Journal of Nutrition **91**(02): 301-305.

Hollman, P. C. H., M. G. L. Hertog and M. B. Katan (1996). "Analysis and health effects of flavonoids." Food Chemistry **57**(1): 43-46.

Hong, V. and R. E. Wrolstad (1990). "Use of HPLC separation/photodiode array detection for characterization of anthocyanins." Journal of Agricultural and Food Chemistry **38**(3): 708-715.

Hong, Y.-J. and A. E. Mitchell (2006). "Identification of glutathione-related quercetin metabolites in humans." Chemical Research in Toxicology **19**(11): 1525-1532.

Hooper, L., P. A. Kroon, E. B. Rimm, J. S. Cohn, I. Harvey, K. A. Le Cornu, J. J. Ryder, W. L. Hall and A. Cassidy (2008). "Flavonoids, flavonoid-rich foods, and cardiovascular risk: A meta-analysis of randomized controlled trials." The American Journal of Clinical Nutrition **88**(1): 38-50.

Hua, Y. and D. Jenke (2012). "Increasing the sensitivity of an LC–MS method for screening material extracts for organic extractables via mobile phase optimization." Journal of Chromatographic Science **50**(3): 213-227.

Huang, H., G. Chen, D. Liao, Y. Zhu and X. Xue (2016). "Effects of berries consumption on cardiovascular risk factors: A meta-analysis with trial sequential analysis of randomized controlled trials." Scientific Reports **6**(23625).

Huang, W.-Y., J. Wang, Y.-M. Liu, Q.-S. Zheng and C.-Y. Li (2014). "Inhibitory effect of malvidin on TNF- α -induced inflammatory response in endothelial cells." European Journal of Pharmacology **723**(0): 67-72.

Hughes, L. A., I. C. Arts, T. Ambergen, H. A. Brants, P. C. Dagnelie, R. A. Goldbohm, P. A. van den Brandt and M. P. Weijenberg (2008). "Higher dietary flavone, flavonol, and catechin intakes are associated with less of an increase in BMI over time in women: A longitudinal analysis from the Netherlands Cohort Study." The American Journal of Clinical Nutrition **88**(5): 1341-1352.

Hui, C., X. Qi, Z. Qianrong, P. Xiaoli, Z. Jundong and M. Mantian (2013). "Flavonoids, flavonoid subclasses and breast cancer risk: A meta-analysis of epidemiologic studies." PLOS ONE **8**(1): e54318.

Ibáñez, A. J., S. R. Fagerer, A. M. Schmidt, P. L. Urban, K. Jefimovs, P. Geiger, R. Dechant, M. Heinemann and R. Zenobi (2013). "Mass spectrometry-based metabolomics of single yeast cells." Proceedings of the National Academy of Sciences **110**(22): 8790-8794.

Impey, G. A. B. M. S. (2005). "Method transfer: Extending compatibility in a multiple instrument laboratory." from http://www3.appliedbiosystems.com/cms/groups/psm_marketing/documents/generaldocuments/cms_041961.pdf.

Ito, H., M.-P. Gonthier, C. Manach, C. Morand, L. Mennen, C. Rémésy and A. Scalbert (2005). "Polyphenol levels in human urine after intake of six different polyphenol-rich beverages." British Journal of Nutrition **94**(04): 500-509.

Jandera, P. (2011). "Stationary and mobile phases in hydrophilic interaction chromatography: A review." Analytica Chimica Acta **692**(1–2): 1-25.

Jenab, M., N. Slimani, M. Bictash, P. Ferrari and S. A. Bingham (2009). "Biomarkers in nutritional epidemiology: Applications, needs and new horizons." Human Genetics **125**(5-6): 507-525.

Jennings, A., A. A. Welch, S. J. Fairweather-Tait, C. Kay, A.-M. Minihane, P. Chowienczyk, B. Jiang, M. Cecelja, T. Spector, A. Macgregor and A. Cassidy (2012). "Higher anthocyanin intake is associated with lower arterial stiffness and central blood pressure in women." The American Journal of Clinical Nutrition **96**(4): 781-788.

Jeong, J.-W., W. Lee, S. Shin, G.-Y. Kim, B. Choi and Y. Choi (2013). "Anthocyanins downregulate lipopolysaccharide-induced inflammatory responses in BV2 microglial cells by suppressing the NF- κ B and Akt/MAPKs signaling pathways." International Journal of Molecular Sciences **14**(1): 1502-1515.

Jia, Z., P. V. A. Babu, H. Si, P. Nallasamy, H. Zhu, W. Zhen, H. P. Misra, Y. Li and D. Liu (2013). "Genistein inhibits TNF- α -induced endothelial inflammation through the protein kinase pathway A and improves vascular inflammation in C57BL/6 mice." International Journal of Cardiology **168**(3): 2637-2645.

Jian, W., R. W. Edom, Y. Xu and N. Weng (2010). "Recent advances in application of hydrophilic interaction chromatography for quantitative bioanalysis." Journal of Separation Science **33**(6-7): 681-697.

Jiménez-Girón, A., I. Muñoz-González, P. J. Martín-Álvarez, M. V. Moreno-Arribas and B. Bartolomé (2014). "Towards the fecal metabolome derived from moderate red wine intake." Metabolites **4**(4): 1101-1118.

Jurd, L. (1963). "Anthocyanins and related compounds. I. Structural transformations of flavylum salts in acidic solutions." The Journal of Organic Chemistry **28**(4): 987-991.

Kalili, K. M. and A. de Villiers (2011). "Recent developments in the HPLC separation of phenolic compounds." Journal of Separation Science **34**(8): 854-876.

Kalt, W., Y. Liu, J. E. McDonald, M. Vinqvist-Tymchuk and S. A. E. Fillmore (2014). "Anthocyanin metabolites are abundant and persistent in human urine." Journal of Agricultural and Food Chemistry **62**(18): 3926-3934.

Kamiloglu, S., E. Capanoglu, C. Grootaert and J. Van Camp (2015). "Anthocyanin absorption and metabolism by human intestinal Caco-2 cells—a review." International Journal of Molecular Sciences **16**(9): 21555-21574.

Karlsen, A., L. Retterstøl, P. Laake, I. Paur, S. Kjølrsrud-Bøhn, L. Sandvik and R. Blomhoff (2007). "Anthocyanins inhibit nuclear factor- κ B activation in monocytes and reduce plasma concentrations of pro-inflammatory mediators in healthy adults." The Journal of Nutrition **137**(8): 1951-1954.

Karmann, K., C. Hughes, J. Schechner, W. C. Fanslow and J. S. Pober (1995). "CD40 on human endothelial cells: Inducibility by cytokines and functional regulation of adhesion molecule expression." Proceedings of the National Academy of Sciences **92**(10): 4342-4346.

Kay, C. D. (2006). "Aspects of anthocyanin absorption, metabolism and pharmacokinetics in humans." Nutrition Research Reviews **19**(1): 137-146.

Kay, C. D., L. Hooper, P. A. Kroon, E. B. Rimm and A. Cassidy (2012). "Relative impact of flavonoid composition, dose and structure on vascular function: A systematic review of randomised controlled trials of flavonoid-rich food products." Molecular Nutrition & Food Research **56**(11): 1605-1616.

Kay, C. D., P. A. Kroon and A. Cassidy (2009). "The bioactivity of dietary anthocyanins is likely to be mediated by their degradation products." Molecular Nutrition & Food Research **53**(S1): S92-S101.

Kay, C. D., G. Mazza and B. J. Holub (2005). "Anthocyanins exist in the circulation primarily as metabolites in adult men." The Journal of Nutrition **135**(11): 2582-2588.

Kay, C. D., G. Mazza, B. J. Holub and J. Wang (2004). "Anthocyanin metabolites in human urine and serum." British Journal of Nutrition **91**(06): 933-942.

Kent, K., K. Charlton, S. Roodenrys, M. Batterham, J. Potter, V. Traynor, H. Gilbert, O. Morgan and R. Richards (2015). "Consumption of anthocyanin-rich cherry juice for 12 weeks improves memory and cognition in older adults with mild-to-moderate dementia." European Journal of Nutrition: 1-9.

Keppler, K. and H.-U. Humpf (2005). "Metabolism of anthocyanins and their phenolic degradation products by the intestinal microflora." Bioorganic & Medicinal Chemistry **13**(17): 5195-5205.

Khymenets, O., C. Andres-Lacueva, M. Urpi-Sarda, R. Vazquez-Fresno, M. M. Mart, G. Reglero, M. Torres and R. Llorach (2015). "Metabolic fingerprint after acute and under sustained consumption of a functional beverage based on grape skin extract in healthy human subjects." Food & Function **6**(4): 1288-1298.

Kim, M.-C., S.-J. Kim, D.-S. Kim, Y.-D. Jeon, S. J. Park, H. S. Lee, J.-Y. Um and S.-H. Hong (2011). "Vanillic acid inhibits inflammatory mediators by suppressing NF- κ B in lipopolysaccharide-stimulated mouse peritoneal macrophages." Immunopharmacology and Immunotoxicology **33**(3): 525-532.

Kong, J.-M., L.-S. Chia, N.-K. Goh, T.-F. Chia and R. Brouillard (2003). "Analysis and biological activities of anthocyanins." Phytochemistry **64**(5): 923-933.

Krga, I., L.-E. Monfoulet, A. Konic-Ristic, S. Mercier, M. Glibetic, C. Morand and D. Milenkovic (2016). "Anthocyanins and their gut metabolites reduce the adhesion of monocyte to TNF α -activated endothelial cells at physiologically relevant concentrations." Archives of Biochemistry and Biophysics **599**: 51-59.

Krogholm, K. (2011). Flavonoids as fruit and vegetable intake biomarkers - development, validation and application of flavonoid biomarkers in nutritional research, University of Copenhagen & Technical University of Denmark.

Kropat, C., D. Mueller, U. Boettler, K. Zimmermann, E. H. Heiss, V. M. Dirsch, D. Rogoll, R. Melcher, E. Richling and D. Marko (2013). "Modulation of Nrf2-dependent gene transcription by bilberry anthocyanins in vivo." Molecular Nutrition & Food Research **57**(3): 545-550.

Kuhnle, G. G. C. (2012). "Nutritional biomarkers for objective dietary assessment." Journal of the Science of Food and Agriculture **92**(6): 1145-1149.

Kuntz, S., H. Asseburg, S. Dold, A. Römpf, B. Fröhling, C. Kunz and S. Rudloff (2015a). "Inhibition of low-grade inflammation by anthocyanins from grape extract in an in vitro epithelial-endothelial co-culture model." Food & Function **6**(4): 1136-1149.

Kuntz, S., S. Rudloff, H. Asseburg, C. Borsch, B. Fröhling, F. Unger, S. Dold, B. Spengler, A. Römpf and C. Kunz (2015b). "Uptake and bioavailability of anthocyanins and phenolic acids from grape/blueberry juice and smoothie in vitro and in vivo." British Journal of Nutrition **113**(07): 1044-1055.

Lambert, N., P. A. Kroon, C. B. Faulds, G. W. Plumb, W. R. McLauchlan, A. J. Day and G. Williamson (1999). "Purification of cytosolic β -glucosidase from pig liver and its reactivity towards flavonoid glycosides." Biochimica et Biophysica Acta **1435**(1-2): 110-116.

Lamport, D. J., L. Dye, J. D. Wightman and C. L. Lawton (2012). "The effects of flavonoid and other polyphenol consumption on cognitive performance: A systematic research review of human experimental and epidemiological studies." Nutrition and Aging **1**(1): 5-25.

Lee, C.-C., S.-H. Huang, Y.-T. Yang, Y.-W. Cheng, C.-H. Li and J.-J. Kang (2012). "Motorcycle exhaust particles up-regulate expression of vascular adhesion molecule-1 and intercellular adhesion molecule-1 in human umbilical vein endothelial cells." Toxicology in Vitro **26**(4): 552-560.

Lee, S. G., B. Kim, Y. Yang, T. X. Pham, Y.-K. Park, J. Manatou, S. I. Koo, O. K. Chun and J.-Y. Lee (2014). "Berry anthocyanins suppress the expression and secretion of proinflammatory mediators in macrophages by inhibiting nuclear translocation of NF- κ B independent of nrf2-mediated mechanism." The Journal of Nutritional Biochemistry **25**(4): 404-411.

Li, G., Y. Zhu, Y. Zhang, J. Lang, Y. Chen and W. Ling (2013). "Estimated daily flavonoid and stilbene intake from fruits, vegetables, and nuts and associations with lipid profiles in Chinese adults." Journal of the Academy of Nutrition and Dietetics **113**(6): 786-794.

Libby, P., P. M. Ridker and A. Maseri (2002). "Inflammation and atherosclerosis." Circulation **105**(9): 1135-1143.

Lin, H. H., J. H. Chen, C. C. Huang and C. J. Wang (2007). "Apoptotic effect of 3, 4-dihydroxybenzoic acid on human gastric carcinoma cells involving JNK/p38 MAPK signaling activation." International Journal of Cancer **120**(11): 2306-2316.

Loke, W. M., A. M. Jenner, J. M. Proudfoot, A. J. McKinley, J. M. Hodgson, B. Halliwell and K. D. Croft (2009). "A metabolite profiling approach to identify biomarkers of flavonoid intake in humans." The Journal of Nutrition **139**(12): 2309-2314.

Louise, C. B. and T. G. Obrig (1991). "Shiga toxin-associated hemolytic-uremic syndrome: Combined cytotoxic effects of shiga toxin, interleukin-1 beta, and tumor necrosis factor alpha on human vascular endothelial cells in vitro." Infection and Immunity **59**(11): 4173-4179.

Maaser, C., S. Schoeppner, T. Kucharzik, M. Kraft, E. Schoenherr, W. Domschke and N. Luegering (2001). "Colonic epithelial cells induce endothelial cell expression of ICAM-1 and VCAM-1 by a NF- κ B-dependent mechanism." Clinical & Experimental Immunology **124**(2): 208-213.

Mäkilä, L., O. A. Laaksonen, A.-L. M. Alanne, M. K. Kortenesniemi, H. P. Kallio and B. Yang (2016). "Stability of hydroxycinnamic acid derivatives, flavonol glycosides and anthocyanins in black currant juice." Journal of Agricultural and Food Chemistry.

Mallet, C. R., Z. Lu and J. R. Mazzeo (2004). "A study of ion suppression effects in electrospray ionization from mobile phase additives and solid-phase extracts." Rapid Communications in Mass Spectrometry **18**(1): 49-58.

Manach, C., A. Scalbert, C. Morand, C. Rémésy and L. Jiménez (2004). "Polyphenols: Food sources and bioavailability." The American Journal of Clinical Nutrition **79**(5): 727-747.

Manach, C., G. Williamson, C. Morand, A. Scalbert and C. Rémésy (2005). "Bioavailability and bioefficacy of polyphenols in humans. I. Review of 97 bioavailability studies." The American Journal of Clinical Nutrition **81**(1): 230S-242S.

Matheny, H. E., T. L. Deem and J. M. Cook-Mills (2000). "Lymphocyte migration through monolayers of endothelial cell lines involves VCAM-1 signaling via endothelial cell NADPH oxidase." The Journal of Immunology **164**(12): 6550-6559.

Matuszewski, B. K., M. L. Constanzer and C. M. Chavez-Eng (2003). "Strategies for the assessment of matrix effect in quantitative bioanalytical methods based on HPLC-MS/MS." Analytical Chemistry **75**(13): 3019-3030.

Mauray, A., C. Felgines, C. Morand, A. Mazur, A. Scalbert and D. Milenkovic (2012). "Bilberry anthocyanin-rich extract alters expression of genes related to atherosclerosis development in aorta of apo E-deficient mice." Nutrition, Metabolism and Cardiovascular Diseases **22**(1): 72-80.

Mazza, G., C. D. Kay, T. Cottrell and B. J. Holub (2002). "Absorption of anthocyanins from blueberries and serum antioxidant status in human subjects." Journal of Agricultural and Food Chemistry **50**(26): 7731-7737.

McCullough, M. L., J. J. Peterson, R. Patel, P. F. Jacques, R. Shah and J. T. Dwyer (2012). "Flavonoid intake and cardiovascular disease mortality in a prospective cohort of US adults." The American Journal of Clinical Nutrition **95**(2): 454-464.

McGhie, T. K., G. D. Ainge, L. E. Barnett, J. M. Cooney and D. J. Jensen (2003). "Anthocyanin glycosides from berry fruit are absorbed and excreted unmetabolized by both humans and rats." Journal of Agricultural and Food Chemistry **51**(16): 4539-4548.

McGhie, T. K. and M. C. Walton (2007). "The bioavailability and absorption of anthocyanins: Towards a better understanding." Molecular Nutrition & Food Research **51**(6): 702-713.

McKay, D. L., C.-Y. O. Chen, C. A. Zampariello and J. B. Blumberg (2015). "Flavonoids and phenolic acids from cranberry juice are bioavailable and bioactive in healthy older adults." Food Chemistry **168**: 233-240.

Merken, H. M. and G. R. Beecher (2000). "Measurement of food flavonoids by high-performance liquid chromatography: A review." Journal of Agricultural and Food Chemistry **48**(3): 577-599.

Milbury, P. E., G. Cao, R. L. Prior and J. Blumberg (2002). "Bioavailability of elderberry anthocyanins." Mechanisms of Ageing and Development **123**(8): 997-1006.

Milbury, P. E., J. A. Vita and J. B. Blumberg (2010). "Anthocyanins are bioavailable in humans following an acute dose of cranberry juice." The Journal of Nutrition **140**(6): 1099-1104.

Milenkovic, D., B. Jude and C. Morand (2013). "miRNA as molecular target of polyphenols underlying their biological effects." Free Radical Biology and Medicine **64**: 40-51.

Minihane, A. M. (2010). "Fatty acid–genotype interactions and cardiovascular risk." Prostaglandins, Leukotrienes and Essential Fatty Acids **82**(4): 259-264.

Mink, P. J., C. G. Scrafford, L. M. Barraj, L. Harnack, C.-P. Hong, J. A. Nettleton and D. R. Jacobs (2007). "Flavonoid intake and cardiovascular disease mortality: A prospective study in postmenopausal women." The American Journal of Clinical Nutrition **85**(3): 895-909.

Miyazaki, K., K. Makino, E. Iwadate, Y. Deguchi and F. Ishikawa (2008). "Anthocyanins from purple sweet potato Ipomoea batatas cultivar Ayamurasaki suppress the development of atherosclerotic lesions and both enhancements of oxidative stress and soluble vascular cell adhesion molecule-1 in apolipoprotein E-deficient mice." Journal of Agricultural and Food Chemistry **56**(23): 11485-11492.

Moridani, M. Y., H. Scobie, P. Salehi and P. J. O'Brien (2001). "Catechin metabolism: Glutathione conjugate formation catalyzed by tyrosinase, peroxidase, and cytochrome p450." Chemical Research in Toxicology **14**(7): 841-848.

Morrison, D. J., B. Dodson, C. Slater and T. Preston (2000). "¹³C natural abundance in the British diet: Implications for ¹³C breath tests." Rapid Communications in Mass Spectrometry **14**(15): 1321-1324.

Mülleder, U., M. Murkovic and W. Pfannhauser (2002). "Urinary excretion of cyanidin glycosides." Journal of Biochemical and Biophysical Methods **53**(1–3): 61-66.

Mullen, W., C. A. Edwards, M. Serafini and A. Crozier (2008). "Bioavailability of pelargonidin-3-O-glucoside and its metabolites in humans following the ingestion of strawberries with and without cream." Journal of Agricultural and Food Chemistry **56**(3): 713-719.

Nakamura, Y., H. Matsumoto, M. Morifuji, H. Iida and Y. Takeuchi (2009). "Development and validation of a liquid chromatography tandem mass spectrometry method for simultaneous determination of four anthocyanins in human plasma after black currant anthocyanins ingestion." Journal of Agricultural and Food Chemistry **58**(2): 1174-1179.

Németh, K., G. W. Plumb, J.-G. Berrin, N. Juge, R. Jacob, H. Y. Naim, G. Williamson, D. M. Swallow and P. A. Kroon (2003). "Deglycosylation by small intestinal epithelial cell β -glucosidases is a critical step in the absorption and metabolism of dietary flavonoid glycosides in humans." European Journal of Nutrition **42**(1): 29-42.

Neveu, V., J. Perez-Jiménez, F. Vos, V. Crespy, L. du Chaffaut, L. Mennen, C. Knox, R. Eisner, J. Cruz, D. Wishart and A. Scalbert (2010). "Phenol-explorer: An online comprehensive database on polyphenol contents in foods. Database, doi: 10.1093/database/bap024 (version 1.5.2, available at <http://www.phenol-explorer.eu>)." Database **2010**.

Nguyen, H. P. and K. A. Schug (2008). "The advantages of ESI-MS detection in conjunction with HILIC mode separations: Fundamentals and applications." Journal of Separation Science **31**(9): 1465-1480.

Nielsen, I. L. F., L. O. Dragsted, G. Ravn-Haren, R. Freese and S. E. Rasmussen (2003). "Absorption and excretion of black currant anthocyanins in humans and watanabe heritable hyperlipidemic rabbits." Journal of Agricultural and Food Chemistry **51**(9): 2813-2820.

Nielsen, S. E., R. Freese, P. Kleemola and M. Mutanen (2002). "Flavonoids in human urine as biomarkers for intake of fruits and vegetables." Cancer Epidemiology Biomarkers & Prevention **11**(5): 459-466.

Nurmi, T., J. Mursu, M. Heinonen, A. Nurmi, R. Hiltunen and S. Voutilainen (2009). "Metabolism of berry anthocyanins to phenolic acids in humans." Journal of Agricultural and Food Chemistry **57**(6): 2274-2281.

Oak, M. H., J. Bedoui, S. F. Madeira, K. Chalupsky and V. Schini-Kerth (2006). "Delphinidin and cyanidin inhibit PDGFAB-induced VEGF release in vascular smooth muscle cells by preventing activation of p38 MAPK and JNK." British Journal of Pharmacology **149**(3): 283-290.

Ohnishi, R., H. Ito, N. Kasajima, M. Kaneda, R. Kariyama, H. Kumon, T. Hatano and T. Yoshida (2006). "Urinary excretion of anthocyanins in humans after cranberry juice ingestion." Bioscience, Biotechnology, and Biochemistry **70**(7): 1681-1687.

Oliveira, H. I., I. Fernandes, N. r. F. Brás, A. Faria, V. De Freitas, C. a. o. Calhau and N. Mateus (2015). "Experimental and theoretical data on the mechanism by which red wine anthocyanins are transported through a human MKN-28 gastric cell model." Journal of Agricultural and Food Chemistry **63**(35): 7685-7692.

Ostrowski, W., A. Wojakowska, M. Grajzer and M. Stobiecki (2014). "Mass spectrometric behavior of phenolic acids standards and their analysis in the plant samples with LC/ESI/MS system." Journal of Chromatography B **967**: 21-27.

Paixão, J., T. C. Dinis and L. M. Almeida (2012). "Malvidin-3-glucoside protects endothelial cells up-regulating endothelial NO synthase and inhibiting peroxynitrite-induced NF-κB activation." Chemico-Biological Interactions **199**(3): 192-200.

Pamukcu, B., G. Y. Lip, V. Snezhitskiy and E. Shantsila (2011). "The CD40-CD40L system in cardiovascular disease." Annals of Medicine **43**(5): 331-340.

Passamonti, S., A. Vanzo, U. Vrhovsek, M. Terdoslavich, A. Cocolo, G. Decorti and F. Mattivi (2005). "Hepatic uptake of grape anthocyanins and the role of bilitranslocase." Food Research International **38**(8–9): 953-960.

Passamonti, S., U. Vrhovsek and F. Mattivi (2002). "The interaction of anthocyanins with bilitranslocase." Biochemical and Biophysical Research Communications **296**(3): 631-636.

Peiffer, D. S., N. P. Zimmerman, L.-S. Wang, B. W. Ransom, S. G. Carmella, C.-T. Kuo, J. Siddiqui, J.-H. Chen, K. Oshima and Y.-W. Huang (2014). "Chemoprevention of esophageal cancer with black raspberries, their component anthocyanins, and a major anthocyanin metabolite, protocatechuic acid." Cancer Prevention Research **7**(6): 574-584.

Penczynski, K. J., D. Krupp, A. Bring, K. Bolzenius, T. Remer and A. E. Buyken (2015). "Relative validation of 24-h urinary hippuric acid excretion as a biomarker for dietary flavonoid intake from fruit and vegetables in healthy adolescents." European Journal of Nutrition: 1-10.

Pérez-Jiménez, J., L. Fezeu, M. Touvier, N. Arnault, C. Manach, S. Hercberg, P. Galan and A. Scalbert (2011). "Dietary intake of 337 polyphenols in French adults." The American Journal of Clinical Nutrition **93**(6): 1220-1228.

Pierce, J. W., R. Schoenleber, G. Jesmok, J. Best, S. A. Moore, T. Collins and M. E. Gerritsen (1997). "Novel inhibitors of cytokine-induced I κ B α phosphorylation and endothelial cell adhesion molecule expression show anti-inflammatory effects in vivo." Journal of Biological Chemistry **272**(34): 21096-21103.

Pietrini, F., M. Iannelli and A. Massacci (2002). "Anthocyanin accumulation in the illuminated surface of maize leaves enhances protection from photo-inhibitory risks at low temperature, without further limitation to photosynthesis." Plant, Cell & Environment **25**(10): 1251-1259.

Pimpão, R. C., T. Dew, M. E. Figueira, G. J. McDougall, D. Stewart, R. B. Ferreira, C. N. Santos and G. Williamson (2014). "Urinary metabolite profiling identifies novel colonic metabolites and conjugates of phenolics in healthy volunteers." Molecular Nutrition & Food Research **58**(7): 1414-1425.

Pimpão, R. C., M. R. Ventura, R. B. Ferreira, G. Williamson and C. N. Santos (2015). "Phenolic sulfates as new and highly abundant metabolites in human plasma after ingestion of a mixed berry fruit purée." British Journal of Nutrition **113**(03): 454-463.

Polson, C., P. Sarkar, B. Incledon, V. Raguvaran and R. Grant (2003). "Optimization of protein precipitation based upon effectiveness of protein removal and ionization effect in liquid chromatography–tandem mass spectrometry." Journal of Chromatography B **785**(2): 263-275.

Pompella, A., A. Visvikis, A. Paolicchi, V. De Tata and A. F. Casini (2003). "The changing faces of glutathione, a cellular protagonist." Biochemical Pharmacology **66**(8): 1499-1503.

Potischman, N. (2003). "Biologic and methodologic issues for nutritional biomarkers." The Journal of Nutrition **133**(3): 875S-880S.

Prior, R. L., X. Wu, L. Gu, T. J. Hager, A. Hager and L. R. Howard (2008). "Whole berries versus berry anthocyanins: Interactions with dietary fat levels in the c57bl/6j mouse model of obesity." Journal of Agricultural and Food Chemistry **56**(3): 647-653.

Queipo-Ortuño, M. I., M. Boto-Ordóñez, M. Murri, J. M. Gomez-Zumaquero, M. Clemente-Postigo, R. Estruch, F. C. Diaz, C. Andrés-Lacueva and F. J. Tinahones (2012). "Influence of red wine polyphenols and ethanol on the gut microbiota ecology and biochemical biomarkers." The American Journal of Clinical Nutrition **95**(6): 1323-1334.

Rabassa, M., A. Cherubini, R. Zamora-Ros, M. Urpi-Sarda, S. Bandinelli, L. Ferrucci and C. Andres-Lacueva (2015). "Low levels of a urinary biomarker of dietary polyphenol are associated with substantial cognitive decline over a 3-year period in older adults: The Invecchiare in Chianti Study." Journal of the American Geriatrics Society **63**(5): 938-946.

Raju, B., M. Ramesh, R. M. Borkar, R. Padiya, S. K. Banerjee and R. Srinivas (2012). "Identification and structural characterization of in vivo metabolites of ketorolac using liquid chromatography electrospray ionization tandem mass spectrometry (LC/ESI-MS/MS)." Journal of Mass Spectrometry **47**(7): 919-931.

Ramalingam, P. and Y. T. Ko (2016). "Validated LC–MS/MS method for simultaneous quantification of resveratrol levels in mouse plasma and brain and its application to pharmacokinetic and brain distribution studies." Journal of Pharmaceutical and Biomedical Analysis **119**: 71-75.

Ramana, K. V., A. Bhatnagar and S. K. Srivastava (2004). "Aldose reductase regulates TNF- α -induced cell signaling and apoptosis in vascular endothelial cells." FEBS Letters **570**(1–3): 189-194.

Rangel-Huerta, O. D., B. Pastor-Villaescusa, C. M. Aguilera and A. Gil (2015). "A systematic review of the efficacy of bioactive compounds in cardiovascular disease: Phenolic compounds." Nutrients **7**(7): 5177-5216.

Rauha, J.-P., H. Vuorela and R. Kostianen (2001). "Effect of eluent on the ionization efficiency of flavonoids by ion spray, atmospheric pressure chemical ionization, and atmospheric pressure photoionization mass spectrometry." Journal of Mass Spectrometry **36**(12): 1269-1280.

Rein, M. (2005). Copigmentation reactions and color stability of berry anthocyanins, University of Helsinki.

Rice-Evans, C. (1995). "Plant polyphenols: Free radical scavengers or chain-breaking antioxidants?" Biochemical Society Symposia **61**: 103-116.

Robbins, R. J. (2003). "Phenolic acids in foods: An overview of analytical methodology." Journal of Agricultural and Food Chemistry **51**(10): 2866-2887.

Rodriguez-Mateos, A., C. Rendeiro, T. Bergillos-Meca, S. Tabatabaee, T. W. George, C. Heiss and J. P. Spencer (2013). "Intake and time dependence of blueberry flavonoid-induced improvements in vascular function: A randomized, controlled, double-blind, crossover intervention study with mechanistic insights into biological activity." The American Journal of Clinical Nutrition **98**(5): 1179-1191.

Rodriguez-Mateos, A., D. Vauzour, C. Krueger, D. Shanmuganayagam, J. Reed, L. Calani, P. Mena, D. Del Rio and A. Crozier (2014). "Bioavailability, bioactivity and impact on health of dietary flavonoids and related compounds: An update." Archives of Toxicology: 1-51.

Romanelli, A., L. Olson, T. Biesenthal and H. Ghobarah. (2012). "The AB SCIEX triple quad™ 6500 and QTRAP^(r) 6500 systems for bioanalysis - a new level of sensitivity." from <http://sciex.com/Documents/tech%20notes/6500%20System%20for%20High%20Sensitivity%20Bioanalysis%20TN%205780212-01.pdf>.

Sabio, G. and R. J. Davis (2014). "TNF and MAP kinase signalling pathways." Seminars in Immunology **26**(3): 237-245.

Sadilova, E., F. Stintzing and R. Carle (2006). "Thermal degradation of acylated and nonacylated anthocyanins." Journal of Food Science **71**(8): C504-C512.

Sánchez-Patán, F., C. Cueva, M. Monagas, G. E. Walton, G. R. Gibson M, J. E. Quintanilla-López, R. Lebrón-Aguilar, P. J. Martín-Álvarez, M. V. Moreno-Arribas and B. Bartolomé (2012). "In vitro fermentation of a red wine extract by human gut microbiota: Changes in microbial groups and formation of phenolic metabolites." Journal of Agricultural and Food Chemistry **60**(9): 2136-2147.

Sawa, Y., T. Ueki, M. Hata, K. Iwasawa, E. Tsuruga, H. Kojima, H. Ishikawa and S. Yoshida (2008). "LPS-induced IL-6, IL-8, VCAM-1, and ICAM-1 expression in human lymphatic endothelium." Journal of Histochemistry and Cytochemistry **56**(2): 97-109.

Scalbert, A., I. T. Johnson and M. Saltmarsh (2005). "Polyphenols: Antioxidants and beyond." The American Journal of Clinical Nutrition **81**(1): 215S-217S.

Scalbert, A. and G. Williamson (2000). "Dietary intake and bioavailability of polyphenols." The Journal of Nutrition **130**(8): 2073S-2085S.

Schoenheimer, R. and D. Rittenberg (1935). "Deuterium as an indicator in the study of intermediary metabolism. I." Journal of Biological Chemistry **111**(1): 163-168.

Schuett, H., M. Luchtefeld, C. Grothusen, K. Grote and B. Schieffer (2009). "How much is too much? Interleukin-6 and its signalling in atherosclerosis." Thrombosis and Haemostasis **102**(2): 215-222.

Schwartz, R. and C. C. Giesecke (1979). "Mass spectrometry of a volatile Mg chelate in the measurement of stable ²⁶Mg when used as a tracer." Clinica Chimica Acta **97**(1): 1-8.

Selma, M. a. V., J. C. Espín and F. A. Tomás-Barberán (2009). "Interaction between phenolics and gut microbiota: Role in human health." Journal of Agricultural and Food Chemistry **57**(15): 6485-6501.

Sesink, A. L. A., I. C. W. Arts, M. Faassen-Peters and P. C. H. Hollman (2003). "Intestinal uptake of quercetin-3-glucoside in rats involves hydrolysis by lactase phlorizin hydrolase." The Journal of Nutrition **133**(3): 773-776.

Smith, D. L. (1983). "Determination of stable isotopes of calcium in biological fluids by fast atom bombardment mass spectrometry." Analytical Chemistry **55**(14): 2391-2393.

Sommer, M. O. (2015). "Advancing gut microbiome research using cultivation." Current Opinion in Microbiology **27**: 127-132.

Speciale, A., S. Anwar, R. Canali, J. Chirafisi, A. Saija, F. Virgili and F. Cimino (2013). "Cyanidin-3-O-glucoside counters the response to TNF-alpha of endothelial cells by activating Nrf2 pathway." Molecular Nutrition & Food Research **57**(11): 1979-1987.

Speciale, A., F. Cimino, A. Saija, R. Canali and F. Virgili (2014). "Bioavailability and molecular activities of anthocyanins as modulators of endothelial function." Genes & Nutrition **9**(4): 1-19.

Spencer, J. P., M. M. Abd El Mohsen, A.-M. Minihiene and J. C. Mathers (2008). "Biomarkers of the intake of dietary polyphenols: Strengths, limitations and application in nutrition research." British Journal of Nutrition **99**(01): 12-22.

Stintzing, F. C. and R. Carle (2004). "Functional properties of anthocyanins and betalains in plants, food, and in human nutrition." Trends in Food Science & Technology **15**(1): 19-38.

Stokvis, E., H. Rosing and J. H. Beijnen (2005). "Stable isotopically labeled internal standards in quantitative bioanalysis using liquid chromatography/mass spectrometry: Necessity or not?" Rapid Communications in Mass Spectrometry **19**(3): 401-407.

Sun, Y., B. Xia, X. Chen, C. Duanmu, D. Li and C. Han (2015). "Rapid quantification of four anthocyanins in red grape wine by hydrophilic interaction liquid chromatography/triple quadrupole linear ion trap mass spectrometry." Journal of AOAC International **98**(6): 1628-1631.

Talavéra, S., C. Felgines, O. Texier, C. Besson, J.-L. Lamaison and C. Rémésy (2003). "Anthocyanins are efficiently absorbed from the stomach in anesthetized rats." The Journal of Nutrition **133**(12): 4178-4182.

Tanaka, Y., N. Sasaki and A. Ohmiya (2008). "Biosynthesis of plant pigments: Anthocyanins, betalains and carotenoids." The Plant Journal **54**(4): 733-749.

Tedgui, A. and Z. Mallat (2006). "Cytokines in atherosclerosis: Pathogenic and regulatory pathways." Physiological Reviews **86**(2): 515-581.

Thilakarathna, S. H. and H. Rupasinghe (2013). "Flavonoid bioavailability and attempts for bioavailability enhancement." Nutrients **5**(9): 3367-3387.

Thompson, F. E., A. F. Subar, C. M. Loria, J. L. Reedy and T. Baranowski (2010). "Need for technological innovation in dietary assessment." Journal of the American Dietetic Association **110**(1): 48.

Tresserra-Rimbau, A., E. B. Rimm, A. Medina-Remón, M. A. Martínez-González, R. de la Torre, D. Corella, J. Salas-Salvadó, E. Gómez-Gracia, J. Lapetra, F. Arós, M. Fiol, E. Ros, L. Serra-Majem, X. Pintó, G. T. Saez, J. Basora, J. V. Sorlí, J. A. Martínez, E. Vinyoles, V. Ruiz-Gutiérrez, R. Estruch and R. M. Lamuela-Raventós (2014). "Inverse association between habitual polyphenol intake and incidence of cardiovascular events in the PREDIMED study." Nutrition, Metabolism and Cardiovascular Diseases **24**(6): 639-647.

Turnlund, J. R. (1989). "The use of stable isotopes in mineral nutrition research." The Journal of Nutrition **119**(1): 7-14.

United Nations Office on Drugs and Crime (2009). "Guidance for the validation of analytical methodology and calibration of equipment used for testing of illicit drugs in seized materials and biological specimens."

Urpi-Sarda, M., M. Boto-Ordóñez, M. I. Queipo-Ortuño, S. Tulipani, D. Corella, R. Estruch, F. J. Tinahones and C. Andres-Lacueva (2015). "Phenolic and microbial-targeted metabolomics to discovering and evaluating wine intake biomarkers in human urine and plasma." Electrophoresis **36**(18): 2259-2268.

van Dorsten, F. A., C. H. Grün, E. J. van Velzen, D. M. Jacobs, R. Draijer and J. P. van Duynhoven (2010). "The metabolic fate of red wine and grape juice polyphenols in humans assessed by metabolomics." Molecular Nutrition & Food Research **54**(7): 897-908.

Vanholder, R., R. De Smet, G. Glorieux, A. Argilés, U. Baurmeister, P. Brunet, W. Clark, G. Cohen, P. P. De Deyn and R. Deppisch (2003). "Review on uremic toxins: Classification, concentration, and interindividual variability." Kidney International **63**(5): 1934-1943.

Vanzo, A., M. Terdoslavich, A. Brandoni, A. M. Torres, U. Vrhovsek and S. Passamonti (2008). "Uptake of grape anthocyanins into the rat kidney and the involvement of bilitranslocase." Molecular Nutrition & Food Research **52**(10): 1106-1116.

Vassiliadis, E., N. Barascuk and M. A. Karsdal (2012). "Atherofibrosis-a unique and common process of the disease pathogenesis of atherosclerosis and fibrosis-lessons for biomarker development." American Journal of Translational Research **5**(1): 1-14.

Vastag, M., J. Skopál, Z. Voko, É. Csonka and Z. Nagy (1999). "Expression of membrane-bound and soluble cell adhesion molecules by human brain microvessel endothelial cells." Microvascular Research **57**(1): 52-60.

Vitaglione, P., G. Donnarumma, A. Napolitano, F. Galvano, A. Gallo, L. Scalfi and V. Fogliano (2007). "Protocatechuic acid is the major human metabolite of cyanidin-glucosides." The Journal of Nutrition **137**(9): 2043-2048.

Vogel, R. A. (1997). "Coronary risk factors, endothelial function, and atherosclerosis: A review." Clinical Cardiology **20**(5): 426-432.

Wakeling, L. A. and D. Ford (2012). "Polymorphisms in genes involved in the metabolism and transport of soy isoflavones affect the urinary metabolite profile in premenopausal women following consumption of a commercial soy supplement as a single bolus dose." Molecular Nutrition & Food Research **56**(12): 1794-1802.

Walgren, R. A., J.-T. Lin, R. K.-H. Kinne and T. Walle (2000). "Cellular uptake of dietary flavonoid quercetin 4'- β -glucoside by sodium-dependent glucose transporter SGLT1." Journal of Pharmacology and Experimental Therapeutics **294**(3): 837-843.

Wallace, T. C. (2011). "Anthocyanins in cardiovascular disease." Advances in Nutrition: An International Review Journal **2**(1): 1-7.

Wallace, T. C., M. Slavin and C. L. Frankenfeld (2016). "Systematic review of anthocyanins and markers of cardiovascular disease." Nutrients **8**(1): 32.

Wang, J., Y. Liao, J. Fan, T. Ye, X. Sun and S. Dong (2012). "Apigenin inhibits the expression of IL-6, IL-8, and ICAM-1 in DEHP-stimulated human umbilical vein endothelial cells and in vivo." Inflammation **35**(4): 1466-1476.

Wang, S. Y., C.-T. Chen and C. Y. Wang (2009). "The influence of light and maturity on fruit quality and flavonoid content of red raspberries." Food Chemistry **112**(3): 676-684.

Wang, X., Y. Y. Ouyang, J. Liu and G. Zhao (2014a). "Flavonoid intake and risk of CVD: A systematic review and meta-analysis of prospective cohort studies." British Journal of Nutrition **111**(01): 1-11.

Wang, X., X. Zhao, L. Gu, C. Lv, B. He, Z. Liu, P. Hou, K. Bi and X. Chen (2014b). "Simultaneous determination of five free and total flavonoids in rat plasma by ultra HPLC–MS/MS and its application to a comparative pharmacokinetic study in normal and hyperlipidemic rats." Journal of Chromatography B **953–954**: 1-10.

Warner, E. F., Q. Zhang, K. S. Raheem, D. O'Hagan, M. A. O'Connell and C. D. Kay (2016). "Common phenolic metabolites of flavonoids, but not their unmetabolized precursors, reduce the secretion of vascular cellular adhesion molecules by human endothelial cells." The Journal of Nutrition **146**(3): 465-473.

Warth, B., M. Sulyok, P. Fruhmman, H. Mikula, F. Berthiller, R. Schuhmacher, C. Hametner, W. A. Abia, G. Adam and J. Fröhlich (2012). "Development and validation of a rapid multi-biomarker liquid chromatography/tandem mass spectrometry method to assess human exposure to mycotoxins." Rapid Communications in Mass Spectrometry **26**(13): 1533-1540.

Wei, L., X. Wang, P. Zhang, Y. Sun, L. Jia, J. Zhao, S. Dong and L. Sun (2016). "An UPLC–MS/MS method for simultaneous quantitation of two coumarins and two flavonoids in rat plasma and its application to a pharmacokinetic study of Wikstroemia indica extract." Journal of Chromatography B **1008**: 139-145.

Whyte, A. R., G. Schafer and C. M. Williams (2015). "Cognitive effects following acute wild blueberry supplementation in 7- to 10-year-old children." European Journal of Nutrition: 1-12.

Wiczowski, W., D. Szawara-Nowak and J. Romaszko (2016). "The impact of red cabbage fermentation on bioavailability of anthocyanins and antioxidant capacity of human plasma." Food Chemistry **190**: 730-740.

Wilkes, K., L. R. Howard, C. Brownmiller and R. L. Prior (2013). "Changes in chokeberry (Aronia melanocarpa L.) polyphenols during juice processing and storage." Journal of Agricultural and Food Chemistry **62**(18): 4018-4025.

Willemse, C. M., M. A. Stander and A. de Villiers (2013). "Hydrophilic interaction chromatographic analysis of anthocyanins." Journal of Chromatography A **1319**: 127-140.

Williamson, G. (2013). "Possible effects of dietary polyphenols on sugar absorption and digestion." Molecular Nutrition & Food Research **57**(1): 48-57.

Woodward, G., P. Kroon, A. Cassidy and C. Kay (2009). "Anthocyanin stability and recovery: Implications for the analysis of clinical and experimental samples." Journal of Agricultural and Food Chemistry **57**(12): 5271-5278.

World Health Organisation (2014). Global status report on noncommunicable diseases.

Wu, C. H., F. H. Lu, C. S. Chang, T. C. Chang, R. H. Wang and C. J. Chang (2003). "Relationship among habitual tea consumption, percent body fat, and body fat distribution." Obesity Research **11**(9): 1088-1095.

Wu, T., Z. Yu, Q. Tang, H. Song, Z. Gao, W. Chen and X. Zheng (2013). "Honeysuckle anthocyanin supplementation prevents diet-induced obesity in C57BL/6 mice." Food & Function **4**(11): 1654-1661.

Wu, W.-B., D.-K. Hung, F.-W. Chang, E.-T. Ong and B.-H. Chen (2012). "Anti-inflammatory and anti-angiogenic effects of flavonoids isolated from *Lycium barbarum* Linnaeus on human umbilical vein endothelial cells." Food & Function **3**(10): 1068-1081.

Wu, X., G. R. Beecher, J. M. Holden, D. B. Haytowitz, S. E. Gebhardt and R. L. Prior (2006). "Concentrations of anthocyanins in common foods in the United States and estimation of normal consumption." Journal of Agricultural and Food Chemistry **54**(11): 4069-4075.

Wu, X., G. Cao and R. L. Prior (2002). "Absorption and metabolism of anthocyanins in elderly women after consumption of elderberry or blueberry." The Journal of Nutrition **132**(7): 1865-1871.

Wu, X., L. Gu, R. L. Prior and S. McKay (2004). "Characterization of anthocyanins and proanthocyanidins in some cultivars of *Ribes*, *Aronia*, and *Sambucus* and their antioxidant capacity." Journal of Agricultural and Food Chemistry **52**(26): 7846-7856.

Xia, M., W. Ling, H. Zhu, J. Ma, Q. Wang, M. Hou, Z. Tang, H. Guo, C. Liu and Q. Ye (2009). "Anthocyanin attenuates CD40-mediated endothelial cell activation and apoptosis by inhibiting CD40-induced MAPK activation." Atherosclerosis **202**(1): 41-47.

Xia, M., W. Ling, H. Zhu, Q. Wang, J. Ma, M. Hou, Z. Tang, L. Li and Q. Ye (2007). "Anthocyanin prevents CD40-activated proinflammatory signaling in endothelial cells by regulating cholesterol distribution." Arteriosclerosis, Thrombosis, and Vascular Biology **27**(3): 519-524.

- Xie, C., J. Kang, M. E. Ferguson, S. Nagarajan, T. M. Badger and X. Wu (2011). "Blueberries reduce pro-inflammatory cytokine TNF- α and IL-6 production in mouse macrophages by inhibiting NF- κ B activation and the MAPK pathway." Molecular Nutrition & Food Research **55**(10): 1587-1591.
- Xie, L., S. G. Lee, T. M. Vance, Y. Wang, B. Kim, J.-Y. Lee, O. K. Chun and B. W. Bolling (2016). "Bioavailability of anthocyanins and colonic polyphenol metabolites following consumption of aronia berry extract." Food Chemistry **211**: 860-868.
- Xu, J.-W., K. Ikeda and Y. Yamori (2004). "Upregulation of endothelial nitric oxide synthase by cyanidin-3-glucoside, a typical anthocyanin pigment." Hypertension **44**(2): 217-222.
- Yang, Z., L. Deng, Y. Lan, X. Zhang, Z. Gao, C.-W. Chu, D. Cai and Z. Ren (2014). "Molecular extraction in single live cells by sneaking in and out magnetic nanomaterials." Proceedings of the National Academy of Sciences **111**(30): 10966-10971.
- Yu, H., W. Jiang, H. Du, Y. Xing, G. Bai, Y. Zhang, Y. Li, H. Jiang, Y. Zhang, J. Wang, P. Wang and X. Bai (2014). "Involvement of the Akt/NF- κ B pathways in the HTNV-mediated increase of IL-6, CCL5, ICAM-1, and VCAM-1 in HUVECs." PLOS ONE **9**(4): e93810.
- Yuan, L., D. Zhang, M. Jemal and A. F. Aubry (2012). "Systematic evaluation of the root cause of non-linearity in liquid chromatography/tandem mass spectrometry bioanalytical assays and strategy to predict and extend the linear standard curve range." Rapid Communications in Mass Spectrometry **26**(12): 1465-1474.
- Zamek-Gliszczyński, M. J., K. A. Hoffmaster, K.-i. Nezasa, M. N. Tallman and K. L. R. Brouwer (2006). "Integration of hepatic drug transporters and phase II metabolizing enzymes: Mechanisms of hepatic excretion of sulfate, glucuronide, and glutathione metabolites." European Journal of Pharmaceutical Sciences **27**(5): 447-486.
- Zamora-Ros, R., V. Knaze, L. Luján-Barroso, N. Slimani, I. Romieu, M. Touillaud, R. Kaaks, B. Teucher, A. Mattiello and S. Grioni (2011). "Estimation of the intake of anthocyanidins and their food sources in the European Prospective Investigation into Cancer and Nutrition (EPIC) study." British Journal of Nutrition **106**(07): 1090-1099.
- Zamora-Ros, R., C. Not, E. Guinó, L. Luján-Barroso, R. M. García, S. Biondo, R. Salazar and V. Moreno (2013). "Association between habitual dietary flavonoid and lignan intake and colorectal cancer in a Spanish case-control study (the Bellvitge Colorectal Cancer Study)." Cancer Causes & Control **24**(3): 549-557.
- Zeng, Y., S. Li, X. Wang, T. Gong, X. Sun and Z. Zhang (2015). "Validated LC-MS/MS method for the determination of scopoletin in rat plasma and its application to pharmacokinetic studies." Molecules **20**(10): 18988-19001.
- Zhang, Q., K. S. Raheem, N. P. Botting, A. M. Z. Slawin, C. D. Kay and D. O'Hagan (2012). "Flavonoid metabolism: The synthesis of phenolic glucuronides and sulfates as candidate metabolites for bioactivity studies of dietary flavonoids." Tetrahedron **68**(22): 4194-4201.

Zhao, Y., P. M. Vanhoutte and S. W. Leung (2015). "Vascular nitric oxide: Beyond eNOS." Journal of Pharmacological Sciences **129**(2): 83-94.

Zhou, S. and K. D. Cook (2001). "A mechanistic study of electrospray mass spectrometry: Charge gradients within electrospray droplets and their influence on ion response." Journal of the American Society for Mass Spectrometry **12**(2): 206-214.

Zhu, Y., W. Ling, H. Guo, F. Song, Q. Ye, T. Zou, D. Li, Y. Zhang, G. Li and Y. Xiao (2013). "Anti-inflammatory effect of purified dietary anthocyanin in adults with hypercholesterolemia: A randomized controlled trial." Nutrition, Metabolism and Cardiovascular Diseases **23**(9): 843-849.

Zou, T.-B., D. Feng, G. Song, H.-W. Li, H.-W. Tang and W.-H. Ling (2014). "The role of sodium-dependent glucose transporter 1 and glucose transporter 2 in the absorption of cyanidin-3-O- β -glucoside in Caco-2 cells." Nutrients **6**(10): 4165-4177.